Apport des nanocapsules lipidiques dans le traitement local des gliomes malins: application à l'encapsulation de complexes lipophiles métalliques

Emilie Allard

UNIVERSITE D'ANGERS

Année 2008
N°942

APPORT DES NANOCAPSULES LIPIDIQUES DANS LE TRAITEMENT LOCAL DES GLIOMES MALINS: APPLICATION A L'ENCAPSULATION DE COMPLEXES LIPOPHILES METALLIQUES

THÈSE DE DOCTORAT

Spécialité : Pharmacologie expérimentale et clinique

ECOLE DOCTORALE BIOLOGIE ET SANTE

Présentée et soutenue publiquement

Le 5 Décembre 2008

A Angers

Par **Emilie ALLARD**

Devant le jury ci-dessous :

Mr Igor CHOURPA, Professeur à l'Université de Tours	Rapporteur
Mr Philippe LEGRAND, Professeur à l'Université de Montpellier	Rapporteur
Mme Anne VESSIERES-JAOUEN, Directeur de recherche CNRS, UMR-CNRS 7576, Paris	Examinateur
Mr Gérard JAOUEN, Professeur à l'Ecole Nationale Supérieure de Chimie de Paris	Président du jury
Mme Catherine PASSIRANI, Maître de Conférences à l'Université d'Angers	Co-Directeur de thèse
Mr Jean-Pierre BENOIT, Professeur à l'Université d'Angers	Directeur de thèse

INSERM U646, Ingénierie de la vectorisation particulaire
IBT, 10 rue André Boquel, 49100 Angers, France

ED 502

Remerciements

Je tiens à exprimer mes plus sincères remerciements aux membres du jury pour avoir acceptés et pris de leur temps pour juger ce travail.

Je tiens à remercier en premier lieu, Mr Jean-Pierre Benoit, Professeur à l'Université d'Angers et directeur de l'Unité INSERM U646 de m'avoir accueillie dans son laboratoire et de m'avoir fait confiance pour accomplir ce travail de thèse. Merci d'avoir pris le temps de suivre ce travail régulièrement et d'avoir participé à la correction des publications issues de ce projet de recherche.

Je remercie Mr Igor Chourpa, Professeur à l'Université de Tours, et Mr Philippe Legrand, Professeur à l'Université de Montpellier, de me faire l'honneur d'avoir accepté de consacrer du temps à l'évaluation de ce travail en qualité de rapporteurs.

Je remercie également Mme Anne Vessières-Jaouen, Directeur de recherche CNRS et Mr Gérard Jaouen, Professeur à l'Ecole Nationale Supérieure de Chimie de Paris (ENSCP), pour leur participation au jury en tant qu'examinateurs. Merci pour l'enthousiasme dont vous m'avez fait part tout au long de ce travail. Je garderai un très bon souvenir de cette collaboration.

J'exprime enfin ma reconnaissance à Mme Catherine Passirani, Maitre de conférences à l'Université d'Angers et co-encadrante de ce travail de thèse. Merci Catherine, pour ta sympathie, ton enthousiasme et ton extrême disponibilité. Je le dis très sincèrement ; je souhaite à tous les thésards d'avoir une encadrante comme toi. Merci d'avoir valorisé ce travail, et d'avoir fait de cette correction de thèse, une priorité dans ton emploi de temps largement chargé.

J'adresse également mes remerciements à la région des Pays de la Loire, ainsi qu'au "Cancéropole Grand Ouest" pour les aides financières octroyées.

Un grand merci

Aux Docteurs Emmanuel Garcion, François Hindre et Laurent Lemaire, pour leurs collaborations liées à leurs domaines de compétence, respectivement, la biologie cellulaire, la radioactivité et l'imagerie par résonnance magnétique.

Aux Professeurs Frank Boury, Patrick Saulnier, et Marie-Claire Venier pour m'avoir encadré dans mes fonctions de moniteur. Après avoir été une de vos étudiantes, merci de m'avoir fait confiance en me laissant la possibilité d'enseigner avec vous. Je garderai un bon souvenir de cette première expérience d'enseignante à l'Université d'Angers. J'en profite également pour remercier le CIES (Centre d'initiation à l'enseignement supérieur) pour la formation octroyée pendant ces 3 ans et pour l'aide financière apportée.

Aux docteurs Delphine Jarnet et Sandrine Vinchon-Petit pour m'avoir bien aidé en ce qui concerne les manips in vivo. Merci Delphine d'avoir répondu si vite à mes mails en détresse et d'avoir pris de ton temps libre pour les séances de radiothérapie de mes petits rats. Merci Sandrine de m'avoir formé sur les injections en CED sans quoi, ce travail n'aurait pu avoir lieu.

Au docteur Pascal Pigeon, de l'ENSCP pour la synthèse et l'envoi très rapide des complexes lipophiles de fer.

Aux docteurs Nicolas Lepareur et Nicolas Noiret du Centre Eugène Marquis de Rennes et de l'ENSCR pour nous avoir fourni en Rhénium-188.

Au Dr Robert Filmon du service commun d'imagerie et de microscopie de l'Université d'Angers qui a réalisé les clichés de microscopie confocale.

A tout le personnel de l'animalerie : Pierre, Jérôme, Dominique et Laurent. Merci de m'avoir supporté pendant ces nombreuses heures passées dans vos murs. Vous vous êtes bien occupés de mes nombreux groupes de rats, et spécialement quand j'étais en vacances !!! Un spécial merci à mes « survivors » chouchou de surcroît… Pierrot, désolée de ne pas avoir suivi tes conseils mais sache que tu seras le deuxième (après le 1er) au courant si un jour ça m'arrive…

Enfin, j'adresse de sincères remerciements à tous ceux que j'ai côtoyés au laboratoire pendant plus de 3 ans et demi…

Avec une spéciale attention à mes deux collègues de bureau :

Emilie : dit Emilie R, ou Emilie la brune… Ton franc parlé légendaire et nos millions de fous rires vont me manquer. Je te souhaite de réussir (tu le mérites largement !!!) et que tes recherches (quelle qu'elles soient…) soient fructueuses. J'espère juste qu'il restera quelques feuilles au bananier la prochaine fois que je passerai dans le bureau…

Olivier : dit le chanceux… Il ne le sait pas encore mais il est le mieux loti de tout le labo : 2 z'émilie pour le prix d'1 !!! Merci de nous avoir supportés… Bonne chance pour la suite de ta carrière. Je te souhaite vraiment de gravir les échelons au plus vite.

Merci également à :

Edith, notre chère secrétaire de l'unité ; tes réunions tuperwares adossée au radiateur du bureau vont me manquer. Sache que je n'hésiterais pas à revenir de Tours pour la teuf de tes 50 ans (d'ailleurs, il va falloir penser à fixer une date quand même !!!).

Archi, merci pour tes conseils concernant la culture cell' et bon courage pour cette dernière année de thèse ainsi que pour la suite. Je pense qu'un petit post-doc à Barcelone serait tout à fait adapté pour toi ; maintenant que tu connais si bien la ville !!!

Maud, prends soin de tes nanocarottes ! Un petit conseil pour tes prochains congrès internationaux au Mans : kirido élégant, salut royal et rire « cocktail »…

Mathilde, je sais maintenant pourquoi ton pull en était imprégné, c'était pour mieux maîtriser la technique !!! Quel professionnalisme !!! Merci pour les nombreux « Welsh layonnés » du vendredi soir…

Jérome, toi l'unique rescapé, je te souhaite un jour de passer du côté obscur de la force…

Nolwenn, merci pour ton aide quant à la formulation des LNC de magnétite et bonne chance pour cette nouvelle carrière qui t'attend. N'oublie surtout pas de me tenir au courant des prochaines promos chez C… and C-C… !!!

Elisa et Kathy, respectivement espagnoles et belges… Les filles, j'ai vraiment été ravie de vous rencontrer, de me remettre à l'espagnol et d'apprendre quelques bonnes expressions belges. Je vous souhaite chacune de réussir et j'espère qu'on se recroisera un jour dans des congrès ou pour d'autres occasions.

Merci également à toutes les nombreuses personnes que j'ai côtoyées au Laboratoire :

Marie (capt'ain !), Gaétan (dit l'homme qui danse en oscillant les bras), Sandy, Erika, Catherine C, Stéphanie, Kaïs, Alya, Thomas, Kamel, Pascal, Jean-Pierre (dit Dr Corazón), Emilien (dit Brandon…), Florian, Frank, Céline, Thanh, Trinh, Ahmed, Claire, José, Laurence, Anne, David, Claudia, Nathalie…
Je me chargerai bien entendu d'envoyer à chacun de vous un petit mail pour vos anniversaires et fêtes à venir (nouveauté 2008!). Comptez sur moi !!!
Bon courage pour vos recherches et bon vent à tous !!!

Merci également à Jacqueline, Mimy et Gisèle, fraichement parties à la retraite. Je vous souhaite pleins de bonnes choses pour votre nouvelle vie…

Un petit mot également pour les 'vieux' thésards qui ont quitté ce labo avant moi : Alex, Nico, Arnaud B, Arnaud V, Florence, Anne S, Matthieu, Thomas B, Pierre, Ali…

Merci aux stagiaires qui m'ont accompagné dans ce projet: Emilie, Ingrid et Laure

Un énorme merci à mes petites Maugettes (copines des Mauges…) et apparentés qui sont toujours là pour m'écouter et me soutenir : Mano, Hélène, Marie, Ando, Audrey, Matthias (et leur haricot magique…), Catherine, David et Salomé, Pédros, Emilie et Titouan.

Un grand merci également à tous mes amis de Pharma avec qui j'ai débuté cette longue vie étudiante. Et oui, ça fait maintenant 10 ans que je mange au RU de St Serge !!!

J'adresse des remerciements sincères à ma famille ; mes parents, mes sœurs, mes beaux-frères et mes petites nièces pour leur soutien inconditionnel, ainsi qu'à ma belle-famille, mes beaux parents, mes belles sœurs, mes beaux frères, et mes petits neveux pour vos nombreux encouragements.

Le dernier remerciement sera pour toi Fabien, merci d'être là tous les jours à mes côtés…

Sommaire

DISCUSSION GENERALE

Conception des LNC, vecteurs de substances actives

L’application intracérébrale

Le complexe de Rhénium-188

Les ferrocifènes

Intérêt du système LNC dans la thérapie locale des gliomes

Un vecteur adapté à la Convection Enhanced Delivery (CED)

Une meilleure rétention *in situ*

Un vecteur internalisant

Les évaluations *in vivo*

Le gliome sous-cutané

L’administration intracérébrale par CED

Les protocoles de chimio-radiothérapie

CONCLUSION ET PERSPECTIVES

CURRICULUM VITAE

.

Abréviations

A		
	ADN	acide désoxyribonucléique
	AAV2	adéno-associated virus 2
B		
	BBB	blood brain barrier
	BHE	barrière hémato encéphalique
	bFGF	basic fibroblast growth factor
	BNCT	boron neutron capture therapy
	BPA	boronophénylalanine
	BSA	bovine serum albumin
C		
	C-225	cetuximab
	CED	convection-enhanced delivery
	CSF	circulating cerebrospinal fluid
D		
	DMEM	Dulbecco modified eagle medium
	DTI	diffusion tensor imaging
E		
	ECM	extra cellular matrix
	ECS	extra cellular space
	EGFR	epidermal growth factor receptor
	E/H	eau dans huile
	EMEM	Eagle’s minimal essential medium
	ER	estrogen receptor
F		
	FCS	foetal calf serum
	FGF	fibroblast growth factor
	5-FU	5-fluorouracile
	FDA	food and drug administration
G		
	GBM	glioblastome multiforme
	GCV	ganciclovir
	GSH	gluthation
H		
	HBSS	Hanks balanced salt solution
	H/E	huile dans eau
	HSPG	heparan sulfate proteoglycans
	HSA	human serum albumin
	HSV-1	herpes simplex virus type 1
I		
	IL-12	interleukine-12
	IRM	imagerie par resonance magnétique
	IST	increase in survival time
L		
	LNC	lipid nanocapsule

M

MDR	multidrug resistance
Me-β-CD	methylated β cyclodextrins
MEC	matrice extra-cellulaire
MNP	maghemite nanoparticle
MIONs	monocrystalline iron oxide nanocompounds
MRI	magnetic resonance imaging
MRS	magnetic resonance spectroscopy
MTX	methotrexate
Mw	molecular weight

N

NAA	N-acétyl-aspartate
NGF	nerve growth factor
NIH	national institutes of health
NR	nile red

O

OD	optical density
OD	outer diameter

P

PA	principe actif
PBS	phosphate buffer saline
PCNST	primary central nervous system tumors
PEG	polyethylene glycol
P-gp	glycoprotein P
PI	polydispersity index
PLGA	poly (lactic-co-glycolic acid)
PMM	poly(méthylidène malonate)

R

RCP	radiochemical purity
RARE	rapid acquisition with relaxation enhancement
ROS	reactive oxygen species

S

SD	standard deviation
SF2	survival fraction at 2Gy
SNC	système nerveux central
SERM	selective estrogen receptor modulator
SFV	Semliki forest virus

T

THF	tetrahydrofurane
TIP	température d’inversion de phase

W

WHO	world health organisation

X

XRT	external radiotherapy

Z

ZIP	zone d’inversion de phase

INTRODUCTION GENERALE

Les tumeurs gliales

Les tumeurs gliales malignes, ou gliomes, sont des tumeurs primitives du système nerveux central (SNC) dont l'incidence annuelle est en constante évolution [1]. Parmi elles, le glioblastome, dérivé des astrocytes, est la forme la plus agressive des gliomes et la plus grave de l'adulte. Son incidence est estimée à 10,000 nouveaux cas/an aux Etats-Unis et 74,000 cas/an dans le monde [2]. Sa prise en charge est particulièrement difficile en raison de sa radiorésistance et de sa chimiorésistance, expliquant en partie le sombre pronostic.

Le traitement classique implique une résection chirurgicale, lorsque possible, associée à une radiothérapie et/ou une chimiothérapie adjuvante [3]. La radiothérapie focalisée délivre 55 à 60 Gy en une trentaine de fractions selon la taille du volume cible et la proximité des organes à risques. La chimiothérapie de référence est le témozolomide (Témodal®), agent alkylant administré par voie orale de façon concomitante à l'irradiation cérébrale et pendant la période post-radiothérapie. La chimiothérapie est souvent limitée par la barrière hémato-encéphalique (BHE), qui empêche le passage des molécules hydrophiles dans le tissu cérébral lorsqu'elles sont administrées par voie systémique. L'éventail thérapeutique s'en trouve ainsi restreint et se limite aux anticancéreux lipophiles et à certaines molécules hydrophiles qui peuvent traverser la barrière hémato-encéphalique à fortes doses, occasionnant des effets secondaires toxiques. Des techniques de modulation de perméabilité par ouverture transitoire de la BHE après injection de solutions hyperosmotiques ou d'agents vasodilatateurs peuvent favoriser significativement le passage de certains principes actifs dans le cerveau. Cependant, le bénéfice apporté est minime comparé à la toxicité générée par cette technique.

Le glioblastome est une tumeur infiltrante, avec un certain nombre de cellules malignes disséminées. Des biopsies réalisées en zone macroscopiquement saine, à plusieurs centimètres de la tumeur visible en imagerie par résonance magnétique (IRM) permettent d'isoler des cellules tumorales [4]. Malgré des techniques neurochirurgicales plus sûres, permettant des exérèses larges, les patients rechutent quasi-systématiquement avec une reprise tumorale au sein même ou au voisinage immédiat du lit tumoral (Figure 1).

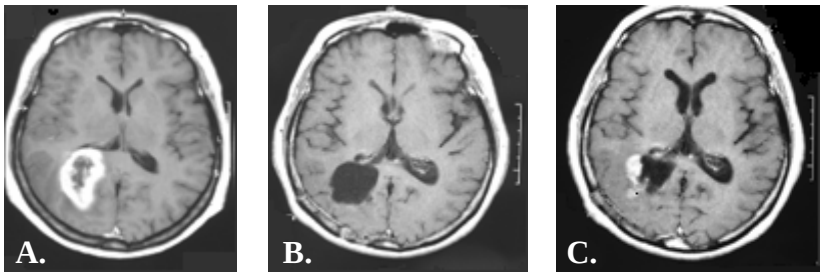

Figure 1 : IRM d'un patient atteint de glioblastome. A : la tumeur apparaît comme une région hyperintense par rapport au tissu cérébral sain, B : l'hyposignal illustre la cavité post-résection, C : le signal hyperintense proche de la cavité illustre la récurrence tumorale.

Ces gliomes sont constitués de cellules non seulement hautement proliférantes mais également exceptionnellement migrantes et possédant de nombreuses altérations génétiques, ce qui les rend très résistantes aux thérapies antiprolifératives.

L'équipe développe depuis maintenant de nombreuses années des systèmes destinés à une implantation locale par stéréotaxie [5, 6]. La chirurgie stéréotaxique est une technique qui permet de cibler avec une très haute précision différentes régions à l'intérieur du cerveau. La stéréotaxie traite le cerveau comme une carte géographique, grâce à un système de coordonnées permettant une localisation en 3D. Cette technique utilise un équipement de repérage appelé " cadre stéréotaxique " fixé à la tête du patient (Figure 2).

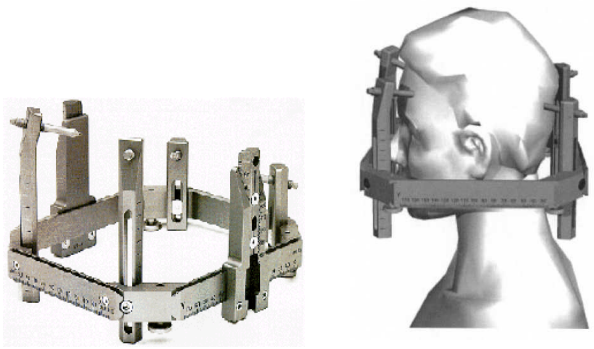

Figure 2 : Cadres de stéréotaxie.

Parmi les systèmes développés, des résultats préliminaires encourageants ont été obtenus chez l'homme dans le traitement du glioblastome multiforme à l'issue de deux essais cliniques réalisés au CHU d'Angers. Un essai de phase I a porté sur l'implantation stéréotaxique de microsphères de copolymères d'acide lactique et glycolique (PLGA) chargées en 5-

fluorouracile (5-FU) dans des gliomes profonds inopérables, montrant la possibilité technique du concept, l'absence de toxicité et la libération locale prolongée du 5-FU [6, 7]. Un essai randomisé multicentrique de phase IIb a également été mis en place avec implantation peropératoire suivant une exérèse complète du glioblastome [8]. Malgré de meilleures médianes de survie pour le groupe chimio-radiothérapie (15.2 mois) en comparaison avec le groupe radiothérapie seule (12.3 mois), il n'a pas été montré de différence significative entre ces deux groupes.

De plus, les microsphères polymères encapsulant un agent anticancéreux empêchent la prolifération du glioblastome à proximité du foyer primitif, mais une récurrence à distance est notée chez un certain nombre de patients. L'autre inconvénient des microsphères de PLGA est qu'elles sont totalement dégradées au bout de deux mois et le 5-FU n'est libéré *in situ* que pendant 20 jours. Pour pallier à ce problème, d'autres tentatives utilisant des polymères se dégradant plus lentement *in vivo* ont été réalisées. Des microsphères de poly(méthylidène malonate 2.1.2) (PMM 2.1.2) ont été formulées et testées dans un modèle de gliome chez le rat [9]. Malgré des résultats de survie prometteurs, les études de biocompatibilité menées en parallèle, ont démontré une toxicité majeure de ces polymères [10].

En définitive, les vecteurs potentiellement intéressants doivent respecter un cahier des charges associant biocompatibilité et capacité à diffuser dans le parenchyme cérébral. Dans cette perspective, ce travail de thèse a consisté à tester l'emploi de nanovecteurs thérapeutiques pour la thérapie des gliomes, en utilisant une technologie brevetée au laboratoire, celle des nanocapsules lipidiques (LNC : lipid nanocapsules). Ces vecteurs, de part leur taille nanométrique (20-100 nm) et leur structure lipidique, sont potentiellement capables de diffuser au sein du SNC afin d'atteindre les cellules disséminées à l'origine des récurrences. De plus, les LNC sont formulées grâce à un procédé original sans solvant organique utilisant des excipients biocompatibles tous approuvés par la Food and Drug Administration (FDA).

Les nanocapsules lipidiques (LNC)

La formulation de ces nanocapsules lipidiques repose sur une série d'inversions de phase entre une émulsion huile dans eau (H/E) et une émulsion eau dans huile (E/H) suite à une augmentation et une diminution de la température du milieu réactionnel [11] (Figure 3A). En fonction des proportions de chaque constituant, une zone d'inversion de phase (ZIP) est déterminée par suivi conductimétrique, permettant de connaître les températures cibles à atteindre au cours des cycles. Une conductivité très faible ($< 10^{-2}$ µS.cm^{-1}) caractérise une émulsion E/H, tandis qu'une conductivité plus forte traduit une émulsion H/E (Figure 3B). La préparation est réalisée en deux étapes : la première consiste à former une micro-émulsion, et à déstructurer cette micro-émulsion pour former les LNC. La deuxième étape consiste à figer le système, refroidi à une température de dilution prédéfinie, en le diluant dans un grand volume d'eau froide. Cette technique permet d'obtenir des LNC sans recours à un solvant organique et sans consommation importante d'énergie.

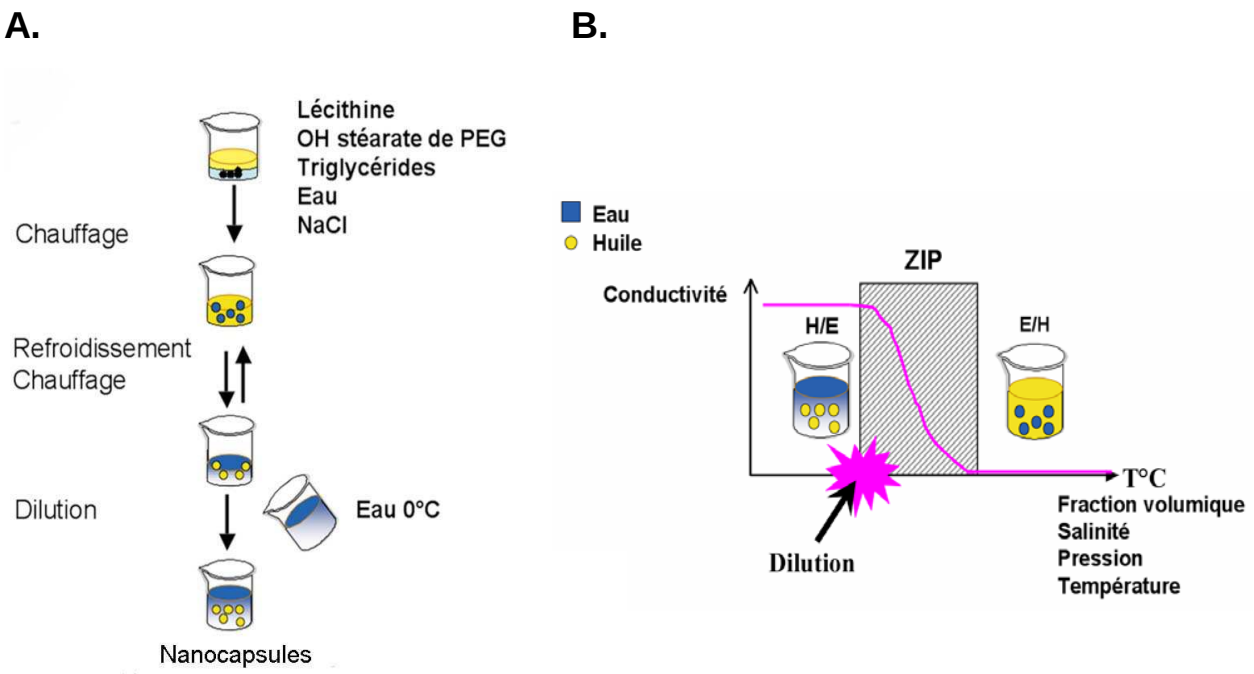

Figure 3. A : Représentation schématique des étapes de la formulation des nanocapsules
B : Mesure de la conductivité en fonction de la température

Les LNC sont formulées à partir d'une phase huileuse, d'une phase aqueuse et de tensioactifs non ioniques. La phase huileuse qui constitue le cœur lipophile de la capsule est composé d'un mélange de triglycérides à chaines moyennes (acides caprique et caprylique (C_8-C_{10})) (Labrafac®CC) (Figure 4). Le tensioactif principal formant la coque est un dérivé fortement polyéthoxylé, le Solutol® HS15 comportant du PEG 660 et de l'hydroxystéarate de PEG 660 dans des proportions 30/70. Une faible proportion de lécithine de soja contenant environ 70% de phosphatidylcholine et 10% de phosphatidyléthanolamine (Lipoid® S75-3) est ajoutée en tant que co-tensioactif pour rigidifier la coque. La phase aqueuse contient du chlorure de sodium (NaCl), celui-ci jouant un rôle sur la température d'inversion de phase (TIP). Quand sa concentration est augmentée, la TIP diminue. Ces nanocapsules lipidiques constituent des particules biocompatibles et biodégradables.

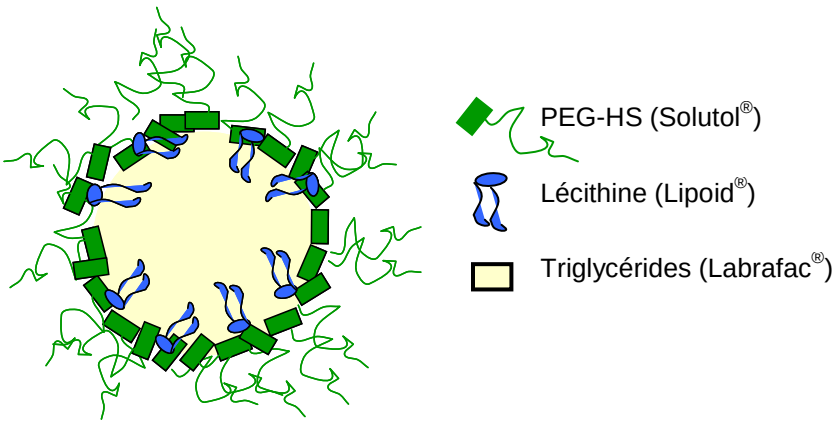

Figure 4. Structure des nanocapsules lipidiques (LNC).

Ces vecteurs hybrides entre les liposomes et les nanoparticules polymères présentent de nombreux intérêts (Figure 5). Parmi eux, leur caractère biocompatible est un critère de choix pour l'administration intracérébrale. Leur capacité à encapsuler des substances hydrophobes actives est un atout majeur pour une visée thérapeutique. De plus, leur échelle nanométrique (20-100 nm) associée à leur dispersion monomodale permet d'envisager une administration par convection enhanced delivery (CED).

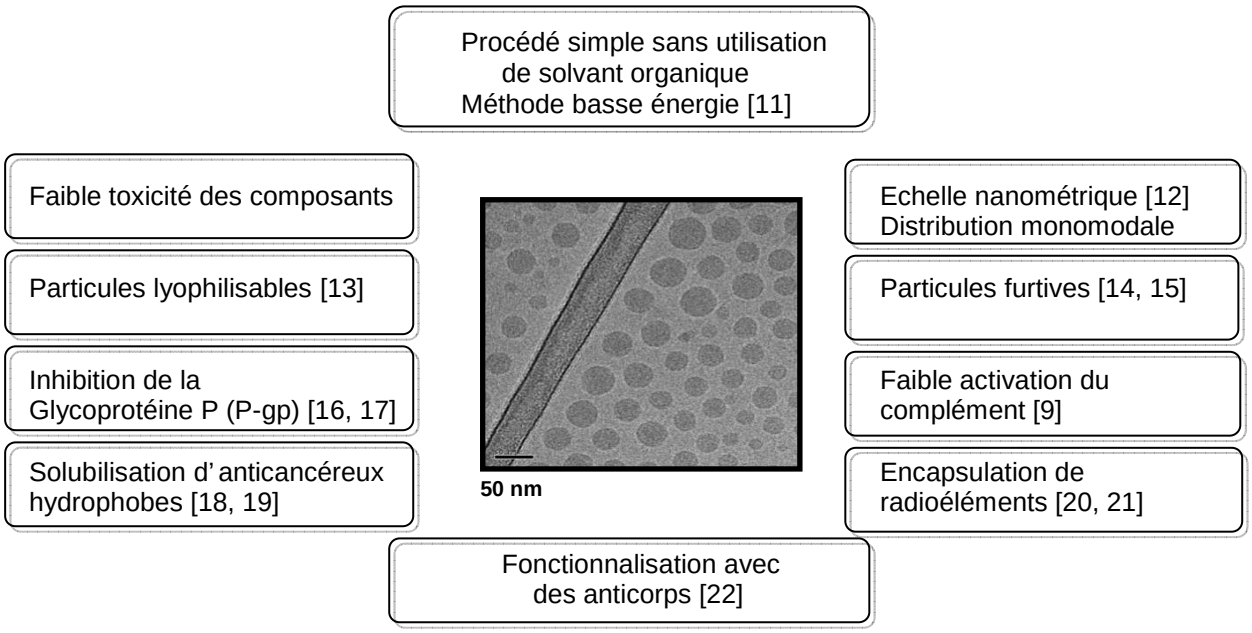

Figure 5 : Avantage des LNC.

La CED est une approche relativement nouvelle, introduite par Bobo et leurs collaborateurs en 1994, pour délivrer des substances actives dans le cerveau [23]. Elle permet la distribution de fortes concentrations de drogues, et ceci dans de larges volumes tissulaires, tout en évitant la toxicité systémique. Par cette technique, l'agent pharmacologique est délivré par convection et non par diffusion, ce qui permet de s'affranchir de paramètres tels que le poids moléculaire de la substance active. Des systèmes colloïdaux tels que des liposomes pégylés [24], des nanoparticules [25], des micelles polymères [26] et des dendrimères [27] ont déjà été infusés en CED. Ces systèmes colloïdaux présentent l'avantage de protéger les actifs et de distribuer uniformément les drogues dans le parenchyme cérébral tout en augmentant leur temps de résidence *in situ*.

Les complexes métalliques lipophiles

Ce travail de thèse s'inscrit dans une stratégie associant l'encapsulation de nouveaux actifs dans les nanocapsules lipidiques et leur administration intracérébrale par convection-enhanced delivery pour la thérapie des gliomes. Dans cette perspective, deux complexes métalliques lipophiles ont été étudiés. Le premier d'entre eux est un radioélément se présentant sous la forme d'un complexe hydrophobe de Rhénium-188 (Figure 6).

Le Rhénium-188 (^{188}Re) présente l'avantage d'être facilement disponible puisqu'il est obtenu à partir d'un générateur. Sa demi-vie physique (T) de 16.9h est suffisamment longue pour réaliser l'étape de formulation ainsi que son administration chez l'animal et suffisamment brève pour limiter les problèmes liés à la radioprotection. De plus, le Rhenium-188 émet des rayonnements gamma (γ) et beta moins (β^-), conférant à ce radioisotope des applications diagnostiques et thérapeutiques. En effet, les rayonnements β^- étant très radiotoxiques, ils peuvent être utilisés en thérapie. La formulation du complexe [^{188}Re(S_3CPh)$_2$(S_2CPh) = ^{188}Re-SSS] [28] ainsi que son incorporation au sein des LNC (^{188}ReSSS-LNC) a déjà fait l'objet d'études préliminaires [20]. L'objectif de ce travail est d'adapter la formulation des LNC à des applications intracérébrales afin d'envisager ce nouveau radiopharmaceutique en tant que vecteur pour la radiothérapie interne des gliomes malins.

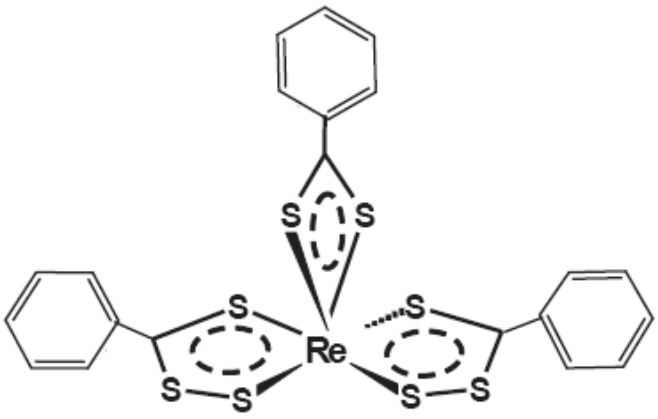

Figure 6 : Structure du complexe de Rhenium-188 étudié

La deuxième molécule étudiée appartient à la famille des organométalliques dérivés d'un métallocène à base de fer (Fe). Ces composés dénommés "ferrocifènes" sont des dérivés du tamoxifène où l'un des groupements phényl est substitué par un groupement ferrocène [Fe(C_5H_5)$_2$] potentiellement cytotoxique (Figure 7). Parmi ces molécules, le ferrociphénol [2-ferroceny-1,1-bis(4-hydroxyphényl)-but-1-ène (Fc-diOH)] apparaît comme la molécule la plus active.

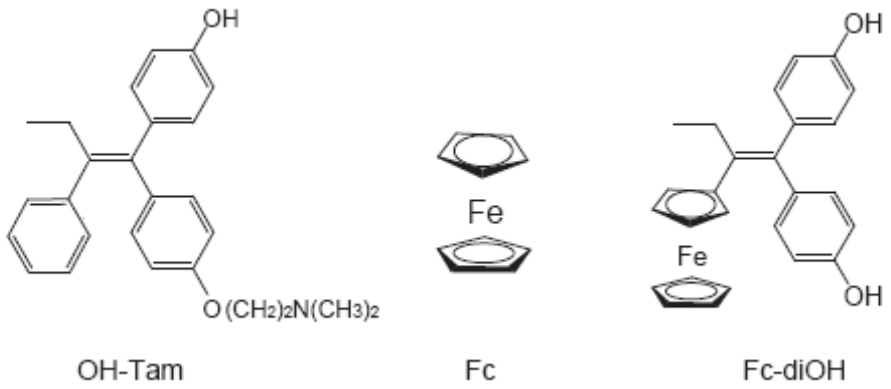

Figure 7: Structure des hydroxytamoxifène (OH-Tam), ferrocène (Fc) et ferrociphenol (Fc-diOH).

Ces molécules ont été largement étudiées sur des modèles *in vitro* de cancer du sein. Elles ont montré un effet antiprolifératif important sur des lignées de cultures cellulaires hormono-dépendantes (MCF7) ou non (MDA-MB231) [29]. Leur efficacité est basée sur deux oxydations intracellulaires successives qui vont d'abord transformer le groupement ferrocène en ferrocenium entraînant le déplacement d'un proton phénolique. La deuxième oxydation implique la formation d'une quinone méthyde, hautement toxique et capable d'interagir avec des macromolécules comme le glutathion, l'ADN ou certaines protéines pour aboutir à une mort cellulaire par sénescence [30].

La première partie de cette thèse est une revue bibliographique s'intéressant aux différents types de nanovecteurs infusés en CED pour le traitement de pathologies malignes de type gliales. La seconde partie, organisée en trois chapitres, porte sur le travail expérimental qui a été réalisé au cours de cette thèse. Le premier s'intéresse à l'évaluation thérapeutique des ^{188}Re-SSS LNC administrées par CED dans un modèle de gliome 9L chez le rat. Le deuxième chapitre concerne la conception et l'évaluation biologique de nanovecteurs lipidiques encapsulant le ferrociphénol Fc-diOH, ainsi que leur administration *in vivo* dans un modèle de gliome ectopique. Le troisième et dernier chapitre de ce travail portera sur l'évaluation thérapeutique de l'association des LNC-Fc-diOH avec une radiothérapie externe dans un modèle *in vitro* d'une part, puis après administration par CED dans un modèle orthotopique chez le rat. Enfin, une discussion générale commentera l'ensemble des résultats sous un aspect plus global, en reprenant également des résultats qui n'ont pas fait l'objet de publication.

Références

1. Jemal A, Murray T, Samuels A, Ghafoor A, Ward E, Thun MJ. Cancer statistics, 2003. CA Cancer J Clin 2003;53(1):5-26.

2. Sampson JH, Raghavan R, Provenzale JM, Croteau D, Reardon DA, Coleman RE, et al. Induction of hyperintense signal on T2-weighted MR images correlates with infusion distribution from intracerebral convection-enhanced delivery of a tumor-targeted cytotoxin. AJR Am J Roentgenol 2007;188(3):703-709.

3. Stupp R, Mason WP, Van Den Bent MJ, Weller M, Fisher B, Taphoorn MJB, et al. Radiotherapy plus concomitant and adjuvant temozolomide for glioblastoma. N Engl J Med 2005;352(10):987-996.

4. Silbergeld DL, Chicoine MR. Isolation and characterization of human malignant glioma cells from histologically normal brain. J Neurosurg 1997;86(3):525-531.

5. Fournier E, Passirani C, Montero-Menei C, Colin N, Breton P, Sagodira S, et al. Therapeutic effectiveness of novel 5-fluorouracil-loaded poly(methylidene malonate 2.1.2)-based microspheres on F98 glioma-bearing rats. Cancer 2003;97(11):2822-2829.

6. Menei P, Boisdron-Celle M, Croue A, Guy G, Benoit JP. Effect of stereotactic implantation of biodegradable 5-fluorouracil-loaded microspheres in healthy and C6 glioma-bearing rats. Neurosurgery 1996;39(1):117-123; discussion 123-114.

7. Menei P, Venier MC, Gamelin E, Saint-Andre JP, Hayek G, Jadaud E, et al. Local and sustained delivery of 5-fluorouracil from biodegradable microspheres for the radiosensitization of glioblastoma: a pilot study. Cancer 1999;86(2):325-330.

8. Menei P, Capelle L, Guyotat J, Fuentes S, Assaker R, Bataille B, et al. Local and sustained delivery of 5-fluorouracil from biodegradable microspheres for the radiosensitization of malignant glioma: a randomized phase II trial. Neurosurgery 2005;56(2):242-248; discussion 242-248.

9. Fournier E, Passirani C, Vonarbourg A, Lemaire L, Colin N, Sagodira S, et al. Therapeutic efficacy study of novel 5-FU-loaded PMM 2.1.2-based microspheres on C6 glioma. Int J Pharm 2003;268(1-2):31-35.

10. Fournier E, Passirani C, Colin N, Sagodira S, Menei P, Benoit JP, et al. The brain tissue response to biodegradable poly(methylidene malonate 2.1.2)-based microspheres in the rat. Biomaterials 2006;27(28):4963-4974.

11. Heurtault B, Saulnier P, Pech B, Proust JE, Benoit JP. A novel phase inversion-based process for the preparation of lipid nanocarriers. Pharm Res 2002;19(6):875-880.

12. Heurtault B, Saulnier P, Pech B, Venier-Julienne M-C, Proust J-E, Phan-Tan-Luu R, et al. The influence of lipid nanocapsule composition on their size distribution. Eur J Pharm Sci 2003;18(1):55-61.

13. Dulieu C, Bazile D. Influence of lipid nanocapsules composition on their aptness to freeze-drying. Pharm Res 2005;22(2):285-292.

14. Beduneau A, Saulnier P, Anton N, Hindre F, Passirani C, Rajerison H, et al. Pegylated nanocapsules produced by an organic solvent-free method: Evaluation of their stealth properties. Pharm Res 2006;23(9):2190-2199.

15. Lacoeuille F, Hindre F, Moal F, Roux J, Passirani C, Couturier O, et al. In vivo evaluation of lipid nanocapsules as a promising colloidal carrier for paclitaxel. Int J Pharm 2007;344(1-2):143-149.

16. Garcion E, Lamprecht A, Heurtault B, Paillard A, Aubert-Pouessel A, Denizot B, et al. A new generation of anticancer, drug-loaded, colloidal vectors reverses multidrug resistance in glioma and reduces tumor progression in rats. Mol Cancer Ther 2006;5(7):1710-1722.

17. Lamprecht A, Benoit J-P. Etoposide nanocarriers suppress glioma cell growth by intracellular drug delivery and simultaneous P-glycoprotein inhibition. J Control Release 2006;112(2):208-213.

18. Lacoeuille F, Garcion E, Benoit JP, Lamprecht A. Lipid nanocapsules for intracellular drug delivery of anticancer drugs. J Nanosci Nanotechnol 2007;7(12):4612-4617.

19. Malzert-Fréon A, Vrignaud S, Saulnier P, Lisowski V, Benoit JP, Rault S. Formulation of sustained release nanoparticles loaded with a tripentone, a new anticancer agent. Int J Pharm 2006;320(1-2):157-164.

20. Ballot S, Noiret N, Hindre? F, Denizot B, Garin E, Rajerison H, et al. 99mTc/188Re-labelled lipid nanocapsules as promising radiotracers for imaging and therapy: Formulation and biodistribution. Eur J Nucl Med Mol Imaging 2006;33(5):602-607.

21. Jestin E, Mougin-Degraef M, Faivre-Chauvet A, Remaud-Le Saec P, Hindre F, Benoit JP, et al. Radiolabeling and targeting of lipidic nanocapsules for applications in radioimmunotherapy. Q J Nucl Med Mol Imaging 2007;51(1):51-60.

22. Beduneau A, Saulnier P, Benoit JP. Active targeting of brain tumors using nanocarriers. Biomaterials 2007;28(33):4947-4967.

23. Hunt Bobo R, Laske DW, Akbasak A, Morrison PF, Dedrick RL, Oldfield EH. Convection-enhanced delivery of macromolecules in the brain. Proceedings of the National Academy of Sciences of the United States of America 1994;91(6):2076-2080.

24. Mamot C, Nguyen JB, Pourdehnad M, Hadaczek P, Saito R, Bringas JR, et al. Extensive distribution of liposomes in rodent brains and brain tumors following convection-enhanced delivery. J Neurooncol 2004;68(1):1-9.

25. Perlstein B, Ram Z, Daniels D, Ocherashvilli A, Roth Y, Margel S, et al. Convection-enhanced delivery of maghemite nanoparticles: Increased efficacy and MRI monitoring. Neuro Oncol 2008;10(2):153-161.

26. Inoue T, Yamashita Y, Nishihara M, Sugiyama S, Sonoda Y, Kumabe T, et al. Therapeutic efficacy of a polymeric micellar doxorubicin infused by convection-enhanced delivery against intracranial 9L brain tumor models. Neuro Oncol 2008:*In press*.

27. Li Y, Owusu A, Lehnert S. Treatment of intracranial rat glioma model with implant of radiosensitizer and biomodulator drug combined with external beam radiotherapy. Int J Radiat Oncol Biol Phys 2004;58(2):519-527.

28. Mevellec F, Roucoux A, Noiret N, Patin H, Tisato F, Bandoli G. Synthesis and characterization of the bis(trithioperoxybenzoate)(dithiobenzoate)rhenium(III) hetero complex. Inorganic Chemistry Communications 1999;2(6):230-233.

29. Vessieres A, Top S, Pigeon P, Hillard E, Boubeker L, Spera D, et al. Modification of the estrogenic properties of diphenols by the incorporation of ferrocene. Generation of antiproliferative effects in vitro. J Med Chem 2005;48(12):3937-3940.

30. Hillard E, Vessieres A, Thouin L, Jaouen G, Amatore C. Ferrocene-mediated proton-coupled electron transfer in a series of ferrocifen-type breast-cancer drug candidates. Angew Chem Int Ed 2006;45(2):285-290.

REVUE BIBLIOGRAPHIQUE

CONVECTION-ENHANCED DELIVERY OF NANOCARRIERS FOR THE TREATMENT OF BRAIN TUMORS

E. Allard[a], C. Passirani[a*] and J-P Benoit[a]

a: INSERM, U646, Université d'Angers, Angers, F-49100, France

*To whom correspondence should be addressed:

Tel: +33 241 735850;

Fax: +33 241 735853;

E-mail address: catherine.passirani@univ-angers.fr

Revue soumise à 'Advanced drug delivery review'

Abstract

Primary brain tumors have a significant infiltrative capacity as their reappearance after resection usually occurs within 2cm of the tumor margin. Local delivery method such as Convection-Enhanced Delivery (CED) has been introduced to avoid this recurrence by delivering active molecules via positive-pressure methods. For an efficient infusion, the distribution volume of the drug has to be optimized while avoiding backflow, since this is responsible for side effects and a reduction of therapeutic efficacy. The encapsulation of the drug infused in nanosized structures can be considered, which would lead to a reduction of both toxicity of the treatment and infusion time during CED. In the present review, we will firstly discuss the technical approach of CED with regard to catheter design and brain characteristics; secondly, we will describe the 'ideal' nanocarrier in terms of size, surface properties, and interaction with the extracellular matrix for optimal diffusion in the brain parenchyma. We also discuss pre-clinical and clinical applications of this new method.

Keywords: brain tumor, convection-enhanced delivery, backflow, distribution volume, nanocarrier, anticancer treatment, real-time imaging.

1. Introduction

The incidence of primary central nervous system tumors (PCNST) is increasing, especially in the younger population as it represents the second cause of cancer death in adults less than 35 years of age. In the United States, about 1-2% of the population is affected and consequently suffer from profound and progressive mortality, as evidenced from the 20,500 new brain cancer cases and the 12,740 deaths estimated in 2007 [1]. A French study has described an incidence of 15.8/100,000 persons per year affected by PCNST [2]. Among the brain tumors, half originate from glial cells and are thus classified as gliomas, and more than three quarters of all gliomas are astrocytomas. Astrocytomas constitute a heterogeneous group of tumors that range from low grade to the most aggressive, glioblastoma multiforme (GBM), based on histopathological classification (from grade I to IV WHO-Word Health Organisation). GBM differs from the other cancers by its diffuse invasion of the surrounding normal tissue and its recurrence after all forms of therapy. The overall incidence of malignant glioma grade III and IV (WHO) in industrialised nations is 5-11 new cases per 100,000 people per year [3].

Conventional therapy includes surgical biopsy for pathological diagnosis and if it is possible, the first treatment is tumor resection, followed by fractioned external beam radiotherapy and systemic or oral chemotherapy [4-6]. Despite these treatments, the prognosis for patients with glioblastoma has remained largely unchanged over the last three decades. Stupp *et al.* described a median survival time of 14.6 months for patients treated with radiotherapy plus temozolomide which is the reference chemotherapy, and 12.1 months with radiotherapy alone [7, 8]. The difficulty with treating brain tumors is the effective delivery of therapeutic agent to the tumor as well as to infiltrate cells that are not located in the tumor bed. If these outlying tissues are not treated, the tumor will reappear.

Because of the presence of the blood brain barrier (BBB), the failure of conventional systemic drug delivery for gliomas has motivated more direct approaches [9-11]. An alternative treatment is the local administration of the agent from a degradable or non-degradable polymer delivery system implanted at the site of the disease [12, 13]. Although this technique

presents some advantages such as sustained and controlled drug release, it is also characterized by poor drug penetration and drug dosage limited by the implant size.

Recently, it was shown that fluid convection, established by maintaining a pressure gradient during interstitial infusion, can supplement simple diffusion to enhance the distribution of small and large molecules in brain and tumor tissue. This technique called Convection-Enhanced Delivery (CED) was proposed and introduced by researchers from the US National Institutes of Health (NIH) by the early 1990s to deliver drugs that would not cross the BBB and that would be too large to diffuse effectively over required distances [14]. In this case, *in situ* drug concentrations can be significantly greater than those achieved by systemic administration [15, 16]. This technique allows the local delivery of a wide range of substances like conventional chemotherapeutic agents [17-19], monoclonal antibodies [20, 21], targeted toxins [22-24], other proteins [25], viruses [26, 27], and nanocarriers [28-30]. During the first decade after the NIH researchers founded this analytical model of drug distribution, the results of several computer simulations that had been conducted according to realistic suppositions were also published, revealing encouraging results [31].

For the effective functioning of CED, the activity of the anticancer agent has to be considered but the technical drug delivery approach appears to be a critical parameter. In fact, a uniform distribution of a truly effective agent in tumors will ultimately influence the therapeutic efficacy. This is the reason why experimental protocols have to take care of different parameters proper to CED injection.

Moreover, properties of each infusate have to be considered. Nanocarriers like polymer and lipid nanoparticles, micelles, liposomes, and dendrimers are often used to vehicle some drugs that are very sensitive, toxic, or hydrophobic, or in order to target a specific organ [32]. Such nanoparticulate systems have some inner properties that have to be considered for optimal convection delivery. This review aims at firstly discussing, the technical approach of CED with regard to the materials used and the model investigated. Then the review will focus on specific properties of the infusate limiting our discussion to the use of non-viral nanocarriers such as liposomes, nanoparticles, dendrimers and micelles. Finally, animal and human trials which deliver nanocarriers in CED for therapeutic applications will be explored.

2. Technical approach of CED

2.1. CED Mechanism

Convection-enhanced delivery (CED) is a novel approach to deliver drugs into brain tissue and is defined as the continuous injection of a therapeutic fluid agent under positive pressure. This recent technique using convection or 'bulk flow' was proposed to supplement simple diffusion which characterizes local intracerebral delivery by stereotactic injections (Figure 1). Stereotaxy is the methodology involved in the three-dimensional localization of structures within the brain, based on diagnostic image information, and the use of stereotactic frame to reach these points. Horsley and Clarke described the first use of an apparatus for neurophysiological animal experiments in 1906 and named their technique 'stereotactic' (Greek: stereo = three dimensional (3D), taxis = to move toward) [33]. The first human stereotactic apparatus was described 40 years later by Spiegel and Wycis [34]. A stereotactic head frame is based on a 3D coordinate system consisting of three orthogonal planes, which are related to external skull points. Stereotaxy can be used to approach deep-seated brain lesions with a probe, a cannula or a high energy ionizing radiation beam [35].

Diffusion is defined as a type of passive transport (non-energy requiring) involving the movement of small molecules from an area where they are highly concentrated to an area where they are less concentrated. The diffusion of a compound in a given tissue depends mainly on 2 parameters: the free concentration gradient and the diffusivity of this compound in the tissue. With the classic diffusion technique, high molecular weight compounds (neurotrophic factors, antibodies, growth factors, enzymes) are not able to diffuse over large distances and drug distribution is very limited, thus reducing the treatment efficacy of neurological disorders [36]. For example, 3 days can be necessary for an IgG to diffuse 1mm from its delivery site. Moreover, small drugs with good diffusion characteristics can be metabolized or quickly eliminated by capillaries reducing their diffusion in surrounding tissues [37, 38]. On the contrary, CED is powered by bulk flow kinetics which occur secondary to pressure gradients. Convection, which can be used to supplement diffusion, relies on a simple pressure gradient, and is independent of molecular weight. In practice, drugs are delivered continuously via a catheter connected to a syringe pump, thus enabling the

distribution of large volumes of high drug concentrations with minimum systemic toxicity (Figure 1).

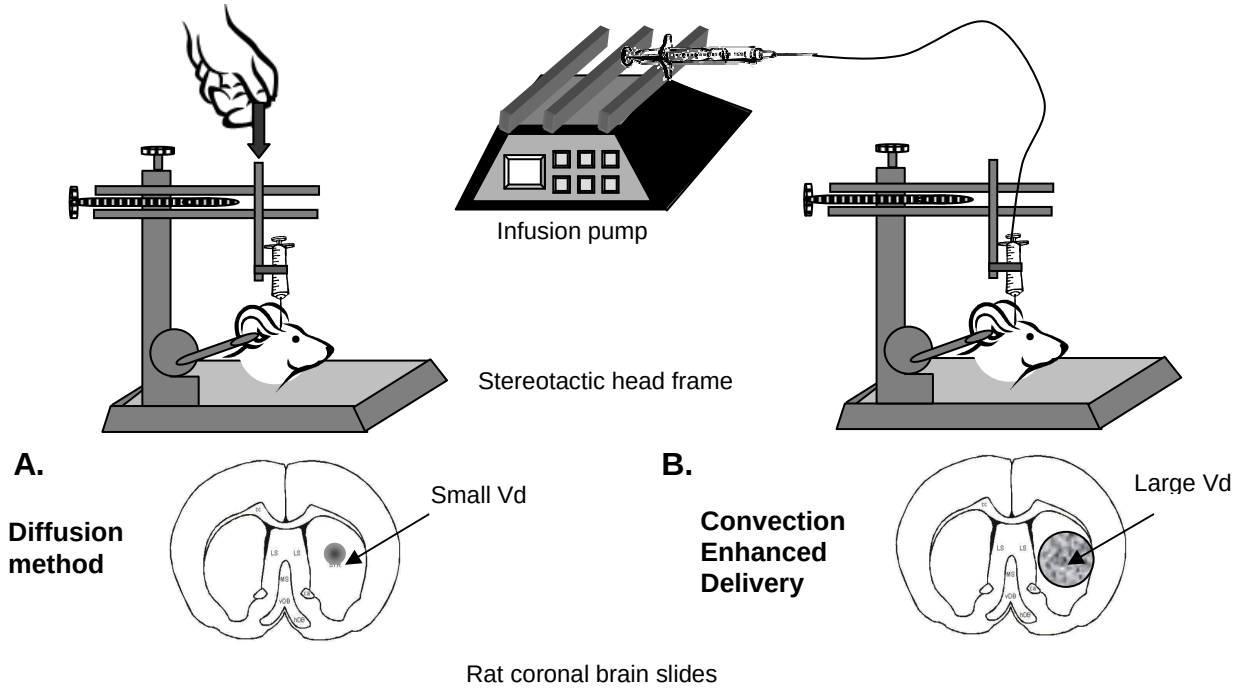

Figure 1: Stereotactic injection in rat brain by classic diffusion method (**A**) versus convection enhanced delivery (**B**). Infusate diffusivity is predominant in CED techniques as large volume of distribution (Vd) can be achieved compared to those obtained after a classic diffusion method.

During CED, backflow, diffusion and convection take place simultaneously (Figure 2). In fact, before the elaboration of a pressure gradient, the phenomenon of backflow (or leakage-leakback) occurs along the cannula. This backflow is defined as a more or less voluminous return of the infusate along the catheter, in a space localized between the external surface of the cannula and the brain environment [39]. Leakback has two main but different causes. First, it can be due to the cannula's introduction into the brain which forms a local injury thus creating a local 'empty' space allowing backflow. Moreover, leakback can also be explained by a more intrinsic property: hydrostatic pressure associated with the injection pushes back the tissues allowing a local detachment from the needle. This backflow can be minimized as detailed below. The second phenomenon is the diffusion and this is strictly dependent on a concentration gradient on the one hand and on the diffusivity of the infusate in a specific tissue on the other hand. Diffusion occurs all the time, but is rigorously dependent on the nature of the infusate. Finally, the agent is distributed within the interstitial spaces of the

tissue by convection itself. The bulk flow, which is strictly dependent on the pressure gradient, occurs throughout the establishment of the pressure gradient. With regard to the shape of drug distribution, the diffusion process leads to a gradient of concentration which decreases exponentially from the point of injection towards surrounding tissues. The convection process allows the obtention of a higher concentration over a longer distance (with reference to the point of injection); the concentration profile is constant during infusion and decreases in an abrupt way at the end of the process (Figure 2). By using convection to supplement simple diffusion, an enhanced distribution of small and large molecules can be obtained in the brain while achieving drug concentration greater than systemic levels [14]. High-flow microinfusion, like the CED technique, offers the potential of treating much larger volumes of brain tissue than is possible with low-flow delivery methods based on diffusion. Morrison *et al.* showed that a 12-h high-flow microinfusion of a designed macromolecule would provide 5 to 10-fold increases in volume over low-flow infusion, and provided total treatment volumes superior to $10cm^3$ [40].

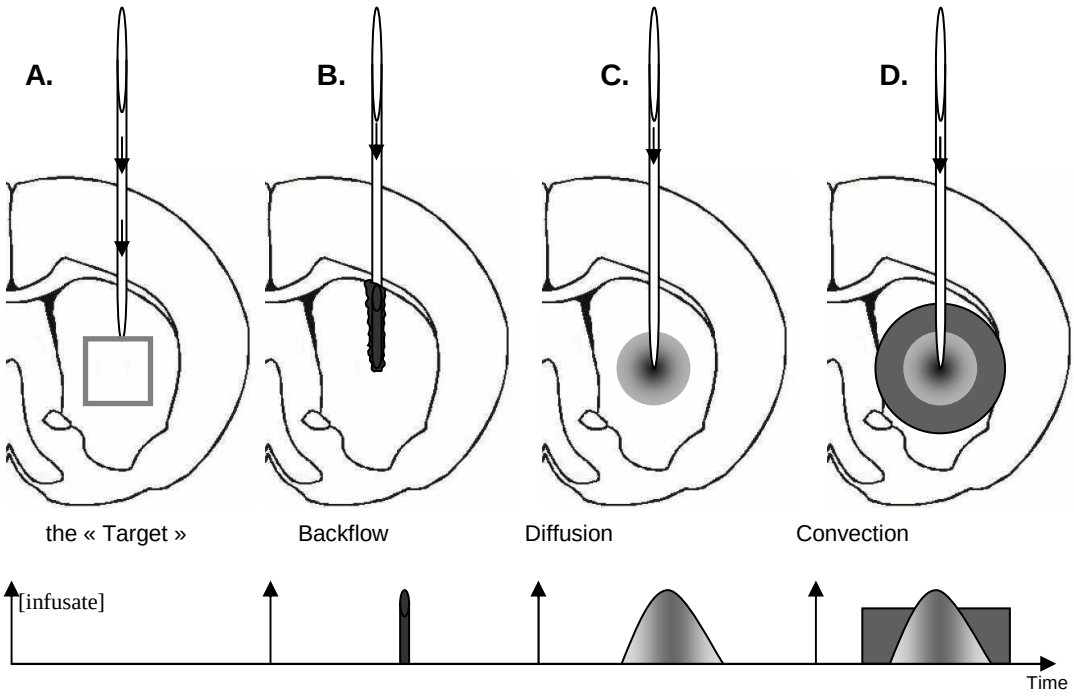

Figure 2: Schematic representation of CED mechanism. A: identification of the target site with correct placement of the catheter according to specific coordinates. B: Backflow (or leakage-leakback) is defined like an upturn of the infusate along the catheter, in a space localised between the external surface of the cannula and the brain environment and takes place before the elaboration of a pressure gradient C: Diffusion occurs all the time but is rigorously dependent of the infusate nature. D: Convection (or bulk flow) is strictly dependent on the pressure gradient and occurs during all the establishment of the pressure gradient.

Some experimental approaches can be considered to follow the distribution of an infusate in a brain structure. Chen *et al.* compared the distribution and pressure profiles obtained after CED of small molecular weight infusates (Mw = 570-700) in pig animal models on the one hand, and in low-concentration agarose gels used as experimental models on the other hand [41]. Even though agarose gels are inert, non-perfused, homogeneous and isotropic, the ratios between distribution volumes (Vd) and infusate volumes (Vi) were in the same range of order and equivalent to 10 and 7.1 for 0.6% agarose gel and pig brain, respectively. In addition, the infusion pressure of the gel at this concentration was typically close to that found in pig brain (10-20mm Hg). They concluded that a 0.6% agarose gel was a useful *in vitro* model to mimic the global behavior of real infusion in pig brains, especially when MR imaging was not available. Linninger *et al.* went further and introduced an innovative mathematical method to calculate the impact of individual tissue properties on molecular transport in CED [31]. This computer-aided methodology allows the reconstruction of the brain geometry for a specific patient, and gives an estimation of heterogeneous anisotropic transport properties by diffusion tensor imaging (DTI) data. Finally, this technique can predict the drug distribution based on rigorous transport principles.

2.2. The key parameters

CED is a complex process that is governed by many parameters. This review aimed at listing the technical parameters directly linked to delivery by convection and especially to the volume of distribution (Vd), and the control of the backflow mechanism.

2.2.1. Regions of the brain

The different regions of the brain are not equivalent in terms of molecular transport mechanism because of a distinct internal structure. Gray matter is mainly composed of the somas of neurons and glial cells. The effective diffusivity in gray matter is almost the same in all directions, and the transport in the gray matter is qualified as isotropic (Figure 3). White matter contains bundles of axons leading to the peripheral nervous system. The permeability of the white matter changes in accordance with directional alignment and density of axonal fibers. Hence, white matter diffusion is anisotropic. A wide spread of agents can be achieved

in both white and gray matter, but white matter exhibits a greater ability to accommodate infusate because it is more densely packed and there is less extracellular space [14, 42, 43]. Because rat brains have very limited white matter in their structure, this parameter would be better studied in larger animal models like primates, dogs and of course, in humans.

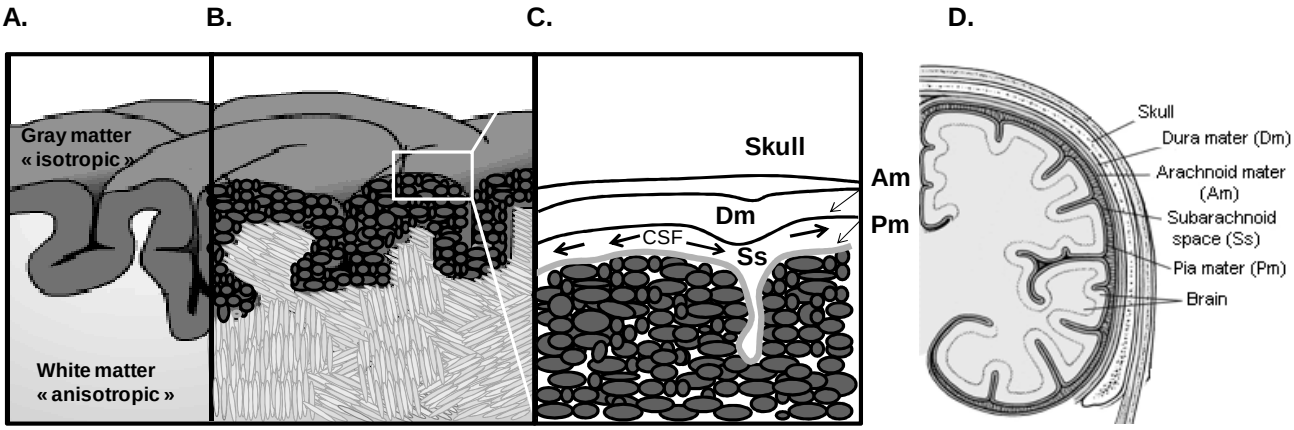

Figure 3: Schematic representation of grey and white matter in human brain **(A**). Gray matter is mainly composed by the somas of neurons and glial cells and the transport in the gray matter is qualified of isotropic (**B**). White matter contains bundles of axons leading to the peripheral nervous system and the diffusion in white matter is qualified of anisotropic. **C** (zoom of picture B): Caused by backflow, the active infused by CED can be melt with circulating cerebrospinal fluid (CSF) in the subarachnoid space (Ss). **D**: Representation of a section across the top of the skull, showing the membranes and the cavity of the human brain including Dura mater (Dm), Arachnoid mater (Am), Subarachnoid space (Ss) and Pia matter (Pm).

Moreover, most studies defining CED parameters have been carried out on normal brain tissue and not in a tumor environment. Vavra *et al.* showed that distribution in a brain tumor model was a parameter not to be ignored since interstitial fluid pressure is higher in intracranial tumors [15] and may be responsible for the asymmetric distribution of drugs in glioma-bearing rats. Moreover, the presence of oedemas, often observed in brain cancer, can reduce the flow of the infused agent. When infused into a tumor, which means into tissue where the hydraulic conductivity and extracellular fraction may change radically, liposomes are characterized by an irregular distribution with the presence of nanocarriers into the encapsulated tumor margins [44]. Globally, there is a lack of knowledge about the distribution of infusate in the brain tumor environment.

2.2.2. Catheter placement

Catheter placement is very important for several reasons and especially for preventing the occurrence of backflow. Backflow can lead to the spreading of the agent into regions of the brain where it is not intended to be and, possibly, to a diminution of the dose otherwise needed within the target tissues. The problem can be particularly acute in cortical infusions, when backflow of the agent along the insertion track and into the subarachnoid space can occur, with the subsequent widespread distribution of the agent via the circulating cerebrospinal fluid (CSF) (Figure 3). Raghavan *et al.* described an example which illustrates the leakage of an infused agent into the subarachnoid space via backflow into the catheter during the infusion. A 0.85mm-diameter catheter was inserted through a bur hole into an *in vivo* pig brain to a depth of 14mm from the cortical surface. A Gd-DTPA in water solution (1:200) was infused at 5 ml/minute and three dimensional MR images were obtained to analyze the dispersion of the Gd marker. Images obtained after 32 minutes of infusion showed evidence that the infused agent had mostly leaked into the subarachnoid space and was widely dispersed along the contours of the cortex, whereas little distribution into the white matter had occurred [45]. Lidar *et al.* described this phenomenon with the infusion of Taxol® in patients with GBM. Leakage of the drug into the CSF was described because of a bad catheter location, and was responsible for side effects such as chemical meningitis [17]. Catheter location is therefore highly important as it can cause complications.

Catheter placement also depends on the Vd of a studied infusate. Linninger *et al.* ask the question: “which injection site is best for maximising the drug distribution in a specific target site without causing side effects and excessive tissue stress damage?” To answer this, they aimed at targeting the human caudate nucleus (gray matter), and studied the final Vd at 4 weeks, for four different catheter locations: the thalamus, the corpus callosum, the internal capsule and the putamen, and for an infusion flow rate of 4µL/min (Figure 4) [31]. Results showed that injections via the gray matter (thalamus injection) yielded to a Vd of 80% in the caudate nucleus because of the relatively short distance between the injection site and the target and because of an isotropic uniform structure. On the contrary, injections via white matter tracts (the corpus callosum and the internal capsule) impregnated the caudate at 72 and 60%, respectively. When injecting into anisotropic media, the infusate travels long distances

due to the higher permeability along white matter tracts, resulting in more infusate loss and consequently, less quantity available for diffusion into the target.

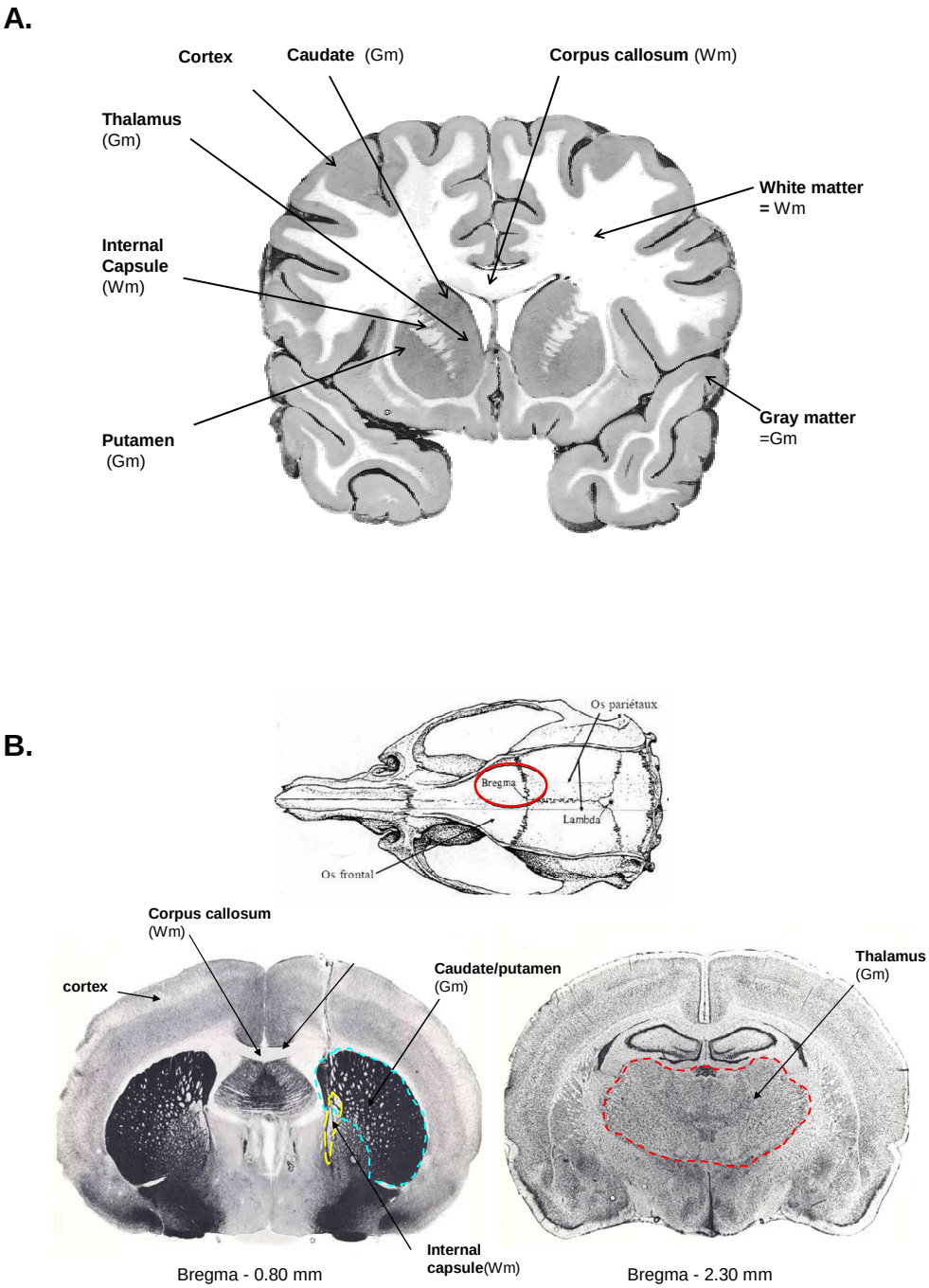

Figure 4: Coronal brain section identifying the location of gray (Gm) and white matter (Wm) in humans (A) and in rats (B).

Although while white matter targets were required to achieve high Vd levels, it was not recommended to place the catheter in an anisotropic structure if the target was not located at the cannula place. Finally, although it was qualified as a gray-matter structure, putamen injections were worst because the studied target received only 10% of the initial drug. This can be explained by the larger distance between the two structures and the presence of white fibers between them.

2.2.3. Rate of infusion - Catheter size

The pressure gradient, which generates the convective movement, is equal to the difference between the skull pressure and the injection pressure. The flow of injection is thus a critical parameter to create convection, and it is known that it is related to the resistance of the considered tissues (gray and white matter). Finding an optimal infusion rate for CED has been elusive because it is often limited by the development of backflow along the cannula track. In most cases, the optimal infusion rate is that which allows the delivery of the therapeutic volume over the least amount of time without any associated reflux. This optimum is also dependent on the cannula size used. In general, the higher the infusion rate and catheter diameter used, the greater the reflux induced.

To obtain effective convection in rodent models, the injection flow must be in the range of 0.5 to 5µl/min [14, 40]. Indeed, weaker flows limit the extent of the distribution volume, whereas too high a flow facilitates backflow. In addition, the use of superior flow levels is not recommended as the generated hydrostatic pressure can damage the tissues [46]. Consequently, the use of a 0.5µl/min rate of infusion is often described to carry out effective CED in rodents [19, 27, 43, 47]. Kroll *et al.* underlines that the infusion rate has to be adjusted according to the model used [48]. When they attempted to establish a rat infusion rate of 4µL/min as reported by Bobo *et al.* in their study in cats [14], leakage up and out of the catheter occurred. Whereas injections took place in white matter for cats, the organisation of the fibers in rat gray matter was characterized by increased resistance, inducing backflow.

In addition, the larger the catheter diameter, the greater the tissue resistivity and reflux induction. Chen *et al.* showed that leakback associated with the smallest cannula (32 gauge) was significantly smaller than that associated with the two larger cannulae: 28 and 22 gauge

[49]. An increase in cannula diameter facilitates the formation of a low-resistance pathway that follows the surface contours of the cannula. Bauman *et al.* demonstrated that, at a fixed flow rate, the backflow distance varies as the four-fifths time of the outer diameter (OD) of the catheter [50].

Moreover, volumetric inflow rates associated with catheter diameter must be carefully chosen to avoid loss or bad distribution associated with backflows that reach the outer boundaries of the target structure. In some studies using low infusion rates, the infusate is almost entirely contained in the target (striatum) whereas at rates ten times higher, there is significantly more infusate outside the target [39, 49]. For example, with a 32-gauge catheter, confinement of the infusate in the rat caudate (radius of 0.22 cm) requires a flow rate not greater than 0.5µl/min. In fact, at this infusion rate, the backflow distance is equivalent to 0.2cm whereas it is near 0.8cm for an infusion rate of 5µl/min. Moreover, for a 22-gauge catheter, the backflow distance increases from 0.5 to 2cm for flow rates equivalent to 0.5µl/min and 5µl/min, respectively [39]. The significance of these observations is that the selection of a too high a flow rate into a gray matter target will lead to diminished delivery and internal leakage to nearby white matter regions and perhaps to external leakage as well.

Others studies performed in human brains showed that for a fixed infusate flow rate, the smaller the catheter used, the greater the volume of distribution, due to higher velocities at the tip [31]. Recent clinical trials using high infusion flow rates (3.3µL/min) and large catheters (1.4 and 2.5 mm OD) described MRI signal changes in the catheter track after infusion in patients due to reflux [51]. We can say, however, that as the volume of brain structure is larger in humans, there is a much higher flexibility concerning the infusion rates employed. Recently, experimentators have increased the infusion rate to 5µL/min without any reflux thanks to the use of an innovative cannula design [46].

2.2.4. Catheter design

The use of a reflux-free cannula in order to enhance the infusion rate of therapeutic agents by CED has been described, thus reducing the duration of treatment and, by the way, the exposure of patients to high risk of infection or side effects [46]. The design used in this study

consisted of a 27-gauge cannula needle with glued-in fused silica tubing attached to the CED infusion system. This catheter allowed the delivery of infusate (0.4%Trypan blue solution) at a flow rate of 50µl/min without any reflux in agarose gel, and rodent and non-human primate brains. But, if there was no leakage, high levels of induced tissue damage appeared in animal models when infusion rates were above 10µl/min.

Multiple-hole catheters are cannulae with 5-6 holes of a few millimeters (outer diameter) on each side, separated at short distances. Studies have shown that the use of this type of catheters leads to high volumes of distribution due to the distributed arrangement of outlet ports [31]. On the contrary, by studying the impact of Vd and pressure profiles with different kinds of neurocatheters, Bauman *et al.* showed a lack of flow predictability when using multiport catheters [50]. They concluded that the simplest solution was to use catheters with a single end port because thin-walled infusion catheters mimic a point source and produce repeatable and spherical symmetric volume of distribution of the infusate within the brain material. Larger catheters or those with air trapped inside produce irregularly-shaped volumes of distribution and can exhibit complex pressure profiles during use. In addition, Kunwar *et al.* underlines the importance of priming the cannula before insertion into brain. This manipulation prevents air bubbles occurring at the end of the catheter tip which can significantly affect distribution and increase the probability of backflow [52].
Sealing the burr hole with bone wax during CED is also of interests. Firstly, it can prevent efflux of the drug used for glioma chemotherapy. For instance, due to an efflux of paclitaxel out of the cranium, some patients developed side effects like severe skin necrosis [53]. Moreover, the effect of sealing the burr hole may increase the volume of distribution (Vd) because sealing might increase the pressure opposing the outflowing fluid which equals the atmospheric pressure when the burr hole is unsealed. Finally, the bone wax can be used to fix the catheters avoiding movement that can create more disruption in the tissue and consequently, exacerbate leakage.

2.2.5. Brain ECM dilatation

The brain's extra cellular matrix (ECM) is the conduit through which drugs and drug delivery nanovectors must diffuse after crossing the BBB or after direct brain administration by CED. If the surface of this brain ECM can be enhanced, the volume of distribution may be

increased. Neeves *et al.* speculated that, like osmotic and hydraulic dilation, enzymatic degradation of the brain ECM could enhance the distribution of nanometric objects [54]. To investigate the hydraulic dilation hypothesis, they injected PBS prior to nanoparticle infusion (30 min before) and they showed that the distribution volume was more than twice as large as the distribution volume of the control group treated by NP in PBS. However, it was difficult to compare these two results as the total infused volume was twice as high for the rats which underwent hydraulic dilation. Furthermore, degradation of hyaluronic acid by the co-administration of hyaluronidase at 20,000U/ml-30 min. before the injection of NP resulted in a 58% increase in the distribution volume of nanoparticles. These results had to be taken with care as the consequences of a hyaluronan depletion are not clearly known and especially in a contact with brain tumor. These results showed that both enzymatic treatment and dilatation of the extracellular space could significantly enhance the transport of nano-objects.

2.2.6. Heart rate enhancement

In order to increase the distribution volume, it should be possible to enhance brain fluid circulation by enhancing the level of this circulation. Hadaczek *et al.* hypothesized that infusate distribution is caused by brain fluid circulation which is itself generated by arterial pulsations [55]. They evaluated the Vd of 7.2nm bovine serum albumin (BSA), 65nm-fluorescent liposomes and 25nm-adeno-associated virus 2 (AAV2) in rat striata. Rats were randomized in three groups: group H with high blood pressures and heart rates induced by epinephrine, group L with low blood pressure and heart rate induced by blood withdrawal, and group N with no heart action. They found first, that whatever the nature of the infusate, the Vd was significantly higher for group H compared to group L and group N. Within this group, the distribution of liposomes - which were even larger than AAV2 particles - was comparable to that of BSA which means that the diffusion was not size-dependent. The affinity of AAV2 particles for their cellular receptor heparin sulphate proteoglycan was very high and can explain their lower diffusion levels as these receptors are found in all neurons. This conclusion was correlated to the study of Nguyen *et al.* who used heparin-like co-infusate to saturate receptors and in this way, to enhance the distribution of AAV2 particles [27].

2.2.7. Volume and nature of the infusate

Vd determination in CED is a complex process which includes the intervention of many parameters. However, when infusions are performed into regions of interest with adequate materials, the Vd is characterized by a direct linear relationship with Vi which represents the volume infused. This information has been checked in different species such as cats [14], rats [56], pigs [41], dogs [57], non-human primates [43, 58], and humans [59, 60]. The relationship between Vi and Vd is linear, but the ratio Vd/Vi is dependent on structural properties of the tissue on the one hand, and characteristics of the infusate on the other hand. Heavy molecules like trophic factors or proteins diffuse more slowly than small molecules such as sucrose. For example, the volume of distribution (Vd) increased linearly with the infusion volume (Vi) in the proportions of 6:1 (Vd/Vi) for ^{111}Indium-labelled transferrin (^{111}In-Tf; Mw= 80,000) and in the proportion of 13:1 for [^{14}C] sucrose (Mw=359) [14]. The same conclusions were made by comparing the infusions of Evans blue (Mw=960) with blue dextran (Mw=2,000 000) [61].

In a word, the diffusivity of a defined infusate is dependent on technical parameters inherent to cannula type/position, brain structure, and infusate rate/volume; the different examples are summarized in Table 1. Diffusivity is also dependent on the nature of the materials infused; the physicochemical properties of each infusate have to be considered in order to optimize the diffusivity, especially when infusates are colloidal systems.

Parameters		Description	Vd	Backflow	Ref
Brain geography	White matter	High conductivity	+++		[14, 42, 43]
	Gray matter	Low conductivity	++		[48]
	Tumor tissue	Modified conductivity	+		[15, 44, 90]
Catheter placement	Location	Bad insertion	+	+++	[17, 45]
	Distance to target	Large distance	+	+++	[31]
	Distance to target	Short distance	+++	+	[31]
Catheter size	Large	< 28 gauge	+	+++	[48, 49]
	Small	≥ 32 gauge	+++	+	[48]
Infusion rate	High	2 - 5µl/min (rodents)	+	+++	[39, 51]
	Low	≤ 0.5µl/min (rodents)	++	+	[19, 27, 47]
Catheter design	Reflux-free	Glued-in fused silica tubing	+++	+	[46]
	Multiple hole	Irregularly shaped Vd	+		[31, 50]
	Single end port	Spherical distribution	+++		[50]
	Bone wax fixed	Increased pressure	+++	+	[53]
	Primed cannula	To prevent air bubbles	+++		[52]
Infusion Volume	Increased Vi	Linear relationship Vd/ Vi	+++		[14, 61]

Table 1: Technical parameters relevant to effective convection-enhanced delivery (CED) and their impact on distribution volume (Vd) and occurrence of backflow. Vd and backflow are qualified as high (+++), moderate (++) or low (+). Vd: distribution volume, Vi: infusate volume

3. The CED of nanocarriers

Nanocarriers are constructed systems that are measured in nanometer size (nm) and that can carry multiple drugs [62], radionuclides [63] and/or imaging agents [64, 65]. Nanomaterials for drug delivery include various architectural designs in terms of size, shape and materials. The characteristics of each nanocarrier differ in structure composition, drug-loading capacity, ability to encapsulate hydrophobic or hydrophilic molecules, carrier stability and targeting possibility. The nanocarrier family includes mainly polymeric or lipid-based carriers such as liposomes, nanoparticles (including nanospheres and nanocapsules), micelles, and dendrimers (Figure 5).

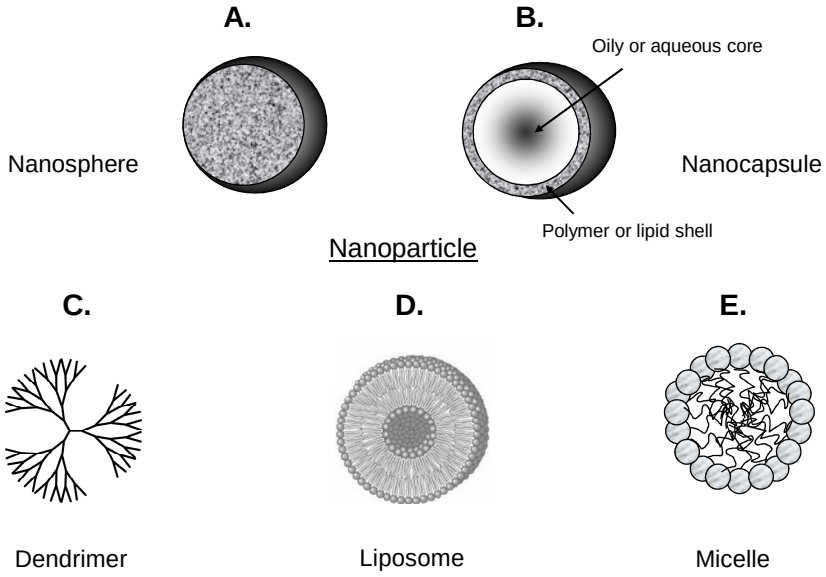

Figure 5: Schematic structure of nanoparticules including nanospheres (A) and nanocapsules (B), dendrimers (C), liposomes (D) and micelles (E) for drug delivery.

With drug delivery, the pharmacokinetic properties of the drug will no longer depend on the properties of the active molecule but on the physicochemical properties of the carrier. Thus, nanoencapsulation offers many advantages such as the protection of sensitive active molecules against *in vivo* degradation, the reduction of toxic side effects which can occur when drugs are administered in solution, better drug pharmacokinetic behavior, and an increase in patient comfort. Thanks to the possibility of grafting specific ligands to their surface, nanocarriers can recognize specific targets [66]. Nanoparticles can also bypass multidrug resistance (MDR) mechanisms by inhibiting efflux pumps such as P-glycoprotein (P-gp), and optimizing the bioavailability of anticancer agents [67-69].

After CED injection, nanocarriers have to diffuse themselves in extra cellular brain conduits. Consequently, the size of these nanocarriers appears to be a critical parameter for the delivery of drugs into the brain. Nanocarriers that have already been injected by CED are liposomes [44], nanoparticles [29, 47], dendrimers [30] and polymeric micelles [70]. Liposomes are artificial phospholipid vesicles varying in size from 50 to 1,000nm and even more, which can be loaded with small therapeutic agents including drugs and genes, and have been considered

as promising drug carriers since over three decades. Hydrophilic drugs can be readily entrapped within the aqueous interior of the vesicles, and neutral and hydrophobic molecules can be carried within the hydrophobic bilayers of the vesicles. Liposomes can provide stable encapsulation and the delivery of a number of potent anticancer drugs [71, 72]. Nanoparticles are defined as solid colloidal particles ranging in size from 10 to 1,000nm. They consist of macromolecular materials or lipids in which the active principle (drug or biologically-active material) is dissolved, entrapped, encapsulated and/or to which the active principle is adsorbed or attached [73, 74]. They are constituted in general from biodegradable and non-biodegradable polymers, or from lipids. They can be classified into two groups according to their inner structure, namely nanospheres and nanocapsules [75, 76]. Dendrimers are spherical, highly-branched polymers with a hierarchical three-dimensional structure [77]. They look treelike in their molecular architecture since they are built from repetitive monomers with branching point units that are radially connected around a template core [78]. Polymeric micelles are supramolecular assemblies of amphiphilic block copolymers with a core-shell structure which maintains physical properties characteristic of conventional micelles, but with enhanced thermodynamic stability [79]. All these nanocarriers, when administered by CED, have a double application: firstly, they can be used as a tracer to monitor the infusion; secondly, they can be loaded with antineoplasic agents for an anticancer therapy approach.

3.1. Nanocarrier labelling

Nanocarriers can be labelled by incorporating a marker in the liposomal/nanoparticle membrane and/or can be loaded by encapsulating of a marker within their interior part (Figure 6). Such applications involve the use of histological [80] or fluorescent markers [81, 82], radiotracers [83-86], and MRI contrast agents [87, 88].

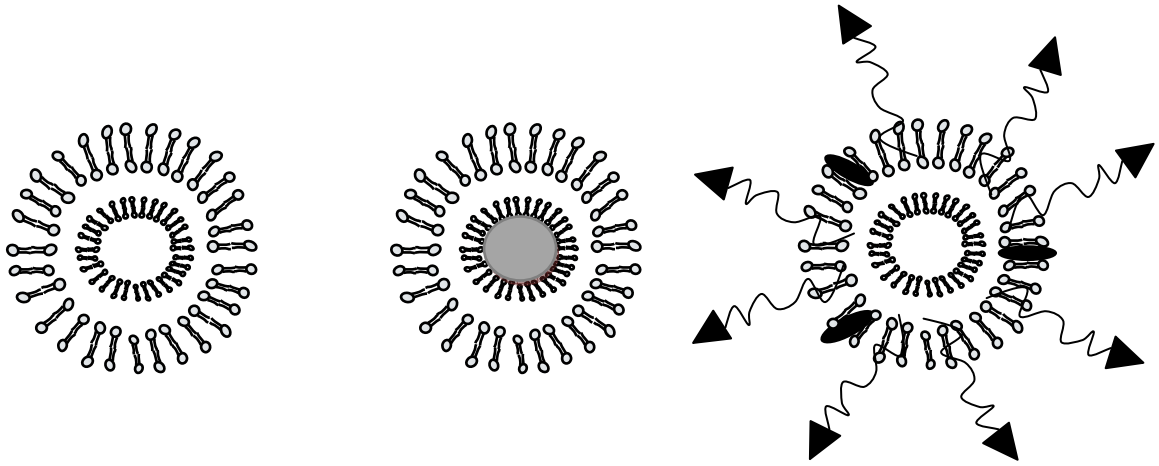

Figure 6: Schematic representation of a blank liposome (A), a loaded liposome (B) and a labelled liposome (C). Loading implies an encapsulation of the marker in the aqueous part of the liposome, whereas labelling means grafting or inclosing the marker in the shell structure.

3.1.1. Histological marker

For a histological analysis of liposome diffusion, liposomes can be loaded via gold particles which are histological markers that can be visualized in tissue sections [89]. Mamot *et al.* described a distribution study using liposomes loaded with colloidal gold in the core and also labelled with a hydrophobic fluorescent indicator DiI-DS (1.1'-dioctadecyl-3,3,3',3'-tetramethylindocarbocyanine-5,5'-disulfonic acid - Molecular Probes) which is a fluorescent, stable lipid that can be incorporated into liposomal membranes [90]. Results showed comparable distribution patterns for the two markers, excluding the possibility of a distribution linked to fluorescent or colometric marker released from the liposomes. With the same idea, Prussian blue staining was performed to demonstrate the micro-distribution of maghemite nanoparticles (Fe_2O_3-MNP) infused by CED in rat striatum. With this marker, it was possible to visualize the nanoparticle either intracellularly or adjacent to the cell surface [29].

3.1.2. Fluorescent labelling

In rodents, studies showed excellent distribution of liposomes containing fluorescent dyes after CED into normal striatum, as well as into implanted brain tumor xenografts. Liposomes

can be labelled and loaded with two kinds of fluorescent marker in order to track diffusion io of the vector in rodent brains [90, 91]. Liposomes were labelled with Dil-DS and loaded with water-soluble rhodamine B disulfonate in the aqueous part [92]. The distribution of these liposomes injected into the CNS was evaluated with comparable results with the two types of marker. This validated the fact that these two markers characterized the distribution of the liposome itself since the distribution volumes of free DiI-DS and free rhodamine occur in very different proportions. In fact, the distribution of free DiI-DS was largely reduced, equivalent to 23% of the liposomal Dil-DS because of a tendency towards aggregation and membrane interactions. On the contrary, the injection of free rhodamine was much greater (+220%) than rhodamine encapsulated in liposome because of an easier diffusion of this small water-soluble compound. These findings confirm the importance of considering the tissue affinity of the infusate when delivering therapeutic agents locally into the brain.

3.1.3. Radiomarkers

Liposomes can be formulated using radiolabelled lipids such as iodinated benzamidine phospholipids (^{125}I-BPE) [93] and cholesteryl hexadecyl ether (^{3}H-Chol). ^{3}H-Chol liposome infused by CED with an increased flow rate from 0.1 to 0.8µL/min, remained in the brain for at least 2 days without the loss of a signal whereas ^{125}I-BPE liposomes rapidly lost their signal in the brain with a 10h half-life. This double radiolabelling indicates that liposome components remained in the brain but underwent degradation [84].

Our research team focuses on the use of lipid nanocapsules (LNC) which are formulated without the use of organic solvents and are characterized by a core shell structure which is a hybrid between polymer nanoparticles and liposomes [94]. These nanocarriers can be loaded in their hydrophobic core with a lipophilic complex [$R(S_3CPh)_2(S_2CPh)$ = (R-SSS)] which can be prepared with either technetium (^{99m}Tc) or rhenium (^{188}Re), providing good stability for labelling [83]. Moreover, ^{188}Re-SSS LNC were obtained with a very high labelling yield and allowed the determination of the brain residence time of Rhenium-188 (Brain $T_{1/2}$) after CED administration [47]. LNC can also be labelled in their shells after the post-insertion of amphiphilic constructs like ^{111}In-labelling DSPE-PEG-DTPA or ^{125}I-DSPE-PEG-Bolton Hunter [95].

3.1.4. MRI markers

To perform magnetic resonance imaging (MRI), nanocarriers can be loaded with contrast agents. These molecules are able to modify the longitudinal (T1) and transverse (T2) relaxation times. The ability of a contrast agent to shorten T1 and T2 is defined as the relaxivity, r_1 or r_2, respectively. In general, there are two classes of MR contrast agents. On the one hand, there are agents that have a low r_2/r_1 ratio and therefore generate positive contrast in T1-weighted images. These positive contrast agents usually are paramagnetic complexes of Gd^{3+}or Mn^{2+} ions [96, 97]. On the other hand, there are superparamagnetic contrast agents with a high r_2/r_1 ratio, which cause dark spots in T2- and T2*-weighted images and are therefore referred to negative contrast agents. These contrast agents are usually based on iron oxide particles [98, 99]. The two kinds of MR contrast agents were encapsulated in nanocarriers for CED injection. As liposomes can be loaded with hydrophilic molecules, it was possible to formulate liposomes containing paramagnetic agent such as Gadoteridol, a chelated gadolinium (Gd). Saito *et al.* established a method for using MRI to monitor the CED of liposomes in the brain in real time [100]. They concluded that, although histological methods are much more sensitive, MRI monitoring provide distribution patterns with precise information and in real time. With this technique, they were able to see the difference between the invasive properties of two tumor models in rats such as the C6 and the 9L-2 glioma models. In a word, MRI appears to be a real-time imaging technique to track the brain delivery of liposomes [101].

Perlstein *et al.* evaluated the distribution of maghemite nanoparticles (Fe_2O_3-MNP) of approximately 80nm average diameter, prepared by controlled nucleation and growth of thin maghemite films onto appropriate nuclei [102]. These superparamagnetic particles were injected by CED in normal rat brain with different viscosities and evaluated regardless of their diffusion properties [29]. The results showed a very good correlation between MRI and fluorescent acquisitions after loading the Fe_2O_3-MNP with rhodamine, establishing the use of MRI for reliable maghemite nanoparticle imaging. Nevertheless, superparamagnetic iron particles are characterized by a very high sensitivity to MR imaging [103]. Thus, iron signals sometimes give excessive results, especially when compared to histological findings. After the CED administration of iron particles in rat brain, the Vd measured by MRI was overestimated by a factor of 0.38 compared to histological methods [48].

3.2. Nanocarrier physicochemical properties

In this chapter, we will focus on the parameters influencing a nanocarrier's aptitude to diffuse to be diffused in brain parenchyma, depending on their size, charge, composition, surface properties, and physicochemical characteristics. All these data are resumed in Table 2.

Parameters	Optimal conditions	Explanation	Ref
Size	20-50nm (< 100nm)	To diffuse in brain ECM	[84, 104, 105]
Charge	Neutral or negative charge Ex: PEG chains	To reduce non-specific binding	[84, 91, 108]
Surface coating	Steric coating Ex: PEG, dextran, albumin	To reduce binding to brain cells	[29, 84, 105]
Osmolarity	Slightly hyperosmolar Ex: mannitol, sucrose	To increase ECM channel size	[54, 90]
Viscosity	Slightly viscous Ex: PEG, sucrose	To reduce backflow	[29, 112]
Concentration	Highly concentrated Ex: excess of nanocarriers	To block the binding sites	[48, 84]
Tissue affinity	Use of co-infusates Ex: heparin, bFGF, mannitol	To reduce specific binding sites	[27, 114, 115, 119]
Pharmacokinetic	Nanoencapsulation Ex : LNC, liposomes	To enhance drug brain $T_{1/2}$	[29, 47, 91]

Table 2 : Physicochemical properties of nanosized structures and their influence on brain diffusivity.
ECM: extra cellular matrix, PEG: polyethylene glycol, bFGF: basic fibroblast growth factor; LNC: lipid nanocapsules

3.2.1. Size

Many studies have focused on the optimum in size for nanocarriers used in CED. The conclusions are quite unanimous since the distribution volume of nanocarriers in rat striatum is inversely proportional to the size of the particle. Mackay *et al.* worked on the physicochemical properties of liposomes in order to optimize post-CED diffusion [84]. They concluded that ideal liposomes for CED should be less than 100nm in diameter, because above this size, liposomes are retained near the site of injection and are characterized by restricted mobility. Studies on brain extracellular space (ECS) gave more precise informations: the ECS has been estimated at between 35 and 64nm in diameter in normal rat brain [104] which means that many vectors beyond 100nm will be too large to transit normal neocortical extra-cellular space. The size of some polystyrene nanospheres administered by

CED were also evaluated in rats in order to mimic the behavior of viral vectors [105]. The conclusions were that the Vd of these nanocarriers in rat striatum were about $9mm^3$ for 20nm nanospheres and about $1mm^3$ for 100 and 200nm particles. Nevertheless, when the nanospheres were covered by albumin, the effect of size was reduced. Indeed, albumin coating can mask the hydrophobic structures of the polystyrene nanospheres, reducing the risk of the eventual aggregation and binding to proteins in the extracellular space.

3.2.2. Surface properties

Surface properties have a considerable impact on the diffusivity of colloidal vectors especially because of the presence of a steric coating. Polyethylene glycol (PEG) and dextran coating significantly increase the distribution of liposomes and nanoparticles delivered by CED [29, 84]. Biocompatible polymers such as dextran and PEG are known to extend the systemic circulation of such nanocarriers because they significantly reduce interactions with proteins [106, 107]. Following CED infusions, these same excipients may reduce the binding of nanocarriers to brain cells, allowing a greater diffusion compared to those without any coating. Surface charge has also been studied concerning the diffusivity of liposomes in the rat brain. Mackay *et al.* observed that when liposomes were charged with modest amounts of positive charge (10% per Mole lipid), the distribution of such liposomes was significantly decreased compared to neutral nanocarriers ($p < 0.0005$) [84]. Cationic liposomes were found adjacent to the needle tract because of non-specific binding to negatively-charged structures in the brain parenchyma [108]. The diffusivity of cationic liposomes is a challenge as they are used as vectors for gene delivery [109]. However, the pegylation of these carriers enhanced the distribution volume reducing tissue affinity as demonstrated above [91]. On the contrary, negative charges have no effect on the diffusivity of such liposomes. Based on these findings, a neutral or negative surface charge is required to obtain a good diffusion [84].

3.2.3. Osmolarity

The use of mannitol has been described to increase the convective effects of liposomes, especially a few hours after infusion. The CED of 40nm-liposomes co-infused with 25% mannitol produced an enhancement of the distribution from 52.5 ± 2.1 to 78.5 ±5.5 units immediately after CED and was even more pronounced after 48h (34.8 ± 7.5 compared to

13.5 ± 3.2 units) [90]. This phenomenon was explained by the hyperosmotic power of mannitol which may increase the size of channels of the interstitial space through which liposomes could transit. Similarly, Neeves *et al.* co-infused BSA-coated polystyrene nanoparticles with 25% mannitol (Osmolarity = 1568 ±12 mOsmol/kg) in normal rat brain and showed that the distribution was enhanced by about 50% [54].

On the contrary, Chen *et al.* studied the influence of BSA solution osmolarity and revealed that there were no dramatic effects on the Vd when the BSA osmolarities varied between 145 and 450mOsmol/kg [105]. They, then, injected nanospheres coated with BSA and studied the Vd in rat striatum. They concluded that the distribution of nanospheres coated with BSA was not affected by osmolarity. But, they considered that the transport of such a small molecule as BSA (7.2nm) was comparable to nanocarriers of about 20 to 200nm in size. The diffusivity of nanoparticles in porous media was reduced when compared to that of small molecules in solution because of a combination of hydrodynamic and steric factors [110, 111].

3.2.4. Viscosity

By increasing the viscosity of the infusate, Mardor *et al.* demonstrated that CED efficacy could be enhanced [112]. In fact, a linear correlation was found between Vd and viscosity. It is easy to increase the viscosity of a nanocarrier formulation by dissolving sugar or polymers in the aqueous external phase of such a suspension. Perlstein *et al.* increased the viscosity of their nanoparticle suspension by incorporating PEG (3-6%) or sucrose and the results were characterized by an improved distribution capability [29]. High viscosity of the infusate may also reduce backflow, thus increasing the possibility of efficient convection. Moreover, the efficient formation and extent of convection obtained by using high-viscosity infusates enables the coverage of larger volumes of distribution in less time, thus reducing the time of infusion and consequently the appearance of related side effects [113]. After the CED injection of two formulations of carboplatin (4mg/ml) and carboplatin + sucrose (4mg/ml + 12%), Mardor *et al.* showed that not only the Vd was enhanced but also the cytotoxic treatment effects measured by MRI (performed on Day 1 and 4) [112]. This significant correlation suggests that, by increasing the infusate viscosity, it is possible to significantly increase the efficiency of CED, and consequently improve the efficacy of treatment.

3.2.5. Concentration

Chen *et al.* showed that the concentration of the infusate had no impact on the calculated Vd, nor on the global distribution of the infusate in brains [49]. Indeed, when the ^{14}C-BSA concentration increased from 25 to 50 and 100%, the corresponding Vd were about 20.6±1.8, 21.5±2.6 and 19.6±2.7 mm^3, which means that the differences in concentration did not alter the distribution pattern. They explained that the administration of a pharmacological agent by convection is based on the transport of a material through the interstitial space which is not dependent on concentration gradients as in diffusion methods. But the reality is more complex and seems to be linked to the nature of the materials infused. When infusion is carried out with monocrystalline iron oxide nanocompounds (MIONs), Kroll *et al.* concluded that concentration was a principal parameter [48]. Evaluating which parameters between dosage, volume and infusion time, may have the greatest influence on increasing the Vd, they evidenced a major impact of the dose effect. By increasing the iron dose contained in monocrystalline iron oxide nanocompounds (MIONs) from 5.3 to 26.5µg, the MRI calculated Vd increased by 4.9- and 2.5-fold for infusion rates of 0.2 and 1.2µl/min, respectively. The overall effect of dosage, at these two different rates, was significant ($P<0.001$). It is especially interesting to note that the Vd associated with either dose was greatest with the lowest flow rate tested because of the occurrence of backflow for the higher rate. Even if superparamagnetic iron particles are known to overestimate the signal, histological sections confirmed the same Vd ratio for the different formulations tested. With the same idea in mind, Mackay *et al.* demonstrated that when the liposome concentration was increased, the distribution volumes also increased. They postulated that the liposome-engulfing cells could be responsible for reducing the penetration of liposomes into the brain. This process would require particle adsorption, and the excess of liposomes was used to block the binding sites reducing the adsorption of the nanocarriers left along the conduction pathway [84].

3.2.6. Brain affinity

The use of co-infusates (e.g. heparin, basic fibroblast growth factor or mannitol) has been widely described as reducing the affinity of infusates to the brain environment. Hamilton *et al.* demonstrated the influence of receptor binding on the distribution of trophic factors in the CNS [114]. They showed that heparin co-infusion significantly enhanced the Vd of GDNF and GDNF-homologous trophic factors, probably by binding and blocking heparin-binding

sites in the extracellular matrix. The same observations were made to enhance the distribution of viral particles such as adeno-associated virus type 2 (AAV-2) particles [27]. Working on the same vectors, Hadaczek *et al.* indicates that the simultaneous injection of basic fibroblast growth factor (bFGF) with AAV-2-thymidine kinase (AAV-2-TK) can greatly enhance the volume of transduced tissue, probably by way of a competitive block of AAV-2-binding sites within the striatum [115]. Similarly, heparan sulfate proteoglycans (HSPG) have been identified as primary viral receptors [116] and are known to be abundantly present on neurons [117, 118]. The use of mannitol was described as blocking the adeno-associated virus type 2 (rAAV) binding to HSPG thus facilitating the spread of the virus [119]. For a nanosized structure, a compromise had to be made between weak interactions with brain ECM and cellular interactions with tumor cells. Indeed, on the one hand, interaction with brain ECM has to be controlled for optimal distribution, but on the other hand, the carrier loaded with its anticancer agent has to play its 'toxic' rule to eradicate the tumor. Most of the time, anticancer agents have to penetrate the cells to be active as their targets are sub-cellular entities.

3.2.7. Pharmacokinetic behavior

Modification of drug pharmacokinetic behavior is one of the many advantages linked to to nanoencapsulation strategy [120]. For example, Saito *et al.* compared the distribution of doxorubicin hydrochloride, which is a small, hydrophilic molecule, infused by CED, with a pegylated liposomal formulation of doxorubicin (Doxil®) [91]. The results showed that the drug alone had poor tissue distribution and did not cover the entire tumor mass, whereas liposomal formulations did. Due to the affinity of free doxorubicin for cellular components, the accumulation of free doxorubicin was found in cellular nuclei whereas most of the Doxil® was found in the intercellular spaces.

However, elimination routes for the nanocarriers infused by CED may vary substantially between formulations and need to be understood. Each nanocarrier infused by CED can be characterized by a brain half-life which is defined as the time when half the quantity has disappeared from the brain. For example, Mackay *et al.* described a brain half-life of about 9.9h for neutral pegylated liposomes and 15 min. for positively-charged liposomes [84]. We have previously shown that the elimination of lipid nanocapsules (LNC) loaded with a hydrophobic complex of rhenium-188 (^{188}Re-SSS) was significantly lower when compared to a hydrophilic solution of rhenium-188 perrhenate [47]. The CED infusion of Rhenium-188

perrhenate solution revealed that more than 80% was eliminated in 12h and about 94% after 72h post CED. ^{188}Re perrhenate brain half-life (brain $T_{1/2}$) was equivalent to 7h, and the solution was mainly excreted by the kidneys as 99.4% of the total excreted radioactivity was recovered in urine. On the contrary, only 10% of rhenium-188 encapsulated in LNC was detected in urine and feces 72h post-CED infusion. ^{188}Re-SSS LNC were found to be a sustained residency system which constitutes a major advantage (1% elimination after 12h). The lipophilic nature of LNC and their intracellular glioma location [121] leads to a long radionuclide brain retention time allowing improved tumor irradiation. Maghemite nanoparticles (Fe_2O_3-MNP) were also characterized by a high time residency (t½ brain = 10d), with about 10 to 20% remaining at Day 40 and no toxicity being observed up to 120 days after CED [29]. This long time residency was also correlated with an intracellular co-localization or surface adsorption of the Fe_2O_3-MNP as detected after Prussian blue staining. If the infusion time surpasses the nanoparticle half-life, it is impossible to deliver the particle for large volumes without blocking the source of elimination. On the contrary, if it is possible to increase the brain half-life, particles can be infused for longer periods and achieve greater volumes of distribution.

4. Survival studies and clinical trials

In the context of CED, nanocarriers can be used as vectors to track infusion and/or as vectors to treat solid tumors. As the results are different between species because of difference in brain structure, we separated the results obtained from rodent brains and larger brain models including studies on non-human primate brains and dogs. To conclude, a few comments have been made for clinical trials involving the use of nanocarriers. The main preclinical and clinical studies involving the use of nanocarriers infused by CED are summarized in Table 3 (page 61).

4.1. Rodent models

Pegylated liposomal doxorubicin (Doxil®, Alza Pharmaceuticals, Inc., Mountain View, CA; Caelyx®, Schering-Plough, Inc., Kenilworth, NJ) and liposomal daunorubicin (Daunoxome®, Gilead, Inc., Foster City, CA) are approved as liposomal formulations for clinical use [122-

124]. Saito *et al.* proved the concept feasibility of a co-infusion of Doxil® and liposomes loaded with gadolinium to provide direct evidence of the drug Vd in tissue during CED [44]. The conclusions were that CED effectively distributed Doxil® liposomes in the tumor and the surrounding normal brain tissue that contained invasive tumor cells. The CED of Doxil® into rodent brain tumors demonstrated that doxorubicin is present in the tissue several weeks after a single administration [125].

In terms of pure cancer therapy, a novel nanoliposomal formulation has been developed and loaded with a campthotecin derivative, Irinotecan or CPT-11, in order to use it in rodent brain tumor models [126]. Following CED in rat brains, the tissue retention of nanoliposomal CPT-11 (nLs-CPT-11) was greatly prolonged as compared to free drugs, with >20% of the injected dose remaining at 12 days for all doses. Brain tissue residence was dose-dependent and increased as the dose increased. At equivalent doses, brain $t_{1/2}$ was 22-fold higher for nanoliposomal CPT-11 than for free CPT-11, without signs of toxicity, increasing the tolerance of the molecule, more than 4-fold. The median survival time of rats bearing 9L-2 glioma was largely increased for the group treated by the highest dose tested (1.6mg/rat) with 62.5% of the rats treated being long-term survivors (> 100 days) [28]. Although no great difference was seen in low-dose free CPT-11 versus low dose nLs-CPT-11, the fact that high-dose nLs-CPT-11 could be used in the absence of limiting brain toxicity confirmed the possibility of the direct clinical application of this technology for the treatment of brain tumors.

The same kinds of results were observed with nanoliposomal Topotecan (nLs-TPT). Topotecan is a water-soluble campthotecin derivative that inhibits the topoisomerase I leading to DNA damage in tumors. The analysis of brain tissue revealed a dramatic improvement in brain retention of nLs-TPT as compared to free drugs as the brain half-lifes were about 1.5 and 0.1 days, respectively. The study showed that the CED of nLs-TPT resulted in the perivascular accumulation and consequent disruption of tumor vessels suggesting a possible antiangiogenic mechanism of liposomes loaded with a chemotherapeutic cargo. The CED of nLs-TPT inhibited growth or completely eradicated orthotopic U87MG or U251MG xenografts, whereas free drugs exerted almost no effect at an equivalent dose of 10µg [127].
These liposomal formulations can be mixed in order to enhance the effects of antineoplasic molecules, because these three drugs (topotecan, irinotecan and doxorubicin) decrease

different key enzymes involved in *in vitro* tumor cell replication. Topotecan and irinotecan are topoisomerase I inhibitors whereas doxorubicin is known to inhibit topoisomerase II, enzymes involved in regulating DNA topology. Pegylated liposomal doxorubicin (Doxil®) and nLs-TPT were first mixed and tested *in vitro* and *in vivo* on U87MG glioma cell lines and on corresponding tumor xenografts [128]. The results showed a synergistic effect between the two topoisomerase I inhibitors and a significant improvement in survival time compared to the control groups and to the groups treated with both drugs separately. These results were all the more significant as the liposome treatment took place 10 days after cell inoculation, which means that the tumor was an advanced tumor with a well-stablished vasculature.

Doxil® and nLs-CPT11 were also mixed and evaluated *in vitro* and *in vivo* with respect of toxicity, tissue half-life, and efficacy in U87MG and U251MG xenografts to learn about the synergy of action of these two molecules [129]. Although the dose of Doxil® used was 400-fold lower than that of nLs-CPT11, their brain half-lives were similar and equivalent to 16.7 and 10.9 days, respectively. The synergy between the two agents was only observed in one of the two cell lines tested (U251MG cells), in *in vitro* cell cycle profile as well as *in vivo* survival xenografts studies: this may be due to the reduced growth of U251MG cells compared to U87MG and higher sensitivity to the doxorubicin and irinotecan combination. Even so, a better liposome distribution was observed in U87MG xenografts when compared to U251MG tumors characterized by the presence of large necrotic areas. This means that the growth of the cell lines used for implanted xenografts was a principal factor for *in vivo* survival results.

Dendrimers are synthetic polymers with a well-defined globular structure. They are composed of a core molecule, repeated units that have three or more functionalities, and reactive surface groups. A fifth generation (G5) polyamidoamine dendrimer containing methotrexate (MTX), a folate antimetabolite-like anticancer agent covently linked to cetuximab, a monoclonal antibody was prepared and administered by CED in rats with F98 gliomas [30]. Cetuximab (Erbitux® or IMC-C225) was able to bind the epidermal growth factor receptor (EGFR) and its mutant isoform (EGFRvIII), frequently overexpressed in malignant gliomas [130-132]. The amount of the so-called C225-G5-MTX dendrimer after CED was more than 5-fold higher in EGFR-positive gliomas compared to receptor negative tumors, which means that there was direct interaction between the vector and the glioma cells. Unfortunately, there was

no impact on the median survival time as no significant difference between the control group, the group treated by the C225-G5-MTX dendrimer, and the group treated by MTX alone, was observed. This could be due to a loss of activity of MTX after the linkage of this antifolate molecule to the dendrimer structure, altering the interaction with dihydrofolate reductase which is essential for a biological activity. Moreover, no investigation was carried out concerning the diffusion of this carrier C225-G5-MTX dendrimer in the rat brain.

Dendrimers have also been used for boron neutron capture therapy (BNCT) [133, 134]. Briefly, BNCT is a binary radiation therapy modality that brings together two components that, when kept separate, have only minor effects on cells. The first component is a stable boron isotope (^{10}B) that can be concentrated in tumor cells by grafting it onto dendrimers. The second is a beam of low-energy neutrons that produce ^{11}B in an unstable form which instantaneously produces α-particles (^{4}He) and recoiling lithium nuclei (^{7}Li). These high, linear-energy, transfer particles restrict their destructive effects to cells containing ^{10}B. A heavily-boronated polyamidoamine dendrimer was chemically linked to cetuximab, and was designed at BD-C225. This dendrimer was administered by CED in rats with a F98 tumor that expressed the epidermal growth factor receptor (EGFR). These rats were also treated with an intravenous injection of boronophenylalanine (IV-BPA), drug that has been used clinically for BNCT of brain tumors. The survival data of rats treated by CED with BD-C225 following BNCT +/- IV-BPA [135] gave significant results compared to the irradiated and untreated controls [136]. Indeed, the corresponding mean percentage increase in life span was 170% for the combination versus 107% for CED of BD-C225 alone and 52% for i.v. BPA alone. These results indicate that the CED of BD-C225 plus IV-BPA was significantly different from the IV- BPA alone group ($p = 0.0002$), and that the difference between the groups that received BD-C225 alone or in combination with BPA was also significant ($p = 0.017$).

Thanks to the high level of retention of lipid nanocapsules (LNC) in rat brains, conclusive dose-dependent results were obtained with internal radiotherapy using ^{188}Re-SSS LNC administered by CED [47]. LNC with an equivalent dose of 8Gy constituted the most efficient group treatment in terms of survival because a high increase in the median survival time of 80% was noted compared to the control group and because two rats from this group (33%) were long-term survivors. CED injection at this dosage seemed to be well tolerated since no

side effects were observed except for a very slight weight loss observed over a few days after treatment.
Micellar doxorubicin (DOX) infused by CED resulted in prolonged median survival (36 days) compared to free DOX (19.6 days; P=0.0173) and liposomal DOX (16.6 days; P=0.0007) at the same dose (0.2 mg/mL) in a 9L glioma model [70].

4.2. Studies in large brain models

Differences have to be made between the diffusion of liposomes in rodents compared to primate brains since the brain anatomy of each species is quite different. For example, it has been underlined in section 1 (§ 2.2.1) that the proportion of white matter is much higher in primate brains suggesting an easier diffusion. Moreover, to consider such nanocarriers in future clinical trials in the human brain, the transposition to a larger brain model is necessary.
As in rodent models, the injection of liposomes loaded with fluorescent markers or with paramagnetic agents has been performed in the normal primate brain [100]. A linear correlation between infusion volume (Vi) and distribution volume (Vd) was established with a 2:1 ratio between the volume of liposome infused and the distribution volume observed in brains, and this occurred whatever the amount of gadolinium encapsulated [137]. The co–infusion of liposomes, fluorescently loaded with rhodamine, and liposomes encapsulating gadoteridol, showed a perfect superposition of the images obtained by histological acquisitions and magnetic resonance techniques. This observation highlights MRI as a real-time imaging technique in the treatment of brain tumors, and to monitor the distribution of the encapsulated drug. No toxicity was observed during and after the infusion of such liposomes except for some minor tissue damage due to the presence of the cannula.

In larger models like primate models, it was possible to target different structures of the brain. In their first study on the primate brain, Saito *et al.* aimed at targeting corona radiata, putamen and brainstem with a maximum of 100µl-liposome infusion; they described robust and clearly-defined distribution of liposomal Gd in each infusion site [100]. Then, they injected a fixed and considerable volume of liposomes (700 µl) into each of these three regions to investigate the regional difference in brain structure. The results of all three infusion sites showed a linear correlation between Vi and Vd with a maximum distribution observed in the brainstem (Vd/Vi = 2.3) and a minimum for the putamen (Vd/Vi = 1)[138]. Lonser *et al.*

described a Vd/ Vi ratio of up to 8.7 in primate brainstems with an infusion of albumin-bound Gd, showing that not only the brain region had to be considered, but also the physicochemical properties of the infusate [43]. The limited size of primate putamen seems to restrict Vi and was characterized by a leakage of liposomes out of this structure. This leakage was correlated with the perivascular transport of liposomes throughout CNS arteries [139]. These findings suggest that every therapeutic agent infused into putamen should be closely monitored for distribution, since the possibility of side effects increases greatly with leakage out of the infusion site. Nevertheless, a principal advantage of CED is that liposomal distribution stops immediately once the CED pumps are turned off.

In order to mimic a real intervention for human brain-tumor patients, three consecutive infusions of liposomes with an increased volume of infusate was performed in the same region in a primate brain. No change in distribution was noted after repeated infusions and the linear relationship between Vi and Vd was also maintained in the brainstem and in the corona radiata. After histological examinations of the right and left hemispheres, no modifications were noted in both parts of the brain, suggesting that multiple injections appear to be a safe and conceivable treatment approach.

In order to work in conditions very closed to human ones, and as only a few data can be collected concerning the distribution in tumor models, the next step will be the administration of such nanocarriers in large models bearing tumors. Dogs are able to generate spontaneous brain tumors with an incidence near to that observed in humans. Moreover, canine tumors are on the scale of human tumor patients with biological, histological and molecular characteristics very similar to those reported in humans [140-143]. For the first time, Dickinson *et al.* investigated the infusion of liposome by CED in a canine model but in healthy brains [57]. They injected a mixture of liposomes loaded with Gd and with CPT-11 as a potential treatment strategy. The CED resulted in robust Vd in both gray and white matter, with minimal adverse effects. Leakage was only observed in one of the 11 infusions performed and was mainly due to poor catheter placement. No adverse clinical effects were associated with leaving the infusion cannulae *in situ*, and second infusions were successful in all cases. In brief, this study confirmed the results observed in rodents and primate studies on normal brains. The next step will be the administration of nanocarriers in spontaneous canine tumors first, and in human glioma very shortly.

4.3. Clinical trials

The clinical trials randomized patients who had failed conventional therapy (surgery, radiotherapy and/or chemotherapy) [144]. The first therapeutic agent infused via CED for malignant glioma was diphtheria toxin conjugated to transferring Tf-CRM107 [145]. This active agent belongs to the targeted toxin family which is mostly composed of recombinant polypeptides designed with two segments that represent a new class of agents with a high specificity for tumor cells [146-148]. Others clinical trials using CED reported in literature are trials infusing anticancer drugs like paclitaxel [17], or radioimmunotherapy drugs like Cotara®, a ^{131}I-labelled chimeric monoclonal antibody [21].

Among the clinical trials described in the literature using CED, only a few studies described the use of drug-loaded nanocarriers. The concept of gene therapy has been investigated to fight against malignant glioma and has been the object of encapsulation in nanocarriers such as liposomes. Ren *et al.* studied the antitumor efficacy of a genetically-modified replication-disabled Semliki forest virus vector (SFV) carrying the human interleukin 12 (IL-12) gene, encapsulated in cationic liposomes (LSFV-IL12) [149]. Virus encapsulation has several advantages such as reduced recognition of the virus by the immune system, virus protection from an *in vivo* inactivation process and a prolonged *in situ* residency time. Unfortunately, this study gave no therapeutic results and settled for providing the description of the phase I/II clinical protocol.

Others studies have investigated the encapsulation of a retrovirally mediated HSV-1-*tk* gene transfer, which sensitizes tumor cells for ganciclovir (GCV) in liposomal structures [150, 151]. In this concept, the use of synthetic nanocarriers has been investigated to avoid the use of viral vectors because of easier preparation, a lack of immunogenicity and higher stability over time. In fact, Voges *et al.* presented the results of a prospective phase I/II clinical study using CED of an HSV-1-*tk* gene-bearing cationic liposomal vector (LIPO- HSV-1-*tk*) and systemic GCV for the treatment of GBM [152]. The results showed that the treatment was tolerated with minor side effects indicating the safety and feasibility of this technique. Within the 8 patients treated, two of them had a 50% reduction of tumor volume, whereas for the others, only a focal effect was noted. Nevertheless, the main critical aspect of this study was that the monitoring of the CED injection by MRI was performed after the injection of Gd-

DTPA (550 Da, no charge) and not with the liposomes encapsulating Gd (180 ± 20 nm, negative charge) given that the distribution volume is known to be strictly dependent on the physicochemical properties of the nanocarrier.

5. Conclusion

Local delivery of agents to brain tumors by Convection Enhanced Delivery offers the advantage of better drug distribution compared to other strategies only governed by diffusion. Because this technique was also characterized by the appearance of side effects caused by backflow along the catheter and drug leakage in non-desired regions, the encapsulation of active molecules within the concept of CED has been investigated to overcome this problem. The encapsulation of such a drug, a toxin, or a gene is under investigation on experimental models rather than in clinical trials, but seems to be very promising for the treatment of brain malignancies. In the context of solid brain tumors, the nanocarriers have to be characterized by a high, drug-loading level to eradicate the tumor and to be labelled with a contrast agent in order to realize real-time imaging. In terms of pure structure, the ideal nanocarrier would be about 20 to 50nm in size, with a global neutral or negative charge, and shielded by a steric coating made of PEG or dextran (Figure 7A). The final infused suspension would be viscous, hyperosmolar, with the eventual presence of co-infusate to saturate the binding sites along the nanocarrier route (Figure 7B). It should be infused at high concentrations especially for carriers that have to target the intracellular compartment. The elimination route has to be controlled in order to prevent the rapid elimination by blood capillaries in a brain extracellular matrix (Figure 7C). In a word, the objective for using CED for drug delivery nanomaterials is twofold: Firstly, thanks to specific structural properties, the nanocarrier has to diffuse into the brain parenchyma in order to obtain an optimal volume of distribution to cover tumor mass and infiltrating cells. Secondly, the nanocarrier has to be internalized by cancer cells in order to exert its cytotoxicity, mediated by anticancer agents.

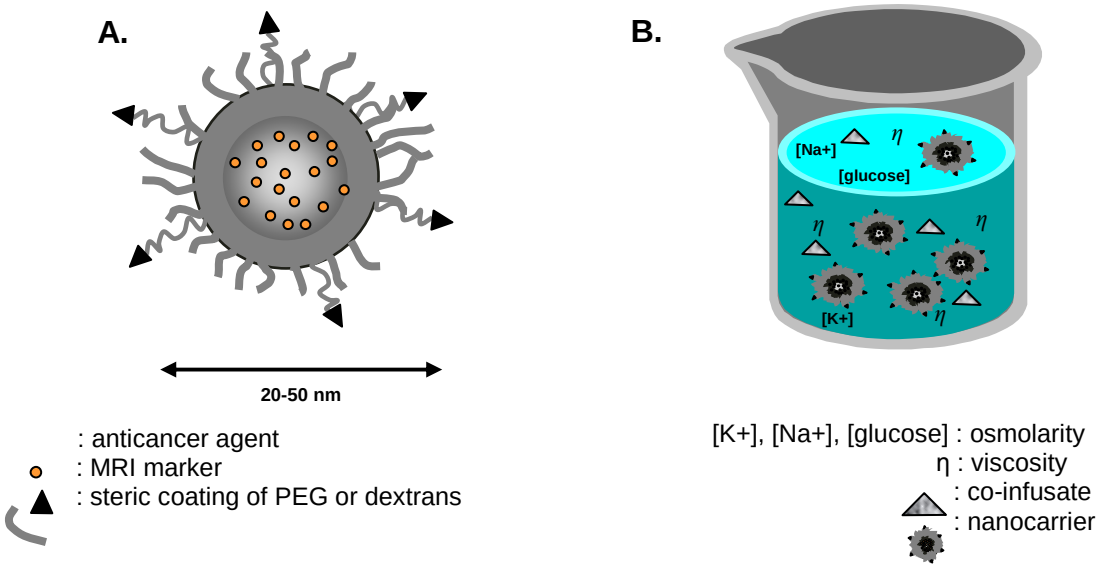

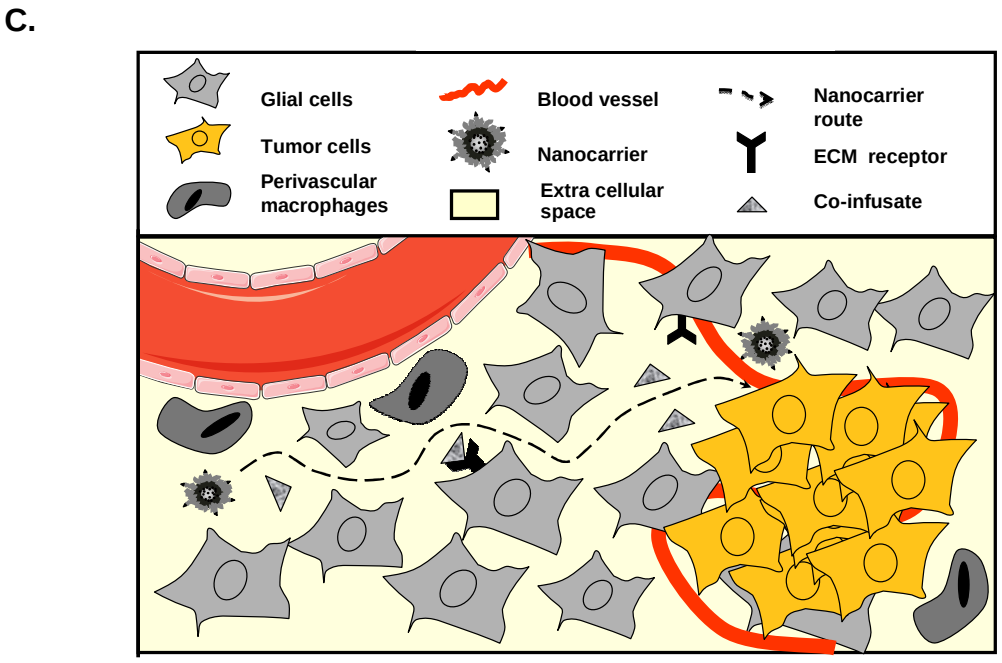

Figure 7: Representation of the "ideal' nanocarrier infused by CED. The ideal nanocarrier has to be characterized by a high drug loading level to eradicate the tumor and labelled with contrast agent in order to realize real time imaging. It should be about 20 to 50 nm in size, with a global neutral or negative charge, and shielded by a steric coating made of PEG or dextrans (**A**). The final suspension infused should be viscous, hyperosmolar, with eventually the presence of co-infusate to saturate the binding sites along the nanocarrier route (**B**). It should be infused at high concentration and especially for carriers that have to target the intracellular compartment. The elimination route has to be controlled in order to prevent a rapid elimination by blood capillaries in brain extracellular matrix (**C**).

Table 3: Preclinical and clinical studies of CED nanocarriers (liposomes, dendrimers or nanoparticles) for therapeutic or diagnostic applications

Designation	Active molecules	Animal Model	Tumor cell line	Applications	Significant results	Ref
Liposome	Gold particles Dil-DS, Rhodamine Gadodiamide	Rats Mice	U87MG	Histology Fluorescence MRI	First report of CED infusion of liposomes in CNS. Labelled liposomes could be sensitively and specifically detected in CNS in tumor and safe brains as in flank tumor models.	[90]
Lip/Gd/Dil-DS Doxil®	Dil-DS, Gadoteridol Doxorubicin	Rats	C6, 9L-2	Fluorescence MRI	Distribution of Lip/Gd/Dil-DS and Lip/Gd + Doxil® covers the tumor mass and can be monitored by MRI.	[44]
Liposome	^{125}I-BPE, ^{3}H-Chol, DNA, DiD, DiO	Rats	-	Autoradiography Fluorescence	Description of the ideal properties for liposomes infused by CED: < 100nm, shielded PEG, neutral or negative charge, infused as a high lipid concentration to saturate the binding sites.	[84]
Nanoliposomal-CPT-11 (nLs-CPT-11)	Irinotecan or CPT-11	Rats	9L-2	Therapy	CED of Ls-CPT11 greatly prolonged tissue residence while reducing toxicity, resulting in a highly effective treatment strategy in brain tumor models.	[28]
Nanoliposomal-TPT (nLs-TPT)	Topotecan	Rats	U87MG, U251MG	Therapy	Ls-TPT produced a significant survival benefit on U87MG (P= 0.0002) and on U251MG (P=0.0005) tumor models compared to controls.	[127]
nLs-TPT Doxil®	Topotecan + Doxorubicin	Rats	U87MG	Therapy	The combination of these two topoisomerase inhibitors loaded liposomes gave synergic effects on U87MG tumor models and median survival was significantly enhanced compared to controls.	[128]
nLs-CPT-11 Doxil®	Irinotecan + Doxorubicin	Rats	U87MG, U251MG	Therapy	The synergy between the two agents was only observed in one of the two cell lines tested (U251MG), in *in vitro* cell cycle profile as well as *in vivo* survival xenografts studies.	[129]
Liposome	Gadoteridol Dil-DS Rhodamine	Monkeys	-	MRI Fluorescence	CED of liposomes in primates was characterized by linear correlation of Vi/Vd in the corona radiata, the putamen and the brain stem. In the putamen, leakage of liposomes was correlated with the transport of carriers throughout CNS arteries.	[100, 138, 139]
Liposome	Gadoteridol Rhodamine	Monkeys	-	MRI Fluorescence	This retrospective analysis showed that real-time imaging of GDL-loaded liposomes was a reproducible and safe procedure for future clinical applications.	[137]
Liposome	Gadoteridol Rhodamine CPT-11	Dogs	-	MRI Fluoresence	The CED of liposomal Gd/CPT-11 was associated with minimal adverse effects in a large safe animal model. Real-time imaging allowed accurate Vd determination. Canine models are interesting as they can spontaneously develop gliomas.	[57]
Dendrimer (C225-G5-MTX)	Methotrexate or MTX	Rats	$F98_{EGFR}$	Therapy	Whereas C225-G5-MTX dendrimer quantites after CED was more than 5-fold higher in EGFR(+) gliomas compared to EGFR(-) tumors, there was no impact on median survival compared to control groups.	[30]
Dendrimer (BD-C225)	Boron	Rats	$F98_{EGFR}$	Therapy	The corresponding mean percentage increase in life span was 170% for the combination BNCT of BD-C225 + BPA_{IV} versus 107% for CED of BD-C225 alone and 52% for i.v. BPA alone.	[136]
Polystyrene Nanospheres (NP and BSA-NP)	^{14}C-phenanthrene	Rats	-	Autoradiography	The Vd of nanospheres in rat striata was inversely proportional to the size of the particle but when they were recovered by albumin, the effect of size was reduced. The surface properties limited the diffusivity of the nanospheres.	[105]
Maghemite nanoparticles (Fe_2O_3 MNP)	Fe_2O_3 Rhodamine	Rats	-	MRI Fluorescence Histology	By adding sucrose or PEG to MNPs, infusate viscosity was increased and distribution volumes were greater. MRI showed that dextran-MNPs were able to penetrate the cells which could explain the high brain T1/2 of 10 days.	[29]
Lipid nanocapsules (^{188}Re-SSS LNC)	^{188}Re-	Rats	9L	Therapy	When administered in LNC, ^{188}Re tissue retention was greatly prolonged. Rat median survival was significantly improved for the group treated with 8Gy ^{188}Re-SSS LNC compared to the control groups.	[47]
Cationic liposomes (LIPO-HSV-1-*Tk*)	HSV-1-*tk*	Humans	-	Therapy	The treatment was tolerated with minor side effects indicating the safety and feasibility of this technique. Of the 8 patients treated, two of them had a 50% reduction of tumor volume, whereas for the others, only a focal effect was noted.	[152]

BD = boronated polyamidoamine dendrimer, BNCT = boron neutron capture therapy, BPA = boronophenylalanine, BSA = bovine serum albumine, C225 = cetuximab, CNS = central nervous system, CPT-11 = irinotecan, Dil-DS = 1.1'-dioctadecyl-3,3,3',3'-tetramethylindocarbocyanine-5,5'-disulfonic acid, DiO (D-275) and DiD (D-307) = fluorescent lipid tracers (Molecular probes), EGFR = epidermal growth factor, G5 = fifth generation of polyamidoamine dendrimer, HSV-1-*tk* = herpes simplex virus type-1 thymidine kinase, ^{125}I-BPE = iodinated benzamidine phospholipids, MNP = maghemite nanoparticle, MRI = magnetic resonance imaging, MTX= methotrexate, PEG = polyethylene glycol, ^{188}Re = rhenium-188.

References

1. Gralow J, Ozols RF, Bajorin DF, Cheson BD, Sandler HM, Winer EP, et al. Clinical cancer advances 2007: Major research advances in cancer treatment, prevention, and screening - A report from the American Society of Clinical Oncology. J Clin Oncol 2008;26(2):313-325.

2. Bauchet L, Rigau V, Mathieu-Daude H, Figarella-Branger D, Hugues D, Palusseau L, et al. French brain tumor data bank: Methodology and first results on 10,000 cases. J Neurooncol 2007;84(2):189-199.

3. Ohgaki H, Kleihues P. Epidemiology and etiology of gliomas. Acta Neuropathol 2005;109(1):93-108.

4. Mason WP. Progress in clinical neurosciences: Advances in the management of low-grade gliomas. Can J Neurol Sci 2005;32(1):18-26.

5. Lonardi S, Tosoni A, Brandes AA. Adjuvant chemotherapy in the treatment of high grade gliomas. Cancer Treat Rev 2005;31(2):79-89.

6. Nieder C, Adam M, Molls M, Grosu AL. Therapeutic options for recurrent high-grade glioma in adult patients: recent advances. Crit Rev Oncol Hematol 2006;60(3):181-193.

7. Stupp R, Mason WP, Van Den Bent MJ, Weller M, Fisher B, Taphoorn MJB, et al. Radiotherapy plus concomitant and adjuvant temozolomide for glioblastoma. N Engl J Med 2005;352(10):987-996.

8. Nieder C, Adam M, Grosu AL. Combined modality treatment of glioblastoma multiforme: the role of temozolomide. Rev Recent Clin Trials 2006;1(1):43-51.

9. Boiardi A, Eoli M, Salmaggi A, Lamperti E, Botturi A, Solari A, et al. Local drug delivery in recurrent malignant gliomas. Neurol Sci 2005;26 Suppl 1:S37-39.

10. Wang PP, Frazier J, Brem H. Local drug delivery to the brain. Adv Drug Deliv Rev 2002;54(7):987-1013.

11. Sawyer AJ, Piepmeier JM, Saltzman WM. New methods for direct delivery of chemotherapy for treating brain tumors. Yale J Biol Med 2006;79(3-4):141-152.

12. Raza SM, Pradilla G, Legnani FG, Thai QA, Olivi A, Weingart JD, et al. Local delivery of antineoplastic agents by controlled-release polymers for the treatment of malignant brain tumours. Expert Opin Biol Ther 2005;5(4):477-494.

13. Guerin C, Olivi A, Weingart JD, Lawson HC, Brem H. Recent advances in brain tumor therapy: local intracerebral drug delivery by polymers. Invest New Drugs 2004;22(1):27-37.

14. Bobo RH, Laske DW, Akbasak A, Morrison PF, Dedrick RL, Oldfield EH. Convection-enhanced delivery of macromolecules in the brain. Proc Natl Acad Sci U S A 1994;91(6):2076-2080.

15. Vavra M, Ali MJ, Kang EW, Navalitloha Y, Ebert A, Allen CV, et al. Comparative pharmacokinetics of 14C-sucrose in RG-2 rat gliomas after intravenous and convection-enhanced delivery. Neuro Oncol 2004;6(2):104-112.

16. Groothuis DR, Ward S, Itskovich AC, Dobrescu C, Allen CV, Dills C, et al. Comparison of 14C-sucrose delivery to the brain by intravenous, intraventricular, and convection-enhanced intracerebral infusion. J Neurosurg 1999;90(2):321-331.

17. Lidar Z, Mardor Y, Jonas T, Pfeffer R, Faibel M, Nass D, et al. Convection-enhanced delivery of paclitaxel for the treatment of recurrent malignant glioma: a phase I/II clinical study. J Neurosurg 2004;100(3):472-479.

18. Rousseau J, Boudou C, Barth RF, Balosso J, Esteve F, Elleaume H. Enhanced survival and cure of F98 glioma-bearing rats following intracerebral delivery of carboplatin in combination with photon irradiation. Clin Cancer Res 2007;13(17):5195-5201.

19. Degen JW, Walbridge S, Vortmeyer AO, Oldfield EH, Lonser RR. Safety and efficacy of convection-enhanced delivery of gemcitabine or carboplatin in a malignant glioma model in rats. J Neurosurg 2003;99(5):893-898.

20. Vandergrift WA, Patel SJ, Nicholas JS, Varma AK. Convection-enhanced delivery of immunotoxins and radioisotopes for treatment of malignant gliomas. Neurosurg Focus 2006;20(4):E13.

21. Patel SJ, Shapiro WR, Laske DW, Jensen RL, Asher AL, Wessels BW, et al. Safety and feasibility of convection-enhanced delivery of Cotara for the treatment of malignant glioma: initial experience in 51 patients. Neurosurgery 2005;56(6):1243-1252; discussion 1252-1243.

22. Weber FW, Floeth F, Asher A, Bucholz R, Berger M, Prados M, et al. Local convection enhanced delivery of IL4-Pseudomonas exotoxin (NBI-3001) for treatment of patients with recurrent malignant glioma. Acta Neurochir Suppl 2003;88:93-103.

23. Rainov NG, Soling A. Clinical studies with targeted toxins in malignant glioma. Rev Recent Clin Trials 2006;1(2):119-131.

24. Muro K, Das S, Raizer JJ. Convection-enhanced and local delivery of targeted cytotoxins in the treatment of malignant gliomas. Technol Cancer Res Treat 2006;5(3):201-213.

25. Saito R, Bringas JR, Panner A, Tamas M, Pieper RO, Berger MS, et al. Convection-enhanced delivery of tumor necrosis factor-related apoptosis-inducing ligand with systemic administration of temozolomide prolongs survival in an intracranial glioblastoma xenograft model. Cancer Res 2004;64(19):6858-6862.

26. Cunningham J, Oiwa Y, Nagy D, Podsakoff G, Colosi P, Bankiewicz KS. Distribution of AAV-TK following intracranial convection-enhanced delivery into rats. Cell Transplant 2000;9(5):585-594.

27. Nguyen JB, Sanchez-Pernaute R, Cunningham J, Bankiewicz KS. Convection-enhanced delivery of AAV-2 combined with heparin increases TK gene transfer in the rat brain. Neuroreport 2001;12(9):1961-1964.

28. Noble CO, Krauze MT, Drummond DC, Yamashita Y, Saito R, Berger MS, et al. Novel nanoliposomal CPT-11 infused by convection-enhanced delivery in intracranial tumors: pharmacology and efficacy. Cancer Res 2006;66(5):2801-2806.

29. Perlstein B, Ram Z, Daniels D, Ocherashvilli A, Roth Y, Margel S, et al. Convection-enhanced delivery of maghemite nanoparticles: Increased efficacy and MRI monitoring. Neuro Oncol 2008;10(2):153-161.

30. Wu G, Barth RF, Yang W, Kawabata S, Zhang L, Green-Church K. Targeted delivery of methotrexate to epidermal growth factor receptor-positive brain tumors by means of cetuximab (IMC-C225) dendrimer bioconjugates. Mol Cancer Ther 2006;5(1):52-59.

31. Linninger AA, Somayaji MR, Mekarski M, Zhang L. Prediction of convection-enhanced drug delivery to the human brain. J Theor Biol 2008;250(1):125-138.

32. Prokop A, Davidson JM. Nanovehicular intracellular delivery systems. J Pharm Sci 2008:*in press*.

33. Clarke RH, Horsley V. On a method of investigating the deep ganglia and tracts of the central nervous system (cerebellum). Br Med J 1906(2):1799-1800.

34. Spiegel EA, Wycis HT, Marks M, Lee AJ. Stereotaxic Apparatus for Operations on the Human Brain. Science 1947;106(2754):349-350.

35. Roberge D, Souhami L. Stereotactic radiosurgery in the management of intracranial gliomas. Technol Cancer Res Treat 2003;2(2):117-125.

36. Jain RK. Delivery of novel therapeutic agents in tumors: physiological barriers and strategies. J Natl Cancer Inst 1989;81(8):570-576.

37. Kroin JS, Penn RD. Intracerebral chemotherapy: chronic microinfusion of cisplatin. Neurosurgery 1982;10(3):349-354.

38. Morrison PF, Dedrick RL. Transport of cisplatin in rat brain following microinfusion: an analysis. J Pharm Sci 1986;75(2):120-128.

39. Morrison PF, Chen MY, Chadwick RS, Lonser RR, Oldfield EH. Focal delivery during direct infusion to brain: role of flow rate, catheter diameter, and tissue mechanics. Am J Physiol 1999;277(4 Pt 2):R1218-1229.

40. Morrison PF, Laske DW, Bobo H, Oldfield EH, Dedrick RL. High-flow microinfusion: tissue penetration and pharmacodynamics. Am J Physiol 1994;266(1 Pt 2):R292-305.

41. Chen ZJ, Gillies GT, Broaddus WC, Prabhu SS, Fillmore H, Mitchell RM, et al. A realistic brain tissue phantom for intraparenchymal infusion studies. J Neurosurg 2004;101(2):314-322.

42. Laske DW, Morrison PF, Lieberman DM, Corthesy ME, Reynolds JC, Stewart-Henney PA, et al. Chronic interstitial infusion of protein to primate brain: determination of drug distribution and clearance with single-photon emission computerized tomography imaging. J Neurosurg 1997;87(4):586-594.

43. Lonser RR, Walbridge S, Garmestani K, Butman JA, Walters HA, Vortmeyer AO, et al. Successful and safe perfusion of the primate brainstem: in vivo magnetic resonance imaging of macromolecular distribution during infusion. J Neurosurg 2002;97(4):905-913.

44. Saito R, Bringas JR, McKnight TR, Wendland MF, Mamot C, Drummond DC, et al. Distribution of liposomes into brain and rat brain tumor models by convection-enhanced delivery monitored with magnetic resonance imaging. Cancer Res 2004;64(7):2572-2579.

45. Raghavan R, Brady ML, Rodriguez-Ponce MI, Hartlep A, Pedain C, Sampson JH. Convection-enhanced delivery of therapeutics for brain disease, and its optimization. Neurosurg Focus 2006;20(4):E12.

46. Krauze MT, Saito R, Noble C, Tamas M, Bringas J, Park JW, et al. Reflux-free cannula for convection-enhanced high-speed delivery of therapeutic agents. J Neurosurg 2005;103(5):923-929.

47. Allard E, Hindre F, Passirani C, Lemaire L, Lepareur N, Noiret N, et al. (188)Re-loaded lipid nanocapsules as a promising radiopharmaceutical carrier for internal radiotherapy of malignant gliomas. Eur J Nucl Med Mol Imaging 2008:*In press*.

48. Kroll RA, Pagel MA, Muldoon LL, Roman-Goldstein S, Neuwelt EA. Increasing volume of distribution to the brain with interstitial infusion: dose, rather than convection, might be the most important factor. Neurosurgery 1996;38(4):746-752; discussion 752-744.

49. Chen MY, Lonser RR, Morrison PF, Governale LS, Oldfield EH. Variables affecting convection-enhanced delivery to the striatum: a systematic examination of rate of infusion, cannula size, infusate concentration, and tissue-cannula sealing time. J Neurosurg 1999;90(2):315-320.

50. Bauman MA, Gillies GT, Raghavan R, Brady ML, Pedain C. Physical characterization of neurocatheter performance in a brain phantom gelatin with nanoscale porosity: Steady-state and oscillatory flows. Nanotechnology 2004;15(1):92-97.

51. Fiandaca MS, Forsayeth JR, Dickinson PJ, Bankiewicz KS. Image-guided convection-enhanced delivery platform in the treatment of neurological diseases. Neurotherapeutics 2008;5(1):123-127.

52. Kunwar S. Convection enhanced delivery of IL13-PE38QQR for treatment of recurrent malignant glioma: presentation of interim findings from ongoing phase 1 studies. Acta Neurochir Suppl 2003;88:105-111.

53. Tanner PG, Holtmannspotter M, Tonn JC, Goldbrunner R. Effects of drug efflux on convection-enhanced paclitaxel delivery to malignant gliomas: technical note. Neurosurgery 2007;61(4):E880-882; discussion E882.

54. Neeves KB, Sawyer AJ, Foley CP, Saltzman WM, Olbricht WL. Dilation and degradation of the brain extracellular matrix enhances penetration of infused polymer nanoparticles. Brain Res 2007;1180:121-132.

55. Hadaczek P, Yamashita Y, Mirek H, Tamas L, Bohn MC, Noble C, et al. The "perivascular pump" driven by arterial pulsation is a powerful mechanism for the distribution of therapeutic molecules within the brain. Mol Ther 2006;14(1):69-78.

56. Sandberg DI, Edgar MA, Souweidane MM. Convection-enhanced delivery into the rat brainstem. J Neurosurg 2002;96(5):885-891.

57. Dickinson PJ, LeCouteur RA, Higgins RJ, Bringas JR, Roberts B, Larson RF, et al. Canine model of convection-enhanced delivery of liposomes containing CPT-11 monitored with real-time magnetic resonance imaging: laboratory investigation. J Neurosurg 2008;108(5):989-998.

58. Croteau D, Walbridge S, Morrison PF, Butman JA, Vortmeyer AO, Johnson D, et al. Real-time in vivo imaging of the convective distribution of a low-molecular-weight tracer. J Neurosurg 2005;102(1):90-97.

59. Sampson JH, Raghavan R, Provenzale JM, Croteau D, Reardon DA, Coleman RE, et al. Induction of hyperintense signal on T2-weighted MR images correlates with infusion distribution from intracerebral convection-enhanced delivery of a tumor-targeted cytotoxin. AJR Am J Roentgenol 2007;188(3):703-709.

60. Sampson JH, Brady ML, Petry NA, Croteau D, Friedman AH, Friedman HS, et al. Intracerebral infusate distribution by convection-enhanced delivery in humans with malignant gliomas: descriptive effects of target anatomy and catheter positioning. Neurosurgery 2007;60(2 Suppl 1):ONS89-98; discussion ONS98-89.

61. Prabhu SS, Broaddus WC, Gillies GT, Loudon WG, Chen ZJ, Smith B. Distribution of macromolecular dyes in brain using positive pressure infusion: a model for direct controlled delivery of therapeutic agents. Surg Neurol 1998;50(4):367-375; discussion 375.

62. Cho K, Wang X, Nie S, Chen ZG, Shin DM. Therapeutic nanoparticles for drug delivery in cancer. Clin Cancer Res 2008;14(5):1310-1316.

63. Hamoudeh M, Kamleh MA, Diab R, Fessi H. Radionuclides delivery systems for nuclear imaging and radiotherapy of cancer. Adv Drug Deliv Rev 2008;60(12):1329-1346.

64. Kobayashi H, Brechbiel MW. Dendrimer-based nanosized MRI contrast agents. Curr Pharmaceut Biotechnol 2004;5(6):539-549.

65. Lanza GM, Winter PM, Caruthers SD, Morawski AM, Schmieder AH, Crowder KC, et al. Magnetic resonance molecular imaging with nanoparticles. J Nucl Cardiol 2004;11(6):733-743.

66. Peer D, Karp JM, Hong S, Farokhzad OC, Margalit R, Langer R. Nanocarriers as an emerging platform for cancer therapy. Nat Nanotechnol 2007;2(12):751-760.

67. Garcion E, Lamprecht A, Heurtault B, Paillard A, Aubert-Pouessel A, Denizot B, et al. A new generation of anticancer, drug-loaded, colloidal vectors reverses multidrug resistance in glioma and reduces tumor progression in rats. Mol Cancer Ther 2006;5(7):1710-1722.

68. Jabr-Milane LS, van Vlerken LE, Yadav S, Amiji MM. Multi-functional nanocarriers to overcome tumor drug resistance. Cancer Treat Rev 2008:*in press*.

69. Wong HL, Bendayan R, Rauth AM, Xue HY, Babakhanian K, Wu XY. A mechanistic study of enhanced doxorubicin uptake and retention in multidrug resistant breast cancer cells using a polymer-lipid hybrid nanoparticle system. J Pharmacol Exp Ther 2006;317(3):1372-1381.

70. Inoue T, Yamashita Y, Nishihara M, Sugiyama S, Sonoda Y, Kumabe T, et al. Therapeutic efficacy of a polymeric micellar doxorubicin infused by convection-enhanced delivery against intracranial 9L brain tumor models. Neuro Oncol 2008:*In press*.

71. Drummond DC, Meyer O, Hong K, Kirpotin DB, Papahadjopoulos D. Optimizing liposomes for delivery of chemotherapeutic agents to solid tumors. Pharmacol Rev 1999;51(4):691-743.

72. Samad A, Sultana Y, Aqil M. Liposomal drug delivery systems: An update review. Curr Drug Deliv 2007;4(4):297-305.

73. Kreuter J. Nanoparticles. In: Swarbrick J, Boylan, J.C. , editor. Encyclopedia of Pharmaceutical Technology
New York M. Dekker 1994. p. 165-190.

74. Kreuter J. Nanoparticles as drug delivery systems In: Nalwa HS, editor. Encyclopedia of Pharmaceutical Technology
Stevenson Ranch, USA: American Scientific Publishers 2004. p. 161-180.

75. Kreuter J. Nanoparticles-a historical perspective. Int J Pharm 2007;331(1):1-10.

76. Jain KK. Use of nanoparticles for drug delivery in glioblastoma multiforme. Expert Rev Neurother 2007;7(4):363-372.

77. Gingras M, Raimundo JM, Chabre YM. Cleavable dendrimers. Angew Chem Int Ed 2007;46(7):1010-1017.

78. Bai S, Thomas C, Rawat A, Ahsan F. Recent progress in dendrimer-based nanocarriers. Crit Rev Ther Drug Carrier Syst 2006;23(6):437-495.

79. Sutton D, Nasongkla N, Blanco E, Gao J. Functionalized micellar systems for cancer targeted drug delivery. Pharm Res 2007;24(6):1029-1046.

80. Frank JA, Kalish H, Jordan EK, Anderson SA, Pawelczyk E, Arbab AS. Color transformation and fluorescence of Prussian blue-positive cells: implications for histologic verification of cells labeled with superparamagnetic iron oxide nanoparticles. Mol Imaging 2007;6(3):212-218.

81. Maysinger D, Lovric J. Quantum dots and other fluorescent nanoparticles: quo vadis in the cell? Adv Exp Med Biol 2007;620:156-167.

82. Mulder WJM, Griffioen AW, Strijkers GJ, Cormode DP, Nicolay K, Fayad ZA. Magnetic and fluorescent nanoparticles for multimodality imaging. Nanomedicine 2007;2(3):307-324.

83. Ballot S, Noiret N, Hindre F, Denizot B, Garin E, Rajerison H, et al. 99mTc/188Re-labelled lipid nanocapsules as promising radiotracers for imaging and therapy: formulation and biodistribution. Eur J Nucl Med Mol Imaging 2006;33(5):602-607.

84. MacKay JA, Deen DF, Szoka FC, Jr. Distribution in brain of liposomes after convection enhanced delivery; modulation by particle charge, particle diameter, and presence of steric coating. Brain Res 2005;1035(2):139-153.

85. Celebi O, Uzum C, Shahwan T, Erten HN. A radiotracer study of the adsorption behavior of aqueous Ba(2+) ions on nanoparticles of zero-valent iron. J Hazard Mater 2007;148(3):761-767.

86. Pereira MA, Mosqueira VC, Vilela JM, Andrade MS, Ramaldes GA, Cardoso VN. PLA-PEG nanocapsules radiolabeled with 99mTechnetium-HMPAO: release properties and physicochemical characterization by atomic force microscopy and photon correlation spectroscopy. Eur J Pharm Sci 2008;33(1):42-51.

87. Duguet E, Vasseur S, Mornet S, Devoisselle JM. Magnetic nanoparticles and their applications in medicine. Nanomedicine (London, England) 2006;1(2):157-168.

88. Jun YW, Jang JT, Cheon J. Magnetic nanoparticle assisted molecular MR imaging. Advances in experimental medicine and biology 2007;620:85-106.

89. Huang SK, Lee KD, Hong K, Friend DS, Papahadjopoulos D. Microscopic localization of sterically stabilized liposomes in colon carcinoma-bearing mice. Cancer Res 1992;52(19):5135-5143.

90. Mamot C, Nguyen JB, Pourdehnad M, Hadaczek P, Saito R, Bringas JR, et al. Extensive distribution of liposomes in rodent brains and brain tumors following convection-enhanced delivery. J Neurooncol 2004;68(1):1-9.

91. Saito R, Krauze MT, Noble CO, Tamas M, Drummond DC, Kirpotin DB, et al. Tissue affinity of the infusate affects the distribution volume during convection-enhanced delivery into rodent brains: implications for local drug delivery. J Neurosci Methods 2006;154(1-2):225-232.

92. Litzinger DC, Buiting AM, van Rooijen N, Huang L. Effect of liposome size on the circulation time and intraorgan distribution of amphipathic poly(ethylene glycol)-containing liposomes. Biochim Biophys Acta 1994;1190(1):99-107.

93. Abra RM, Schreier H, Szoka FC. The use of a new radioactive-iodine labeled lipid marker to follow in vivo disposition of liposomes: comparison with an encapsulated aqueous space marker. Res Commun Chem Pathol Pharmacol 1982;37(2):199-213.

94. Heurtault B, Saulnier P, Pech B, Proust JE, Benoit JP. A novel phase inversion-based process for the preparation of lipid nanocarriers. Pharm Res 2002;19(6):875-880.

95. Jestin E, Mougin-Degraef M, Faivre-Chauvet A, Remaud-Le Saec P, Hindre F, Benoit JP, et al. Radiolabeling and targeting of lipidic nanocapsules for applications in radioimmunotherapy. Q J Nucl Med Mol Imaging 2007;51(1):51-60.

96. Caravan P, Ellison JJ, McMurry TJ, Lauffer RB. Gadolinium(III) Chelates as MRI Contrast Agents: Structure, Dynamics, and Applications. Chem Rev 1999;99(9):2293-2352.

97. Kotek J, Lebduskova P, Hermann P, Vander Elst L, Muller RN, Geraldes CF, et al. Lanthanide(III) complexes of novel mixed carboxylic-phosphorus acid derivatives of diethylenetriamine: a step towards more efficient MRI contrast agents. Chemistry 2003;9(23):5899-5915.

98. Bulte JW, Brooks RA, Moskowitz BM, Bryant LH, Jr., Frank JA. T1 and T2 relaxometry of monocrystalline iron oxide nanoparticles (MION-46L): theory and experiment. Acad Radiol 1998;5 Suppl 1:S137-140; discussion S145-136.

99. Bulte JW, Kraitchman DL. Iron oxide MR contrast agents for molecular and cellular imaging. NMR Biomed 2004;17(7):484-499.

100. Saito R, Krauze MT, Bringas JR, Noble C, McKnight TR, Jackson P, et al. Gadolinium-loaded liposomes allow for real-time magnetic resonance imaging of convection-enhanced delivery in the primate brain. Exp Neurol 2005;196(2):381-389.

101. Krauze MT, Forsayeth J, Park JW, Bankiewicz KS. Real-time imaging and quantification of brain delivery of liposomes. Pharm Res 2006;23(11):2493-2504.

102. Hergt R, Hiergeist R, Hilger I, Kaiser WA, Lapatnikov Y, Margel S, et al. Maghemite nanoparticles with very high AC-losses for application in RF-magnetic hyperthermia. J Magn Magn Mater 2004;270(3):345-357.

103. Neuwelt EA, Weissleder R, Nilaver G, Kroll RA, Roman-Goldstein S, Szumowski J, et al. Delivery of virus-sized iron oxide particles to rodent CNS neurons. Neurosurgery 1994;34(4):777-784.

104. Thorne RG, Nicholson C. In vivo diffusion analysis with quantum dots and dextrans predicts the width of brain extracellular space. Proc Natl Acad Sci U S A 2006;103(14):5567-5572.

105. Chen MY, Hoffer A, Morrison PF, Hamilton JF, Hughes J, Schlageter KS, et al. Surface properties, more than size, limiting convective distribution of virus-sized particles and viruses in the central nervous system. J Neurosurg 2005;103(2):311-319.

106. Berry CC, Wells S, Charles S, Curtis AS. Dextran and albumin derivatised iron oxide nanoparticles: influence on fibroblasts in vitro. Biomaterials 2003;24(25):4551-4557.

107. Lemarchand C, Gref R, Passirani C, Garcion E, Petri B, Muller R, et al. Influence of polysaccharide coating on the interactions of nanoparticles with biological systems. Biomaterials 2006;27(1):108-118.

108. Natsume A, Mizuno M, Ryuke Y, Yoshida J. Antitumor effect and cellular immunity activation by murine interferon-beta gene transfer against intracerebral glioma in mouse. Gene Ther 1999;6(9):1626-1633.

109. Gao X, Huang L. Cationic liposome-mediated gene transfer. Gene Ther 1995;2(10):710-722.

110. Johnson EM, Berk DA, Jain RK, Deen WM. Hindered diffusion in agarose gels: test of effective medium model. Biophys J 1996;70(2):1017-1023.

111. Kosto KB, Panuganti S, Deen WM. Equilibrium partitioning of Ficoll in composite hydrogels. J Colloid Interface Sci 2004;277(2):404-409.

112. Mardor Y, Rahav O, Zauberman Y, Lidar Z, Ocherashvilli A, Daniels D, et al. Convection-enhanced drug delivery: increased efficacy and magnetic resonance image monitoring. Cancer Res 2005;65(15):6858-6863.

113. Vogelbaum MA. Convection enhanced delivery for treating brain tumors and selected neurological disorders: symposium review. J Neurooncol 2007;83(1):97-109.

114. Hamilton JF, Morrison PF, Chen MY, Harvey-White J, Pernaute RS, Phillips H, et al. Heparin coinfusion during convection-enhanced delivery (CED) increases the distribution of

the glial-derived neurotrophic factor (GDNF) ligand family in rat striatum and enhances the pharmacological activity of neurturin. Exp Neurol 2001;168(1):155-161.

115. Hadaczek P, Mirek H, Bringas J, Cunningham J, Bankiewicz K. Basic fibroblast growth factor enhances transduction, distribution, and axonal transport of adeno-associated virus type 2 vector in rat brain. Hum Gene Ther 2004;15(5):469-479.

116. Summerford C, Samulski RJ. Membrane-associated heparan sulfate proteoglycan is a receptor for adeno-associated virus type 2 virions. J Virol 1998;72(2):1438-1445.

117. Hsueh YP, Sheng M. Regulated expression and subcellular localization of syndecan heparan sulfate proteoglycans and the syndecan-binding protein CASK/LIN-2 during rat brain development. J Neurosci 1999;19(17):7415-7425.

118. Hsueh YP, Yang FC, Kharazia V, Naisbitt S, Cohen AR, Weinberg RJ, et al. Direct interaction of CASK/LIN-2 and syndecan heparan sulfate proteoglycan and their overlapping distribution in neuronal synapses. J Cell Biol 1998;142(1):139-151.

119. Mastakov MY, Baer K, Xu R, Fitzsimons H, During MJ. Combined injection of rAAV with mannitol enhances gene expression in the rat brain. Mol Ther 2001;3(2):225-232.

120. Heath JR, Davis ME. Nanotechnology and cancer. Annu Rev Med 2008;59:251-265.

121. Allard E, Passirani C, Garcion E, Pigeon P, Vessieres A, Jaouen G, et al. Lipid nanocapsules loaded with an organometallic tamoxifen derivative as a novel drug-carrier system for experimental malignant gliomas. J Control Release 2008:*in press*.

122. Muggia FM. Liposomal encapsulated anthracyclines: new therapeutic horizons. Curr Oncol Rep 2001;3(2):156-162.

123. Gabizon AA. Liposomal anthracyclines. Hematol Oncol Clin North Am 1994;8(2):431-450.

124. Gabizon A, Isacson R, Libson E, Kaufman B, Uziely B, Catane R, et al. Clinical studies of liposome-encapsulated doxorubicin. Acta Oncol 1994;33(7):779-786.

125. Park JW, Hong K, Kirpotin DB, Meyer O, Papahadjopoulos D, Benz CC. Anti-HER2 immunoliposomes for targeted therapy of human tumors. Cancer Lett 1997;118(2):153-160.

126. Drummond DC, Noble CO, Guo Z, Hong K, Park JW, Kirpotin DB. Development of a highly active nanoliposomal irinotecan using a novel intraliposomal stabilization strategy. Cancer Res 2006;66(6):3271-3277.

127. Saito R, Krauze MT, Noble CO, Drummond DC, Kirpotin DB, Berger MS, et al. Convection-enhanced delivery of Ls-TPT enables an effective, continuous, low-dose chemotherapy against malignant glioma xenograft model. Neuro Oncol 2006;8(3):205-214.

128. Yamashita Y, Krauze MT, Kawaguchi T, Noble CO, Drummond DC, Park JW, et al. Convection-enhanced delivery of a topoisomerase I inhibitor (nanoliposomal topotecan) and a topoisomerase II inhibitor (pegylated liposomal doxorubicin) in intracranial brain tumor xenografts. Neuro Oncol 2007;9(1):20-28.

129. Krauze MT, Noble CO, Kawaguchi T, Drummond D, Kirpotin DB, Yamashita Y, et al. Convection-enhanced delivery of nanoliposomal CPT-11 (irinotecan) and PEGylated liposomal doxorubicin (Doxil) in rodent intracranial brain tumor xenografts. Neuro Oncol 2007;9(4):393-403.

130. Arwert E, Hingtgen S, Figueiredo JL, Bergquist H, Mahmood U, Weissleder R, et al. Visualizing the dynamics of EGFR activity and antiglioma therapies in vivo. Cancer Res 2007;67(15):7335-7342.

131. Ren H, Yang BF, Rainov NG. Receptor tyrosine kinases as therapeutic targets in malignant glioma. Rev Recent Clin Trials 2007;2(2):87-101.

132. Weppler SA, Li Y, Dubois L, Lieuwes N, Jutten B, Lambin P, et al. Expression of EGFR variant vIII promotes both radiation resistance and hypoxia tolerance. Radiother Oncol 2007;83(3):333-339.

133. Wu G, Barth RF, Yang W, Lee RJ, Tjarks W, Backer MV, et al. Boron containing macromolecules and nanovehicles as delivery agents for neutron capture therapy. Anticancer Agents Med Chem 2006;6(2):167-184.

134. Yamamoto T, Nakai K, Matsumura A. Boron neutron capture therapy for glioblastoma. Cancer Lett 2008;262(2):143-152.

135. Barth RF, Coderre JA, Vicente MG, Blue TE. Boron neutron capture therapy of cancer: current status and future prospects. Clin Cancer Res 2005;11(11):3987-4002.

136. Wu G, Yang W, Barth RF, Kawabata S, Swindall M, Bandyopadhyaya AK, et al. Molecular targeting and treatment of an epidermal growth factor receptor-positive glioma using boronated cetuximab. Clin Cancer Res 2007;13(4):1260-1268.

137. Krauze MT, Vandenberg SR, Yamashita Y, Saito R, Forsayeth J, Noble C, et al. Safety of real-time convection-enhanced delivery of liposomes to primate brain: a long-term retrospective. Exp Neurol 2008;210(2):638-644.

138. Krauze MT, McKnight TR, Yamashita Y, Bringas J, Noble CO, Saito R, et al. Real-time visualization and characterization of liposomal delivery into the monkey brain by magnetic resonance imaging. Brain Res Brain Res Protoc 2005;16(1-3):20-26.

139. Krauze MT, Saito R, Noble C, Bringas J, Forsayeth J, McKnight TR, et al. Effects of the perivascular space on convection-enhanced delivery of liposomes in primate putamen. Exp Neurol 2005;196(1):104-111.

140. Foster ES, Carrillo JM, Patnaik AK. Clinical signs of tumors affecting the rostral cerebrum in 43 dogs. J Vet Intern Med 1988;2(2):71-74.

141. Lipsitz D, Higgins RJ, Kortz GD, Dickinson PJ, Bollen AW, Naydan DK, et al. Glioblastoma multiforme: clinical findings, magnetic resonance imaging, and pathology in five dogs. Vet Pathol 2003;40(6):659-669.

142. Snyder JM, Shofer FS, Van Winkle TJ, Massicotte C. Canine intracranial primary neoplasia: 173 cases (1986-2003). J Vet Intern Med 2006;20(3):669-675.

143. Heidner GL, Kornegay JN, Page RL, Dodge RK, Thrall DE. Analysis of survival in a retrospective study of 86 dogs with brain tumors. J Vet Intern Med 1991;5(4):219-226.

144. Lopez KA, Waziri AE, Canoll PD, Bruce JN. Convection-enhanced delivery in the treatment of malignant glioma. Neurol Res 2006;28(5):542-548.

145. Laske DW, Youle RJ, Oldfield EH. Tumor regression with regional distribution of the targeted toxin TF-CRM107 in patients with malignant brain tumors. Nat Med 1997;3(12):1362-1368.

146. Hall WA, Rustamzadeh E, Asher AL. Convection-enhanced delivery in clinical trials. Neurosurg Focus 2003;14(2).

147. Ferguson S, Lesniak MS. Convection enhanced drug delivery of novel therapeutic agents to malignant brain tumors. Curr Drug Deliv 2007;4(2):169-180.

148. Rainov NG, Gorbatyuk K, Heidecke V. Clinical trials with intracerebral convection-enhanced delivery of targeted toxins in malignant glioma. Rev Recent Clin Trials 2008;3(1):2-9.

149. Ren H, Boulikas T, Lundstrom K, Soling A, Warnke PC, Rainov NG. Immunogene therapy of recurrent glioblastoma multiforme with a liposomally encapsulated replication-incompetent Semliki forest virus vector carrying the human interleukin-12 gene--a phase I/II clinical protocol. J Neurooncol 2003;64(1-2):147-154.

150. Klatzmann D, Valery CA, Bensimon G, Marro B, Boyer O, Mokhtari K, et al. A phase I/II study of herpes simplex virus type 1 thymidine kinase "suicide" gene therapy for recurrent glioblastoma. Study Group on Gene Therapy for Glioblastoma. Hum Gene Ther 1998;9(17):2595-2604.

151. Rainov NG. A phase III clinical evaluation of herpes simplex virus type 1 thymidine kinase and ganciclovir gene therapy as an adjuvant to surgical resection and radiation in adults with previously untreated glioblastoma multiforme. Hum Gene Ther 2000;11(17):2389-2401.

152. Voges J, Reszka R, Gossmann A, Dittmar C, Richter R, Garlip G, et al. Imaging-guided convection-enhanced delivery and gene therapy of glioblastoma. Ann Neurol 2003;54(4):479-487.

CHAPITRE 1

Radiothérapie interne par administration de nanocapsules lipidiques encapsulant un complexe de Rhénium-188 pour la thérapie des gliomes.

Radiothérapie interne par administration de nanocapsules lipidiques encapsulant un complexe de Rhénium-188 pour la thérapie des gliomes.

Les nanocapsules lipidiques encapsulant un complexe lipophile de Rhénium-188 (^{188}Re-SSS LNC) ont été évaluées en tant que radiopharmaceutique pour la radiothérapie interne des gliomes malins. Cette étude vise à évaluer leur efficacité antitumorale après administration locale par "convection enhanced delivery" (CED) dans un modèle de tumeur 9L chez le rat. Ce chapitre décrit tout d'abord les modifications apportées à la formulation des ^{188}Re-SSS LNC initialement décrite par Ballot *et al.* dans l'optique d'une application intracérébrale et caractérise l'encapsulation du complexe radioactif. Elle évalue également l'intérêt du vecteur dans cette application en suivant l'élimination du ^{188}Re pour des rats traités par les nanocapsules lipidiques ou par une solution aqueuse de perrhénate de ^{188}Re, qui est la substance directement éluée du générateur. La rétention du traceur est appréciée en maintenant les animaux dans des cages à métabolisme pendant 72H après injection. L'efficacité du traitement est ensuite évaluée par la mise en place d'une étude de survie. Des rats femelles Fisher sont traités par une injection unique de ^{188}Re-SSS LNC en CED 6 jours après l'implantation de la tumeur. Les rats sont randomisés dans différents groupes selon les doses reçues (12, 10, 8, et 3Gy) et comparés à des animaux traités par une solution de perrhénate de ^{188}Re (4Gy), par une suspension de LNC blanches ou à des animaux non traités. Pendant toute la durée de l'étude, la toxicité du traitement est évaluée par le suivi des variations de poids des animaux. Enfin, ce travail évalue la toxicité locale d'une telle administration par l'étude des animaux longs survivants (médiane de survie > 100 jours) en imagerie et en spectroscopie par résonance magnétique.

Eur J Nucl Med Mol Imaging (2008) 35:1838–1846
DOI 10.1007/s00259-008-0735-z

ORIGINAL ARTICLE

^{188}Re-loaded lipid nanocapsules as a promising radiopharmaceutical carrier for internal radiotherapy of malignant gliomas

E. Allard · F. Hindre · C. Passirani · L. Lemaire · N. Lepareur · N. Noiret · P. Menei · J-P. Benoit

Received: 14 November 2007 / Accepted: 22 January 2008 / Published online: 9 May 2008

Abstract
Purpose Lipid nanocapsules (LNC) entrapping lipophilic complexes of ^{188}Re (^{188}Re(S_3CPh)$_2$(S_2CPh) [^{188}Re-SSS]) were investigated as a novel radiopharmaceutical carrier for internal radiation therapy of malignant gliomas. The present study was designed to evaluate the efficacy of intra-cerebral administration of ^{188}Re-SSS LNC by means of convection-enhanced delivery (CED) on a 9L rat brain tumour model.
Methods Female Fischer rats with 9L glioma were treated with a single injection of ^{188}Re-SSS LNC by CED 6days after cell implantation. Rats were put into random groups according to the dose infused: 12, 10, 8 and 3Gy in comparison with blank LNC, perrhenate solution (4Gy) and non-treated animals. The radionuclide brain retention level was evaluated by measuring ^{188}Re elimination in faeces and urine over 72h after the CED injection. The therapeutic effect of ^{188}Re-SSS LNC was assessed based on animal survival.
Results CED of ^{188}Re perrhenate solution resulted in rapid drug clearance with a brain $T_{1/2}$ of 7h. In contrast, when administered in LNC, ^{188}Re tissue retention was greatly prolonged, with only 10% of the injected dose being eliminated at 72h. Rat median survival was significantly improved for the group treated with 8Gy ^{188}Re-SSS LNC compared to the control group and blank LNC-treated animals. The increase in the median survival time was about 80% compared to the control group; 33% of the animals were long-term survivors. The dose of 8Gy proved to be a very effective dose, between toxic (10–12Gy) and ineffective (3–4Gy) doses.
Conclusions These findings show that CED of ^{188}Re-loaded LNC is a safe and potent anti-tumour system for treating malignant gliomas. Our data are the first to show the in vivo efficacy of ^{188}Re internal radiotherapy for the treatment of brain malignancy.

Keywords Lipid nanocapsules · ^{188}Re · 9L glioma model · convection-enhanced delivery · MRI

E. Allard · F. Hindre (✉) · C. Passirani · L. Lemaire · P. Menei · J.-P. Benoit
INSERM U646, Université d'Angers,
Angers 49100, France
e-mail: francois.hindre@univ-angers.fr

P. Menei
Département de Neurochirurgie, CHU d'Angers,
Angers 49033, France

N. Noiret
UMR CNRS 6052, ENSCR,
Rennes-Beaulieu 35700, France

N. Lepareur
Centre Eugène Marquis, Centre de médecine nucléaire,
Rennes 35700, France

Introduction

Malignant gliomas are still associated with a poor prognosis despite advances in neurosurgery, radiotherapy and chemotherapy [1]. The median survival time after tumour resection, external beam irradiation and various forms of chemotherapy still lies in the range of 12months, and more than 80% of patients have fatal local tumour recurrence [2]. Among many attempts to fight this disease,

conclusive results have often been associated with the use of radiotherapy, alone or in combination with chemotherapy. Whereas classic radiotherapy involves external sources of radiation, internal tumour radiotherapy uses a radioisotope that is conjugated to a suitable agent such as an antibody, a peptide or a nanocarrier. Several nanoscale carriers (nanoparticles, liposomes, water-soluble polymers, micelles and dendrimers) have been developed for the targeted delivery of diagnostic and therapeutic cancer agents [3]. These carriers can selectively target cancer sites and carry large payloads, thereby improving cancer detection and therapy effectiveness. However, for therapeutic cancer applications, only a few attempts of internal radiotherapy have been described for the treatment of malignant gliomas [4, 5]. Among all the therapeutic radiopharmaceuticals used for radionuclide imaging and therapy, ^{188}Re is of widespread interest due to its attractive physical and chemical properties [6] linked to its short physical half-life of 16.9h with 155keV gamma emissions for imaging and its 2.12MeV beta emission for therapy [7]. Furthermore, the availability of ^{188}Re from a generator at a reasonable cost has increased the clinical applications of ^{188}Re-labelled radiopharmaceuticals [8].

In a previous study, the formulation and biodistribution of ^{188}Re-labelled lipid nanocapsules (LNC) were assessed [9]. Neutral lipophilic complexes chosen for their affinity for hydrophobic substrates allowed the encapsulation of the radioelement in the LNC lipid core as well as labelling stability [10]. Prepared from a phase-inversion process [11], these LNC are characterised by a stable monodispersal size distribution and a small diameter in the range of 20 to 100nm. The present work has focused on the therapeutic application of such ^{188}Re$(S_2CPh)_2(S_2CPh)$ complex (^{188}Re-SSS) LNC on a 9L rat glioma model. Convection-enhanced delivery (CED) [12], a direct intra-cerebral drug delivery technique that uses a bulk flow mechanism to distribute molecules to clinically significant volumes of tissue, was used to administer ^{188}Re-SSS LNC into rat brains. The aim of this work was to test the capacity of different ^{188}Re dose-loaded nanocapsules to eradicate tumours by studying the prolonged survival time of 9L glioma-bearing rats in comparison with the injection of ^{188}Re perrhenate solution and blank LNC.

Materials and methods

Materials

Lipophilic Labrafac® CC (caprylic–capric acid triglycerides) was kindly provided by Gattefosse S.A. (Saint-Priest, France). Lipoïd® S75-3 (soybean lecithin at 69% of phosphatidylcholine) and Solutol® HS15 (a mixture of free polyethylene glycol 660 and polyethylene glycol 660 hydroxystearate) were a gift from Lipoïd Gmbh (Ludwigshafen, Germany) and BASF (Ludwigshafen, Germany), respectively. NaCl, dichloromethane and acetone were obtained from Prolabo (Fontenay-sous-bois, France). Deionised water was obtained from a Milli-Q plus system (Millipore, Paris, France).

Complex preparation

The lipophilic ^{188}Re-SSS [(*bis*(perthiobenzoato)(dithiobenzoato)rhenium(III)] was prepared according to a previously described process [9]. The radiochemical purity (RCP) of the ^{188}Re-SSS complex was checked by thin-layer chromatography as the ratio of migrated radioactivity to total radioactivity. Thin-layer chromatography was carried out using silica gel 60 F_{254} alumina plates (Merck) and a solution of petroleum ether/dichloromethane (6/4, v/v) as an eluant (Rf 0.70). The detection was evaluated by a phospho-imager apparatus (Packard, Cyclone storage phosphor system).

Nanocapsule formulation

The preparation of ^{188}Re-SSS LNC was based on a phase-inversion process described by Heurtault et al. [11]. The suspension was prepared by mixing all the components under magnetic stirring (37.5mg Lipoïd®, 423mg Solutol®, 514mg Labrafac®, 44.5mg NaCl and 1,481mg deionised water). Because of its precipitation in aqueous media, the ^{188}Re-SSS complex was first extracted with dichloromethane (1ml) and then added to the other components of the emulsion. The organic solvent was then removed by heating at 60°C for 15min. Three cycles of progressive heating and cooling between 85°C and 60°C were then carried out allowing the residual organic solvent to evaporate. At 70°C and during the last cycle, an irreversible shock was induced by dilution with cold deionised water (1ml at 2°C), leading to the formation of stable nanocapsules. Afterwards, slow magnetic stirring was applied to the suspension for 5min.

Nanocapsule characterisation

LNC were analysed for their size distribution using a Malvern Zetasizer® Nano Serie DTS 1060 (Malvern Instruments S.A., Worcestershire, UK). The complex formation yield was determined with a gamma counter (Packard Auto-Gamma 5,000 series) according to Eq. 1, and encapsulate rate was estimated according to Eq. 2. Before injection, ^{188}Re-SSS LNC were dialysed with deionised water at room temperature under magnetic stirring. Following this, dialysate samples were collected and counted to determine a dialysis recovery as shown in

Eq. 3. As referred to the starting perrhenate activity, labelling yield was calculated by Eq. 4.

$$\text{Complex formation yield (\%)} = \frac{^{188}\text{Re} - \text{SSS complex activity}}{\text{starting perrhenate solution activity}} \times 100 \quad (1)$$

$$\text{Encapsulation rate (\%)} = \frac{\text{LNC suspension activity}}{^{188}\text{Re} - \text{SSS complex activity}} \times 100 \quad (2)$$

$$\text{Dialysis recovery (\%)} = \frac{\text{LNC suspension activity after dialysis}}{\text{LNC suspension activity before dialysis}} \times 100 \quad (3)$$

$$\text{Labeling yield (\%)} = \frac{\text{LNC suspension activity after dialysis}}{\text{starting perrhenate solution activity}} \times 100 \quad (4)$$

Animal study

Animals and anaesthesia

Syngeneic Fischer F344 female rats weighing 150–175g were obtained from Charles River Laboratories France (L'Arbresle, France). All experiments were performed on 10- to 11-week-old female Fisher rats. The animals were anaesthetised with an intraperitoneal injection of 0.75–1.5ml/kg of a solution containing 2/3 ketamine (100mg/ml) (Clorketam®, Vétoquinol, Lure, France) and 1/3 xylazine (20mg/ml; Rompun®, Bayer, Puteaux, France). Animal care was carried out in strict accordance to the French Ministry of Agriculture regulations.

Cell culture and cell implantation

Rat gliosarcoma 9L cells were obtained from the European Collection of Cell Culture (Salisbury, UK, no. 94110705). The cells were grown at 37°C/5% CO_2 in Dulbecco's modified Eagle medium with glucose and L-glutamine (BioWhittaker, Verviers, Belgium) containing 10% foetal calf serum (FCS; BioWhittaker) and 1% antibiotic and antimycotic solution (Sigma, Saint-Quentin Fallavier, France). A cultured tumour monolayer was detached with trypsin-ethylenediamine tetraacetic acid, washed twice with Eagle's minimal essential medium without FCS or antibiotics, counted and re-suspended to the final concentration desired. For intra-cranial implantation, 10µl of 10^3 9L cell suspension were injected into the rat striatum at a flow rate of 2µl/min using a 10-µl syringe (Hamilton® glass syringe 700 series RN) with a 32-G needle (Hamilton®). For that purpose, rats were immobilised in a stereotaxic head frame (Lab Standard Stereotaxic; Stoelting, Chicago, IL). A sagittal incision was made through the skin, and a burr hole was drilled into the skull with a twist drill. The cannula coordinates were 1mm posterior from the bregma, 3mm lateral from the sagittal suture and 5mm below the dura (with the incisor bar set at 0mm). The needle was left in place for an additional 5min to avoid expulsion of the suspension from the brain during removal of the syringe, which was withdrawn very slowly (0.5mm/min).

Convection-enhanced delivery procedure

On day6, 60µl of the LNC suspension was injected by CED at the coordinates of the tumour cells. Infusions were performed at the depth of 5mm from the brain surface using a 10-µl Hamilton® syringe with a 32-G needle. This syringe was connected to a 100-µl Hamilton 22-G syringe containing the product (Harvard Apparatus, Les Ulis, France) through a cannula (CoExTM PE/PVC tubing, Harvard Apparatus). CED was performed with an osmotic pump PHD 2,000 infusion (Harvard Apparatus) by controlling a 0.5 µl/min rate for 2h.

Sub-groups

The rats treated with ^{188}Re-SSS LNC were put into four random sub-groups and received rhenium activity equivalent to 1.1 (group 1: $n = 5$; 3Gy), 2.8 (group 2: $n = 6$; 8Gy), 3.7 (group 3: $n = 4$; 10Gy) and 4.4MBq (group 4: $n = 4$; 12Gy), respectively. Group 5 received 60µl of ^{188}Re perrhenate solution equivalent to 1.5MBq ($n = 4$; 4Gy). Group 6 received blank LNC ($n = 7$), and rats of group 7 (control group) did not receive treatment by CED on day6 but were anaesthetised with the same protocol compared to the rats who underwent a CED infusion ($n = 8$). After treatment, rats from groups 4 and 5 were maintained in metabolism cages for 72h and were fed ad libitum. Urine and faeces were collected every 12h and measured with a gamma counter (Packard Auto-Gamma 5,000 series) to evaluate ^{188}Re elimination. Doses delivered to tumours were estimated according to Eq. 5:

$$D = \frac{A \times E_{\beta\text{moy}} \times 0.576 \times T}{d \times V \times \ln 2} \quad (5)$$

where $A = ^{188}$Re activity delivered to each rat, $E_{\beta\text{moy}}$ = mean energy, T = physical half-life (16.9h) and d and V = density and volume of the irradiated organ. The irradiated organ was considered to be a sphere with a radius equivalent to ^{188}Re range of beta particles in tissue (^{188}Re $R_{\text{tissue}} = 10.15$mm) [7] and with a density of 1.

MRI and ^{1}H-magnetic resonance spectroscopy

MRI was performed with a Bruker Avance DRX 300 (Germany) apparatus equipped with a vertical superwide-

Table 1 Physico-chemical characteristics of blank and ^{188}Re SSS LNC

	Mean particle size (nm)	Polydispersity index	Complex formation yield (%)	Encapsulation rate (%)	Dialysis recovery (%)	Labelling yield (%)
Blank LNC	55.7±1.7	0.084±0.003	–	–	–	–
^{188}Re-SSS LNC	55.5±11.5	0.208±0.051	77.6	96.7	98.5	73.9

bore magnet of 7T. Rapid qualitative T2-weighted images were obtained using rapid acquisition with relaxation enhancement (RARE) sequence (TR = 2,000ms; mean echo time (Tem) = 31.7ms; RARE factor = 8; FOV = 3 × 3cm; matrix 128 × 128; nine contiguous slices of 1mm, eight acquisitions). Magnetic resonance spectroscopy (MRS) was performed using a PRESS sequence with water suppression and cardiac triggering (Rapid Biomed GmbH, Germany). ^{1}H spectra were acquired with the following parameters: TR/TE = 1,500/11ms; NEX = 128; vowel size 27µl (3 × 3 × 3mm).

Statistical analysis

The Kaplan–Meier method was used to plot animal survival. Statistical significance was calculated using the log-rank test (Mantel–Cox Test). StatView software version 5.0 (SAS Institute) was used for that purpose, and tests were considered as significant with p values of less than 0.05. The different treatment groups were compared in terms of survival time, increase in survival time (IST_{median}%), maximal survival time and long-term survivors.

Results

Complex and nanocapsule characterisation

^{188}Re-SSS complexes were obtained with satisfactory RCP. Physico-chemical properties of the LNC are given in Table 1. In the proportions described, blank LNC were obtained with a mean size of 55.7 ± 1.7nm with a good polydispersity index (PI < 0.1). ^{188}Re-SSS LNC were measured at 55.5 ± 11.5nm, but an increase in polydispersity index (PI = 0.20) was observed. Measurement of LNC mean particle size before and after CED infusion showed that there was no size modification (data not shown). ^{188}Re complex formation yield was around 78%. Encapsulation of the ^{188}Re complex into LNC was very efficient (96.7%). Radiolabelling occurred during LNC formulation with important yields (98.5%) after elimination of ^{188}Re perrhenate, which was not incorporated into the complex by dialysis. ^{188}Re-SSS LNC were obtained with a final labelling yield of 73.9%.

Internal radiotherapy study

Descriptive and statistical data from the radiotherapy study are summarised in Table 2. Rats were considered as long-term survivors if they survived up to 100days after tumour implantation (four times the median survival of non-treated rats). As shown in Fig. 1, all animals of the control group died due to tumour progression by day27, and median survival was only 25days. Rats of group 6, which received a CED infusion of blank LNC, died within 33days post-implantation, and the median survival was 26days. There was no significant difference between these two groups (p > 0.05). The experiments established that rat median survival was improved significantly for group 3, which was treated

Table 2 Descriptive and statistical data from the radiotherapy study

		Median survival time (days)	IST median (%)	Maximal survival time (days)	Long-term survivors	p values versus control	p values versus blank LNC
1	12 Gy ^{188}Re-SSS LNC	27.5	10	>100	1	0.3210	0.3205
2	10 Gy ^{188}Re-SSS LNC	28.5	14	>100	1	0.0294	0.2386
3	8 Gy ^{188}Re-SSS LNC	45.0	80	>100	2	0.0003	0.0010
4	3 Gy ^{188}Re-SSS LNC	28.0	12	33	0	0.0277	0.4858
5	4 Gy ^{188}Re perrhenate	23.5	0	26	0	0.1575	0.0942
6	Blank LNC	26.0	4	33	0	0.1729	–
7	Control=no treatment	25.0	–	27	0	–	0.1729

The increases in median survival time (IST_{median}%) are calculated in comparison to the control group. Survival data were analysed using the log-rank test (Mantel–Cox test), which was considered as significant when the p values were less than 0.05.

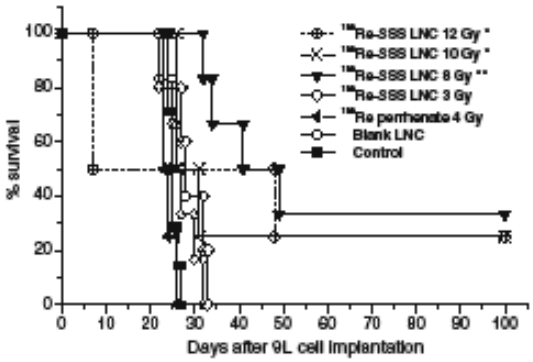

Fig. 1 Graph of Kaplan–Meier survival curve associated with treatment of rat bearing 9L glioma with single CED infusion of blank LNC, ^{188}Re-SSS LNC or ^{188}Re perrhenate. On day 6, rats were treated with 12 Gy ^{188}Re-SSS LNC (n=4; –⊕–), 10 Gy ^{188}Re-SSS LNC (n=4; –X–), 8 Gy ^{188}Re-SSS LNC (n=6; –▼–), 3 Gy ^{188}Re-SSS LNC (n=5; –◇–), 4 Gy ^{188}Re perrhenate (n=4; –◀–), blank LNC (n=7; –○–) or no treatment (n=8; –■–). Four rats (*asterisks*) were long-term survivors (>100 days)

with 8Gy ^{188}Re-SSS LNC compared with group 6 (blank LNC) and the control group (no treatment; $p = 0.0010$ and $p = 0.0003$, respectively). Animals treated with 8Gy ^{188}Re-SSS LNC showed excellent survival, with two of six rats surviving beyond day100, a median survival of 45days and an increase in the median survival time (IST_{median}) of 80% compared to the control group. At the highest dose of ^{188}Re activity (12Gy; group 1), 50% of the treated rats died after treatment, and median survival was only 27.5days. In spite of the presence of one long-term survivor in this group, comparisons with group 6 or 7 were not significant ($p = 0.32$). At the equivalent dose of 10Gy, treatment with ^{188}Re-SSS LNC resulted in median survival of 28.5days with one long-term survivor and an IST_{median} that relapsed to 14%. No significant difference was observed with the group treated with blank LNC ($p = 0.2386$), whereas a slight significant difference was noted for this group compared to the control group ($p = 0.0294$). Rats in group 4 treated with 3Gy ^{188}Re-SSS LNC died within 33days post-implantation; their median survival was 28.0days with an IST_{median} of 12%. A significant difference was only observed with the control group ($p = 0.0277$), whereas the significance was not shown with rats treated with blank LNC infusion ($p = 0.4858$). Group 5 treated with ^{188}Re perrhenate solution gave no positive results in terms of survival time because the median survival time was about 23.5days, and no significant difference was observed with rats from the control group ($p = 0.1575$).

To assess ^{188}Re elimination, urine and faeces in two groups (groups 4 and 5) were collected and measured. CED infusion of ^{188}Re perrhenate solution revealed that more than 80% was eliminated in 12h and about 94% after 72h post-CED (Fig. 2a). Rhenium brain half-disappearance time (brain $T_{1/2}$) was equivalent to 7h, and ^{188}Re perrhenate was mainly excreted by the kidneys as 99.4% of the total excreted radioactivity was recovered in urine (Fig. 2b). On the contrary, only 10% of ^{188}Re encapsulated in LNC was detected in urine and faeces 72h post-CED infusion. Among the 10% eliminated, LNC was mainly excreted in urine (75.8%; Fig. 2c).

Internal radiotherapy side effects

Two of the four rats infused with the highest dose of ^{188}Re-SSS LNC (12Gy) died on day7, which was 1day post-treatment. The two other rats showed clinical signs of toxicity including lethargy and a significant weight loss of 25% by day18 (Fig. 3). None of the other animals that underwent CED of 10, 8 or 3Gy ^{188}Re-SSS LNC died post-

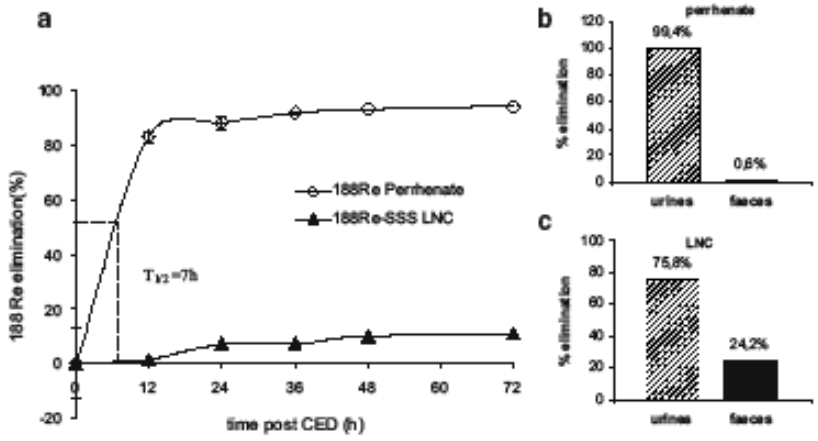

Fig. 2 ^{188}Re elimination measured in urine and faeces by a gamma counter during 72 h after CED infusion of ^{188}Re perrhenate and ^{188}Re-SSS LNC in 9L glioma bearing rats 6 days post-9L cell implantation (a). Repartition between urines and faeces for ^{188}Re perrhenate solution (b) and ^{188}Re-SSS LNC (c)

treatment. A slight weight loss of 3.5% and 4.3% was observed for the two groups treated with 10 and 8Gy ^{188}Re-SSS LNC, respectively, up to day12. However, a very quick revival of weight was detected for the group treated with 8Gy ^{188}Re-SSS LNC from day12 and up to day30. No weight loss was observed for the groups treated with the lowest ^{188}Re doses, i.e. 3Gy ^{188}Re-SSS LNC and 4Gy ^{188}Re perrhenate solution.

Tumour proliferation was evaluated by MRI images. In vivo MRI images were assessed at day16 (10days post-CED) on one rat of the control group versus one rat treated with 10Gy ^{188}Re-SSS LNC (Fig. 4). T2-weighted images of the non-treated rat showed a hyper-intense signal on the right striatum caused by tumour tissue (Fig. 4a). On the contrary, images taken on the rat treated by internal radiotherapy showed a hypo-intense signal probably due to the CED infusion of ^{188}Re-SSS LNC (Fig. 4b).

Late side effects were also followed by MRI and by ^{1}H-MRS (Fig. 5). Images taken on day 83 revealed that the rat treated by internal radiotherapy presented a lesion localised in the right brain, mainly in the striatum but which also affected the ventricle (Fig. 5a). This lesion was still present on days 100 and 140 (Fig. 5b–c). ^{1}H-MRS performed on day 100 revealed that spectral data for *N*-acetylaspartate (NAA), creatine (Cr) and choline were different in the right and left striata. In fact, the striatum affected by the lesion was characterised by a decrease in NAA and Cr associated with the presence of lactate (Fig. 5d).

Discussion

The development of an in-house ^{188}W/^{188}Re-generator has greatly increased the use of ^{188}Re for treating various diseases [13]. Many new radiopharmaceuticals labelled with ^{188}Re have been developed, and some of them are currently used in clinical trials. Among different carriers, LNC labelled with a lipophilic complex of ^{188}Re (^{188}Re-SSS) can be obtained with high yield and satisfactory RCP [9]. This study investigated the therapeutic potential of this carrier for the treatment of malignant brain tumours. Due to the presence of the blood–brain barrier (BBB), which restricts the delivery of systemically administered agents, in situ administration was carried out using a direct intracranial drug delivery technique, CED [14]. This technique, introduced in 1994 as a method to circumvent the BBB and enhance the distribution of therapeutic agents by local administration, represents a promising technique for brain tumour therapy [15].

The incorporation of ^{188}Re complexes in LNC did not change the size of the particles. Only the polydispersity index was slightly enhanced (PI=0.208) which represents a higher degree of heterogeneity but remained still inferior to 0.3. This can be explained by the presence of the lipophilic SSS complexes, which were required for ^{188}Re insertion inside the LNC core. ^{188}Re-SSS LNC could be obtained with a very high labelling yield. This result was expected as the incorporation of lipophilic molecules during the LNC formulation process generally led to high encapsulation efficiency whatever the radionuclide used [16, 17]. These rates are above those obtained in liposome formulations in which the radionuclides are generally post-inserted [18, 19]. In addition, agents directly infused into the brain in a small volume cannot readily disperse from their infusion site [20]; this is the reason why CED infusion was used to administer the nanocapsules. MacKay et al. studied the different parameters that can influence the distribution of liposomes in the brain [21]. Based upon these findings, the ideal nanoparticle for CED would be less than 100 nm in diameter, have a neutral or negative surface charge and would need a targeting ligand to adhere to a target cell. To minimise the dose fraction that could be scavenged by perivascular cells, mainly perivascular macrophages, nanoparticles should be shielded by polyethylene glycol (PEG) and infused at a high total lipid concentration. Our LNC, loaded with a ^{188}Re neutral complex, have a mean particle size of 55 nm, are mainly composed of lipids and are covered by a soft layer formed by PEG. They can be conjugated with the OX26 antibody, which binds them to transferrin receptors that are over-expressed both on brain

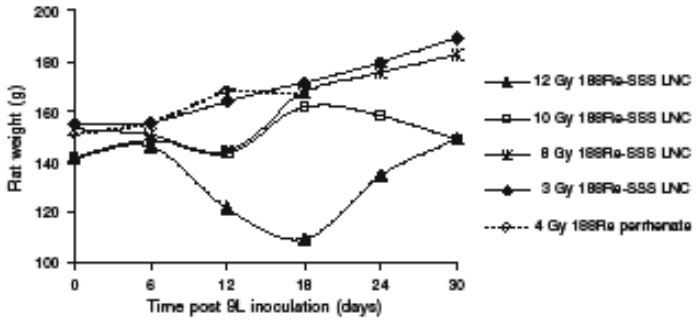

Fig. 3 Evolution of weight measurements during 30 days after 9L inoculation in rats that received ^{188}Re-SSS LNC or ^{188}Re perrhenate solution for internal radiotherapy

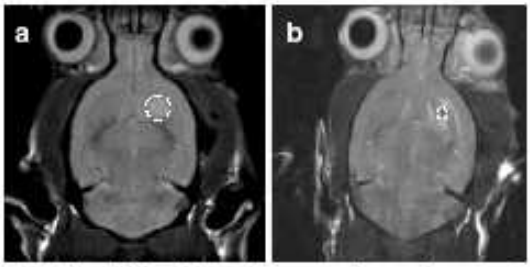

Fig. 4 T2-weighted axial magnetic resonance images of a non-treated rat (a) at day 16 after 9L inoculation compared with a long-term survivor rat which received 10 Gy ^{188}Re-SSS LNC at day 16 (b)

cerebral endothelial cells and on glioma cells [22]. Furthermore, Garcion et al. showed that LNC were able to penetrate intracellular compartments of glioma cells by interacting with cholesterol-rich microdomains [23]. Such characteristics confer ideal properties to LNC to be administered by CED in the rat brain.

To obtain a therapeutic effect, the elimination of the radionuclides deposed by CED in the brain must be as slow as possible. Because perrhenate ($^{188}ReO_4^-$) is the chemical form of ^{188}Re, which is obtained from the ^{188}W/^{188}Re generator by elution with physiological saline, $^{188}ReO_4^-$ infusion in Fisher rat brains was compared to ^{188}Re-SSS LNC. While it has been largely described that perrhenate is rapidly excreted via the urinary bladder following an intravenous injection [24], nothing was known about the elimination of such a solution following brain administration. A largely significant difference between a CED infusion of perrhenate and of ^{188}Re-SSS LNC was observed. Eighty percent of ^{188}Re in solution was eliminated after 12 h in accordance with findings by Knapp et al. [13] with 70% of free perrhenate in urine excretions after 12 h following an IV injection. ^{188}Re-SSS LNC were found to be a sustained residency system, which constitutes a major advantage (1% of elimination after 12 h). Like Noble et al. who showed that the encapsulation of CPT-11 in liposome resulted in at least 196-fold prolongation of residence time in brain tissue compared to free CPT-11 [25], we demonstrated that the lipophilic nature of LNC led to a long radionuclide brain retention time allowing improved tumour irradiation.

The internal radiotherapy study by CED administration of ^{188}Re-SSS LNC was carried out on a well-known 9L rat brain tumour model [26]. The inoculation of 9L cells usually results in 100% tumour take with untreated Fisher 344 rats with a median survival between 20 and 30 days after tumour inoculation [27]. In our study, neither the anaesthetic procedure nor the injection of blank LNC

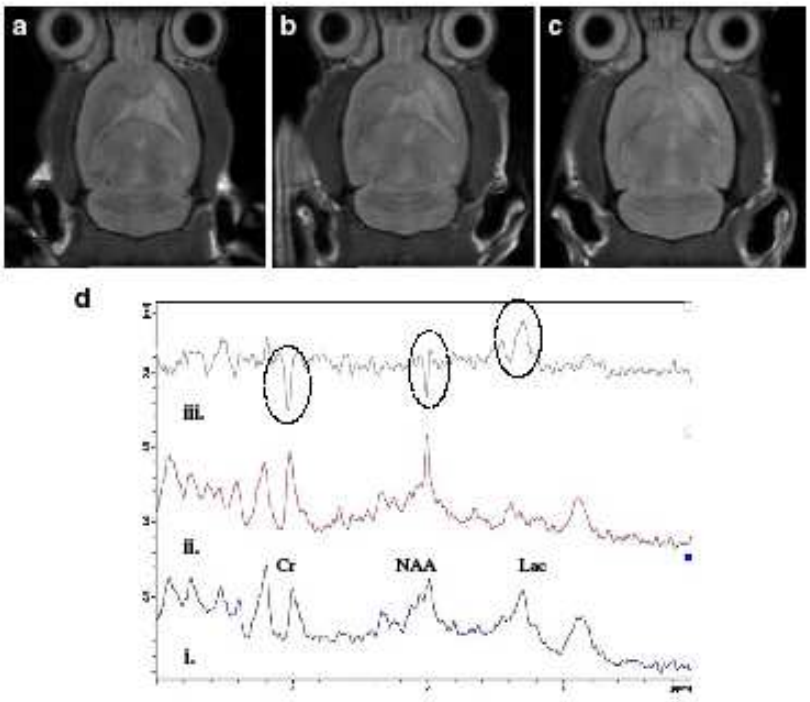

Fig. 5 T2-weighted axial magnetic resonance images of one long-term survivor rat that received 10 Gy ^{188}Re-SSS LNC at days 83, 100 and 140, respectively, for a, b and c. d represents the ^{1}H-MRS spectra realised at day 100. Signal intensities of creatine (*Cr*), *N*-acetyl aspartate (*NAA*) and Lactate (*Lac*) were compared between affected striatum (*i*) and safe striatum (*ii*). *iii* represents the difference between the two spectra

significantly modified the growth or lethality of the 9L gliomas, since the median survival time was 25 and 26 days for the untreated and the blank LNC groups, respectively. This was confirmed by MRI images where a tumour lesion is visible in a non-treated rat on day 16. As shown by Vonarbourg et al., 9L tumour growth is exponential since the tumour lesion volume is between 17±10 and 167± 19 μl between days 14 and 24 [28]. The median survival of the group treated by a CED infusion of ^{188}Re perrhenate solution was in the same range as none of the rats survived beyond 26 days. The hydrophilic nature of this solution provoked a very rapid elimination from the brain, which made tumour eradication impossible. Similar results were found by Vavra et al. for the administration of ^{14}C-sucrose, a small water-soluble compound in RG-2 rat gliomas, after CED infusion with less than 3% of the administered dose still present after 1 h in either the tumour or in surrounding brain tissues [29].

On the contrary, thanks to the high retention of LNC in rat brains, conclusive dose-dependent results were obtained with internal radiotherapy by ^{188}Re-SSS LNC. Toxicity was observed with the highest studied doses, especially for 12 Gy ^{188}Re-SSS LNC. In fact, 50% of the rats died 1 day post-treatment, and a significant weight loss was observed for the two rats left, combined with other signs of toxicity like lethargy, passivity and poor grooming. Despite the presence of a long-term survivor within this group, an internal irradiation dose of 12 Gy can be considered as a toxic dose. For the intermediate dose of 10 Gy, results were mitigated. A significant difference in median survival time was observed compared to the control group but not with the group that received blank LNC. The increase in the median survival time of 14% and the presence of one long-term survivor make this dosage midway between the effective and toxic doses. LNC with an equivalent dose of 8 Gy constituted the most efficient group treatment in terms of survival because a high increase in the median survival time of 80% was noted compared to the control group and because two rats from this group (33%) were long-term survivors. CED injection at this dosage seemed to be well tolerated since no side effects were observed except a very slight weight loss observed in the few days after treatment. For the smaller dose equivalent to 3 Gy, internal radiotherapy with ^{188}Re-SSS LNC had no effect on survival time. This dosage was considered to be ineffective.

A comparison between our technique and external beam radiotherapy (XRT) is difficult, since the schemes of irradiation for many studies are very varied and often associated with chemotherapy [30–32]. The main theoretical advantage of internal radionuclide therapy with ^{188}Re-SSS LNC is that radiation can be delivered selectively to subclinical tumours and metastases that are too small to be imaged and thereby cannot be treated by surgical excision or local XRT.

However, despite obvious benefits noted with internal radiotherapy, side effects in rats were observed in the latter phase of the study. Magnetic resonance images carried out on one long-term survivor treated with 10 Gy ^{188}Re-SSS LNC revealed lesions mainly contained in the right striatum, which was obviously not related to tumour tissue as it was still present on day 140 of the study. The histologic nature of the lesion was not identified but was linked to radiation injury. In fact, a decrease of the signal intensity for NAA and Cr with an increase of the lactate signal has often been described in cases of radiation injury [33, 34]. In an attempt to improve the therapeutic ratio, the delivery of ^{188}Re-SSS LNC in multiple fractions separated in time may improve efficacy by decreasing late effects on critical normal structures, while maintaining a high radiation dose distribution within tumour tissue. In terms of dosimetric evaluation, a more detailed study that may consider these parameters should be pursued. To mimic clinical practice and because multi-therapy might be a solution in the fight against gliomas, chemotherapy could be included since LNC can be loaded with radiosensitive anti-cancer drugs such as etoposide or paclitaxel [17, 23, 35].

Acknowledgements The authors are very grateful to Sandrine Vinchon-Petit for CED experiences and to Myriam Moreau for her help in LNC formulation (INSERM U646, Angers, France) for her help in LNC formulation. We are also grateful to Pierre Legras and Jérome Roux (Service Commun d'Animalerie Hospitalo—Universitaire, Angers, France) for their technical assistance in animal experiments. This work was supported by a 'Région des Pays de la Loire' grant and by the county committee of Maine et Loire of 'La ligue contre le cancer.' Animal care was carried out in strict accordance to French Ministry of Agriculture regulations.

References

1. Nieder C, Adam M, Molls M, Grosu AL. Therapeutic options for recurrent high-grade glioma in adult patients: recent advances. Crit Rev Oncol Hematol 2006;60:181–93.
2. Behin A, Hoang-Xuan K, Carpentier AF, Delattre J-Y. Primary brain tumours in adults. Lancet 2003;361:323–31.
3. Mitra A, Nan A, Line BR, Ghandehari H. Nanocarriers for nuclear imaging and radiotherapy of cancer. Curr Pharm Des 2006; 12:4729–49.
4. Barth RF, Yang W, Coderre JA. Rat brain tumor models to assess the efficacy of boron neutron capture therapy: a critical evaluation. J Neuro-Oncol 2003;62:61–74.
5. Ljunggren K, Liu X, Erlandsson K, Ljungberg M, Salford L, Strand SE. Absorbed dose distribution in glioma tumors in rat brain after therapeutic intratumoral injection of 201Tl-chloride. Cancer Biother Radiopharm 2004;19:562–9.
6. Jeong JM, Chung J-K. Therapy with 188Re-labeled radiopharmaceuticals: an overview of promising results from initial clinical trials. Cancer Biother Radiopharm 2003;18:707–17.

7. Iznaga-Escobar N. 188Re-direct labeling of monoclonal antibodies for radioimmunotherapy of solid tumors: biodistribution, normal organ dosimetry, and toxicology. Nucl Med Biol 1998; 25:441–7.
8. Lambert B, De Klerk JMH. Clinical applications of 188Re-labelled radiopharmaceuticals for radionuclide therapy. Nucl Med Commun 2006;27:223–9.
9. Ballot S, Noiret N, Hindre F, Denizot B, Garin E, Rajerison H, et al. 99mTc/188Re-labelled lipid nanocapsules as promising radiotracers for imaging and therapy: formulation and biodistribution. Eur J Nucl Med Mol Imaging 2006;33:602–7.
10. Mevellec F, Roucoux A, Noiret N, Patin H, Tisato F, Bandoli G. Synthesis and characterization of the bis(trithioperoxybenzoate) (dithiobenzoate)rhenium(III) hetero complex. Inorg Chem Commun 1999;2:230–3.
11. Heurtault B, Saulnier P, Pech B, Proust J-E, Benoit J-P. A novel phase inversion-based process for the preparation of lipid nanocarriers. Pharm Res 2002;19:875–80.
12. Mardor Y, Rahav O, Zauberman Y, Lidar Z, Ocherashvilli A, Daniels D, et al. Convection-enhanced drug delivery: increased efficacy and magnetic resonance image monitoring. Cancer Res 2005;65:6858–63.
13. Knapp FF Jr., Guhlke S, Beets AL, Lin WY, Stabin M, Amols H, et al. Endovascular beta irradiation for prevention of restenosis using solution radioisotopes: pharmacologic and dosimetric properties of rhenium-188 compounds. Cardiovasc Radiat Med 1999;1:86–97.
14. Hunt Bobo R, Laske DW, Akbasak A, Morrison PF, Dedrick RL, Oldfield EH. Convection-enhanced delivery of macromolecules in the brain. Proc Natl Acad Sci USA 1994;91:2076–80.
15. Vogelbaum MA. Convection enhanced delivery for the treatment of malignant gliomas: symposium review. J Neuro-Oncol 2005;73:57–69.
16. Jestin E, Mougin-Degraef M, Faivre-Chauvet A, Remaud-Le Saec P, Hindre F, Benoit JP, et al. Radiolabeling and targeting of lipidic nanocapsules for applications in radioimmunotherapy. Q J Nucl Med Mol Imaging 2007;51:51–60.
17. Lacoeuille F, Hindre F, Moal F, Roux J, Passirani C, Couturier O, et al. In vivo evaluation of lipid nanocapsules as a promising colloidal carrier for paclitaxel. Int J Pharm 2007;344:143–9.
18. Bao A, Goins B, Klipper R, Negrete G, Mahindaratne M, Phillips WT. A novel liposome radiolabeling method using 99mTc-"SNS/S" complexes: in vitro and in vivo evaluation. J Pharm Sci 2003;92:1893–904.
19. Judge LM, O'Leary DJ, Fujii G, Skenes C, Paquette T, Proffitt RT. A hydrazino nicotinamide derivative of cholesterol for radiolabelling liposomes with 99mTc. J Labelled Compd Radiopharm 1999;42:23–8.
20. Sendelbeck SL, Urquhart J. Spatial distribution of dopamine, methotrexate and antipyrine during continuous intracerebral microperfusion. Brain Res 1985;328:251–58.
21. MacKay JA, Deen DF, Szoka FC Jr. Distribution in brain of liposomes after convection enhanced delivery: modulation by particle charge, particle diameter, and presence of steric coating. Brain Res 2005;1035:139–53.
22. Beduneau A, Saulnier P, Hindre F, Clavreul A, Leroux JC, Benoit JP. Design of targeted lipid nanocapsules by conjugation of whole antibodies and antibody Fab′ fragments. Biomaterials 2007; 28:4978–90.
23. Garcion E, Lamprecht A, Heurtault B, Paillard A, Aubert-Pouessel A, Denizot B, et al. A new generation of anticancer, drug-loaded, colloidal vectors reverses multidrug resistance in glioma and reduces tumor progression in rats. Mol Cancer Ther 2006;5:1710–22.
24. Hsieh BT, Hsieh JF, Tsai SC, Lin WY, Huang HT, Ting G, et al. Rhenium-188-Labeled DTPA: a new radiopharmaceutical for intravascular radiation therapy. Nucl Med Biol 1999;26:967–72.
25. Noble CO, Krauze MT, Drummond DC, Yamashita Y, Saito R, Berger MS, et al. Novel nanoliposomal CPT-11 infused by convection-enhanced delivery in intracranial tumors: pharmacology and efficacy. Cancer Res 2006;66:2801–6.
26. Barth RF. Rat brain tumor models in experimental neuro-oncology: the 9L, C6, T9, F98, RG2 (D74), RT-2 and CNS-1 gliomas. J Neurooncol 1998;36:91–102.
27. Kimler BF. The 9L rat brain tumor model for pre-clinical investigation of radiation-chemotherapy interactions. J Neuro-oncol 1994;20:103–9.
28. Vonarbourg A, Sapin A, Lemaire L, Franconi F, Menei P, Jallet P, et al. Characterization and detection of experimental rat gliomas using magnetic resonance imaging. MAGMA 2004; 17:133–9.
29. Vavra M, Ali MJ, Kang EW, Navalitloha Y, Ebert A, Allen CV, et al. Comparative pharmacokinetics of 14C-sucrose in RG-2 rat gliomas after intravenous and convection-enhanced delivery. Neuro Oncol 2004;6:104–12.
30. Kimler BF, Martin DF, Evans RG, Morantz RA, Vats TS. Combination of radiation therapy and intracranial bleomycin in the 9L rat brain tumor model. Int J Radiat Oncol Biol Phys 1990;18:1115–21.
31. Lemaire L, Roullin VG, Franconi F, Venier-Julienne MC, Menei P, Jallet P, et al. Therapeutic efficacy of 5-fluorouracil-loaded microspheres on rat glioma: a magnetic resonance imaging study. NMR Biomed 2001;14:360–6.
32. Li Y, Owusu A, Lehnert S. Treatment of intracranial rat glioma model with implant of radiosensitizer and biomodulator drug combined with external beam radiotherapy. Int J Radiat Oncol Biol Phys 2004;58:519–27.
33. Schlemmer H-P, Bachert P, Herfarth KK, Zuna I, Debus J, Van Kaick G. Proton MR spectroscopic evaluation of suspicious brain lesions after stereotactic radiotherapy. Am J Neuroradiol 2001;22:1316–24.
34. Zeng Q-S, Li C-F, Liu H, Zhen J-H, Feng D-C. Distinction between recurrent glioma and radiation injury using magnetic resonance spectroscopy in combination with diffusion-weighted imaging. Int J Radiat Oncol Biol Phys 2007;68:151–58.
35. Lamprecht A, Benoit J-P. Etoposide nanocarriers suppress glioma cell growth by intracellular drug delivery and simultaneous P-glycoprotein inhibition. J Control Release 2006; 112:208–13.

CHAPITRE 2

Conception et évaluation biologique de nanocapsules lipidiques encapsulant un agent anticancéreux organométallique pour le traitement local des gliomes

Conception et évaluation biologique de nanocapsules lipidiques encapsulant un agent anticancéreux organométallique pour le traitement local des gliomes.

Ce chapitre décrit la conception de nanovecteurs lipidiques encapsulant un complexe métallique lipophile dérivé du tamoxifène et du ferrocène : le Fc-diOH. Lors de la mise au point initiale du procédé de formulation des nanocapsules lipidiques, une étude systématique a mis en évidence la zone de faisabilité des LNC sur un diagramme ternaire eau / huile / tensioactif. En modifiant les proportions de ces mêmes constituants, il est possible de formuler des objets micellaires. Puisque très lipophile, la molécule Fc-diOH a donc été encapsulée dans ces deux types de nanovecteurs lipidiques qui ont été caractérisés en terme de taille, charge et rendement d'encapsulation. Le marquage des nanovecteurs lipidiques avec un marqueur fluoré hydrophobe (Nile Red) nous a permis d'évaluer le devenir de ces vecteurs dans la cellule par des techniques de cytométrie de flux et microscopie confocale. Ces nanovecteurs encapsulant Fc-diOH ainsi que les molécules non encapsulées ont fait l'objet de tests de cytotoxicité *in vitro* mettant en parallèle des cellules cancéreuses à fort pouvoir de division, les cellules 9L, et des cellules au pouvoir de division faible voire nul, mimant le comportement de cellules saines, les astrocytes. Enfin, ces nanovecteurs ont été administrés par injection intratumorale chez le rat dans un modèle de gliome ectopique. L'appréciation de l'efficacité des traitements est évaluée par estimation des volumes tumoraux à J10, J16, J22 et J30 après inoculation des tumeurs et mesure des masses tumorales en fin d'étude (J30), après sacrifice des animaux.

Journal of Controlled Release 130 (2008) 146–153

Contents lists available at ScienceDirect

Journal of Controlled Release

journal homepage: www.elsevier.com/locate/jconrel

Lipid nanocapsules loaded with an organometallic tamoxifen derivative as a novel drug-carrier system for experimental malignant gliomas

Emilie Allard [a,b], Catherine Passirani [a,b], Emmanuel Garcion [a,b], Pascal Pigeon [c,d], Anne Vessières [c,d], Gérard Jaouen [c,d], Jean-Pierre Benoit [a,b,*]

[a] INSERM, U646, Angers, F-49100, France
[b] Université d'Angers, Angers, F-49000, France
[c] CNRS, UMR 7576, Paris 05, F-75231, France
[d] ENSCP Paris V, Paris, F-75231, France

ARTICLE INFO

Article history:
Received 16 April 2008
Accepted 22 May 2008
Available online 5 June 2008

Keywords:
Lipid nanocarrier
Organometallic compound
Cell uptake
Drug delivery
9L tumour model

ABSTRACT

Ferrocenyl diphenol tamoxifen derivative (Fc-diOH) is one of the most active molecules of a new class of organometallic drugs, showing *in vitro* antiproliferative effects on both hormone-dependent and independent breast cancer cells. For the first time, Fc-diOH was tested on a 9L glioma model according to two encapsulation strategies: lipid nanocapsules (LNC) and swollen micelles. LNC showed a higher drug loading capacity because of a larger oily core in their structure and were able to be up taken by glioma cells. The large amount of PEG present at the micellar interface prevented interaction with cytoplasm membrane which led to a low level of micelle cell uptake and no biological activity. On the contrary, Fc-diOH cytostatic activity was conserved after its encapsulation in LNC and was very effective on 9L-glioma cells as the IC_{50} was about 0.6 μM. Interestingly, Fc-diOH-loaded LNC showed low toxicity levels when in contact with healthy cells, conferring a functional specificity of this compound on tumour cells. Finally, Fc-diOH LNC treatment was able to lower significantly both tumour mass and volume evolution after 9L-cell implantation into rats which evidenced for the first time the *in vivo* efficacy of this new kind of organometallic compound.

1. Introduction

Gliomas are the most common type of primary brain tumours. The prognosis for patients with glioblastoma, the most aggressive type of brain malignancy, has remained largely unchanged over the last three decades. Recent studies give a median survival time of 14.6 months for patients treated with radiotherapy plus temozolomide, which is the reference chemotherapy, and 12.1 months with radiotherapy alone [1]. Clearly, new and effective therapies are desperately awaited.

Tamoxifen, a member of the Selective Estrogen Receptor Modulator (SERM) family, has been widely used in the treatment of estrogen receptor (ER)-expressing breast cancer [2–4]. Because antitumour effects have been predominantly observed in patients with ER-positive tumours, it is generally accepted that the primary action of hydroxytamoxifen, its active metabolite, is mediated through inhibition of the ER pathway. But, it has previously been shown that some ER-negative cancers also respond to tamoxifen, [5,6] which means that the molecule can be active because of an ER-independent antitumour mechanism that has not yet been clearly identified [7].

Taking into account that gliomas are ER-negative [8–10], the moderate beneficial effect of tamoxifen in glial neoplasms has been linked to an ER-independent antitumour mechanism. For the treatment of patients with recurrent malignant gliomas, only trials using high-dose tamoxifen alone or in combination with other cytotoxic agents have demonstrated positive results [11–13]. As a consequence, SERM represent a promising therapy for gliomas if their antitumour activity can be improved.

Previously, a potentially cytotoxic moiety, ferrocene, was incorporated into the tamoxifen skeleton [14]. A series of these molecules, called organometallic tamoxifen derivatives by analogy, was prepared and their cytotoxic effects were studied, initially on breast cell lines [15,16]. By modifying various structural aspects of the ferrocenyl derivatives, one of the most effective compounds to date in terms of cytotoxicity is the ferrocenyl diphenol compound Fc-diOH (Fig. 1). This compound showed high levels of *in vitro* antiproliferative activity against both hormone-dependent (MCF7, IC_{50} = 0.7 μM) and independent (MDA-MB231, IC_{50} = 0.6 μM) breast cancer cell lines [16], and has become the standard to which the activity of novel organometallic anticancer drugs can be compared. The observed antiproliferative effect of these molecules can be divided into two actions: anti-oestrogenic in ER(+) cells and cytotoxic in both ER(+) and ER(−) cells. The efficacy of these drugs has been related to an activation pathway which involves the *in vitro* oxidation of the ferrocene and phenol

* Corresponding author. Université d'Angers, Angers, F-49000, France. Tel.: +33 241 735858; fax: +33 241 735853.
E-mail address: jean-pierrebenoit@univ-angers.fr (J.-P. Benoit).

0168-3659/$ – see front matter © 2008 Elsevier B.V. All rights reserved.
doi:10.1016/j.jconrel.2008.05.027

Fig. 1. Chemical formulas of hydroxytamoxifen (OH-Tam), ferrocene (Fc) and 2-ferrocenyl-1,1-bis(4-hydroxyphenyl)-but-1-ene called ferrocenyl diphenol compound (Fc-diOH).

functions [17,18]. These organometallic tamoxifen derivatives could have an enormous impact on medicine, in particular in the treatment of cancer [19]. As demonstrated by Rosenberg's discovery of cisplatin [20] which revolutionized the treatment of testicular cancer, organometallic complexes can be a powerful weapon as antitumour agents [21].

In the present study, the antitumoural efficacy of Fc-diOH was tested on glioma cells. As this product is very hydrophobic, and since its water-insolubility can impede its potential biological activity [22], we aimed at developing a new way to administer this molecule. Two strategies were investigated: a ferrocenyl diphenol compound was encapsulated in lipid nanocapsules (LNC) for one strategy and in swollen micelles for another, according to an organic solvent-free process recently developed in our laboratory [23]. These lipid nanocarriers obtained by a low-energy emulsification method were characterised by the absence of organic solvent in their formulation. They presented a low particle size, ranging from 10 to 20 nm for swollen micelles and from 20 to 100 nm for LNC, with a narrow polydispersity size and the capacity to carry lipophilic molecules. Taking into account these various advantages, Fc-diOH-loaded nanocarriers were developed and tested on glioma culture cells and on a subcutaneous 9L-rat glioma model.

2. Materials and methods

2.1. Materials

Ferrocenyl diphenol compound (2-ferrocenyl-1,1-bis(4-hydroxyphenyl)-but-1-ene) named Fc-diOH was prepared by McMurry coupling [24]. Its purity was assessed by HPLC, NMR and elemental analysis. Hydroxytamoxifen, Ferrocene and Nile Red were supplied by Sigma-Aldrich (Saint-Quentin Fallavier, France). The lipophilic Labrafac® CC (caprylic-capric acid triglycerides) was kindly provided by Gattefosse S.A. (Saint-Priest, France). Lipoid® S75-3 (soybean lecithin at 69% of phosphatidylcholine) and Solutol® HS15 (a mixture of free polyethylene glycol 660 and polyethylene glycol 660 hydroxystearate) were a gift from Lipoid Gmbh (Ludwigshafen, Germany) and BASF (Ludwigshafen, Germany), respectively. NaCl, acetone, ethanol and tetrahydrofurane (THF) were obtained from Prolabo (Fontenay-sous-bois, France). Deionised water was obtained from a Milli-Q plus system (Millipore, Paris, France).

2.2. Preparation of Fc-diOH-loaded nanocarriers

Lipid nanocarriers were prepared according to a previously described original process [23]. In order to obtain LNC, Solutol® HS15 (17% w/w), Lipoid® (1.5% w/w), Labrafac® (20% w/w), NaCl (1.75% w/w) and water (59.75% w/w) were mixed and heated under magnetic stirring up to 85 °C. Three cycles of progressive heating and cooling between 85 and 60 °C were then carried out and followed by an irreversible shock induced by dilution with 2 °C deionised water (45 or 70% v/v) added to the mixture at 70–75 °C. To formulate Fc-diOH-loaded LNC, two parameters will be changed: the amount of Fc-diOH in triglycerides (1.7% and 4% (w/w)) and the volume of cold water for LNC dilution (70% and 45% v/v) for drug loading of 1 mg/g (0.84% w/w dry weight) and 6.5 mg/g (2% w/w dry weight) respectively.

To form swollen micelles, Solutol® HS15 (64.25% w/w), Labrafac® (5% w/w), NaCl (1.75% w/w) and water (29% w/w) were mixed and the same formulation flow chart was applied as previously described. To formulate Fc-diOH-loaded micelles 1 mg/g (0.24% w/w dry weight), the amount of Fc-diOH in triglycerides was equivalent to 3.4% (w/w) and the volume of dilution was about 42% (v/v).

Fluorescent lipid nanocarriers were obtained by using Nile Red, a hydrophobic fluorescent marker, previously dissolved in acetone at 2 µg/µl. The resulting Nile Red solution was incorporated in the triglyceride phase at 50:50 (w/w) and the acetone was evaporated before use. Fluorescent LNC and micelles were then prepared as described above.

2.3. Characterisation of the nanocarriers

2.3.1. Particle size and zeta potential

The nanocarriers were analysed for their size and charge distribution using a Malvern Zetasizer® Nano Serie DTS 1060 (Malvern Instruments S.A., Worcestershire, UK). The nanocarriers were diluted 1:100 (v/v) in deionised water in order to ensure a convenient scattered intensity on the detector.

2.3.2. LNC drug payload and encapsulation efficiency

Because of the orange colour of the anticancer drug, the Fc-diOH payload was determined by spectrophotometry at 450 nm after dissolving LNC and swollen micelles in solvent mixtures as described below. As the water solubility of Fc-diOH was inferior to 0.001 µg/ml, if the product was not entrapped in nanocarriers, drug precipitation occurred and the precipitate could be retained by a filter. Consequently, a part of the formulation of each batch was filtrated using a Minisart® 0.1-µm filter (Sartorius). Three samples of each batch of Fc-diOH-loaded nanocarriers (filtrated and non-filtrated) were prepared by dissolving 250 mg of nanocarriers in 2.25 ml of 22/67/11 (v/v/v) acetone/THF/water solution. Quantification was achieved by comparing the absorbency of ferrocenyl derivative samples to a calibration curve made with blank nanocarriers and Fc-diOH ethanol/THF/water solution. Mean drug payload (milligrams of drug per gram of LNC dispersion or micellar solution) and encapsulation efficiency (%) were calculated.

2.4. Cell experiments

2.4.1. Cell culture

Rat 9L gliosarcoma cells were obtained from the European Collection of Cell Culture (Salisbury, UK, N°94110705). Purified newborn rat primary astrocytes were obtained by the mechanical dissociation method from cultures of cerebral cortex as originally described [25]. The cells were grown at 37 °C/5% CO2 in Dulbecco modified Eagle medium (DMEM) with glucose and l-glutamine (BioWhittaker, Verviers, Belgium) containing 10% foetal calf serum (FCS) (BioWhittaker) and 1% antibiotic and antimycotic solution (Sigma, Saint-Quentin Fallavier, France).

2.4.2. Observation of nanocarrier internalisation by confocal images

9L cells were plated at 10^4/ml on 24-well plates covered with 14 mm microscope cover glasses coated with a solution of 5 µg/ml in PBS of poly-d-lysine hydrobromide mol wt 70,000–150,000 (Sigma, Saint-Quentin Fallavier, France). After 48 h of culture, the culture medium was removed and changed to a serum-free medium containing 50% DMEM, 50% Ham's F12 and N1 complement. At Day 3, the medium was totally removed and the cells were incubated for 2 h with a medium containing the medium alone as a negative control, fluorescent LNC 1:1000 or fluorescent micelles 1:1000. The cells were

then washed twice with Hanks balanced salt solution (HBSS, BioWhittaker) and fixed with 4% paraformaldehyde in PBS for 15 min at 4 °C. They were washed three times with HBSS, the cover glasses were removed and finally mounted on slides in glycerol/PBS 1:1. The cells and fluorescent nanocarriers were observed by confocal microscopy (Olympus light microscope Fluoview FU 300 Laser Scanning Confocal Imaging System, Paris, France) with a helium–argon laser (λ_{ex}: 543 nm, λ_{em}: 572 nm). The morphology of the 9L cells was shown by Nomarsky contrast.

2.4.3. Quantification of nanocarrier internalisation by flow cytometry

A BD FACSCalibur fluorescent-activated flow cytometer and the BD CellQuest software (BD Biosciences, Le Pont de Claix, France) were used to perform flow cytometry analysis. Nile Red-loaded micelles (1/1000) and Nile Red-loaded LNC (1/1000) were incubated with 9L glioma cells in a serum-free medium containing 50% DMEM, 50% Ham's F12 (BioWhittaker) and N1 complement (Sigma). After 2 h of incubation, the removal of the attached nanocarriers was accomplished by washing the cells three times with HBSS. The cells were then detached by trypsinisation. After centrifugation, they were resuspended in a 0.4% (w/v) Trypan Blue solution in HBSS to quench the extracellular fluorescence, thus enabling the determination of the fraction that was actually internalised. The treated samples were subsequently washed twice, and analysed by flow cytometry in at least triplicate experiments, with 10,000 cells being measured in each sample. For quantification analysis, no treatment (9L cells) was considered to be the 100% of fluorescence intensity.

2.4.4. In vitro cell viability

The cells were first plated at 10^4 cells/ml on 24-well plates for 48 h in DMEM containing 10% FCS and 1% antibiotic/antimycotic and then treated with increasing concentrations of various preparations. To test the impact of the drug alone (non-encapsulated) on cells, solvent like ethanol (for Fc-diOH and OH-Tam) and acetone (for Fc) were used to solubilise the drugs. The drugs in solution were prepared at a concentration of 0.1 M and a dilution of 1:1000 in culture medium was realised to obtain the higher concentration tested on cells (100 μmol/l). To test drugs encapsulated in micelles or in LNC at this concentration, a dilution of 1:23.5 was realised in culture medium. For the others concentrations, 1:10 cascade dilution was performed. Blank LNC and micelles were tested as controls and with the same excipient concentration than that needed for Fc-diOH ones. The cells were incubated at 37 °C/5% CO_2 for 96 h. Thereafter, cell viability was determined by the MTT test according to the procedure described by Mosmann [26]. Briefly, 40 μl of MTT solution at 5 mg/ml in PBS 1X was added to each well, and the plates were incubated at 37 °C for 4 h. The medium was removed and 200 μl of acid–isopropanol 0.06 N was added to each well and mixed thoroughly to completely dissolve the dark blue crystals. The optical density values were measured at 580 nm using a multiwell-scanning spectrophotometer (Multiskan Ascent, Labsystems SA, Cergy-pontoise, France). Two independent repetition experiments are conducted, each with a least 6 repeated samples.

2.5. Animal study

2.5.1. Animals and anaesthesia

Syngeneic Fischer F344 female rats weighing 160–175 g were obtained from Charles River Laboratories France (L'Arbresle, France). All experiments were performed on 10 to 11-week old female Fisher rats. The animals were manipulated under isoflurane/oxygen anaesthesia. Animal care was provided in strict accordance to the French Ministry of Agriculture regulations.

2.5.2. Tumour and nanocarrier implantation

A cultured tumour monolayer was detached with trypsin-ethylene diamine tetraacetic acid, washed twice with EMEM without FCS or antibiotics, counted, and resuspended to the final concentration desired. For tumour growth analysis, animals received subcutaneous injections (s.c) of 1.5×10^6 9L cells into the right thigh. On Day 6 after cell injection, rats implanted with 9L cells were treated by an intratumoural (i.t.) single injection (400 μl) of different treatments. Group 1 was injected with physiological saline (control; $n=7$ animals). Group 2 received blank LNC ($n=7$ animals). Group 3 received Fc-diOH-loaded micelles 1 mg/g (2.5 mg/kg; $n=8$ animals). Group 4 received Fc-diOH-loaded LNC 1 mg/g (2.5 mg/kg; $n=8$ animals) and Group 5 was treated with Fc-diOH-loaded LNC at a higher dose of 6.5 mg/g (16.2 mg/kg; $n=5$ animals). The length and width of each tumour were regularly measured using a digital caliper, and tumour volume was estimated with the mathematical ellipsoid formula given in Eq. (1). At the end of the study (Day 30), the rats were sacrificed and the weight of each tumour was evaluated.

$$\text{Volume}(V) = (\pi/6) \times \text{width}^2(l) \times \text{length}(L) \quad (1)$$

2.6. Statistical analysis

For *in vitro* cell survival tests, statistics and analysis of the Similarity Factor f2 were employed to evidence significant curve profiles ($f2<50$ was considered to be significant). The statistical significance for the *in vivo* study was determined for each experiment between groups by a Student *t*-test ($P<0.05$ was considered to be significant).

3. Results and discussion

3.1. Preparation and characterisation of Fc-diOH-loaded nanocarriers

By mixing Fc-diOH with excipients at well-characterised concentrations described by a ternary diagram [23] and by applying the phase inversion process, lipid nanocapsules and swollen micelles loaded with Fc-diOH were obtained. LNC loaded with the anticancer drug presented a very narrow size between 44.7 and 51.7 nm, depending on the drug payload, and were monodispersed (PI < 0.15) (Table 1). Fc-diOH-loaded LNC were also characterised in terms of surface charge. Zeta potential values ranged from −10.0 to −11.5 mV. The physicochemical properties were very similar to the previously-studied standard blank LNC [27,28]. Indeed, because of the presence of PEG dipoles in their shells, 50 nm blank LNC have a low zeta potential of approximately −10 mV [29]. The presence of the active drug did not affect the zeta potential value which means that the entrapment of Fc-diOH was very efficient. Due to the

Table 1
Mean particle size, polydispersity index, and zeta potential values of the different nanocarrier formulations

		Mean particle size (nm)	Polydispersity (PDI)	Zeta potential (mV)
Lipid nanocapsules (LNC)	Blank LNC ($n=3$)	50.7±0.2	0.087±0.009	−10.0±4.1
	Fc-diOH-LNC 0.5 mg/g ($n=3$)	51.7±0.2	0.129±0.003	−11.5±6.9
	Fc-diOH-LNC 1 mg/g ($n=3$)	51.3±0.6	0.093±0.006	−11.1±1.6
	Fc-diOH-LNC 6.5 mg/g ($n=3$)	44.7±0.9	0.036±0.008	−10.5±1.0
	Nile Red-LNC ($n=3$)	53.0±5.0	0.087±0.018	−10.7±1.9
Swollen micelles	Blank micelles ($n=3$)	13.0±0.1	0.053±0.025	−1.9±2.8
	Fc-diOH-Micelles 1 mg/g ($n=3$)	13.2±0.3	0.070±0.059	−1.8±0.3
	Nile Red Micelles ($n=3$)	12.9±0.4	0.095±0.002	−2.7±0.8

Measurements were made in triplicates ($n=3$) and results were expressed as mean values ± standard deviation (SD).

Table 2
Encapsulation efficiency of Fc-diOH in the different nanocarrier formulations (n= 3)

	Exp. drug load (mg/g)	Encapsulation efficiency (%)
Fc-diOH-LNC 0.5 mg/g	0.49 ± 0.02	99.1 ± 4.2
Fc-diOH-LNC 1 mg/g	1.03 ± 0.02	98.1 ± 1.7
Fc-diOH-LNC 6.5 mg/g	6.43 ± 0.07	98.2 ± 1.2
Fc-diOH-Micelles 1 mg/g	1.07 ± 0.04	103.2 ± 3.5

Experimental drug load were expressed as the amount of Fc-diOH in milligrams per gram of lipid nanocapsule suspension. Encapsulation efficiency was expressed as mean percentage (%) ± SD.

nearly negligible solubility of ferrocenyl compound in water and its high solubility in triglycerides (Labrafac®), it was possible to reach high drug loading levels, up to 6.5 mg of Fc-diOH per gram of LNC suspension (2% w/w dry weight). Like many hydrophobic drugs [30–32], Fc-diOH was well-encapsulated in LNC with a high encapsulation efficiency above 98% (Table 2).

Due to a low quantity of triglycerides present in swollen micelles and because of the limit of solubility for Fc-diOH in triglycerides, it was only possible to obtain micelles with a drug load equivalent to 1 mg/g (0.24% w/w dry weight). Nevertheless, they were obtained with the same size and zeta potential as blank micelles (Table 1). The Fc-diOH-loaded micelles were characterised by a very small particle size, 13.2 ± 0.3 nm, the same as for blank ones (13.0 ± 0.1 nm) and exhibited a very weak negative charge with values around −2 mV. The incorporation of Fc-diOH in swollen micelles was very effective, as demonstrated by the high encapsulation efficiency and the stability of the zeta potential (Tables 1 and 2).

3.2. Cell line experiments

3.2.1. Nanocarrier cell uptake

The internalisation of lipid nanocarriers in glioma cells was investigated by confocal microscopy and flow cytometry after the formulation of Nile Red (NR)-loaded LNC and micelles. As their size and charge measurements were very similar to those of blank nanocarriers (Table 1), NR-loaded LNC and micelles were considered to mimic the behaviour of nanocarriers entrapping the anticancer drug. Quantitative cellular uptake by FACS analysis (Fig. 2) and images taken after the incubation of fluorescent nanocarriers with 9L cells (Fig. 3) showed that there was a significant difference between the two nanocarriers in terms of cell uptake. Fig. 2A shows that LNC were rapidly taken up by 9L cells. Cell fluorescence intensity increased from 100% for cells alone (control) to 354.4% for cells incubated with NR-LNC (Fig. 2B). As seen in Fig. 3A, all the fluorescence was found inside the cell, while avoiding the nucleus, demonstrating an uptake of the nanocapsules. This uptake could be attributed to the interactions between 50 nm LNC and cholesterol-rich microdomains as previously observed [33]. On the contrary, a very weak level of fluorescence was observed after the incubation of Nile Red-loaded micelles with 9L cells which means that only a few micelles are able to penetrate the cells (Fig. 3B). Cytometry results confirmed that fluorescent micelles were taken up by 9L cells at much lower levels than LNC (205.2%) (Fig. 2B). Dunn et al. investigated the effect of an increased surface density of PEG with constant chain length, on the uptake of pegylated nanoparticles by non-parenchymal liver cells. The interaction of the particles with cells was shown to decrease as the surface density of PEG increased [34]. The surfactant barrier in swollen micelles was more than 7 times higher in proportion to those used for LNC formulations for the same drug load. So, whereas micelles are smaller than LNC, the presence of high density PEG coating certainly decreased interaction with cells and could be responsible of the low internalisation of swollen micelles in 9L glioma cells. This phenomenon had already been described by others groups. In fact, when the concentration of Solutol® HS15 was above its CMC (0.03% w/v), the amount of colchicine taken up into rat hepatocytes, as well as its uptake velocity, were significantly decreased [35]. This phenomenon was explained by an inhibition of colchicine transport either due to direct interaction at the transport site or due to alteration of membrane properties in the presence of Solutol® HS15 micelles.

3.2.2. Cell viability

Fc-diOH was tested *in vitro* in a survival assay on 9L glioma cell and on newborn rat astrocyte primary cultures. Ferrocene (Fc) and hydroxytamoxifen (OH-Tam), which are the main molecules of the Fc-diOH structure, were also tested. No toxic effect was observed for the ethanol/acetone solutions used to solubilise drugs in solution (data not shown). Glioma cell culture studies revealed that a distinct and large decrease in cancer cell viability could be achieved with Fc-diOH, contrary to OH-Tam and Fc (Fig. 4A). The IC_{50} for Fc-diOH was about 0.5 μM whereas OH-Tam was totally inactive at this concentration range (IC_{50}= 35 μM). Similar results had already been found in MDA-MB231 cells which are classified as ER(−) breast cancer cell lines, since the IC_{50} for ferrocenyl tamoxifen derivative and OH-Tam were about 0.5 μM [36] and 34 μM respectively [37,38]. Tamoxifen, the reference molecule of the SERM family, is well known to act through its inhibition of ER. However, it has been already described that the oxidation of tamoxifen to quinoids is a recognised pathway of cytotoxicity [39,40]. As glioma cells are classified as ER(−) cell lines [9], the moderate effect of tamoxifen on 9L cells can be attributed to its oxidant activity. Furthermore, ferrocene was totally inactive on 9L cells. The same result has already been observed on

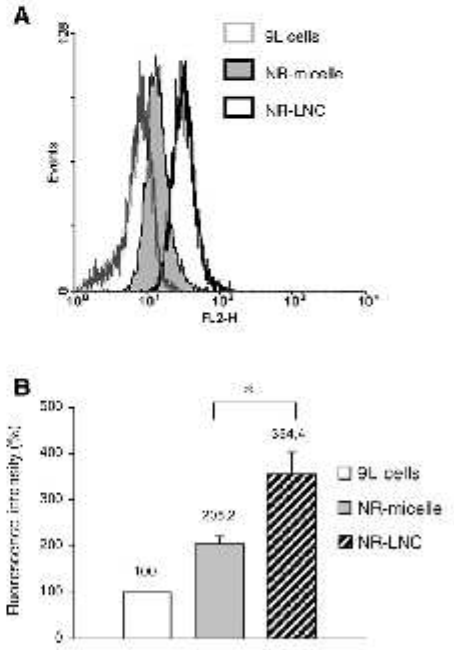

Fig. 2. Evaluation of Nile Red-loaded nanocarrier uptake by 9L cells after 2 h of incubation in serum-free conditions. (A) represents the fluorescence intensity (FL2-H) as a function of the number of collected cells (events) for control (9L cells), Nile Red–loaded micelles (NR-micelle) and Nile Red-loaded LNC (NR-LNC). The percentage value given for each histogram indicates the fluorescence intensity (%) ± SD. No treatment (9L cells) was considered as 100% of fluorescence intensity (B). Note that there is a significant difference between the uptake of NR-LNC and NR-micelle (P = 0.007) (n=3). "*" means P<0.05 — Student t-test.

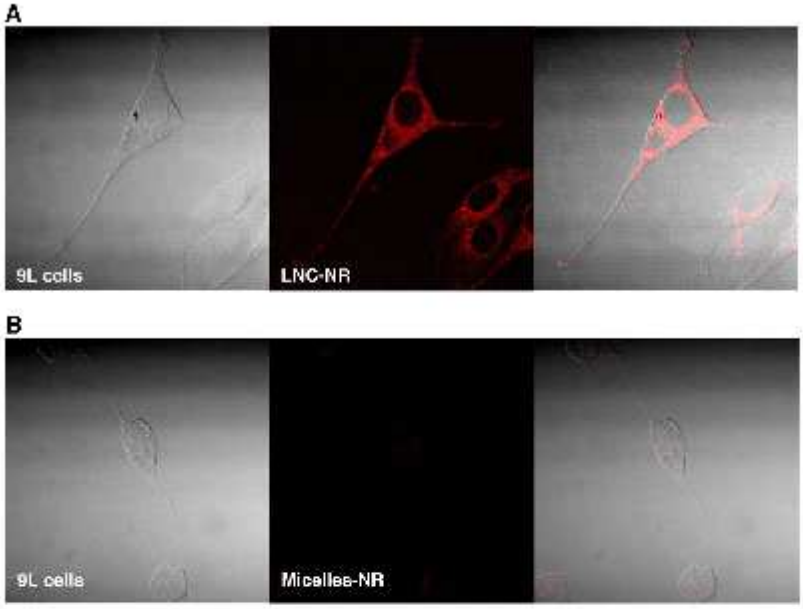

Fig. 3. Confocal images of 9L cells after 2 h of incubation with fluorescent LNC (LNC-NR) (A) and fluorescent micelles (Micelles-NR) (B) in serum-free conditions. Images were taken with a Nomarsky contrast, with a red fluorescence filter and by the superposition of Nomarsky and fluorescent acquisitions. In A, all the fluorescence was found inside the cell, while avoiding the nucleus, demonstrating an uptake of the nanocapsules. On the contrary, a very weak level of fluorescence was observed after the incubation of Nile Red-loaded micelles with 9L cells which means that only a few micelles are able to penetrate the cells (B).

ER(+) and ER(−) breast cell lines [15], even though it showed some antitumour potential, though at high concentrations (10^{-4} M), when oxidized into the ferrocenium ion [41]. The fact that Fc-diOH showed cytotoxic activity at much lower concentrations than OH-Tam suggests that the Fc group has a role in the observed cytotoxic effect. The easier oxidation of ferrocene in comparison to phenol, makes the oxidative metabolism of ferrocenyl derivatives easier, and consequently leads to better antiproliferative activity. As shown in Fig. 4B, in astrocyte cells which are slow- or non-dividing cells, Fc-diOH at equivalent doses to those added to glioma cells demonstrated a largely reduced level of cell toxicity (IC_{50}= 50 μM) equivalent to OH-Tam, whereas ferrocene was characterised overall by a total absence of cytotoxicity. These results indicate that Fc-diOH is toxic to brain tumour cells with a high potential for cell division, and harmless towards healthy cells.

Cell survival curves were not significantly different between Fc-diOH in solution and Fc-diOH-loaded LNC, showing that the activity of the drug was totally recovered *in vitro* after encapsulation (Fig. 4C). Moreover, Fc-diOH-loaded LNC demonstrated cytotoxic activity on 9L cells 150-fold higher than blank LNC. Taking into account the cytotoxic mechanism of ferrocenyl molecules proposed by Hillard et al. [17], these results suggest that LNC improved intracellular bioavailability of Fc-diOH. Indeed, it was demonstrated that upon electrochemical oxidation of the ferrocene group, a partial positive charge is imparted to the hydroxyl group of the molecule, thus acidifying the proton, which may then be easily abstracted by basic species like DNA, glutathione (GSH), or proteins, only present in the intracellular compartment. In a subsequent second oxidative step, quinone methide is formed, and is activated for nucleophilic attack by sulphur and nitrogen donor groups from biomolecules which may lead to cell death. Furthermore, an advantageous effect was found for Fc-diOH when in contact with astrocytes (Fig. 4D). In fact, Fc-diOH in solution or entrapped in LNC, was found to be much less cytotoxic on astrocytes compared to cancer cells. The higher cytotoxic effect of Fc-diOH-loaded LNC in glioma cells than in astrocytes could be triggered by easier accessibility of the intracellular target during cell division. Additionally, astrocytes are considered to play an important role in the defence of the brain against reactive oxygen species (ROS) [42]. They are known to contain higher levels of various antioxidants, especially GSH, than other brain cell types like neurons and oligodendrocytes [43–45]. As GSH may be a potential target of the ferrocenyl tamoxifen derivatives, it can explain the reduced cell death of Fc-diOH on astrocytes. The higher cytotoxic effect of Fc-diOH-loaded LNC on glioma cells than on astrocytes cannot be explained by increased endocytosis during cell division, since LNC uptake is quantitatively equivalent in the two types of cells (A. Paillard et al., unpublished observation). Consequently, Fc-diOH can be considered as a cytostatic anticancer molecule from an *in vitro* concentration of 0.5–0.6 μM.

The results obtained with Fc-diOH-loaded micelles were different (Fig. 4E–F). Firstly, the activity of Fc-diOH in solution was not recovered after its encapsulation in swollen micelles. Moreover, there was no significant difference between blank and Fc-diOH-loaded micelles on 9L cell survival percentage, which means that the observed toxicity was related to the nanocarrier and not to the anticancer drug. The toxicity of swollen micelles was certainly due to the presence of excipients, especially surfactant molecules like Solutol®. In fact, the use of Solutol® HS15 in pharmaceutical preparations for *in vitro* applications should be considered with care. Woodcock et al. studied the toxicity of different surfactants on cells and their capability to reverse multidrug resistance (MDR) [46]. Concerning Solutol® HS15, they concluded that 2/3 of the R100 cells (MDR-derivative of human leukaemia cell line) were lysed when incubated for only 1 h with this polyethoxylated solubilising agent at concentrations equivalent to 1:100 (w/v) and 100% were lysed by 1:10 (w/v). Despite lower concentration of Solutol® HS15 in our micelles

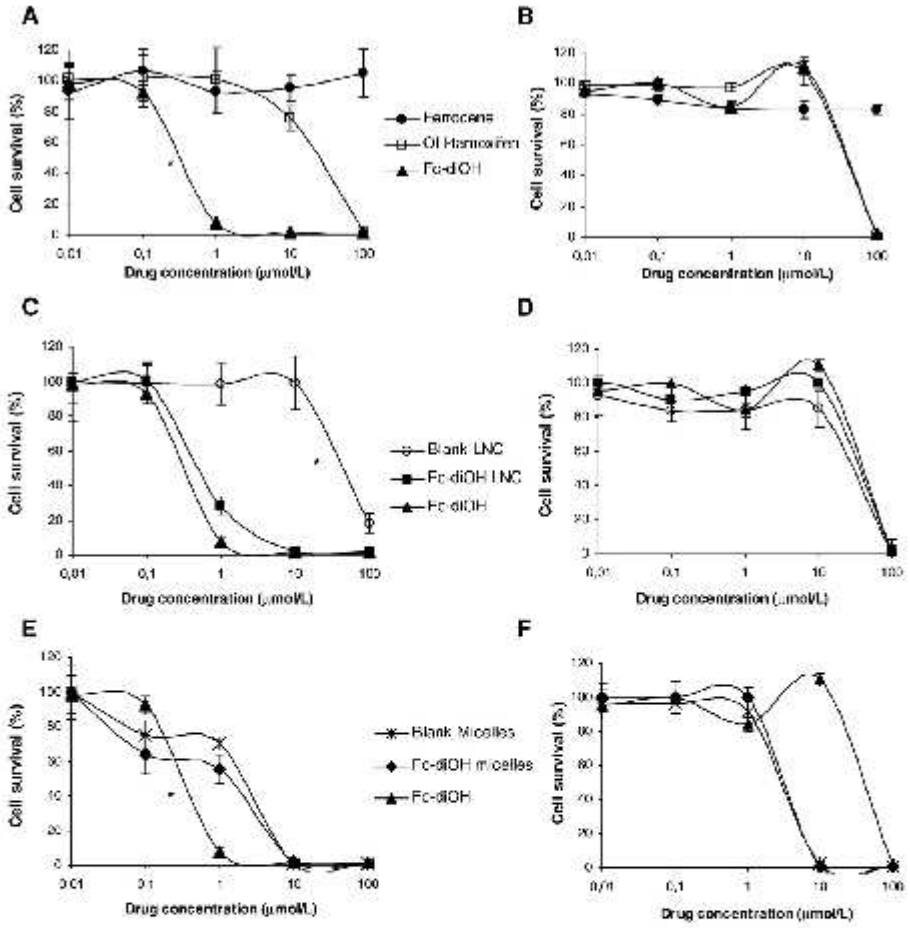

Fig. 4. Effects of ferrocene (Fc), hydroxytamoxifen (OH-Tam), ferrocenyl tamoxifen derivatives (Fc-diOH), Fc-diOH-loaded LNC, blank LNC, Fc-diOH-loaded micelles and blank micelles on the proliferation of 9L cells (A, C and E) and astrocytes (B, D and F) after 96 h of incubation and at concentrations between 0.01 and 100 µM (MTT assay). Blank nanocarriers are tested with the same excipient concentration than for Fc-diOH loaded LNC. No toxic effect was observed for the ethanol/acetone solutions used to solubilise drugs in solution (data not shown). Data refer to the untreated control and are expressed as the mean of six wells repeated 2 times ± SD (n= 2 in 6 wells). "*" means f2 <50 compared to the other curves of the same graph — Similarity factor f2.

(0.037%), toxicity on 9L glioma cells was noted for blank micelles after 2 h of incubation. In addition, swollen micelles were found to be toxic on healthy cells as well as on cancer cells as the IC_{50} was about 5 µM on both cell types (Fig. 4F). The cytotoxic activity of Fc-diOH on 9L decreased dramatically when it was encapsulated in micelle which confirms that swollen micelles were poorly internalised in 9L cells.

3.3. In vivo study

A 9L subcutaneous glioma model was used to evaluate the efficacy of Fc-diOH LNC and micelles. After tumours had developed to about 100 mm^3, we performed comparative efficacy studies by dividing animals into five groups according to the treatment they received. Rats were separated in random samples in a way to minimize weight and tumour size differences among the groups. Rats of the control and LNC groups were characterised by a very quick progression of tumour volume which reached 2500 and 2000 mm^3 by Day 30, respectively. (Fig. 5). On the contrary, Fc-diOH-loaded LNC significantly inhibited tumour growth ($P<0.05$) which means that the cytostatic activity of Fc-diOH was preserved *in vivo*. Indeed, rats treated with a single injection of LNC at an equivalent dose of 2.5 mg/kg presented tumours three times smaller (700 mm^3 at Day 30) than the ones treated by blank LNC (Fig. 5A). In contrast, rats treated by Fc-diOH-loaded micelles with the same anticancer drug dose had tumours that grew very quickly and reached 1600 mm^3 by the end of the study. These *in vivo* data can be linked to the conclusions made about nanocarrier uptake in 9L cells as an intratumoural treatment with Fc-diOH-loaded micelles was less effective than Fc-diOH-loaded LNC injection. Similarly, tumour growth assessed by tumour mass at the end of the study showed that the mean tumour mass had significantly decreased from 1.1 to 0.6 g for 1 mg/g loaded swollen micelles and LNC, respectively (Fig. 5B).

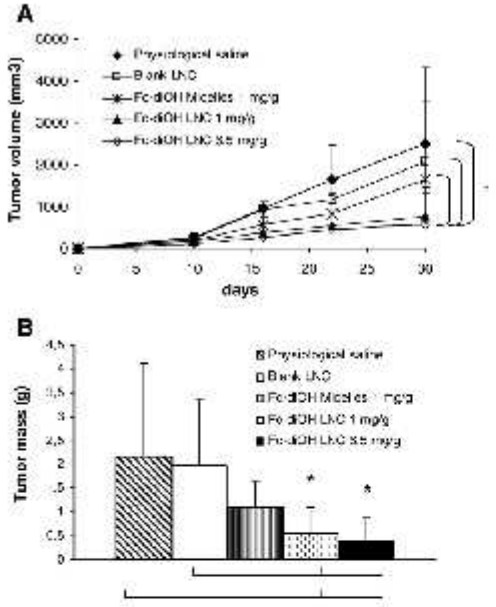

Fig. 5. *In vivo* effects of Fc-diOH-loaded nanocarrier treatment on the growth of 9L glioma cells implanted subcutaneously on Fisher rats. Efficacy of the treatments with Fc-diOH-loaded nanocarriers was compared with controls made after a single injection of physiological serum or blank LNC. (A) was an estimation of tumour growth assessed by tumour size measurements ± SD. Tumours were measured four times a month with callipers and tumour volume was approximated as an ellipsoid. (B) represents values of tumour mass weighted at Day 30±SD. Statistical analysis by pairs shows significant differences in A on Day 30 for Fc-diOH LNC treatment (1 and 6.5 mg/g) compared to both control injection and to Fc-diOH-loaded micelles (1 mg/g). Same conclusions were made with tumour mass at Day 30 (B). "*" means $P<0.05$ — Student *t*-test.

Nevertheless, no dose effect was evidenced as rats treated with Fc-diOH-loaded LNC at an equivalent dose of 16.2 mg/kg (6.5 mg/g load) had s.c. tumour growth similar to LNC ones at an equivalent dose of 2.5 mg/kg (1 mg/g load). The systematic diminution of size observed for 6.5 mg/g loaded LNC (44.7 nm as opposed to 51.3 or 51.7 nm for 1 mg/g and 0.5 mg/g, respectively, see Table 1) could be due to an intramolecular association between Fc-diOH molecules at this concentration which could explain the absence of dose effect. Moreover, a loss of Fc-diOH oxidative activity during the solubilising step using ultrasound or during the LNC formulation is not impossible. The phenol functions of two nearby molecules could react together leading to the unavailability of the pattern ferrocene–C=C–phenol required for internal electron-transfer. The protection of these phenol functions by grafting an acetate chain in order to make a prodrug, so that hydrolysis takes place *in situ*, should allow prolonged activity of Fc-diOH-loaded LNC. Work on this protection is in progress. Finally, it is also possible that the maximum effective dose was already reached with 1 mg/g loaded LNC (0.84% w/w dry weight) but that, as intratumoural administration does not permit to target all the disseminated cells, a unique injection may not be sufficient to provide the right dose at the right time. Extensive research is still required to optimise administration conditions for effective tumour reduction in rats.

4. Conclusions

In this work, we aimed at comparing two lipid nanocarriers produced by a similar process and composed with the same excipients in order to enhance the bioavailability of ferrocenyl tamoxifen derivative (Fc-diOH) in a 9L subcutaneous tumour model. Lipid nanocapsules exhibited great advantages compared to swollen micelles. Quantitatively, LNC were better internalised by glioma cancer cells compared to micelles; they were less toxic to healthy cells in culture and they could be loaded by hydrophobic molecules with high drug loading levels. Fc-diOH-loaded LNC showed interesting cytotoxic effects on 9L glioma cells with an IC_{50} equivalent to 0.6 μM, and furthermore, this organometallic compound was not active on normal brain cells in a concentration range < 10 μM. Promising *in vivo* results were obtained after intratumoural s.c administration of this new drug-carrier as it dramatically reduced the tumour mass and glioma volume.

Acknowledgments

The authors would like to thank Archibald Paillard (Inserm U646, Angers, France) for fruitful discussions, Pierre Legras and Jerome Roux (Service Commun d'Animalerie Hospitalo-Universitaire, Angers, France) for skillful technical support with animals, and Dr. R. Filmon and R. Mallet (Service Commun d'Imagerie et d'Analyses Microscopiques, Angers, France) for confocal images. This work was supported by a "Région des Pays de la Loire" grant and by "La Ligue Nationale Contre le Cancer" (équipe labellisée 2007).

References

[1] R. Stupp, W.P. Mason, M.J. Van Den Bent, M. Weller, B. Fisher, M.J.B. Taphoorn, K. Belanger, A.A. Brandes, C. Marosi, U. Bogdahn, J. Curschmann, R.C. Janzer, S.K. Ludwin, T. Gorlia, A. Allgeier, D. Lacombe, J.G. Cairncross, E. Eisenhauer, R.O. Mirimanoff, Radiotherapy plus concomitant and adjuvant temozolomide for glioblastoma, N. Engl. J. Med. 352 (10) (2005) 987–996.
[2] B.J.A. Furr, V.C. Jordan, The pharmacology and clinical uses of tamoxifen, Pharmacol. Ther. 25 (2) (1984) 127–205.
[3] V.C. Jordan, Tamoxifen (ICI46,474) as a targeted therapy to treat and prevent breast cancer, Br. J. Pharmacol. 147 (Suppl. 1) (2006).
[4] L. Wickerham, Tamoxifen — an update on current data and where it can now be used, Breast Cancer Res. Treat. 75 (Suppl. 1) (2002).
[5] G.J. Goldenberg, E.K. Froese, Drug and hormone sensitivity of estrogen receptor-positive and -negative human breast cancer cells *in vitro*, Cancer Res. 42 (12) (1982) 5147–5151.
[6] E.P. Gelmann, Tamoxifen for the treatment of malignancies other than breast and endometrial carcinoma, Semin. Oncol. 24 (1 suppl. 1) (1997).
[7] P. De Medina, G. Favre, M. Poirot, Multiple targeting by the antitumor drug tamoxifen: a structure-activity study, Curr. Med. Chem. Anti. Canc. Agents 4 (6) (2004) 491–508.
[8] R.S. Carroll, J. Zhang, K. Dashner, M. Sar, P.M. Black, C. Raffel, Steroid hormone receptors in astrocytic neoplasms, Neurosurgery 37 (3) (1995) 496–504.
[9] H. Khalid, A. Yasumaga, M. Kishikawa, S. Shibata, Immunohistochemical expression of the estrogen receptor-related antigen (ER-D5) in human intracranial tumors, Cancer 75 (10) (1995) 2571–2578.
[10] M. Assimakopoulou, G. Sotiropoulou-Bonikou, T. Maraziotis, J. Varakis, Does sex steroid receptor status have any prognostic or predictive significance in brain astrocytic tumors? Clin. Neuropathol. 17 (1) (1998) 27–34.
[11] F.T. Ventosick Jr., R.G. Seiler, I.F. Pollack, V. Arena, R.A. Morantz, R. Savaya, The treatment of intracranial malignant gliomas using orally administered tamoxifen therapy: preliminary results in a series of failed patients, Neurosurgery 30 (6) (1992) 897–903.
[12] M.F. Clougherty, R.P. Woods, K.L. Black, W.T. Couldwell, R.E. Law, D.R. Hinton, Prolonged treatment with biologic agents for malignant glioma: a case study with high dose tamoxifen, J. Neurooncol. 35 (1) (1997) 39–45.
[13] A.A. Brandes, M. Ermani, S. Turazzi, E. Scelzi, E Berti, P. Amista, A. Bonllo, C. Licata, M.V. Fiorentino, Procarbazine and high-dose tamoxifen as second-line regimen in recurrent high-grade gliomas: a phase II study, J. Clin. Oncol. 17 (2) (1999) 645–650.
[14] S. Top, J. Tang, A. Vessieres, D. Carrez, C. Provot, G. Jaouen, Ferrocenyl hydroxytamoxifen: a prototype for a new range of oestradiol receptor site-directed cytotoxics, Chem. Commun. (8) (1996) 955–956.
[15] S. Top, A. Vessieres, G. Leclercq, J. Quivy, J. Tang, J. Vaissermann, M. Huche, G. Jaouen, Synthesis, biochemical properties and molecular modelling studies of organometallic specific estrogen receptor modulators (SERMs) the ferrocifens and hydroxyferrocifens: evidence for an antiproliferative effect of hydroxyferrocifens on both hormone-dependent and hormone-independent breast cancer cell lines, Chem. Eur. J. 9 (21) (2003) 5223–5236.
[16] A. Vessieres, S. Top, P. Pigeon, E. Hillard, L. Boubeker, D. Spera, G. Jaouen, Modification of the estrogenic properties of diphenols by the incorporation of ferrocene. Generation of antiproliferative effects *in vivo*, J. Med. Chem. 48 (12) (2005) 3937–3940.

[17] E. Hillard, A. Vessieres, L. Thouin, G. Jaouen, C. Amatore, Ferrocene-mediated proton-coupled electron transfer in a series of ferrocifen-type breast-cancer drug candidates, Angew. Chem. Int. Ed. 45 (2) (2006) 285–290.
[18] U. Schatzschneider, N. Metzler-Nolte, New principles in medicinal organometallic chemistry, Angew. Chem. Int. Ed. 45 (10) (2006) 1504–1507.
[19] G. Jaouen, Bioorganometallics, Wiley-VCH, Weinheim, Nov 2005.
[20] B. Rosenberg, L. Van Camp, T. Krigas, Inhibition of cell division in *Escherichia coli* by electrolysis products from a platinum electrode, Nature 205 (1965) 698–699.
[21] P.J. Dyson, G. Sava, Metal-based antitumour drugs in the post genomic era, Dalton Trans. (16) (2006) 1929–1933.
[22] A. Nguyen, V. Marsaud, C. Bouclier, S. Top, A. Vessieres, P. Pigeon, R. Gref, P. Legrand, G. Jaouen, J.M. Renoir, Nanoparticles loaded with ferrocenyl tamoxifen derivatives for breast cancer treatment, Int. J. Pharm. 347 (1–2) (2008) 128–135.
[23] B. Heurtault, P. Saulnier, B. Pech, J.-E. Proust, J.-P. Benoit, A novel phase inversion-based process for the preparation of lipid nanocarriers, Pharm. Res. 19 (6) (2002) 875–880.
[24] G. Jaouen, S. Top, A. Vessieres, G. Leclercq, J. Quivy, L. Jin, A. Croisy, The first organometallic antioestrogens and their antiproliferative effects, C.R. Acad. Sci. Sec. IIc 3 (2) (2000) 89–93.
[25] K.D. McCarthy, J. De Vellis, Preparation of separate astroglial and oligodendroglial cell cultures from rat cerebral tissue, J. Cell. Biol. 85 (3) (1980) 890–902.
[26] T. Mosmann, Rapid colorimetric assay for cellular growth and survival: application to proliferation and cytotoxicity assays, J. Immunol. Methods 65 (1–2) (1983) 55–63.
[27] A. Vonarbourg, C. Passirani, P. Saulnier, P. Simard, J.C. Leroux, J.P. Benoit, Evaluation of pegylated lipid nanocapsules versus complement system activation and macrophage uptake, J. Biomed. Mater. Res. A 78 (3) (2006) 620–628.
[28] B. Heurtault, P. Saulnier, B. Pech, M.-C. Venier-Julienne, J.-E. Proust, R. Phan-Tan-Luu, J.-P. Benoit, The influence of lipid nanocapsule composition on their size distribution, Eur. J. Pharm. Sci. 18 (1) (2003) 55–61.
[29] A. Vonarbourg, P. Saulnier, C. Passirani, J.-P. Benoit, Electrokinetic properties of noncharged lipid nanocapsules: influence of the dipolar distribution at the interface, Electrophoresis 26 (11) (2005) 2066–2075.
[30] A. Lamprecht, Y. Ubrich, J.-P. Benoit, New lipid nanocapsules exhibit sustained release properties for amiodarone, J. Control. Release 84 (1–2) (2002) 59–68.
[31] A. Malzert-Fréon, S. Vrignaud, P. Saulnier, V. Lisowski, J.P. Benoit, S. Rault, Formulation of sustained release nanoparticles loaded with a tripentone, a new anticancer agent, Int. J. Pharm. 320 (1–2) (2006) 157–164.
[32] S. Peltier, J.-M. Oger, F. Lagarce, W. Couet, J.-P. Benoit, Enhanced oral paclitaxel bioavailability after administration of paclitaxel-loaded lipid nanocapsules, Pharm. Res. 23 (6) (2006) 1243–1250.
[33] E. Garcion, A. Lamprecht, B. Heurtault, A. Paillard, A. Aubert-Pouessel, B. Denizot, P. Menei, J.P. Benoit, A new generation of anticancer, drug-loaded, colloidal vectors reverses multidrug resistance in glioma and reduces tumor progression in rats, Mol. Cancer Ther. 5 (7) (2006) 1710–1722.
[34] S.E. Dunn, A. Brindley, S.S. Davis, M.C. Davies, L. Illum, Polystyrene-poly (ethylene glycol) (PS-PEG2000) particles as model systems for site specific drug delivery. 2. The effect of PEG surface density on the *in vitro* cell interaction and *in vivo* biodistribution, Pharm. Res. 11 (7) (1994) 1016–1022.
[35] R.C. Bravo Gonzalez, E Boess, E. Durr, N. Schaub, B. Bittner, *In vitro* investigation on the impact of Sdiutol HS 15 on the uptake of colchicine into rat hepatocytes, Int. J. Pharm. 279 (1–2) (2004) 27–31.
[36] S. Top, A. Vessieres, C. Cabestaing, I. Laios, G. Leclercq, C. Provot, G.E. Jaouen, Studies on organometallic selective estrogen receptor modulators. (SERMs) Dual activity in the hydroxy-ferrocifen series, J. Organomet. Chem. 637–639 (2001) 500–506.
[37] R.L. Sutherland, C.K.W. Watts, R.E. Hall, P.C. Ruenitz, Mechanisms of growth inhibition by nonsteroidal antioestrogens in human breast cancer cells, J. Steroid Biochem. 27 (4–6) (1987) 891–897.
[38] D. Yao, F. Zhang, L. Yu, Y. Yang, R.B. Van Breemen, J.L. Bolton, Synthesis and reactivity of potential toxic metabolites of tamoxifen analogues: droloxifene and toremifene o-quinones, Chem. Res. Toxicol. 14 (12) (2001) 1643–1653.
[39] P.W. Fan, F. Zhang, J.L. Bolton, 4-Hydroxylated metabolites of the antiestrogens tamoxifen and toremifene are metabolized to unusually stable quinone methides, Chem. Res. Toxicol. 13 (1) (2000) 45–52.
[40] F. Zhang, P.W. Fan, X. Liu, L. Shen, R.B. Van Breemen, J.L. Bolton, Synthesis and reactivity of a potential carcinogenic metabolite of tamoxifen: 3,4-Dihydroxytamoxifen-o-quinone, Chem. Res. Toxicol. 13 (1) (2000) 53–62.
[41] D. Osella, M. Ferrali, P. Zanello, F. Laschi, M. Fontani, C. Nervi, G. Cavigiolio, On the mechanism of the antitumor activity of ferrocenium derivatives, Inorg. chim. acta 306 (1) (2000) 42–48.
[42] J.X. Wilson, Antioxidant defense of the brain: a role for astrocytes, Can. J. Physiol. Pharmacol. 75 (10–11) (1997) 1149–1163.
[43] B.H. Juurlink, Response of glial cells to ischemia: roles of reactive oxygen species and glutathione, Neurosci. Biobehav. Rev. 21 (2) (1997) 151–166.
[44] S. Peuchen, J.P. Bolanos, S.J. Heales, A. Almeida, M.R. Duchen, J.B. Clark, Interrelationships between astrocyte function, oxidative stress and antioxidant status within the central nervous system, Prog. Neurobiol. 52 (4) (1997) 261–281.
[45] R. Dringen, Metabolism and functions of glutathione in brain, Prog. Neurobiol. 62 (6) (2000) 649–671.
[46] D.M. Woodcock, M.E. Linsenmeyer, G. Chojnowski, A.B. Krieger, V. Nink, L.K. Webster, W.H. Sawyer, Reversal of multidrug resistance by surfactants, Br. J. Cancer 66 (1) (1992) 62–68.

CHAPITRE 3

Effet synergique de l'administration locale de ferrociphénol et de la radiothérapie externe dans un modèle intracérébral de gliome 9L.

Effet synergique de l'administration locale de ferrociphénol et de la radiothérapie externe dans un modèle intracérébral de gliome 9L.

Ce chapitre décrit l'effet de la radiothérapie externe sur la molécule Fc-diOH encapsulée dans les nanocapsules lipidiques sur un modèle de gliome 9L. Les cellules 9L subissent différents types de traitements et la survie cellulaire est évaluée en réalisant un test au MTT (bromure de 3-(4,5-dimethylthiazol-2-yl)-2,5-diphenyl tetrazolium). Le premier protocole associe à J1 une radiothérapie à différentes doses (5 à 40 Gy) et à J2 une chimiothérapie avec des LNC-Fc-diOH 1µmol/L, tandis que le second délivre la chimiothérapie préalablement à l'irradiation. Les cellules 9L sont traitées par des concentrations croissantes en LNC-Fc-diOH (de 0.01 à 1µmol/L) et irradiées avec des doses croissantes en radiothérapie (de 2 à 40 Gy) afin de déterminer les doses létales 50 (IC_{50}) de chimiothérapie et radiothérapie seules. Ces doses vont permettre de déterminer, dans des conditions *in vitro*, si l'interaction thérapeutique est synergique ou simplement supra-additive. Enfin, ce chapitre présente l'administration des LNC-Fc-diOH dans un modèle de gliome orthotopique par "convection enhanced delivery" (CED). Afin d'augmenter les volumes de distribution tout en diminuant le reflux, les viscosités des formulations de LNC ont été augmentées par ajout de sucrose en phase externe. Après avoir vérifié l'innocuité du disaccharide sur les cellules en culture, les rats ont été infusés avec des formulations de LNC-Fc-diOH ou LNC blanches 6 jours après implantation de la tumeur 9L. Les rats ont ensuite subi trois séances de radiothérapie de 6Gy chacune sur l'encéphale *in toto* à J8, J11 et J14. L'efficacité du traitement est ensuite appréciée par des études de survie.

LOCAL DELIVERY OF FERROCIPHENOL LIPID NANOCAPSULES FOLLOWED BY EXTERNAL RADIOTHERAPY AS A SYNERGISTIC TREATMENT AGAINST INTRACRANIAL 9L GLIOMA XENOGRAFT

E. Allard[1], C. Passirani[1*], D. Jarnet[2], S. Petit[1,2], A. Vessières[3], G. Jaouen[3] and JP Benoit[1]

[1] INSERM, U646, Université d'Angers, Angers, F-49100 France.

[2] Centre Paul Papin, Angers, F-49100, France.

[3] CNRS, UMR 7576, Ecole Nationale Supérieure de Chimie de Paris, F-75231 France.

*To whom correspondence should be addressed:

Tel: +33 241 735850;

Fax: +33 241 735853;

E-mail address: catherine.passirani@univ-angers.fr

Article soumis à 'Clinical Cancer Research'

Abstract

Purpose: The goal of the present study was to evaluate the efficacy of a new organometallic drug, ferrociphenol (Fc-diOH) in combination with external radiotherapy in intracerebral 9L glioma model. Previously, we reported that Fc-diOH could be encapsulated in lipid nanocapsules (LNC) with high drug loading compatible with *in vivo* applications. The cytostatic activity of Fc-diOH-LNC was shown to be very effective on 9L glioma cells (IC_{50} = 0.6µM) and harmless towards healthy cells. Here, we tested the hypothesis that the combination of external radiotherapy with Fc-diOH could potentiate the action of this drug, conferring a synergistic effect.

Experimental Design: 9L cells were treated with increasing concentrations of Fc-diOH-LNC (from 0.01 to 1µmol/L) and irradiated with a rising dose of radiotherapy (from 2 to 40 Gy). The MTT test was used to investigate the cytotoxicity of the combination treatment. *In vivo* assessment of synergistic activity was evaluated by the inoculation of 9L cells in Fisher rats. Chemotherapy with Fc-diOH-LNC (0.36mg/rat) was administered by means of convection enhanced delivery (CED), and the treatment was followed by three irradiations of 6 Gy doses at Day 8, 11, 14 (total dose = 18 Gy). The therapeutic effect was assessed based on animal survival.

Results: *In vitro* evaluations evidenced that a combined treatment with Fc-diOH-LNC and irradiations showed synergistic antitumor activity on 9L glioma cells. Combining cerebral irradiation with CED of Fc-diOH-LNC led to a significant longer survival *in vivo* and the existence of long term survivors compared to Fc-diOH-LNC treated animals ($p<0.0001$) and to the group treated with blank LNC + radiotherapy ($p= 0.032$).

Conclusions: The synergistic effect between ferrociphenol-loaded lipid nanocapsules and radiotherapy may be due to a closely oxidative relationship. Radiations may initiate the oxidation of Fc-diOH phenol moiety into a quinone methide structure strongly cytotoxic for the tumor cells. Upon these considerations, Fc-diOH-LNC appear to be an efficient radiosensitive anticancer drug delivery system.

Introduction

Even with aggressive multi-modality treatment strategies, the life expectancy of patients with glioblastoma multiforme (GBM), the most aggressive primary brain tumor, is a bit more than 1 year after diagnosis. Surgery and radiotherapy with concomitant and adjuvant temozolomide, a novel oral alkylating agent, is the standard therapy regimen for newly diagnosed GBM. Patients treated with radiotherapy plus temozolomide show a median survival time of 14.6 months versus 12.1 months with radiotherapy alone after surgery [1]. This moderate result underlines the critical role of chemotherapy, the utility of which is very often controversial [2]. In an attempt to overcome the limitations of systemic delivery of anticancer drugs aimed at brain targeting, especially because of the presence of the Blood brain barrier (BBB), several methods of regional delivery have been developed [3, 4]. Convection enhanced delivery (CED) was introduced in the early nineties as a technique to enhance drug distribution, especially compared to local delivery methods based on diffusion [5, 6]. Many anticancer drugs have been investigated in CED like nitrosoureas - BCNU and ACNU [7, 8] , paclitaxel [9], topotecan [10], carboplatin [11] and gemcitabine [12]. But many problems relating to local CNS toxicity, short drug tissue retention and heterogeneous distribution within tumors were reported. To circumvent these problems, some drugs have been encapsulated in nanocarriers and infused by CED. Nanoencapsulation offers many advantages, such as protection of the active species, reducing both the interaction with the brain extra cellular matrix (ECM) [13] and brain toxicity [14], a better drug distribution [15] and a higher brain half-life [16, 17]. In this context, our group focused on the administration and study of the infusion of lipid nanocapsules (LNC) in rat brain by CED. These lipid nanocarriers obtained by a low-energy emulsification method are characterized by the absence of organic solvent in their formulation [18]. They present ideal characteristics for CED infusion such as a low particle size < 100 nm, a global negative charge, and are shielded by a PEG steric coating (Allard *et al.*, review submitted). Moreover, LNC can be loaded with lipophilic molecules such as many anticancer drugs [19, 20], radionuclides [21] and contrast agents. In the field of GBM therapy, hydrophobic bioorganometallic compounds were encapsulated in LNC and investigated as a new class of active molecules [22]. Bioorganometallic molecules are defined as active molecules that contain at least one carbon directly bound to a metal or metalloid. The metal studied here is iron (Fe) and the metallocene

derivative is ferrocene [η^5-$Fe(C_5H_5)_2$] chemically grafted on a polyphenolic skeleton. The resulting molecules are ferrocenyl phenols compounds that we called “ferrocifen”. They were first studied on breast cancer cell lines where they showed dual effects: an antiestrogenic effect on estrogen receptor positive cell lines and a cytotoxic effect on hormone independent cell lines [23, 24]. These compounds are thought to be susceptible to an oxidation of the ferrocenyl antenna to give intracellular quinone methides that are cytotoxic via interaction with the nucleophiles present in the cell, such as glutathione [25]. We previously demonstrated that LNC could be loaded with the ferrocenyl diphenol molecule called “ferrociphenol” (Fc-diOH) with high drug loading levels and that LNC were an ideal cargo to solubilise and infuse this drug, which is totally insoluble in water [22]. Fc-diOH-LNC were cytotoxic on 9L glioma cells (IC_{50} = 0.6µM) and harmless on healthy brain cells up to a concentration range of 10µM. Promising *in vivo* results were also obtained after intratumoral administration of this new drug-carrier in a subcutaneous injected 9L model as it dramatically reduced the tumor mass and glioma volume.

In the present study, we first evaluated the synergistic effect between radiotherapy and Fc-diOH activity after its nanoencapsulation, on 9L cells in culture. Then, a combined treatment using CED of Fc-diOH-LNC with external beam radiotherapy was evaluated on 9L glioma-bearing rats.

Materials and methods

Materials

Ferrocenyl diphenol compound (2-ferrocenyl-1,1-bis(4-hydroxyphenyl)-but-1-ene) named Fc-diOH was prepared by a McMurry coupling reaction [26]. The lipophilic Labrafac® CC (caprylic-capric acid triglycerides) was kindly provided by Gattefosse S.A. (Saint-Priest, France). Lipoïd® S75-3 (soybean lecithin at 69% of phosphatidylcholine) and Solutol® HS15 (a mixture of free polyethylene glycol 660 and polyethylene glycol 660 hydroxystearate) were a gift from Lipoïd Gmbh (Ludwigshafen, Germany) and BASF (Ludwigshafen, Germany), respectively. NaCl was obtained from Prolabo (Fontenay-sous-bois, France). Deionized water was acquired from a Milli-Q plus system (Millipore, Paris, France) and sterile water from Cooper (Melun, France). Sucrose was obtained from Merck KGaA (Darmstadt, Germany).

Preparation of Fc-diOH-LNC

Lipid nanocapsules were prepared according to a previously described original process [18]. In order to obtain LNC, Solutol® HS15 (17% w/w), Lipoid® (1.5% w/w), Labrafac® (20% w/w), NaCl (1.75% w/w) and water (59.75% w/w) were mixed and heated under magnetic stirring up to 85°C. Three cycles of progressive heating and cooling between 85 and 60°C were then carried out and followed by an irreversible shock induced by dilution with 2°C deionised water added to the mixture at 70-75°C. To formulate Fc-diOH-LNC, a first step consisted in dissolving the anticancer drug in triglycerides (Labrafac®) using ultrasound during 1.5 hours. Two parameters were varied: the amount of Fc-diOH in triglycerides (1.7% and 4% (w/w)) and the volume of cold water for LNC dilution (70% and 28.5% v/v) to obtain drug loadings of 1mg/g (0.84% w/w dry weight) and 6.5mg/g (2% w/w dry weight) respectively. For *in vivo* applications, sucrose (20% w/w) was dissolved in the aqueous phase of the LNC suspension after formulation.

LNC physicochemical properties

LNC were analyzed for their size and charge distribution using a Malvern Zetasizer® Nano Serie DTS 1060 (Malvern Instruments S.A., Worcestershire, UK). LNC were diluted 1:60 (v/v) in deionised water in order to ensure a convenient scattered intensity on the detector. The viscosities of the solutions were measured at room temperature using Schott Geräte AVS 400 Model automatic viscometer (Oswald viscosimeter). Each value was reported as an average of five measurements ± standard deviation.

Tumor cell line

Rat 9L gliosarcoma cells were obtained from the European Collection of Cell Culture (Salisbury, UK, N°94110705). The cells were grown at 37°C/5% CO_2 in Dulbecco modified eagle medium (DMEM) with glucose and L-glutamine (BioWhittaker, Verviers, Belgium) containing 10% foetal calf serum (FCS) (BioWhittaker) and 1% antibiotic and antimycotic solution (Sigma, Saint-Quentin Fallavier, France).

Irradiation

Radiotherapy was conducted with a linear accelerator (Clinac®, Varian Medical Systems, Salt Lake City, USA). The irradiations were delivered by one beam with energy of 6 MV and with an adapted field according to the material irradiated. For *in vitro* irradiations, cells were irradiated at room temperature as a single exposure to doses of photon of 2, 5, 6, 10, 20, and 40Gy or in 3 fractions of 6 Gy spaced in time. For animal irradiations, fractionated radiotherapy consisted of 18 Gy given in 3 fractions of 6 Gy over 2 weeks, on Day 8, 11 and 14. The dose rate for the irradiation was 4 Gy/min and four rats were irradiated at a time. The animals were anesthetized before irradiation under light sedation (isoflurane/oxygen anesthesia 3%/3l min^{-1}) and placed on the Clinac® couch in prone position with laser alignment.

Cell protocol

The 9L cells were plated on 24-well plates in DMEM containing 10% FCS and 1% antibiotic/antimycotic solutions and then treated with increasing concentrations of LNC-Fc-diOH chemotherapy (CT) and external radiotherapy (RT) according to three different protocols described below.

Protocol RT+CT versus CT+RT

The 9L cells were plated on 24-well plates for 24h at 40,000 cells/well. At Day 1, cells were irradiated with 5 to 40 Gy or treated with Fc-diOH-LNC 1µmol/L. At Day 2, irradiated cells at Day 1 were treated with Fc-diOH-LNC 1µmol/L (protocol 1) and cells treated with CT were irradiated with 5 to 40 Gy (protocol 2). MTT survival test was then performed 96 h after (Day 6).

Combined effect protocol

9L cells were plated at 3,000 cells/well at Day 0. At Day 2, they were treated with increasing concentrations of Fc-diOH-LNC from 0.01 to 1 µmol/L. At Day 3, cells were irradiated with 2, 6, 10, 20 or 40 Gy and MTT was performed 96h after (Day 7). The synergy of the combined treatment was assessed using isobologram analysis [27]. To that, the IC_{50} values, i.e. the Fc-diOH concentrations and the irradiation dose at which 50% of the 9L cells survived, were determined. To establish the IC_{50} values for CT alone, cells were incubated with increasing concentrations of Fc-diOH from 0.001 to 100µmol/L. For the evaluation of the IC_{50} in RT alone, cells were irradiated at 5, 10, 20 and 40 Gy in a single fraction.

Multi-irradiation protocol

9L cells were plated at 500 cells/well at Day 0, treated with increasing concentrations of Fc-diOH-LNC from 0.01 to 1µmol/L at Day 4 and irradiated with 3 fractions of 6 Gy at Day 5, 8 and 11. MTT survival test was performed at Day 15.

MTT survival test

After 96h within any treatment, cell survival percentage was estimated by the MTT survival test. 40µl of MTT solution at 5mg/ml in PBS were added to each well, and the plates were incubated at 37°C for 4h. The medium was removed and 200µl of acid–isopropanol 0.06N was added to each well and mixed to completely dissolve the dark blue crystals. The optical density values (OD) were measured at 580nm for blue intensity and at 750 nm for turbidity using a multiwell-scanning spectrophotometer (Multiskan Ascent, Labsystems SA, Cergy-pontoise, France). The maximal absorbance was determined by incubating cells with free media and was considered as 100% survival ($OD_{control}$). Cell survival percentage was estimated according to equation (1). Each experiment was conducted 2 times with at least 6 repeated samples.

$$(1)\ \text{Cell survival (\%)} = \frac{\text{OD 580 nm} - \text{OD 750 nm}}{OD_{control}\ 580\ \text{nm} - OD_{control}\ 750\ \text{nm}} \times 100$$

Animals and intracranial xenograft technique

Syngeneic Fischer F344 female rats weighing 160-180g were obtained from Charles River Laboratories France (L'Arbresle, France). All experiments were performed on 10 to 11-week old female Fisher rats. The animals were anesthetized with an intraperitoneal injection of 0.75-1.5ml/kg of a solution containing 2/3 ketamine (100mg/ml) (Clorketam®, Vétoquinol, Lure, France) and 1/3 xylazine (20mg/ml) (Rompun®, Bayer, Puteaux, France). Animal care was carried out in strict accordance with French Ministry of Agriculture regulations. A 9L tumor monolayer was detached with trypsin-ethylenediamine tetraacetic acid, washed twice with EMEM (Eagle's Minimal Essential Medium) without FCS or antibiotics, counted and resuspended to the final concentration desired. For intracranial implantation, 10 microliters of 1,000 9L cell suspension were injected into the rat striatum at a flow rate of 2µl per minute using a 10µl syringe (Hamilton® glass syringe 700 series RN) with a 32G needle (Hamilton®). For that purpose, rats were immobilized in a stereotaxic head frame (Lab Standard Stereotaxic; Stoelting, Chicago, IL). A sagittal incision was made through the skin and a burr hole was drilled into the skull with a twist drill. The cannula coordinates were 1mm posterior from the bregma, 3mm lateral from the sagittal suture and 5mm below the dura (with the

incisor bar set at 0mm). The needle was left in place for 5 additional minutes to avoid expulsion of the suspension from the brain during removal of the syringe, which was withdrawn very slowly (0.5mm per minute).

Convection Enhanced Delivery

On Day 6, 60µl of the LNC suspensions were injected by CED at the coordinates of the tumor cells. Infusions were performed at the depth of 5mm from the brain surface using a 10µl Hamilton® syringe with a 32G needle. This syringe was connected to a 100µl Hamilton syringe 22G containing the product (Harvard Apparatus, Les Ulis, France) through a cannula (CoExTM PE/PVC tubing, Harvard apparatus, Les Ulis, France). CED was performed with an osmotic pump PHD 2,000 infusion (Harvard Apparatus, Les Ulis, France) by controlling a 0.5µl/min rate for two hours. Thirty nine rats with 9L tumor cells were randomized into four experimental groups. The groups were as follows: (1) control group without CED but with the same anesthetized scheme (n = 9); (2) a CED group, receiving CED of Fc-diOH-LNC (+ sucrose) at a dose of 0.36 mg/rat (n = 8); (3) a radiotherapy group, receiving CED of blank-LNC (+ sucrose) followed by whole-brain radiation to a total dose of 18Gy (3x 6Gy) (n = 10), (4) a CED plus radiotherapy group, receiving CED of Fc-diOH-LNC (+ sucrose) at a dose of 0.36 mg/rat, followed by whole-brain radiation to a total dose of 18Gy (n = 12).

Statistical analysis

Data from *in vitro* experiments are presented as mean ± SD and statistical analysis between groups was conducted with the two-tailed Student t-test ($p<0.05$ was considered to be significant). The Kaplan-Meier method was used to plot animal survival. Statistical significance was calculated using the log-rank test (Mantel-Cox Test). StatView software version 5.0 (SAS institute Inc.) was used for that purpose and tests were considered as significant with p values <0.05. The different treatment groups were compared in terms of median and mean survival time (days), increase in survival time (IST_{median} and IST_{mean} %), and long term survivors (%).

RESULTS

LNC formulation and cytotoxicity

As shown in previous works [22], Fc-diOH-LNC presented a very narrow size between 45.3 and 48.7nm, depending on the drug payload, and were monodispersed (PI ≤ 0.1) (Table 1). The presence of sucrose in the LNC suspension aqueous phase did not affect the size as there was no significant change in size measurements. Zeta potential values were equivalent from -9.4 to -10.5mV for all the suspensions. On the contrary, viscosity increased from 4.4 ± 0.1 to 8.7 ± 0.2 mm^2/s with the presence of the disaccharide in the formulation. The presence of sucrose had no toxic effect on cells *in vitro* as there was no significant difference in cytotoxicity between blank and Fc-diOH-LNC with or without sucrose (Figure 1). Moreover, a dose effect for Fc-diOH could be observed after its encapsulation, as 9L cell survival percentage was 45-50% for Fc-diOH-LNC 1mg/g and 4-6% for 6.5mg/g loaded nanocapsules.

	Mean particle size (nm)	**Polydispersity index** (PDI)	**Zeta potential** (mV)	**Viscosity** ($mm^2. s^{-1}$)
Blank LNC	48.7 ± 0.5	0.063 ± 0.012	-9.4 ± 0.2	4.4 ± 0.1
Blank LNC + sucrose	47.6 ± 0.1	0.048 ± 0.009	-9.5 ± 1.1	8.7 ± 0.2
Fc-diOH LNC 1mg/g	46.3 ± 0.7	0.050 ± 0.009	-9.6 ± 3.9	-
Fc-diOH LNC 6.5mg/g	45.3 ± 2.5	0.074 ± 0.039	-10.5 ± 1.0	-
Fc-diOH LNC 6.5mg/g + sucrose	46.6 ± 2.1	0.103 ± 0.074	-10.0 ± 1.1	-

Table 1: Physicochemical characteristics of blank and Fc-diOH-LNC.

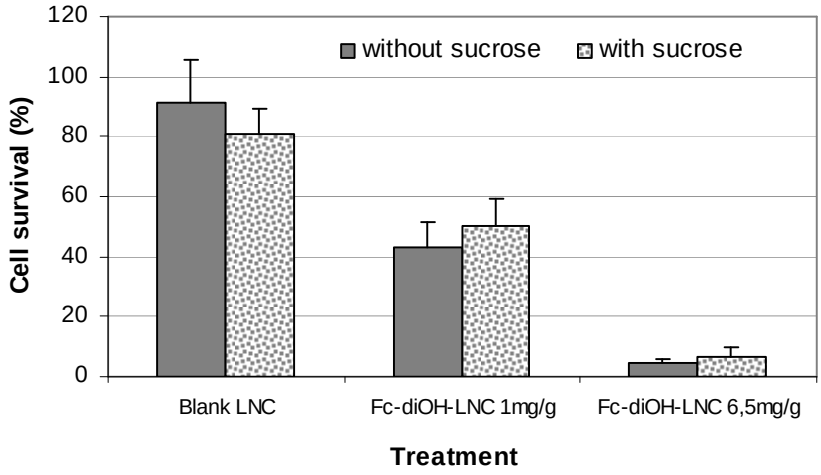

Figure 1: Cell survival test after treatment with Fc-diOH-loaded and blank LNC with or without sucrose in external phase. Blank LNC, Fc-diOH-LNC 1mg/g and Fc-diOH-LNC 6.5mg/g were diluted in culture medium with the same dilution factor (1/ 2.350).

Combined effects of chemotherapy and radiotherapy

Two distinct protocols combining chemotherapy and radiotherapy were performed on 9L cells. One group of cells was treated with radiotherapy followed by chemotherapy with Fc-diOH-LNC (protocol 1= RT+ CT) and another group received the chemotherapy before the RT regimen (protocol 2= CT+RT) (Figure 2a). Firstly, cell survival percentage decreased with the increasing dose of radiotherapy for all conditions tested (Figure 2b). For the first protocol tested (RT+CT), the percentage of cell survival decreased from 34% to 6% for 5 and 40 Gy, respectively. For the protocol 2: CT+RT, cell survival percentages decreased from 8 to 2% for the cells irradiated between 5 and 40 Gy, respectively. The difference in cell viability was shown to be significant between radiotherapy alone and protocol 1 but was also significant for protocol 1: RT+CT versus protocol 2: CT+RT ($p<0.05$). As the treatment was more efficient when cells were first treated by chemotherapy, the sequential utilization of Fc-diOH treatment followed by RT was selected for the following studies.

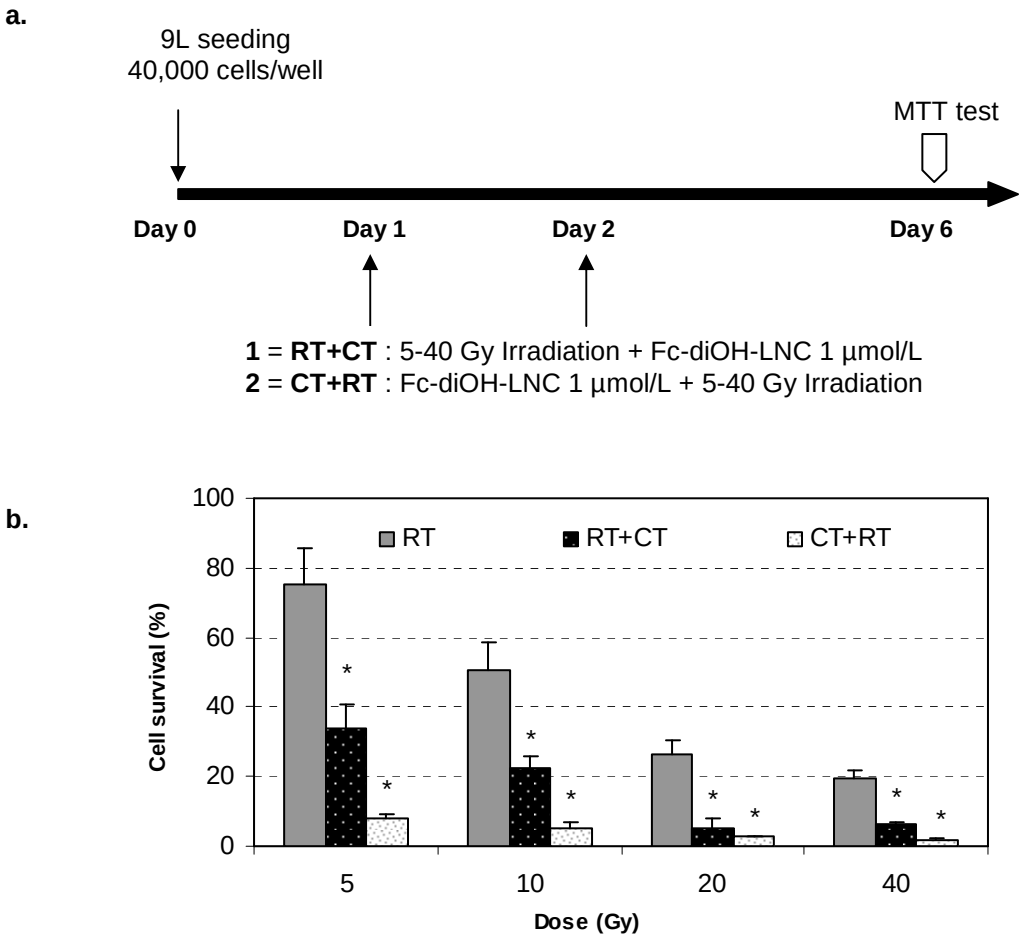

Figure 2: Cell survival percentage of 9L cells according to 2 distinct protocols: radiotherapy + chemotherapy (RT+CT: protocol 1) versus chemotherapy + radiotherapy (CT+RT: protocol 2). Chemotherapy was a treatment with Fc-diOH-LNC 1mg/g at 1µmol/L and Radiotherapy was a single irradiation at 5, 10, 20 and 40 Gy. * means $p<0.05$

Synergistic effects

To determine if the chemotherapy-radiotherapy association with Fc-diOH and external beam photon irradiation was an additive or a synergistic effect, isobologram analysis was performed. Cells were plated at Day 0, treated with increasing concentrations of Fc-diOH-LNC at Day 2 and irradiated 24h after by 2, 6, 10, 20 and 40 Gy (Figure 3a). Median effect doses (IC_{50} values) calculated from this experiment were 0.4µmol/L for Fc-diOH-LNC and about 7.4Gy for irradiation therapy (Figure 3b-c). The combination of Fc-diOH treatment with radiotherapy of 2 and 6Gy allowed the determination of IC_{50} values whereas irradiations with 10, 20 and 40 Gy without chemotherapy always gave cell survival percentage lesser than 50% (Figure 3b). The IC_{50} values were about 0.15 µmol/L and 0.01 µmol/L for 2 Gy and 6

Gy, respectively. As these values divided by the IC_{50} were under the dash line of the isobologram (Figure 3d), this result indicated a synergistic effect between the two treatments.

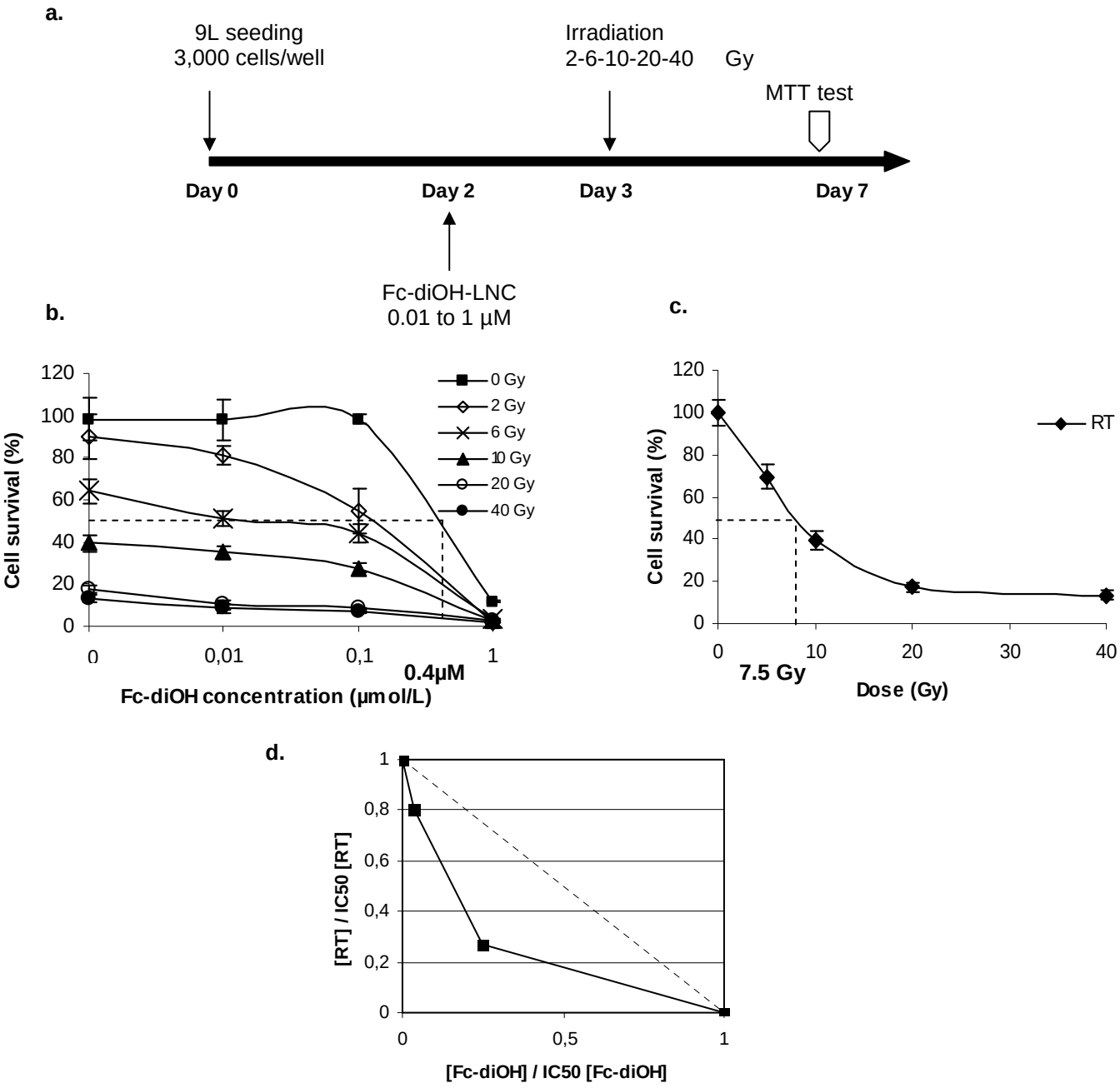

Figure 3: Synergistic effect of cell death by Fc-diOH-LNC and radiotherapy in 9L glioma cells. Cells were treated according to the protocol detailed in (**a**). Cell survival percentage of 9L cells treated with CT (from 0.01 to 1µM) + RT (from 2 to 40 Gy) were expressed in (**b**). IC_{50} for CT alone (RT= 0Gy) was equivalent to 0.4 µM (**b**) and IC_{50} for RT (CT= 0µM) was about 7.5 Gy (**c**). Synergy was determined between the two treatments as seen in the isobologram analysis (points below dotted line) (**d**).

Multi-irradiation

Cultured monolayers of 9L cells were treated with increasing concentrations of Fc-diOH-LNC followed by three irradiations doses leading to a final dose of 6, 12 and 18 Gy (Figure 4a). Cell survival percentage was calculated after performing the MTT survival test (Figure 4b). These results showed that cell death is directly proportional to Fc-diOH concentration. Moreover, cell survival percentage decreased with the repetitive irradiations as 23.9%, 6.1%, 3.2% and 1.9% of the cells were still alive after a treatment with 1µM Fc-diOH-LNC, followed by 0, 1, 2 and 3 irradiations, respectively (Figure 4b).

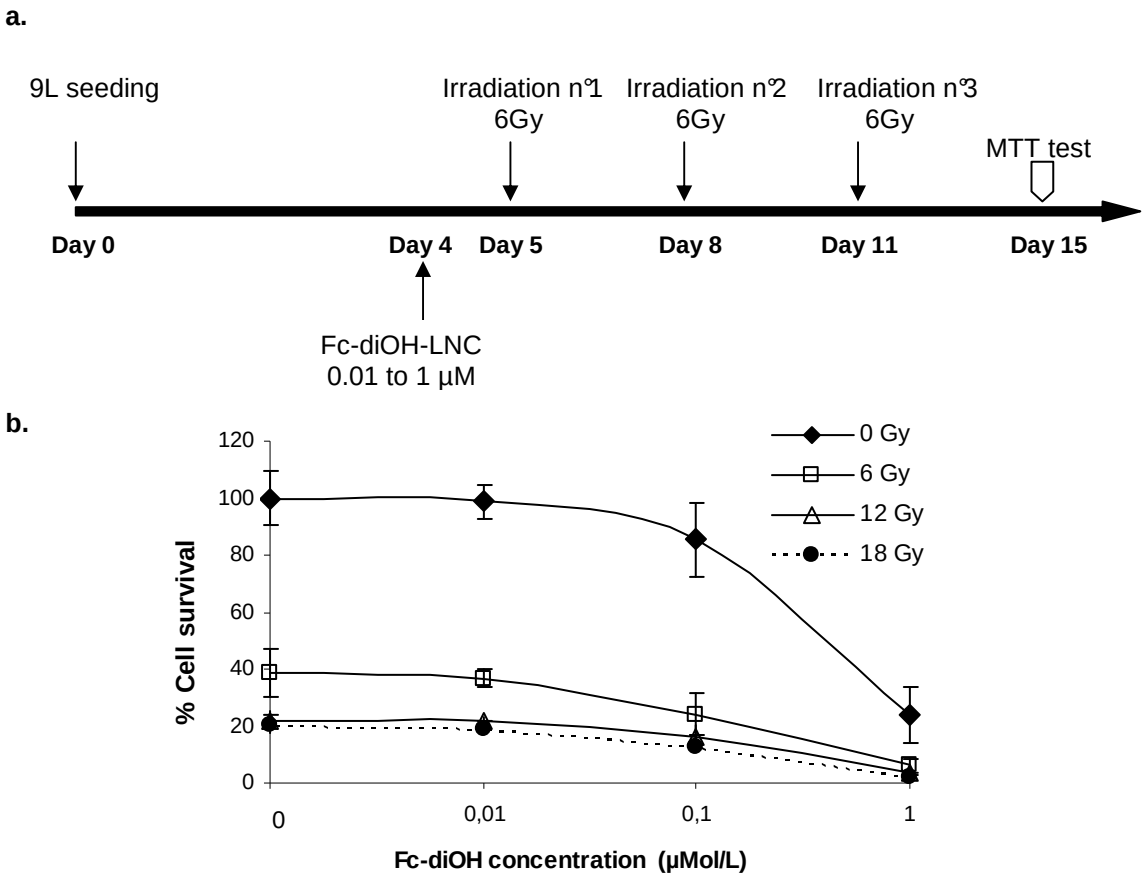

Figure 4: 9L cell viability after a chemotherapy treatment with Fc-diOH-LNC followed by a multi-irradiation scheme of 3x6 Gy. Multi irradiation protocol is detailed in (**a**). (**b**) represents the cell survival percentage after treatment with Fc-diOH-loaded LNC at concentrations between 0.01 and 1µM and followed by a total dose of RT of 0, 6, 12 and 18 Gy (MTT assay).

The effect of cell death was predominant after the first irradiation whatever the chemotherapy scheme as shown in Table 2, which is another representation of the same results. For a chemotherapy treatment without radiotherapy, cell death percentage increased up to 76.1% for a single treatment with Fc-diOH-LNC 1µmol/L. The percentages of cell death spread from 61.4 to 74.4% between 0 and 6 Gy, decreased from 33.0 to 48.4% for the second irradiation (6-12 Gy) and finished between 5.3 to 38.2% for the last irradiation (12-18Gy). After the third irradiation, the cell death percentage was much higher for the cells treated with the highest dose of Fc-diOH especially compared to the group of cells only treated with radiotherapy (38.2% versus 5.3%).

	No irradiation 0Gy	**1 irradiation 6Gy**	**2 irradiations 12Gy**	**3 irradiations 18Gy**
0 µM	0	61,4	44,4	5,3
0,01µM	1,3	62,8	41,7	12,6
0,1 µM	14,7	71,8	33,0	23,2
1 µM	76,1	74,4	48,4	38,2

Table 2: Percentages of cell death after 0, 1, 2, and 3 irradiations of 6Gy according to the dose of chemotherapy received by 9L cells (from 0 to 1 µmol/L).

Survival study

9L tumor bearing rats were treated either by a CED injection of Fc-diOH-LNC 6.5mg/g (0.36mg/rat), a CED injection of blank LNC followed by irradiation with 3 fractions of 6 Gy over 7 days (total dose = 18 Gy) or a CED injection with LNC-Fc-diOH 6.5mg/g (0.36mg/rat) followed by local irradiation (Figure 5a). A control group without CED injection but undergoing the same anesthetized scheme was also preformed. All non treated rats died within 27 days with a median and mean survival of 25 days (Figure 5b and Table 3). There was no increase in life time for the rats which were only treated with chemotherapy as this group had a median survival time of 23 days ($p = 0.1761$ vs control). Rats treated with a CED injection of blank LNC followed by 18Gy irradiation showed an increased median survival time of 32% when compared to controls. The result in survival time was significantly different compared to the control group ($p < 0.0001$).

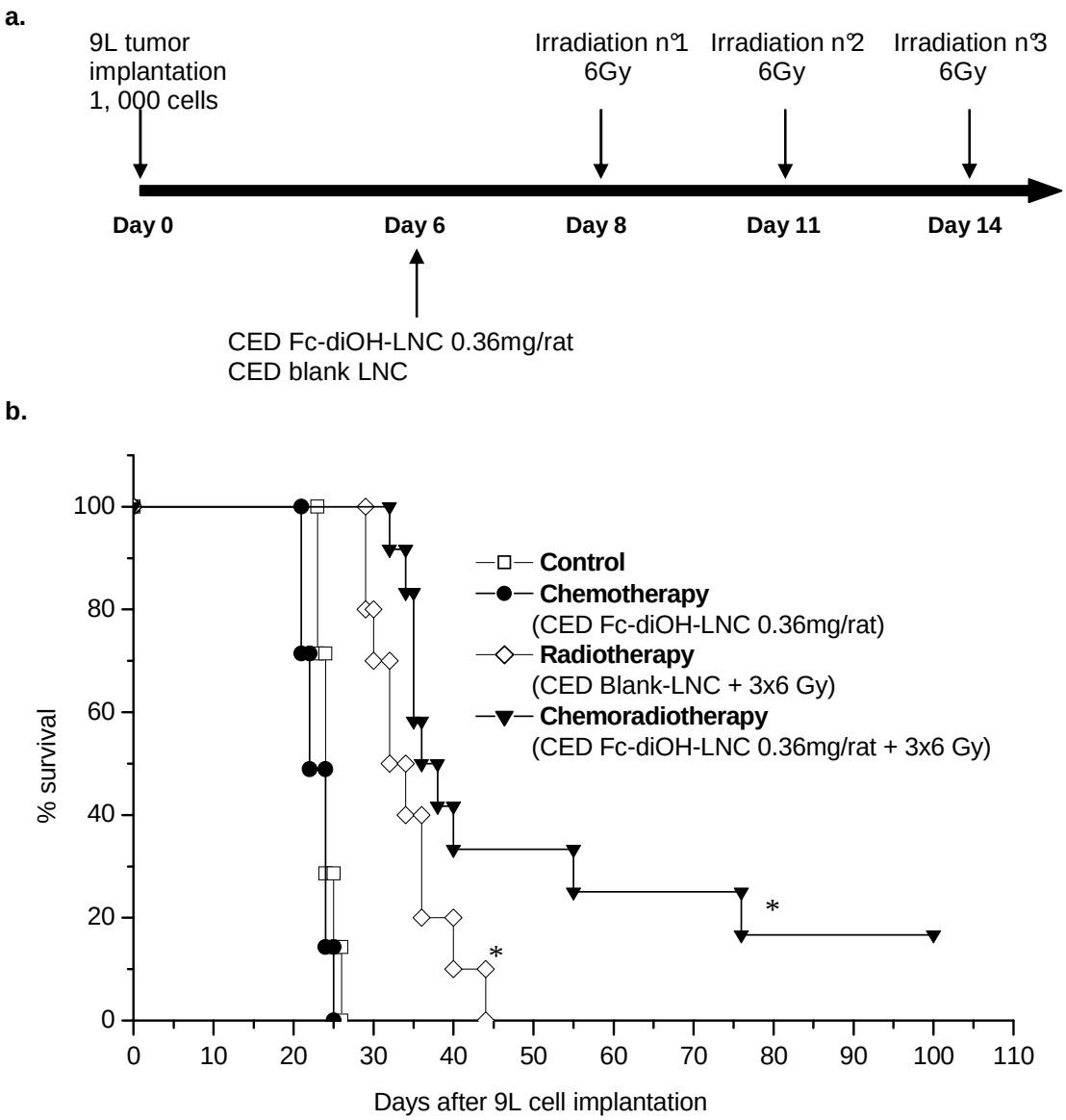

Figure 5: Representation of the chemoradiotherapy protocol applied on 9L glioma-bearing rats (**a**). Kaplan-Meier survival curves for 9L glioma bearing rats after CED of Fc-diOH-LNC and external radiotherapy 3x6 Gy (**b**). Survival times in days after tumor implantation have been plotted for untreated animals (-□-), CED of Fc-diOH-LNC 0.36mg/rat alone (-●-), irradiation 18Gy (three fractions of 6Gy) in combination with CED of blank LNC (-◊-), and irradiation 18Gy in combination with CED of Fc-diOH-LNC 0.36mg/rat (-▼-). Fc-diOH was administrated on Day 6 and X-ray dose fractions were delivered on Days 8, 11 and 14 after tumor implantation. * means $p<0.05$.

Combination of Fc-diOH and RT further improved survival as the median and mean survival time were equivalent to 37 and 53 days, respectively. The experiments established that rat median survival was improved significantly for this group compared to control group ($p<0.0001$) but also compared to the group treated with blank LNC + RT ($p = 0.0328$). In

addition, 2/12 rats (16.7%) in the Fc-diOH + RT group were long term survivors which enhanced the mean increased survival time (IST) up to 105.2% compared to control (Table 3).

Treatment	**n**	**Survival time**(days)			**Increase life time (%)**		
		Range	Median	Mean ± SE	Long term survivors	IST median	IST mean
Fc-diOH-LNC	8	21-27	23.0	23.2 ± 2.1	0	0	0
Blank LNC + radiotherapy	10	29-44	33.0	34.2 ± 4.9	0	32	36.8
Fc-diOH-LNC+ radiotherapy	12	32-100	37.0	51.3 ± 25.9	16.7	48	105.2
Control	9	23-27	25.0	25.0 ± 1.2	0	-	-

Table 3: Descriptive and statistical data from the survival study with Fc-diOH chemotherapy and external radiotherapy of 18Gy (3x6 Gy).
Note: n is the number of animals per group. The increases in median and mean survival time (IST_{median} and IST_{mean}) are calculated in comparison to the control group (%).

DISCUSSION

Polyphenols have a variety of biological activities, ranging from anti-aging or anticancer activities, to the lowering of blood cholesterol levels and bone strength improvement [28, 29]. Among synthetic phenol compounds, ferrocenyl diphenol structures have been particularly studied as anticancer agents [30]. The incorporation of the organometallic group ferrocene in small organic phenols was performed to enhance the cytotoxicity of this type of molecule [26]. Within all these molecules called “ferrocifens”, the most active examples contained the 2-ferrocenyl-1-phenyl-but-1-ene motif [31] and the representative of this class was the 2-ferrocenyl-1,1-bis(4-hydroxyphenyl)-but-1-ene compound called ferrociphenol (Fc-diOH). Nevertheless, this ferrociphenol compound is not sufficiently soluble in water to allow its direct administration. Drug delivery systems outcoming from micelle, liposome, cyclodextrin, or nanoparticle technology have emerged as prominent solutions to allow an *in vivo* administration of this molecule. Recently, the Fc-diOH compound was encapsulated in PEG-PLA nanoparticles [32], in methylated β cyclodextrins (Me-β-CD) [33] and in lipid nanocapsules LNC [22], thus improving its bioavailability without losing its biological activity.

In this study, Fc-diOH was encapsulated in LNC at two different drug loadings and tested *in vitro* on 9L cell lines. The Fc-diOH encapsulation was optimal as LNC size and zeta potential values were not affected by the presence of the organometallic molecule. Moreover, a dose effect was evidenced *in vitro* on 9L cell lines as toxicity was more than 10 times higher for Fc-diOH-LNC 6.5mg/g versus Fc-diOH-LNC 1mg/g. In a previous study, promising *in vivo* results were obtained after intratumoral administration of this drug carrier in a 9L subcutaneous glioma model but no dose effect was demonstrated between the two drug loading formulations [22]. Many of these drugs -polyphenols in general- show promising results *in vitro* but are characterized by a poor bioavailability in animal models. Therefore an urgent issue in the development of polyphenols as anticancer agents is to find strategies to increase their bioavailability. To potentiate the action of the drug, and in a context of multi-therapy, Fc-diOH was associated with external beam irradiation. The radiosensitization effects of Fc-diOH-LNC were first studied *in vitro* on 9L cell cultures. Notably, a higher toxic dose-enhancement ratio was revealed for the chemotherapy (CT)-radiotherapy (RT) protocol in comparison with the RT-CT procedure. A radiosensitizing effect of Fc-diOH can explain the enhanced efficacy of the combined treatment in our model as better results were observed when Fc-diOH was administered before radiotherapy. It is not always the case as some drugs are more sensitive after irradiation because they inhibit enzymes involved in DNA repair for example [34]. Moreover, the treatment combination CT+RT showed synergy and not only additive effects. It means that a real cooperation occurred between the two treatments possibly due to a chemical mechanism. The process responsible for cytotoxicity by Fc-diOH is not clearly understood but seems to be connected to the formation of an intracellular cytotoxic substance in mild oxidizing conditions (Figure 6). Briefly, due to an electron transfer phenomenon, the ferrocene unit can be oxidized to ferrocenium which after some rearrangements generates a quinone methide [25]. This quinone methide, which is an alkylating molecule, may react with GSH, DNA and proteins leading to cell death. This transformation can only occur with a particular structural motif, where the ferrocenyl group is located on carbon 2 of the but-1-ene group, the phenol group resides on carbon 1, and a conjugated π-system exists between the ferrocenyl and phenol groups (Figure 6) [31].

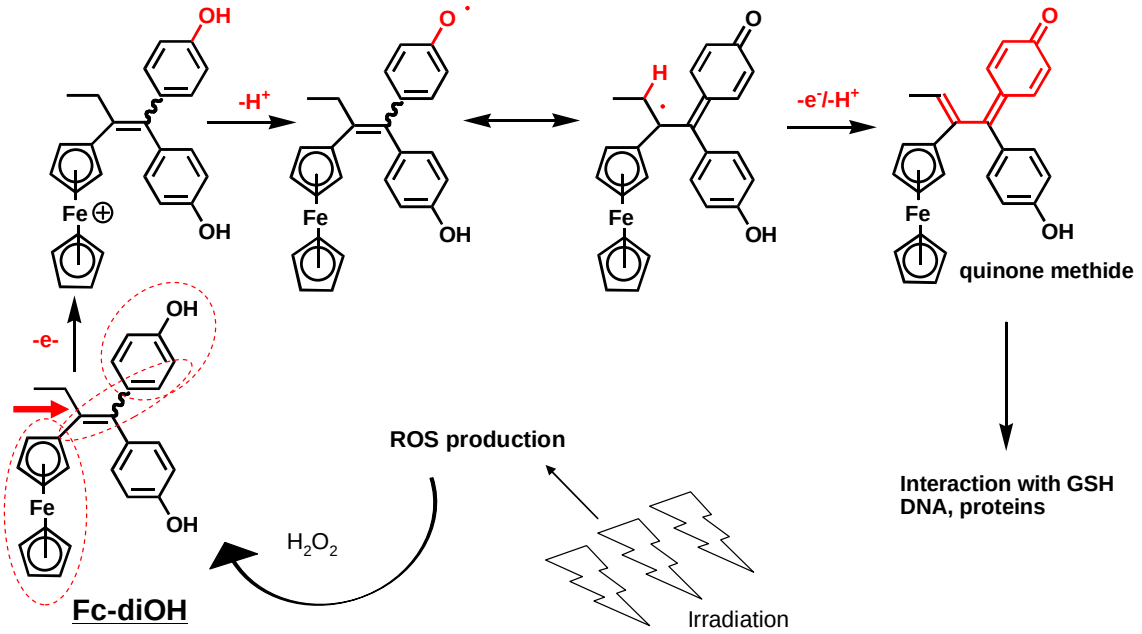

Figure 6: Proposed mechanism for Fc-diOH cytotoxicity based on electron-transfer studies. Irradiation by the generation of reactive oxygen species (ROS) can form hydrogen peroxide (H_2O_2). H_2O_2 which is a strong oxidizing molecule can boost the oxidation of ferrocene in ferrocenium which after rearrangement generates a quinone methide strongly cytotoxic. This substance may interact with intracellular sub-units like GSH, DNA or proteins leading to cell death.

This includes the role of the ferrocene moiety as an intramolecular oxidation antenna but the origin of this oxidative effect has not yet been fully elucidated. We can imagine that radiation can prime the oxidative process, thus enhancing the toxicity of the drug because radiation is known to both enhance the reactive oxygen species (ROS) production and reduce the GSH level [35]. Moreover, as an indirect effect, irradiations are known to produce free radicals originating from water radiolysis. In the presence of oxygen, highly oxidising radicals are created which interact with various compounds to form hydrogen peroxide (H_2O_2), a very strong oxidising molecule (Figure 6).

Fractionated external-beam radiotherapy is the standard treatment for the management of malignant gliomas [36]. For a similar total dose, the biological efficiency varies according to the total number of sessions (fractionation), the dose per session and the total duration of treatment. In our study, we investigated a radiotherapy scheme in 3 fractioned doses of 6 Gray a week and the impact of this scheme was first studied *in vitro* on 9L cell lines. The results showed that cell toxicity was all the more important as the number of doses increased from 1 to 3 and the profit was better for the schemes associated with Fc-diOH-LNC chemotherapy. For all the conditions tested, the main benefit in cell toxicity was obtained after the first irradiation (60-75% cell death), and was slightly reduced after the second and the third irradiation. But the most important observation is that, the synergistic effect between Fc-diOH-LNC and RT was most visible after the third irradiation as toxicity increased from 5.3% to 38.2% for the cells treated with RT alone versus CT + RT respectively (Fc-diOH-LNC with the highest dose tested). After the third irradiation, the percentage of cells still alive was mainly due to a radioresistance mechanism. Indeed, 9L cells are classified as a radioresistant cell line especially compared to other rodent glioma cell lines. Bencokova *et al.* described a surviving fraction at 2Gy (SF2) of 71.9% for 9L cells against 53.0 and 41.4% for C6 and F98 cell lines respectively [37]. This radioresistance seems to be connected to a high expression of BRCA1, a protein involved in the repair of damaged DNA.

The main objective of this work was to confirm the results obtained in *vitro* in an intracranial *in vivo* model. For that, Fc-diOH-loaded LNC with the highest dose entrapped (i.e. 0.36 mg/rat) were administered in 9L glioma bearing rats by convection enhanced delivery (CED) and then followed by an external radiotherapy of 18Gy. The major finding of this work is that Fc-diOH administered by CED in combination with external beam irradiation, resulted in a significant enhancement in median survival time compared to the chemotherapy group ($p<0.0001$) and also compared to the rats treated by blank LNC followed by the same irradiation protocol ($p<0.05$). Radiation therapy is known to be an effective postoperative treatment as it increases the survival time for patients compared to surgery alone [38, 39]. But after high doses of radiotherapy, radiation injuries are often described [40]. In rodent models, toxicity was related to high doses superior to 20Gy and delivered in a single fraction [41]. In this study, the total dose was delivered in 3 fractions of 6Gy to enhance the efficacy of radiations and also to reduce the side effects.

Moreover, many clinical trials addressing the role of adjuvant chemotherapy yielded negative or inconclusive results [2]. In the group of interest, two rats were long term survivors as they survived up to 100 days, which certainly involves a total eradication of the tumor. No enhancement of survival curves was noted for the group treated with chemotherapy alone ($p>0.05$ vs control), whereas in the subcutaneous model, treatment with Fc-diOH-LNC had demonstrated its efficacy in reducing tumor mass and volume [22]. Nonetheless, other studies described a low chemosensibility of 9L cells to metallic compounds like cisplatin in intracranial models [42]. Results obtained *in vitro* or in subcutaneous models for malignant glioma were not shown to be very valuable for predicting therapeutic efficacy [43]. Indeed, as the natural environment of a glioma (i.e. the brain) is of great influence on the response of the tumor to certain agents, orthotopic animal models may be essential for preclinical evaluation of novel therapies, especially for a combination therapy. The IST median of 32% observed for the group radiotherapy compared to the control one was mainly due to the curative effect of irradiation.

In addition, as LNC can be ideally infused by CED, spatial cooperation could be achieved leading to an optimal diffusion of Fc-diOH in rat striatum thanks to its LNC encapsulation. LNC were found to be a sustained residency system which allowed the retention of the active agent in rat brain [16] which is necessary for improved tumor eradication. Because in our last study, the active species was a radioelement (Rhenium-188) acting through irradiation, the distribution of the nanocarrier had not been optimized [16]. In the present work and in an attempt to improve the volume of distribution (Vd), sucrose was dissolved in the external phase of the LNC suspension. Thus, the viscosity was increased twofold with the presence of sucrose in the formulation. Sucrose was shown to be non toxic for 9L cells in culture and was used to enhance the viscosity of the infusate. As already described [44, 45], high viscosity of the infusate may reduce backflow, thus increasing Vd.

Moreover, Fc-diOH appears to be a good candidate for CED infusion for several reasons. Whereas chemotherapy agents infused by CED have produced favorable therapeutic outcomes, brain damage caused by the extensive distribution of highly cytotoxic agents have been described [10]. Hence, good candidates for CED administration into brain tumors would ideally be the agents that show the highest possible therapeutic index against tumor cells over

healthy neuronal cells. In our previous study, Fc-diOH-LNC showed cytostatic activity *in vitro* on 9L brain tumor cells (IC_{50} = 0.6µM) while remaining harmless towards healthy astrocytes. Moreover, because it was possible to reach high drug loading levels, up to 6.5mg of Fc-diOH per gram of LNC suspension (2% w/w dry weight), the ferrociphenol formulation is adapted to *in vivo* brain applications.

This preclinical evidence suggests that combining radiation therapy with the Fc-diOH chemotherapeutic agent may benefit to patients with high-grade malignant brain tumors. Our data represent the first demonstration of a synergy between these organometallic compounds and an external beam RT, and potentially indicate a therapeutic option for this class of molecules which often suffer from problems of bioavailability.

AKNOWLEDGMENTS

The authors would like to thank Emilien Porcher (Inserm U646, Angers, France), Pierre Legras and Jerome Roux (Service Commun d'Animalerie Hospitalo-Universitaire, Angers, France) for skillful technical support with animals. This work was supported by a "Région des Pays de la Loire" grant, by the "Cancéropôle Grand Ouest" and by "La Ligue Nationale Contre le Cancer" (équipe labellisée 2007).

Bibliography

1. Stupp R, Mason WP, Van Den Bent MJ, Weller M, Fisher B, Taphoorn MJB, et al. Radiotherapy plus concomitant and adjuvant temozolomide for glioblastoma. N Engl J Med 2005;352(10):987-996.

2. Lonardi S, Tosoni A, Brandes AA. Adjuvant chemotherapy in the treatment of high grade gliomas. Cancer Treat Rev 2005;31(2):79-89.

3. Sawyer AJ, Piepmeier JM, Saltzman WM. New methods for direct delivery of chemotherapy for treating brain tumors. Yale J Biol Med 2006;79(3-4):141-152.

4. Wang PP, Frazier J, Brem H. Local drug delivery to the brain. Adv Drug Deliv Rev 2002;54(7):987-1013.

5. Bobo RH, Laske DW, Akbasak A, Morrison PF, Dedrick RL, Oldfield EH. Convection-enhanced delivery of macromolecules in the brain. Proc Natl Acad Sci U S A 1994;91(6):2076-2080.

6. Morrison PF, Laske DW, Bobo H, Oldfield EH, Dedrick RL. High-flow microinfusion: tissue penetration and pharmacodynamics. Am J Physiol 1994;266(1 Pt 2):R292-305.

7. Bruce JN, Falavigna A, Johnson JP, Hall JS, Birch BD, Yoon JT, et al. Intracerebral clysis in a rat glioma model. Neurosurgery 2000;46(3):683-691.

8. Sugiyama S, Yamashita Y, Kikuchi T, Saito R, Kumabe T, Tominaga T. Safety and efficacy of convection-enhanced delivery of ACNU, a hydrophilic nitrosourea, in intracranial brain tumor models. J Neurooncol 2007;82(1):41-47.

9. Lidar Z, Mardor Y, Jonas T, Pfeffer R, Faibel M, Nass D, et al. Convection-enhanced delivery of paclitaxel for the treatment of recurrent malignant glioma: a phase I/II clinical study. J Neurosurg 2004;100(3):472-479.

10. Kaiser MG, Parsa AT, Fine RL, Hall JS, Chakrabarti I, Bruce JN. Tissue distribution and antitumor activity of topotecan delivered by intracerebral clysis in a rat glioma model. Neurosurgery 2000;47(6):1391-1398; discussion 1398-1399.

11. Rousseau J, Boudou C, Barth RF, Balosso J, Esteve F, Elleaume H. Enhanced survival and cure of F98 glioma-bearing rats following intracerebral delivery of carboplatin in combination with photon irradiation. Clin Cancer Res 2007;13(17):5195-5201.

12. Degen JW, Walbridge S, Vortmeyer AO, Oldfield EH, Lonser RR. Safety and efficacy of convection-enhanced delivery of gemcitabine or carboplatin in a malignant glioma model in rats. J Neurosurg 2003;99(5):893-898.

13. Neeves KB, Sawyer AJ, Foley CP, Saltzman WM, Olbricht WL. Dilation and degradation of the brain extracellular matrix enhances penetration of infused polymer nanoparticles. Brain Res 2007;1180:121-132.

14. Noble CO, Krauze MT, Drummond DC, Yamashita Y, Saito R, Berger MS, et al. Novel nanoliposomal CPT-11 infused by convection-enhanced delivery in intracranial tumors: pharmacology and efficacy. Cancer Res 2006;66(5):2801-2806.

15. Mamot C, Nguyen JB, Pourdehnad M, Hadaczek P, Saito R, Bringas JR, et al. Extensive distribution of liposomes in rodent brains and brain tumors following convection-enhanced delivery. J Neurooncol 2004;68(1):1-9.

16. Allard E, Hindre F, Passirani C, Lemaire L, Lepareur N, Noiret N, et al. (188)Re-loaded lipid nanocapsules as a promising radiopharmaceutical carrier for internal radiotherapy of malignant gliomas. Eur J Nucl Med Mol Imaging 2008;35(10):1838-1846.

17. Saito R, Krauze MT, Noble CO, Drummond DC, Kirpotin DB, Berger MS, et al. Convection-enhanced delivery of Ls-TPT enables an effective, continuous, low-dose chemotherapy against malignant glioma xenograft model. Neuro Oncol 2006;8(3):205-214.

18. Heurtault B, Saulnier P, Pech B, Proust J-E, Benoit J-P. A novel phase inversion-based process for the preparation of lipid nanocarriers. Pharm Res 2002;19(6):875-880.

19. Lacoeuille F, Garcion E, Benoit JP, Lamprecht A. Lipid nanocapsules for intracellular drug delivery of anticancer drugs. J Nanosci Nanotechnol 2007;7(12):4612-4617.

20. Malzert-Freon A, Vrignaud S, Saulnier P, Lisowski V, Benoit JP, Rault S. Formulation of sustained release nanoparticles loaded with a tripentone, a new anticancer agent. Int J Pharm 2006;320(1-2):157-164.

21. Ballot S, Noiret N, Hindre F, Denizot B, Garin E, Rajerison H, et al. 99mTc/188Re-labelled lipid nanocapsules as promising radiotracers for imaging and therapy: Formulation and biodistribution. European Journal of Nuclear Medicine and Molecular Imaging 2006;33(5):602-607.

22. Allard E, Passirani C, Garcion E, Pigeon P, Vessieres A, Jaouen G, et al. Lipid nanocapsules loaded with an organometallic tamoxifen derivative as a novel drug-carrier system for experimental malignant gliomas. J Control Release 2008;130:146-153.

23. Vessieres A, Top S, Pigeon P, Hillard E, Boubeker L, Spera D, et al. Modification of the estrogenic properties of diphenols by the incorporation of ferrocene. Generation of antiproliferative effects in vitro. J Med Chem 2005;48(12):3937-3940.

24. Top S, Vessieres A, Leclercq G, Quivy J, Tang J, Vaissermann J, et al. Synthesis, biochemical properties and molecular modelling studies of organometallic specific estrogen receptor modulators (SERMs), the ferrocifens and hydroxyferrocifens: evidence for an antiproliferative effect of hydroxyferrocifens on both hormone-dependent and hormone-independent breast cancer cell lines. Chem Eur J 2003;9(21):5223-5236.

25. Hillard E, Vessieres A, Thouin L, Jaouen G, Amatore C. Ferrocene-mediated proton-coupled electron transfer in a series of ferrocifen-type breast-cancer drug candidates. Angew Chem Int Ed 2006;45(2):285-290.

26. Jaouen G, Top S, Vessieres A, Leclercq G, Quivy J, Jin L, et al. The first organometallic antioestrogens and their antiproliferative effects. CR Acad Sci Ser IIc 2000;3(2):89-93.

27. Berenbaum MC. A method for testing for synergy with any number of agents. J Infect Dis 1978;137(2):122-130.

28. Fresco P, Borges F, Diniz C, Marques MP. New insights on the anticancer properties of dietary polyphenols. Med Res Rev 2006;26(6):747-766.

29. Shankar S, Ganapathy S, Srivastava RK. Green tea polyphenols: biology and therapeutic implications in cancer. Front Biosci 2007;12:4881-4899.

30. Hillard E, Vessieres A, Le Bideau F, Plazuk D, Spera D, Huche M, et al. A series of unconjugated ferrocenyl phenols: prospects as anticancer agents. ChemMedChem 2006;1(5):551-559.

31. Hillard EA, Pigeon P, Vessieres A, Amatore C, Jaouen G. The influence of phenolic hydroxy substitution on the electron transfer and anti-cancer properties of compounds based on the 2-ferrocenyl-1-phenyl-but-1-ene motif. Dalton Trans 2007(43):5073-5081.

32. Nguyen A, Marsaud V, Bouclier C, Top S, Vessieres A, Pigeon P, et al. Nanoparticles loaded with ferrocenyl tamoxifen derivatives for breast cancer treatment. Int J Pharm 2008;347(1-2):128-135.

33. Buriez O, Heldt JM, Labbe E, Vessieres A, Jaouen G, Amatore C. Reactivity and Antiproliferative Activity of Ferrocenyl-Tamoxifen Adducts with Cyclodextrins Against Hormone-Independent Breast-Cancer Cell Lines. Chemistry 2008:*In press*.

34. Chen Y, Lin TY, Chen JC, Yang HZ, Tseng SH. GL331, a topoisomerase II inhibitor, induces radiosensitization of human glioma cells. Anticancer Res 2006;26(3A):2149-2156.

35. Lee YY, Kao CL, Tsai PH, Tsai TH, Chiou SH, Wu WF, et al. Caffeic acid phenethyl ester preferentially enhanced radiosensitizing and increased oxidative stress in medulloblastoma cell line. Childs Nerv Syst 2008;24(9):987-994.

36. Laperriere N, Zuraw L, Cairncross G. Radiotherapy for newly diagnosed malignant glioma in adults: a systematic review. Radiother Oncol 2002;64(3):259-273.

37. Bencokova Z, Pauron L, Devic C, Joubert A, Gastaldo J, Massart C, et al. Molecular and cellular response of the most extensively used rodent glioma models to radiation and/or cisplatin. J Neurooncol 2008;86(1):13-21.

38. Larson DA, Wara WM. Radiotherapy of primary malignant brain tumors. Semin Surg Oncol 1998;14(1):34-42.

39. Berg G, Blomquist E, Cavallin-Stahl E. A systematic overview of radiation therapy effects in brain tumours. Acta Oncol 2003;42(5-6):582-588.

40. Schiff D, Wen P. Central nervous system toxicity from cancer therapies. Hematol Oncol Clin North Am 2006;20(6):1377-1398.

41. Wong CS, Van der Kogel AJ. Mechanisms of radiation injury to the central nervous system: implications for neuroprotection. Mol Interv 2004;4(5):273-284.

42. Regnard P, Brauer-Krisch E, Tropres I, Keyrilainen J, Bravin A, Le Duc G. Enhancement of survival of 9L gliosarcoma bearing rats following intracerebral delivery of drugs in combination with microbeam radiation therapy. Eur J Radiol 2008:*In press*.

43. Lamfers ML, Idema S, Bosscher L, Heukelom S, Moeniralm S, van der Meulen-Muileman IH, et al. Differential effects of combined Ad5- delta 24RGD and radiation therapy in in vitro versus in vivo models of malignant glioma. Clin Cancer Res 2007;13(24):7451-7458.

44. Mardor Y, Rahav O, Zauberman Y, Lidar Z, Ocherashvilli A, Daniels D, et al. Convection-enhanced drug delivery: increased efficacy and magnetic resonance image monitoring. Cancer Res 2005;65(15):6858-6863.

45. Perlstein B, Ram Z, Daniels D, Ocherashvilli A, Roth Y, Margel S, et al. Convection-enhanced delivery of maghemite nanoparticles: Increased efficacy and MRI monitoring. Neuro Oncol 2008;10(2):153-161.

DISCUSSION GENERALE

Les thérapies locales des gliomes offrent l'avantage considérable de s'affranchir du passage de la barrière hémato-encéphalique (BHE) qui limite souvent la pénétration des agents cytotoxiques dans le cerveau, tout en minimisant les effets systémiques. La distribution des principes actifs (PA) se fait soit via des systèmes polymères implantés localement, soit via une perfusion cérébrale par Convection Enhanced Delivery (CED) [1, 2]. Les systèmes polymères type implants monolithiques (Gliadel®) ou microparticules libèrent leurs molécules actives par diffusion seule ou par diffusion-érosion, de manière plus ou moins prolongée [3]. L'inconvénient de ces systèmes est une faible distribution tissulaire des cytotoxiques car leur diffusion est fonction d'un gradient de concentration. De plus, ceci impose d'utiliser des polymères biocompatibles et biodégradables et de contrôler les profils de libération des PA. Ils présentent néanmoins l'avantage d'être faiblement invasifs. Les techniques de CED offrent la possibilité de s'affranchir du gradient de concentration puisque les PA sont cette fois-ci délivrés grâce à un gradient de pression [4, 5]. La méthode implique dans ce cas le positionnement d'un cathéter ou d'une aiguille au sein même du tissu à perfuser. Elle est, de ce fait, plus invasive mais permet d'obtenir des volumes de distribution (Vd) beaucoup plus larges, et d'administrer des quantités de PA beaucoup plus importantes.

Dans ce contexte, l'objectif de ce travail a été de combiner l'administration par CED à l'apport des nanotechnologies. Cette combinaison stratégique associant perfusion et nanovecteur n'a été introduite que très récemment puisque les premières études décrivant l'infusion de liposomes datent de 2004 [6]. En effet, de part leur échelle nanométrique, les nanovecteurs peuvent être administrés en CED afin obtenir de larges Vd et ainsi couvrir tout l'environnement tumoral. Le devenir des molécules infusées, dans ce cas, va dépendre des propriétés intrinsèques du vecteur et non de la substance elle-même. Le vecteur va constituer un système réservoir permettant une protection de la molécule active et une meilleure rétention dans le cerveau. Parmi ces nouveaux systèmes nanoparticulaires, les nanocapsules lipidiques (LNC) sont des systèmes biocompatibles qui n'utilisent que des excipients approuvés par la FDA. Ils possèdent également la capacité d'encapsuler des substances lipophiles, comme des complexes métalliques, au sein de leur cœur lipidique.

Ce travail de thèse s'inscrit dans une optique thérapeutique, utilisant les LNC en tant que vecteurs d'anticancéreux et de radioéléments pour la thérapie localisée des gliomes. L'objectif de ce travail vise à éradiquer des tumeurs gliales implantées chez le rat. Nous avons choisi de tester et encapsuler deux types de complexes métalliques lipophiles dont les applications n'en sont encore qu'à un stade préclinique. Comme la majorité des molécules actuellement en recherche et développement, ces complexes métalliques sont très insolubles dans l'eau. Ils nécessitent donc une étape de formulation, pour pouvoir les administrer dans l'organisme. Le premier actif étudié est un complexe de Rhénium-188 hautement souffré [$^{188}Re(S_3CPh)_2(S_2CPh)$ = ^{188}Re-SSS] qui sera utilisé en tant que radioélément émetteur β^- pour la radiothérapie interne. Les seconds types de complexes sont des dérivés du tamoxifène sur lesquels a été greffé un groupement ferrocène et que l'on nomme par analogie « ferrocifènes ». Le mécanisme réactionnel de ces molécules, bien qu'encore non clairement identifié, semble basé sur deux oxydations intracellulaires successives. La première transforme Fe^{2+} en Fe^{3+} et est suivie par le déplacement d'un proton phénolique ; la deuxième implique la formation d'une quinone méthyde, hautement toxique et capable d'interagir avec des macromolécules comme l'ADN ou des protéines, pour aboutir à la mort cellulaire [7]. Dans un contexte de multi-thérapie, l'objectif est aussi d'envisager différents schémas de chimio-radiothérapie où la radiothérapie sera administrée de façon interne ou externe.

Conception des LNC, vecteurs de substances actives

Les LNC ont la capacité d'encapsuler en leur cœur lipidique des molécules lipophiles et amphiphiles. C'est le cas en particulier de l'ibuprofène [8], l'amiodarone [8], et divers agents anticancéreux, comme le paclitaxel [8], l'étoposide [8] ou un anticancéreux de la famille des tripentones [9]. Toutes ces molécules ont conservé leur activité malgré les étapes de chauffage inhérentes au procédé de préparation. Les LNC permettent aussi l'encapsulation de complexes lipophiles radiomarqués. Une étude préalable a porté sur l'encapsulation de complexes marqués au Technétium (^{99m}Tc) et au Rhénium (^{188}Re) dans des LNC natives et a montré une encapsulation sans modification de taille ainsi qu'un important rendement de marquage [10].

L'application intracérébrale

Les nanocapsules lipidiques ont une taille nanométrique, modulable en fonction de la proportion des excipients entrant dans leur formulation [11]. Le tensioactif polyéthoxylé formant la coque (Solutol®) ainsi que les triglycérides formant le cœur (Labrafac®) sont les composés agissant le plus sur la taille des LNC. Classiquement, les proportions utilisées permettent de préparer des nanocapsules de 20, 50 ou 100 nm de diamètre. Dans ce travail, nous avons choisi de formuler des objets de 50 nm pour deux raisons principales. D'une part, les nano-objets d'une telle taille sont adaptés à une application intracérébrale en CED. En effet, après administration, les LNC vont devoir diffuser au travers du compartiment extracellulaire. Cet espace extracellulaire a été récemment estimé entre 35 et 64 nm de diamètre chez un rat sain [12]. D'autre part, le cœur lipidique des LNC de 50 nm est suffisamment important pour pouvoir solubiliser des PA, permettant ainsi d'obtenir des taux d'encapsulation élevés. Puisque les volumes d'injection sont limités en injection intracérébrale pour des raisons de tolérance clinique, les LNC doivent encapsuler un maximum de PA dans un volume final minimal. Dans un souci d'optimisation, nous avons donc fait varier deux paramètres : la quantité de PA solubilisé dans le Labrafac® ainsi que la concentration des LNC par l'intermédiaire du volume d'eau de trempe ajouté à la fin du procédé. Dans ce travail, le volume de trempe a été réduit à 2 ml (28.5% v/v), au lieu des 12.5 ml (70% v/v) utilisés dans la formulation initiale décrite par Heurtault *et al* [11].

Le complexe de Rhénium-188

En premier lieu, nous avons adapté la formulation des LNC encapsulant le complexe de ^{188}Re (^{188}Re-SSS-LNC) initialement décrite par Ballot *et al* [10] à l'administration intracérébrale par CED. L'objectif a été ensuite de formuler des LNC encapsulant des activités croissantes de radioactivité (mesurées en Bequerel=Bq) permettant de délivrer une gamme de doses croissantes (mesurées en Gray=Gy). Dans ce cas, ce sont les activités du perrhénate de ^{188}Re obtenues à la sortie du générateur qui vont influencer les activités encapsulées dans les LNC. Une fois formé, le complexe est solubilisé dans une phase dichlorométhane (CH_2Cl_2), puis mélangé aux divers excipients de la formulation. Une étape d'évaporation est nécessaire pour éliminer le solvant avant de réaliser les 3 cycles de chauffage-refroidissement entre 85 et 60°C. L'inconvénient majeur de cette formulation est une réintroduction de solvant organique

dans une technique qui cherche à s'en affranchir. Cependant, la température élevée atteinte lors des étapes de chauffage devrait permettre une évaporation totale de ce solvant.

Les mesures de taille réalisées sur ces vecteurs montrent que la présence du complexe ne déstabilise pas la capsule puisque les tailles sont globalement inchangées par rapport aux LNC blanches. De plus, la dialyse, comme la chromatographie d'exclusion stérique sur colonne PD10 ne viennent pas déstructurer cet assemblage (Figure 1). Les indices de polydispersité (PI) obtenus sont tous inférieurs à 0.25, témoignant d'une distribution monomodale. Cette technique de formulation présente le considérable avantage d'être rapide, ce qui est un atout majeur quand on cherche à formuler un radioélément dont la demi-vie est de 16.9 heures. Le rendement de marquage final est de 73.9%, la majorité des pertes se produisant lors de la formation du complexe à partir du perrhénate élué du générateur (77.6%).

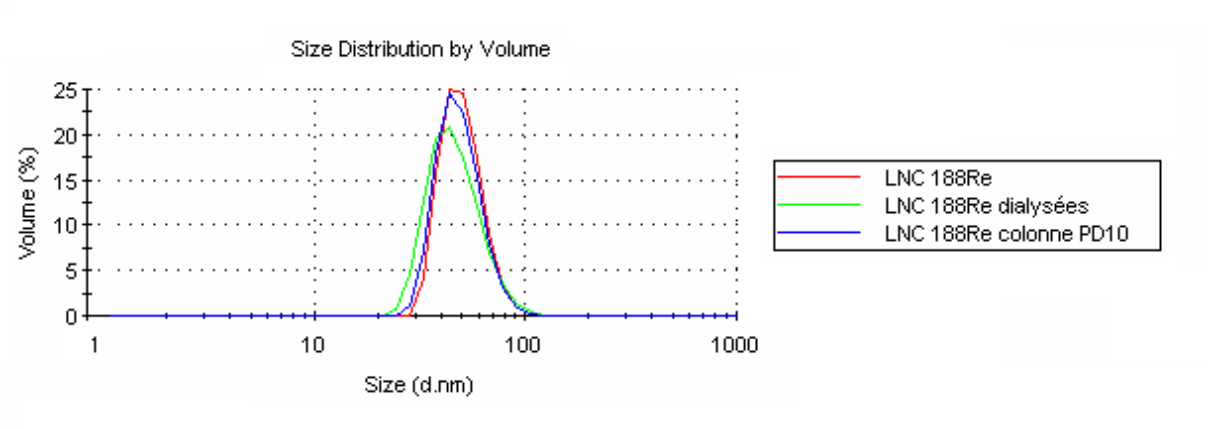

Figure 1 : Distribution de taille des LNC encapsulant le complexe de ^{188}Re effectuée par spectroscopie de corrélation de photons, après formulation (—), après dialyse (—) et après colonne d'exclusion stérique (—).

Les ferrocifènes

Parmi les molécules organométalliques de la famille des ferrocifènes, nous avons testé quatre molécules (Figure 2). La première molécule est le 2-ferrocényl-1,1-bis(4-hydroxyphényl)-but-1-ène que l'on nommera ferrociphénol (Fc-diOH). La seconde est le complexe DP1 où les deux groupements cyclopentadiènes sont liés de façon covalente à la structure diphénolique. Enfin, les deux dernières molécules Fc-diAC et Fc-diPAL sont des prodrogues de la molécule Fc-diOH qui protègent les fonctions phénoliques avec leurs chaînes d'acides gras, respectivement acétate (C2) et palmitate (C16). Pour être actives, ces molécules nécessitent une hydrolyse de cette chaîne afin de libérer la fonction phénol nécessaire au transfert

d'électron. Les prodrogues présentent l'avantage d'être plus hydrophobes et sont supposées plus solubles dans la phase triglycérique (Labrafac®).

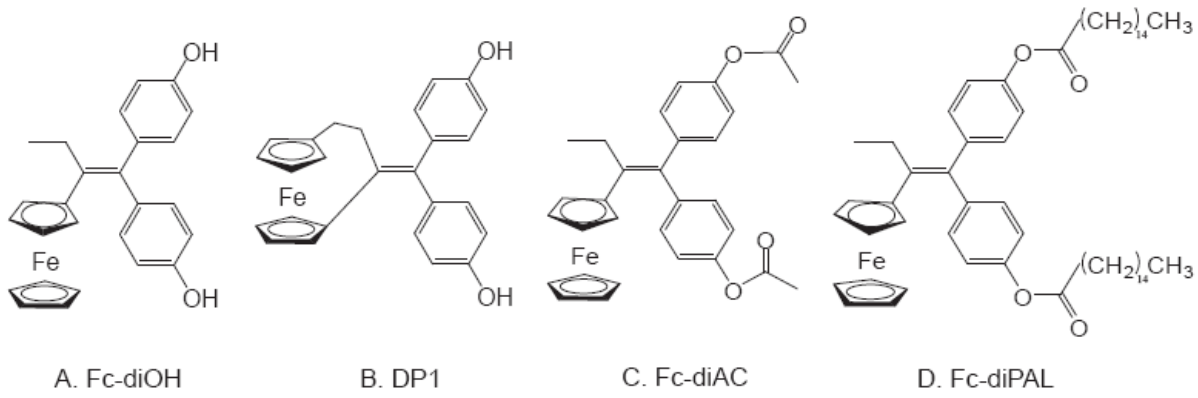

Figure 2 : Formules développées des 4 molécules testées de la famille des ferrocifènes A : Fc-diOH, B : DP1, C : Fc-diAC et D : Fc-diPAL.

Toutes ces drogues ont fait l'objet d'une encapsulation dans les LNC à de faibles taux de charge (1mg PA/ g LNC) et ont été testées à différentes dilutions sur des lignées cellulaires de gliosarcome de rat 9L (Figure 3). Un test MTT permettant de quantifier le nombre de cellules vivantes après traitement a été effectué pour chaque condition, et a permis de déterminer les IC_{50} de chaque composé, c'est-à-dire les concentrations qui inhibent la survie de 50% des cellules.

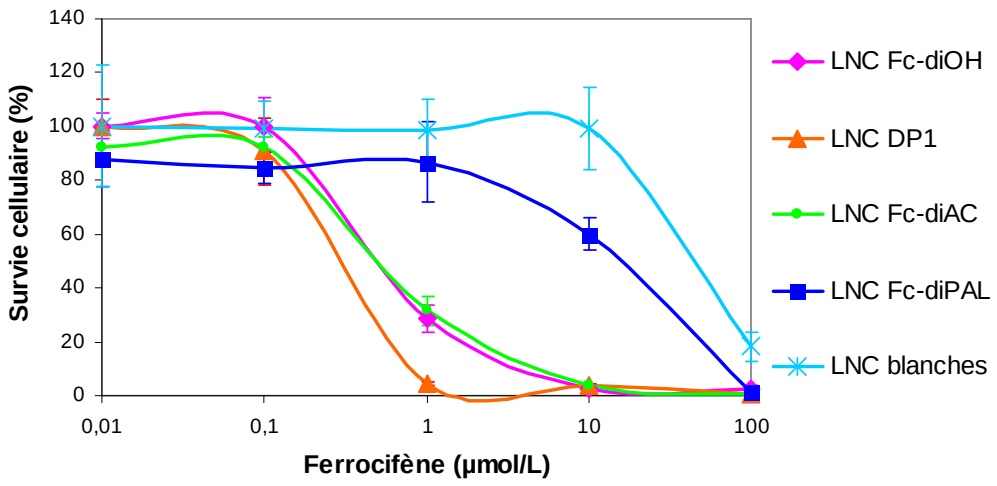

Figure 3 : Courbe de survie des 9L après traitement avec des LNC encapsulant 4 molécules de la famille des ferrocifènes**.**

Malgré une activité cytostatique importante (IC_{50}= 0.35µM), la molécule DP1, la moins soluble des 4 dans le Labrafac®, ne permet pas d'obtenir les forts taux de charge souhaités pour une administration *in vivo*. Fc-diPAL présente une activité cytostatique très réduite sur les cellules tumorales 9L puisque l'IC_{50} se situe autour de 20µM. Ceci peut s'expliquer par une absence d'hydrolyse de la chaîne palmitate *in vitro* rendant impossible le transfert d'électron. En revanche, l'hydrolyse est facilitée avec une chaîne d'acides gras plus courte (en C2) puisque Fc-diAc présente une valeur d'IC_{50} non significativement différente de celle de Fc-diOH, autour de 0.6µM. Pour la suite des tests *in vitro*, nous avons choisi de concentrer nos investigations sur le diphénol Fc-diOH que l'on dénommera ferrociphénol. En effet, cette molécule est jusqu'alors considérée comme la plus active des molécules de cette famille sur des lignées de cancer du sein hormono-dépendantes (MCF7) ou non (MDA-MB231) [13]. Elle est très soluble dans le Labrafac®, ce qui facilite très largement son encapsulation dans les LNC. Fc-diOH peut être dissout dans la phase composée de triglycérides jusqu'à 40mg/g en utilisant les ultras-sons pour accélérer sa vitesse de dissolution. Ainsi, il est donc possible de formuler des lots de LNC-Fc-diOH jusqu'à une concentration de 6.5mg/g (2% w/w poids sec). Les rendements d'encapsulation sont très elevés puisqu'ils sont tous supérieurs à 98% pour des taux d'encapsulation allant de 0.5 à 6.5 mg/g. Les tailles, PDI et potentiels zeta étant inchangés par rapport aux LNC blanches, on peut considérer que le PA encapsulé se retrouve bien au cœur de la capsule.

Les tests de cytotoxicité *in vitro* ont été réalisés sur un modèle de cellules gliales mettant en parallèle des cellules cancéreuses à fort pouvoir de division, les cellules 9L, et des cellules au pouvoir de division faible voire nul, mimant le comportement de cellules saines, les astrocytes. Les molécules testées ont été administrées seules, c'est-à-dire dissoutes dans un solvant organique, ou après leur encapsulation dans les LNC. Administrée seule, la molécule Fc-diOH a montré une activité cytostatique majeure (IC_{50}= 0.5µM) sur les cellules cancéreuses de gliome, notamment par rapport au tamoxifène qui est la molécule de référence du squelette ferrocifène, alors qu'aucune action toxique n'est observée pour le ferrocène seul (chapitre 2). En revanche, sur les astrocytes, Fc-diOH présente une activité toxique très réduite puisque l'IC_{50} est autour de 50µM. Ceci signifie que la molécule Fc-diOH agit sur le cycle de division cellulaire et ne va générer un effet toxique que sur des cellules en division, comme les cellules cancéreuses.

De plus, l'activité du ferrociphénol est conservée après son encapsulation dans les LNC puisque les profils de survie cellulaire pour la molécule encapsulée ou non ne sont pas significativement différents. Cependant, l'activité de la molécule n'est pas majorée après encapsulation comme peut l'être l'activité d'autres agents anticancéreux comme le paclitaxel [14]. En effet, la présence de l'agent tensioactif Solutol® en surface des LNC a été corrélée à une inhibition de la glycoprotéine P (P-gp) à l'origine de nombreux phénomènes de multirésistance (MDR) en cancérologie. Ceci signifie que la molécule Fc-diOH n'est pas un substrat de la P-gp. Par ailleurs, de même que pour le PA administré seul, les LNC encapsulant Fc-diOH présentent une activité cytotoxique 100 fois réduite sur les astrocytes, comparable à celle obtenue avec des LNC blanches. La toxicité observée dans ce cas est non spécifique et liée au vecteur lui-même. En conclusion, l'encapsulation dans les LNC semble être un bon moyen d'administrer ce PA tout en conservant son activité cytostatique.

Intérêt du système LNC dans la thérapie locale des gliomes

Les 2 complexes lipophiles métalliques d'intérêt, à savoir le ^{188}Re-SSS ainsi que le Fc-diOH peuvent être facilement encapsulés dans les LNC. Il est maintenant important de s'intéresser à l'intérêt du vecteur nanocapsule lipidique dans notre application.

Un vecteur adapté à la Convection Enhanced Delivery (CED)

La technique de CED va nous permettre d'injecter un volume plus important (60µl) que ce qu'il est possible de faire avec une injection simple par stéréotaxie (10µl). Les volumes de distribution obtenus devraient également être beaucoup plus importants que ce qu'il est possible d'obtenir en injection simple. Au laboratoire, cette technique a été mise au point par S. Petit *et al* (publication en cours). Elle utilise un pousse-seringue qui va ainsi délivrer le produit sous un effet de gradient de pression. L'infusion des LNC est réalisée grâce à une seringue de 32 gauges à une vitesse de 0.5µL/min pendant 2h pour éviter tout type de reflux (Figure 4).

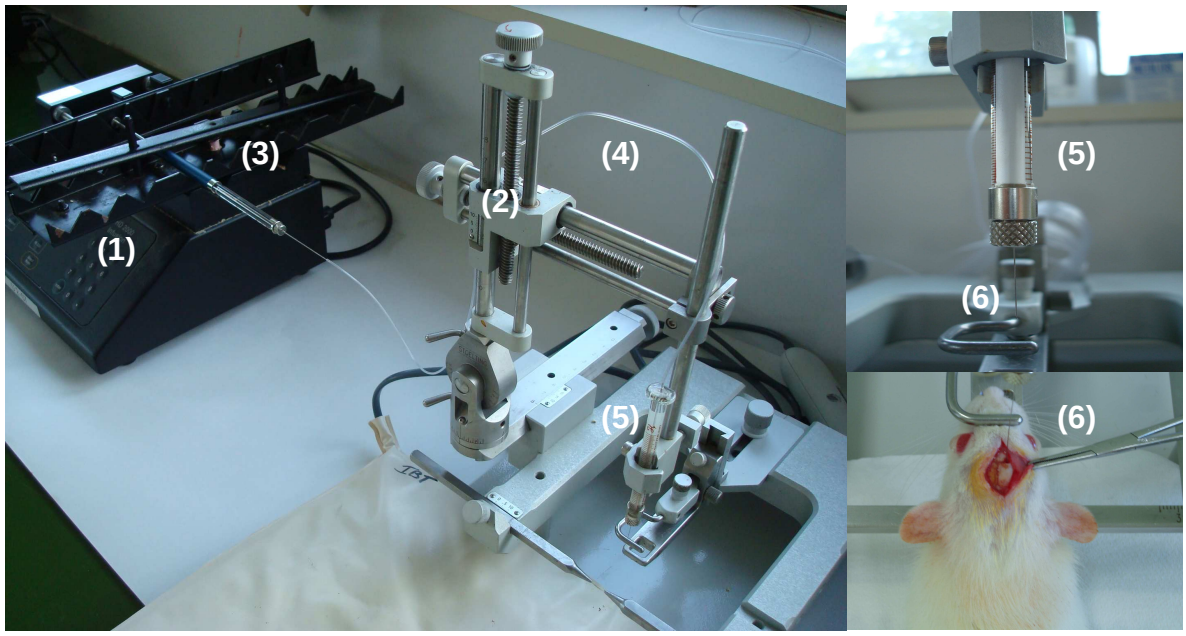

Figure 4: Système d'injection par CED. L'ensemble du dispositif comprend : la pompe Harvard PHD 2,000 (1), le cadre de stéréotaxie (2), la seringue Hamilton 100µl 22G contenant les LNC (3), la tubulure externe en PE/PVC (4), la seringue d'injection 10µL (5) et l'aiguille 32G implantée dans le striatum du rat (6).

D'après la bibliographie (Cf revue), nous avons établi qu'il existe des critères de choix pour infuser un nanovecteur donné en CED. En effet, le vecteur idéal a une taille comprise entre 20 et 50 nm, une charge négative ou neutre avec la présence de molécules de recouvrement à sa surface du type polyéthylène glycol (PEG), dextran ou albumine. La suspension finale est concentrée, légèrement visqueuse et légèrement hyperosmolaire, avec éventuellement la présence de co-infusats qui ont pour but de saturer les sites de fixation des nanovecteurs sur leur trajet d'infusion. Ces systèmes colloïdaux peuvent encapsuler des substances actives et/ou des agents de contraste pour IRM afin de réaliser un suivi en temps réel.

Les LNC utilisées dans cette étude présentent la plupart de ces critères et parmi eux, une taille de 50-55 nm, une charge négative autour de -10mV et la présence d'une brosse de PEG 660 à leur surface. Dans notre application, les LNC ont été concentrées, par réduction du volume d'eau de trempe. De part la présence de NaCl dans la formulation, les formulations concentrées sont légèrement hyperosmolaires (760 ± 2.6 mOsm/kg). De plus, il est possible d'augmenter la viscosité des solutions par ajout de sucrose en phase externe, après formulation. Les formulations passent ainsi d'une viscosité de 4.4 ± 0.1 à 8.7± 0.2 mm^2/s.

De plus, les LNC ont la capacité d'encapsuler de la magnétite Fe_3O_4 (Chapon *et al*, publication en cours), qui est un agent superparamagnétique utilisé pour des applications en IRM. Des infusions en CED de LNC encapsulant cet agent superparamagnétique ont été réalisées afin d'évaluer le volume de distribution suite à une telle injection. Les IRM effectuées après la CED, réalisée à J6 sur trois rats porteurs d'une tumeur 9L (implantée à J0), montrent que la région du striatum est largement imprégnée par les LNC (Figure 5). Les images montrent que les LNC diffusent largement dans le striatum et au-delà de la zone tumorale (Figure 6A-B). La distribution du PA est beaucoup plus importante que celle observée lors de l'implantation striatale de microsphères encapsulant une substance active (Figure 6C). En effet, des études préliminaires réalisées au laboratoire ont montré que l'agent antimétabolite 5-FU se distribuait de façon limitée dans le cerveau, avec un maximum de 3mm autour du site d'implantation des microphères [15].

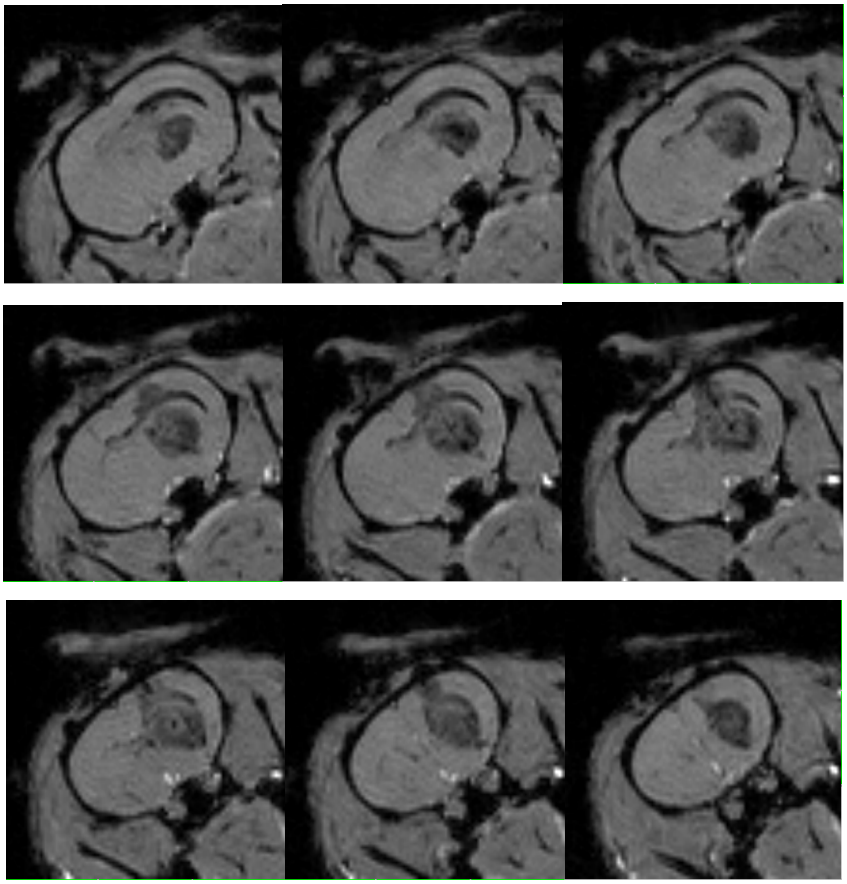

Figure 5 : Images pondérées T2* post-CED (J6) de LNC encapsulant de la magnétite dans le striatum d'un rat porteur d'une tumeur 9L implantée à J0.

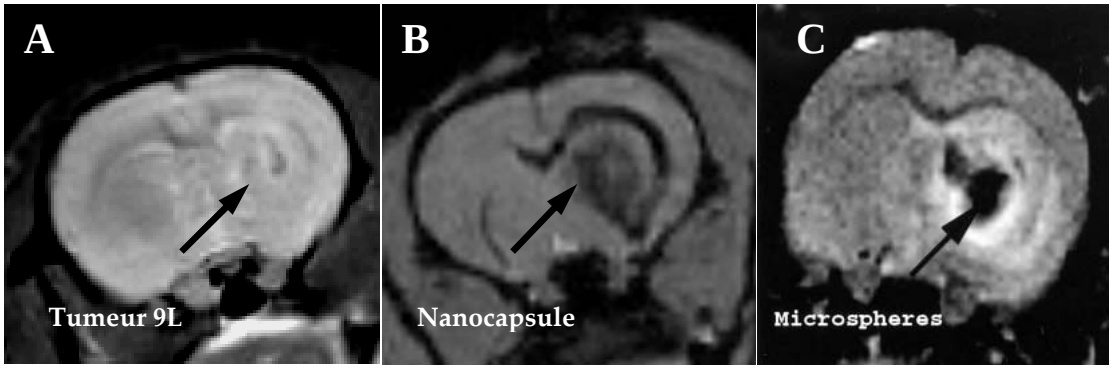

Figure 6 : Image pondérée T2 d'une tumeur 9L à J5 (1 jour avant traitement) (A), images pondérées T2* de LNC-magnétite 30 min après leur infusion en CED (B) et de microsphères-magnétite 2 jours après leur implantation par stéréotaxie (C) (d'après Lemaire *et al.* [16]).

Une meilleure rétention in situ

En parallèle de la CED réalisée avec les LNC chargées en ^{188}Re-SSS, les rats ont été infusés avec du perrhénate de ^{188}Re ($^{188}ReO_4^-$) qui est la substance directement éluée du générateur. Les rats post-CED ont été placés dans une cage à métabolisme pour suivre l'élimination du Rhénium-188, que ce soit sous forme de complexe encapsulé dans les LNC ou sous forme de perrhénate. Après injection de la solution de perrhénate de ^{188}Re, on observe une clairance rapide du traceur avec une demi-vie cérébrale de 7H (Figure 7). 80% de la dose se retrouve éliminée après 12h post CED, contre 2% pour le complexe. Après 72h, 94% de l'activité du ^{188}Re sous forme de perrhénate se retrouve éliminée dans les urines majoritairement (99.4%). Au contraire, une rétention prolongée est observée lorsque celui-ci est complexé à l'intérieur des LNC, 90% de la dose restant après 72h.

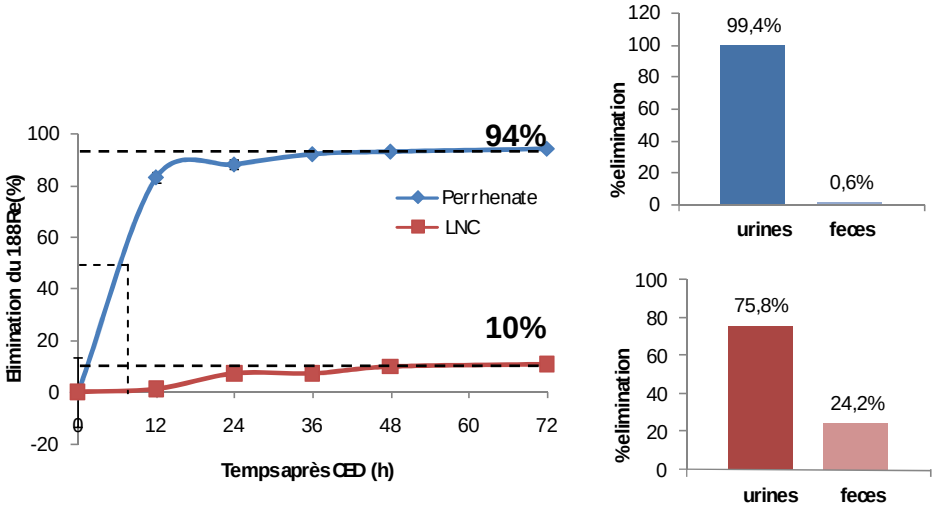

Figure 7 : Elimination du ^{188}Re dans les urines et les feces mesurée par un compteur gamma 72h après l'administration en CED de 60µl de LNC ou perrhénate de ^{188}Re chez un rat porteur d'une tumeur de type 9L.

Les LNC permettent donc la rétention du radioélément *in situ*, nécessaire pour une irradiation des cellules tumorales. Ces résultats montrent bien l'intérêt du système LNC dans cette application d'administration intracérébrale.

Un vecteur internalisant

Lors de la mise au point initiale du procédé, une étude systématique a mis en évidence la zone de faisabilité des LNC sur un diagramme ternaire eau / huile / tensioactif pégylé (Figure 8). Les LNC sont obtenues pour des quantités comprises entre 10 et 40% de tensioactif, entre 35 et 80% d'eau et entre 10 et 25% d'huile. De plus, dans une autre phase du diagramme, il est possible de former des objets micellaires. Pour des quantités comprises entre 60 et 90% de tensioactif, entre 25 et 40% d'eau et 5% d'huile, on forme ce que l'on appelle des micelles gonflées car elles contiennent une faible proportion de triglycérides en leur centre, au contact des parties apolaires des tensioactifs.

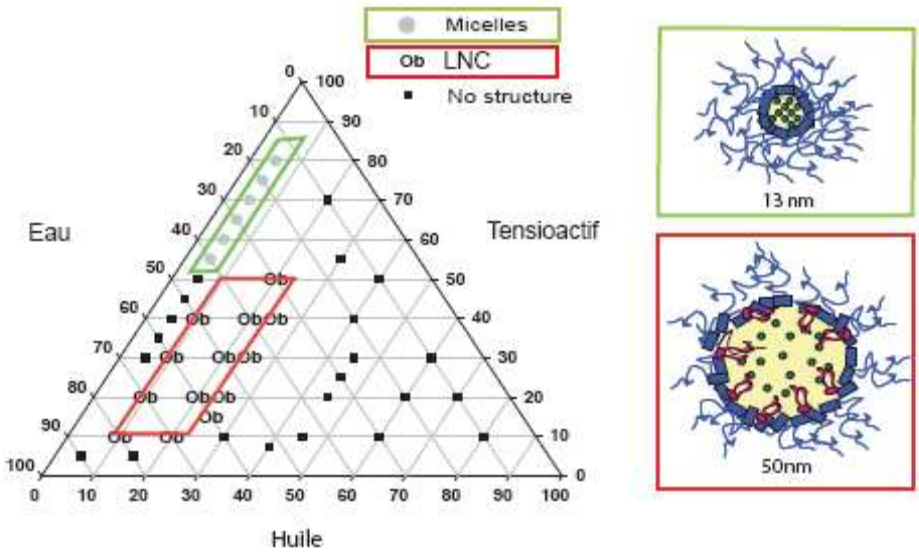

Figure 8 : Diagramme ternaire permettant de définir la zone de faisabilité des LNC (Ob) et des micelles (○) en fonction des quantités respectives d'eau, d'huile et de tensioactif pégylé. D'après Heurtault *et al* [11].

Afin d'évaluer l'intérêt des LNC dans cette application, et dans l'objectif de solubiliser cette molécule lipophile, Fc-diOH a fait l'objet d'une encapsulation dans des LNC et dans des micelles de Solutol®. Comme dans le cas des LNC, les rendements d'encapsulation se sont avérés très élevés pour les micelles encapsulant Fc-diOH. Le premier avantage des LNC par

rapport aux micelles est leur plus importante proportion d'huile permettant de solubiliser les PA jusqu'à 6.5mg/g. Ainsi, les taux d'encapsulation atteints avec les LNC sont beaucoup plus importants que ceux atteints avec les micelles gonflées (1mg/g au maximum). De plus, de part leur très forte proportion de Solutol®, les micelles gonflées sont beaucoup plus toxiques dans des conditions *in vitro* (Figure 9).

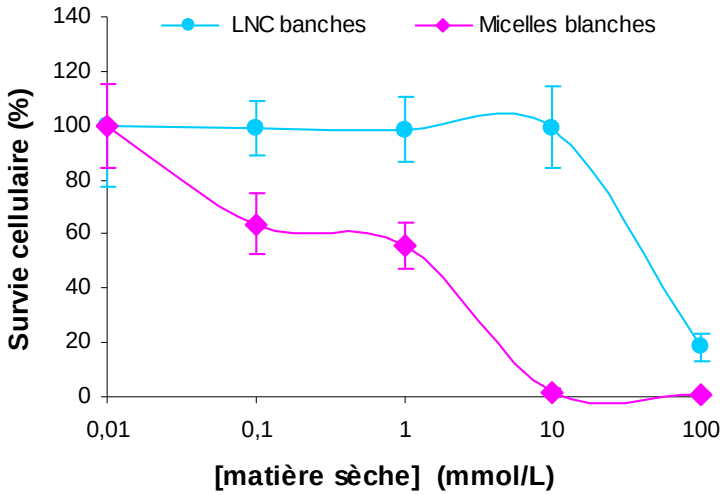

Figure 9 : Survie cellulaire des cellules 9L après traitement par des nanovecteurs non chargés : LNC et micelles gonflées pour des concentrations en matière sèche comprise entre 0.01 et 100 mmol/L.

Enfin, l'activité de la molécule Fc-diOH n'est pas retrouvée après encapsulation dans les micelles, alors qu'elle est inchangée lorsque cette même molécule est encapsulée dans les LNC (chapitre 2).

Le marquage des nanovecteurs lipidiques par un agent fluoré hydrophobe (Nile Red) nous a permis d'aller plus loin et d'envisager le devenir de ces vecteurs dans la cellule. Par des techniques de cytométrie de flux et de microscopie confocale, nous avons pu conclure que les LNC étaient majoritairement internalisées dans les cellules de gliome 9L, contrairement aux micelles (Figure 10). Les chaines de PEG présentes en très forte densité à la surface des micelles empêchent certainement l'internalisation de ces vecteurs dans la cellule. Ceci pourrait expliquer en partie le fait qu'il n'y ait pas de différence de survie cellulaire après traitement des cellules par des micelles blanches ou des micelles encapsulant Fc-diOH.

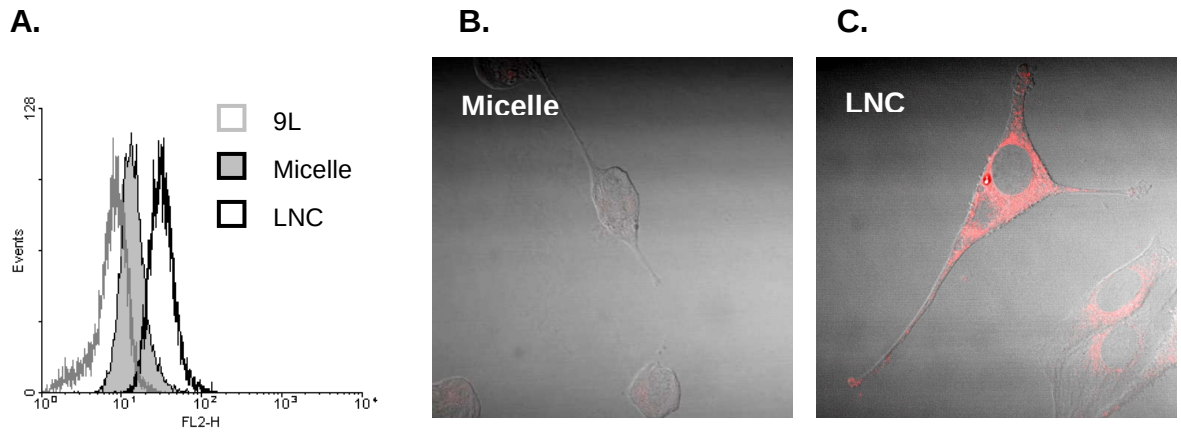

Figure 10 : Internalisation des nanovecteurs dans les cellules de gliome 9L. A : résultats de cytométrie de flux. Superposition des acquisitions en Nomarsky et en fluorescence pour les cellules 9L incubées avec des micelles de Nile Red (B) et avec des LNC-Nile red (C).

En définitif, les LNC diffusent très largement dans le parenchyme cérébral, peuvent encapsuler des substances actives avec de hauts rendements, permettent la rétention des substances actives *in situ* et sont rapidement internalisées dans les cellules. Tous ces critères confèrent aux LNC des propriétés intéressantes pour la thérapie locale des gliomes.

Les évaluations in vivo

Les systèmes nanoparticulaires que sont les LNC encapsulant le complexe de ^{188}Re ainsi que les LNC et micelles encapsulant Fc-diOH ont fait l'objet d'exploration *in vivo*. Les modèles de gliome utilisés dans cette étude reposent sur l'injection de cellules tumorales 9L soit en sous-cutané (injection ectopique), soit dans le cerveau (injection orthotopique).

Le gliome sous-cutané

Le modèle de gliome sous-cutané présente l'avantage de suivre facilement l'évolution du volume tumoral, alors que ce même suivi dans le cerveau implique de réaliser des explorations en IRM. De plus, le modèle de gliome ectopique permet l'administration de volumes de LNC (donc des doses de PA) beaucoup plus importants que ce qu'il est possible

de faire en injection intracérébrale. Dans notre protocole expérimental, les traitements sont administrés à J6, à raison d'un volume de 400µl alors qu'une injection en CED équivaut à un volume de 60µL. Le résultats confirment les données obtenues *in vitro* pour une part. En effet, la croissance tumorale des rats traités par des micelles encapsulant Fc-diOH est importante et non significativement différente de celles des groupes témoins ayant reçu une injection de LNC blanches ou de sérum physiologique (Figure 11). Pour une dose équivalente de PA (2.5mg/rat), l'effet de réduction tumorale est majoré en utilisant des nanocapsules lipidiques en tant que vecteur de Fc-diOH. Ce résultat s'explique probablement par l'internalisation très largement supérieure des LNC comparées aux micelles.

En revanche, l'effet-dose attendu entre un traitement avec des LNC formulées à 1mg/g et celles à 6.5mg/g n'est pas observé *in vivo.* Une perte d'activité de la molécule pour des taux de charge très importants (comme ceux à 6.5mg/g) pourrait être due à des intéractions hydrophobes intermoléculaires. Cependant, des expériences de survie cellulaire par test MTT ont démenti cette hypothèse. En effet, la toxicité est largement majorée sur des cellules recevant un traitement avec LNC-Fc-diOH 6.5mg/g comparativement à la dose de 1mg/g, confirmant une activité de la molécule (Cf chap 3).

Par ailleurs, la protection des fonctions -OH, apportée par la prodrogue Fc-diAC n'a pas entraîné d'amélioration. Due à une forte solubilité de la prodrogue dans le Labrafac®, il est possible de formuler des LNC très concentrées (jusqu'à 16.4mg/g) mais celles-ci sont malheureusement instables, et ce dès J7 pour des études réalisées à température ambiante. Le PA se désolvate de la phase triglycérique et se retrouve sous forme de précipité à l'extérieur des LNC (Figure 12). Ce phénomène est aussi observé pour les formulations plus faiblement concentrées (TE=1.2mg/g) mais pour des stabilités à un mois. Ces problèmes d'instabilité pourraient expliquer les résultats non concluants obtenus *in vivo* sur les modèles ectopiques à forte concentration (Figure 11). Finalement, la différence de concentration en ferrociphénol n'est peut être pas assez importante entre les 2 formulations testées pour avoir un effet *in vivo*, la dose de 1mg/g ayant déjà largement freiné la croissance tumorale.

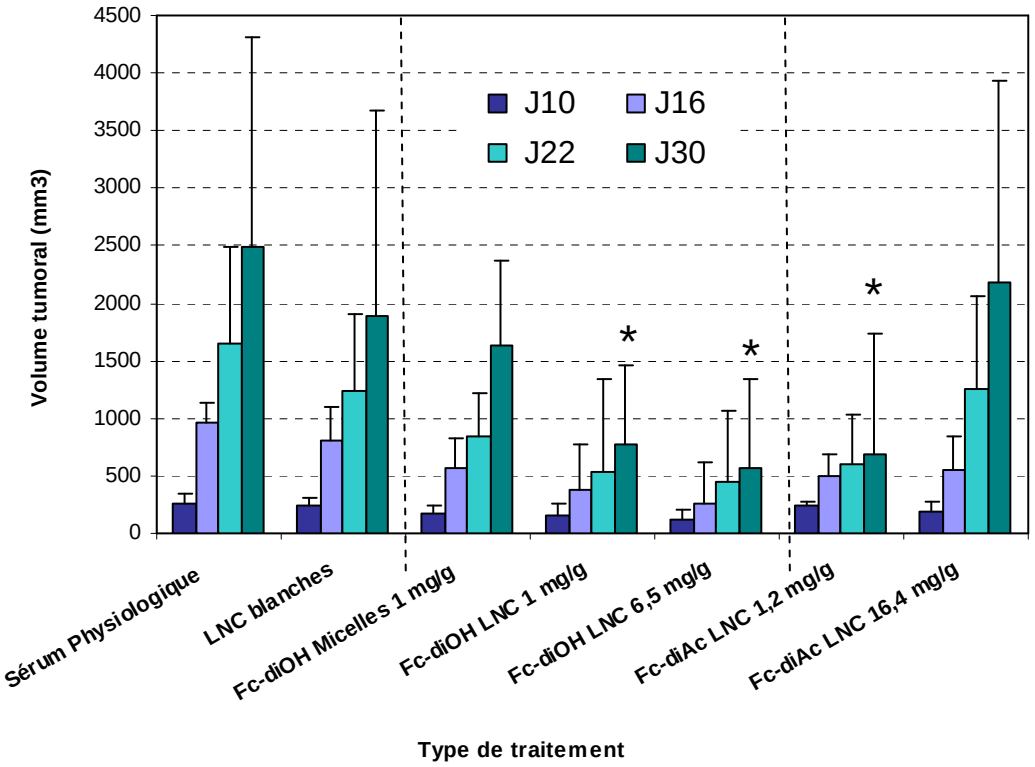

Figure 11 : Suivi du volume tumoral des tumeurs 9L implantées en sous-cutané chez un rat Fischer ayant reçu différents types de traitements (* $p<0.05$ significativement différent pas rapport au groupe témoins : sérum physiologique et LNC blanches).

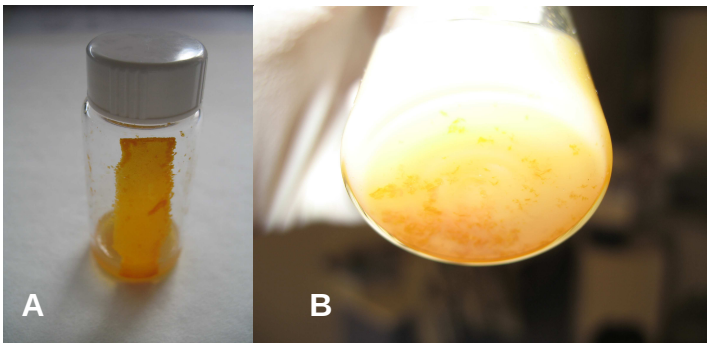

Figure 12 : Illustration de l'instabilité des formulations de LNC encapsulant la prodrogue Fc-diAc, dès J7 pour les formulations très concentrées (A) et à partir de J30 pour les formulations de basses concentrations (B).

Nos résultats sont intéressants puisque ce sont les premiers qui montrent une efficacité de cette famille de molécules dans des explorations *in vivo*, les polyphénols souffrant en général d'un problème de biodisponibilité dans des modèles animaux. Cela met en évidence l'importance du vecteur LNC puisqu'il permet d'administrer des PA très hydrophobes qui ne peuvent pas être administrés tels quels, augmentant ainsi cette biodisponibilité. Cependant, les

résultats obtenus sur un modèle *in vitro* comme sur un modèle de gliome ectopique ne sont pas directement transposables à un modèle de gliome orthotopique [17, 18]. En effet, les tumeurs implantées en sous-cutané sont très largement irriguées [6] et sont moins hypoxiques que les tumeurs cérébrales. De plus, la localisation du cerveau, isolée du reste de l'organisme par la présence de la BHE, confère une spécificité géographique aux tumeurs cérébrales.

L'administration intracérébrale par CED

Les 4 molécules de la famille des ferrocifènes ont fait l'objet d'administrations en CED dans un modèle de gliome 9L chez le rat Fischer. Les tumeurs sont implantées à J0 au niveau du striatum de chaque rat à raison de 1,000 cellules/rat et les traitements sont administrés à J6 à raison de 60µl de LNC. L'efficacité de ces traitements est évaluée par une étude de survie des animaux et par la détermination des médianes et moyennes de survie. Les premiers résultats ont montré une absence d'efficacité des ferrocifènes. En effet, la survie des animaux ayant reçu une CED de LNC chargées n'est pas significativement différente de celle des rats ayant reçus des LNC blanches, et ce, avec les 4 molécules, quelles que soient les doses testées (Figure 13).

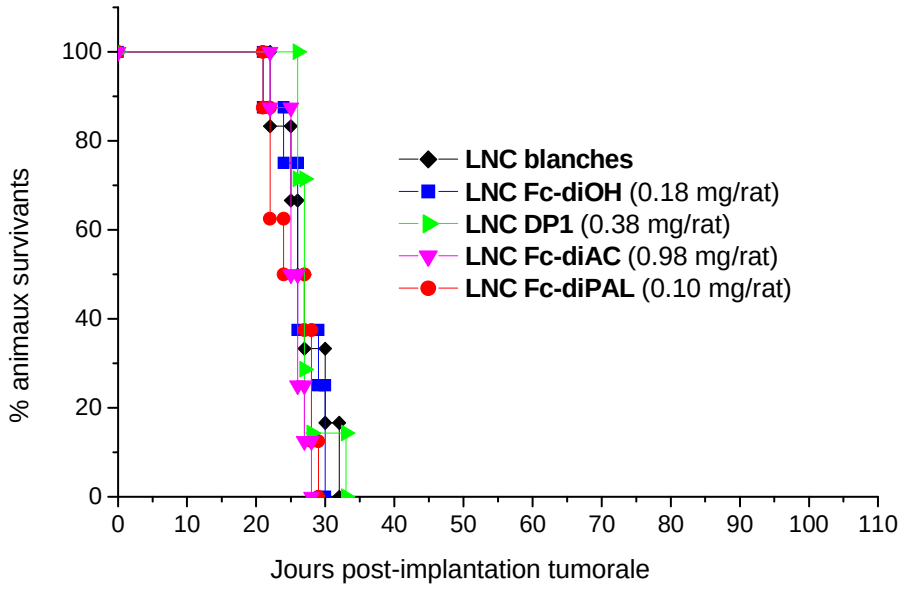

Figure 13 : Courbe de Kaplan-Meier évaluant la survie des animaux traités en CED par des LNC blanches et des LNC encapsulant Fc-diOH, DP1, Fc-diAC et Fc-diPAL.

De la même manière que pour le gliome sous-cutané, un effet-dose a été réalisée avec la molécule Fc-diOH. Puisque dans ce cas, le volume d'injection est limité pour des raisons de pression intracrânienne, deux paramètres ont été ajustés : les volumes d'injection (10 à 60 µL) et la concentration de Fc-diOH injectée (type de formulation). Le premier groupe de rats a été traité par des LNC-FcdiOH pour un TE de 0.5 mg/g par stéréotaxie simple (V= 10µl soit 0.005mg/rat). Le deuxième groupe a reçu une injection par CED de LNC encapsulant Fc-diOH pour un TE de 6.5 mg/g (V= 30µL soit 0.18mg/rat) et le troisième groupe est traité par une CED de Labrafac® solubilisant Fc-diOH à 40mg/g (V= 60µl soit 2.5 mg/rat).

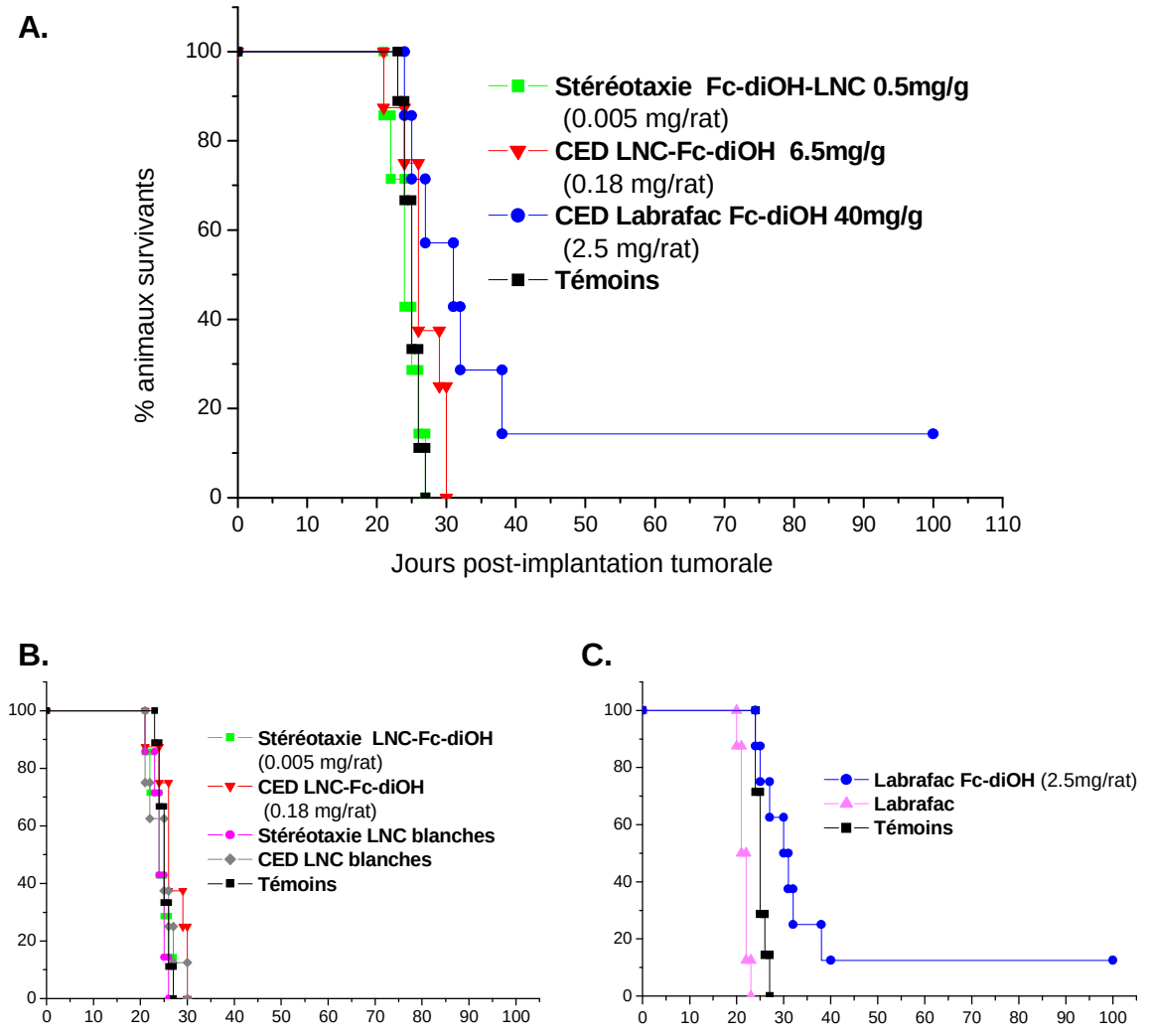

Figure 14 : Courbes de Kaplan-Meier des rats porteurs de gliome 9L, traités avec la molécule Fc-diOH par simple stéréotaxie ou CED suivant différents dosages ; 5, 180 et 2500 µg/rat (A). B et C représentent les courbes de survie de rat traités avec Fc-diOH véhiculé par les LNC (B) ou le Labrafac® (C) comparativement aux courbes de leurs témoins respectifs.

Les résultats de l'étude de survie montrent que l'effet cytostatique de Fc-diOH est proportionnel à la dose puisque les moyennes de survie des rats traités passent de 24.1, à 26.1 puis à 39.6 jours pour des doses de 0.005, 0.18 et 2.5 mg/rat respectivement (Figure 14A). Cependant, pour les rats traités avec les LNC encapsulant Fc-diOH en stéréotaxie simple ou en CED, les moyennes de survie de sont pas significativement différentes comparées aux groupes traités avec les vecteurs blancs ($p = 0.6033$ et $p = 0.5336$; Logrank test) (Figure 14B). En revanche, la différence devient significative si l'on compare le groupe de rats traités avec Fc-diOH dissout dans le Labrafac® à celui traité avec du Labrafac® seul ($p < 0.0001$) (Figure 14C). La molécule Fc-diOH confirme bien son activité cytostatique *in vivo* dans un modèle de gliome orthotopique lorsque la dose injectée est suffisante. La présence d'un rat long-survivant est même observée (médiane de survie > 100 jours). Cependant, il faut noter que l'injection du Labrafac® semble toxique pour le parenchyme cérébral pour plusieurs raisons. En effet, les rats ayant subi une infusion de Labrafac® seul ont une médiane de survie plus courte que les rats non traités (21.5 versus 25 jours). De plus les images IRM réalisées sur le rat long-survivant permettent de détecter la présence des triglycérides par un hypersignal, et ce, jusqu'à J100 (Figure 15). Cette persistance du Labrafac® accompagné de signes cliniques de léthargie est une preuve de la non-biocompatibilité de ce produit.

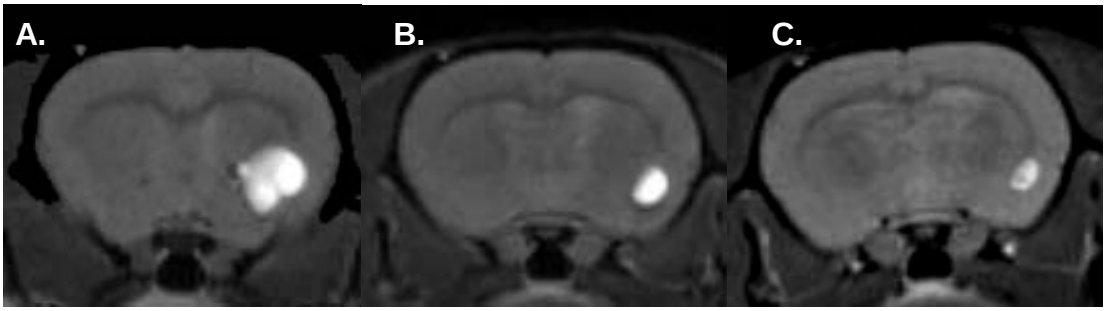

Figure 15 : IRM réalisée sur le rat long-survivant traité par 60µL de Fc-diOH solubilisé dans du Labrafac® à J42 (A), J58 (B) et J100 (C).

Les LNC encapsulant un complexe de ^{188}Re (^{188}Re-SSS LNC) ont été évaluées en tant que radiopharmaceutiques pour la radiothérapie interne des gliomes malins. Des rats femelles Fisher ont été traités par une unique injection de ^{188}Re-SSS LNC en CED 6 jours après implantation de la tumeur 9L. Les rats ont été randomisés dans différents groupes selon les doses reçues équivalentes à 12, 10, 8, et 3 Gy. La survie de ces animaux a été comparée à

celle obtenue pour des rats non traités ou des animaux infusés en CED avec une solution aqueuse de perrhénate de ^{188}Re (4Gy) ou des LNC blanches. Pour le groupe de 8 Gy, la médiane de survie est augmentée de 80% par rapport au groupe contrôle et 33% des animaux sont considérés comme long-survivants (Figure 16). La dose de 8 Gy est donc une dose efficace, intermédiaire entre des doses toxiques (10-12 Gy) ou inefficaces (3-4 Gy). En conclusion de cette étude, ce vecteur s'avère être un radiopharmaceutique très prometteur pour le traitement des tumeurs gliales par radiothérapie interne.

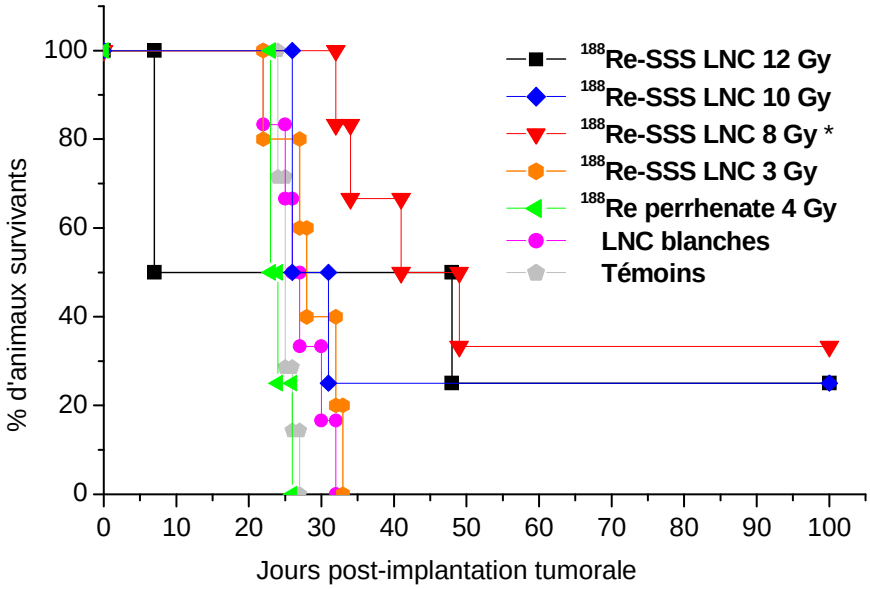

Figure 16 : Courbes de Kaplan-Meier des rats porteurs de gliome 9L, traités par injection intracérébrale de ^{188}Re-SSS LNC pour des doses de 12Gy, 10Gy, 8Gy et 3Gy. Les médianes de survie sont comparées à celles de rats non traités (témoins) ou ayant reçu une CED de LNC blanches ou de perrhenate de ^{188}Re 4Gy (* $p<0.05$).

La technique présente toutefois quelques limites puisque, malgré la présence de long-survivants, des séquelles neurologiques sont observées chez certains rats. La spectroscopie par RMN, réalisée au niveau du striatum atteint (droit) et du striatum sain (gauche) nous renseigne sur la biochimie du tissu cérébral. En effet, elle nous révèle une décroissance du taux de N-acétyl-aspartate (NAA) et de créatine avec une augmentation de lactate. Le NAA étant un marqueur de la viabilité neuronale et la créatine un marqueur du métabolisme énergétique cellulaire, leur diminution témoigne d'une souffrance cellulaire avérée [19]. L'apparition d'un pic de lactate témoigne de conditions d'ischémie cérébrale. Ces perturbations biochimiques sont très largement décrites comme des conséquences de la

radiothérapie externe [20, 21]. L'apparition de ces effets est aussi liée au modèle animal utilisé. Puisque le radioélément ^{188}Re a un diamètre de pénétration tissulaire de 10.15 mm [22], ses rayonnements vont malheureusement couvrir la quasi-totalité du cerveau des rats Fischer utilisés pour cette étude et, ainsi, toucher des parties saines. Même si le protocole expérimental reste perfectible, ces données sont les premières à démontrer l'efficacité thérapeutique de ce radioélément pour la radiothérapie interne des gliomes.

Les protocoles de chimio-radiothérapie

Parallèlement à l'action radiopharmaceutique attendue, un effet de potentialisation pourrait également apparaître par combinaison des deux types de complexes lipophiles, les molécules organométalliques pouvant voir leur efficacité augmentée par l'action du radionucléide. C'est ce que nous avons voulu tester en réalisant une CED combinant les deux types de nanocapsules. Le facteur limitant étant le volume d'injection (V=60µl), le ^{188}Re a été concentré dans les LNC en utilisant des activités très élevées en perrhénate permettant d'obtenir la dose optimisée de 8Gy. De plus, comme l'effet antitumoral du ferrociphénol semble être dépendant de la dose, les LNC ont été concentrées au maximum en modifiant la seconde étape de formulation. Afin de figer le système, et après la réalisation des trois cycles de montée et descente en température, les LNC sont plongées dans un bain de glace. Cette technique nous permet de nous affranchir du volume de trempe qui dilue les échantillons, et autorise la formation de LNC avec un TE de 8.5mg/g. Cette modification de formulation permet d'obtenir une dose de 0.42mg de Fc-diOH/rat pour un volume de 50µl. Les CED sont ensuite réalisées avec des formulations mélangeant 10µl de LNC encapsulant le radioélément avec 50µl de LNC encapsulant l'agent anticancéreux (formulations mixtes).

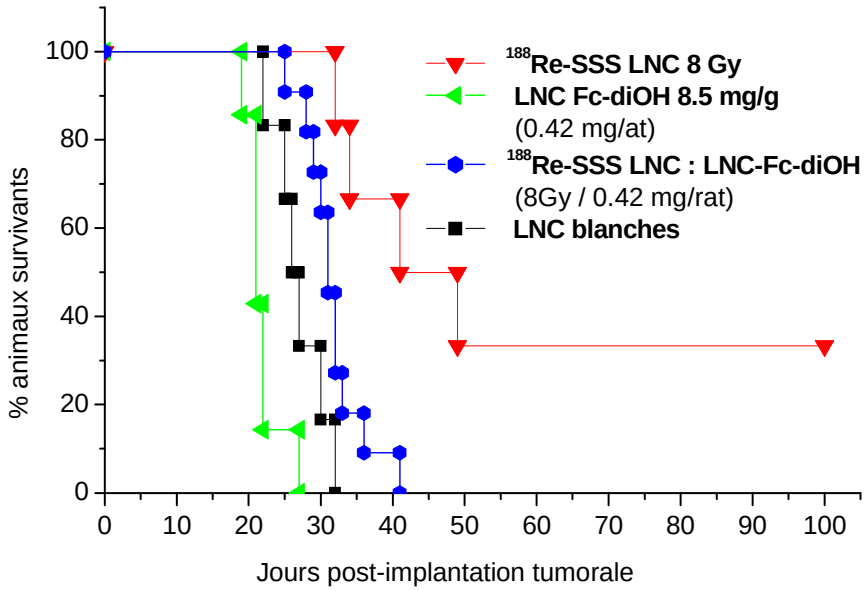

Figure 17 : Courbes de Kaplan-Meier des rats porteurs de gliome 9L, traités par injection intracérébrale en CED de LNC blanches, LNC-^{188}Re 8Gy, LNC FcdiOH 8.5mg/g ou un mélange de LNC FcdiOH et LNC ^{188}Re aux mêmes doses.

Les résultats montrent que la survie des animaux traités par les formulations mixtes n'est pas améliorée par rapport au groupe traité par ^{188}Re-LNC 8Gy puisque les médianes de survie sont de 31 et 45 jours respectivement (Figure 17). De plus, les LNC sans ajout du volume d'eau de trempe apparaissent toxiques pour le parenchyme cérébral puisque les rats traités par ces formulations meurent avec une médiane de survie de 21 jours, donc plus courte que pour les rats non traités (médiane = 25j). Les hypothèses permettant d'expliquer ces résultats négatifs s'orientent tout d'abord vers des problèmes de formulations. En effet, la concentration des 2.8MBq (correspondant à la dose de 8Gy) dans 10µL de LNC est élevée et peut être à l'origine d'un relarguage du complexe hors des nanocapsules. De plus, l'absence de volume de trempe rend les formulations très hyperosmolaires, ce qui peut expliquer leur toxicité vis-à-vis des cellules. D'autre part, dans l'optique d'une potentialisation de l'action du ferrociphénol, les rayonnements doivent avoir des propriétés oxydantes puisque l'action cytostatique de la molécule Fc-diOH est liée à un transfert d'électrons permettant la transformation du groupement ferrocène en ferrocénium [7]. Or, la radioactivité bêta moins (β^-) s'accompagnant de l'émission d'un électron et d'un antineutrino électronique, n'est pas qualifiée d'oxydante. Ainsi, le radioélément ^{188}Re ne permet pas de potentialiser l'action du diphénol Fc-diOH.

Enfin, si l'on combine l'action du ferrociphénol avec de la radiothérapie externe, c'est-à-dire à une source d'irradiation située à l'extérieur de l'animal, les résultats sont plus probants. Les premières expériences *in vitro* sur cellules 9L ont montré un effet prépondérant quand la radiothérapie est délivrée après la chimiothérapie associant LNC et Fc-diOH. De plus, cette association n'est pas seulement une résultante des effets additifs de la radio et de la chimiothérapie, mais apparaît comme "synergique", ce qui signifie qu'il existe une réelle coopération entre la molécule et les radiations. En effet, les rayonnements, dans ce cas, sont des radiations ionisantes non chargées que l'on nomme photons X, obtenues à partir d'accélérateur de particules et provenant du réarrangement des électrons du cortège électronique du métal source. En présence d'oxygène, ces radiations peuvent créer des radicaux à fort pouvoir oxydant entraînant la formation d'eau oxygénée, particulièrement oxydante. Cela permettrait d'engager le processus oxydatif à l'origine de la formation de la quinone méthyde, entraînant la sénescence accélérée des cellules.

Cette association synergique a ensuite fait l'objet d'une exploration *in vivo*. Dans l'idée de s'approcher au maximum de ce qui est réalisé en clinique, la radiothérapie a été effectuée en plusieurs séances. En effet, pour une même dose totale, l'efficacité biologique est différente selon la dose administrée par séance, le nombre total de séances (fractionnement) et la durée du traitement (étalement). La dose totale délivrée choisie est de 18Gy, réalisée en 3 séances de 6Gy chacune, réparties sur une semaine (J8-J11-J14). La CED à base de LNC-Fc-diOH 6.5mg/g est réalisée à J6, soit 2 jours avant la première séance de radiothérapie. L'intérêt de cette triple irradiation a été démontré *in vitro* puisque l'effet de mort, après la troisième irradiation, est évalué à 40% pour les cellules ayant reçu la chimio au préalable contre seulement 5% pour les cellules seulement irradiées. Afin d'optimiser la convection, les formulations de LNC ont vu leur viscosité légèrement augmentée par l'ajout de sucrose en phase externe. L'ajout du disaccharide s'est avéré non toxique sur les cellules en culture. L'ajout de sucrose est décrit dans la littérature pour augmenter la viscosité des suspensions colloïdales, réduisant les risques de reflux et augmentant ainsi les volumes de distribution [23, 24].

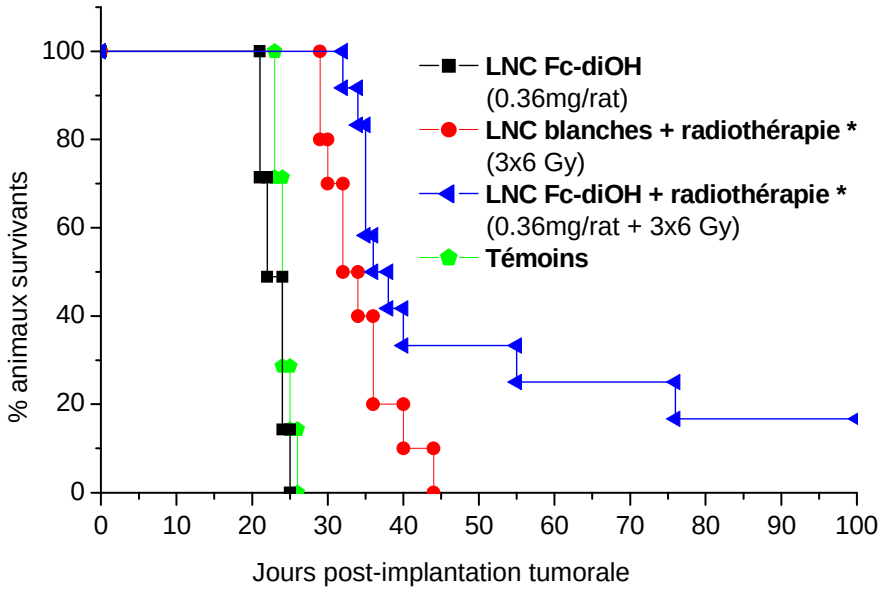

Figure 18 : Courbes de Kaplan-Meier des rats porteurs de gliome 9L, traités par une chimiothérapie de LNC-Fc-diOH 6.5mg/rat (0.36mg.rat), une radiothérapie comprenant une CED de LNC blanches suivie de 3 séances d'irradiation à 6Gy (dose totale = 18Gy) ou une chimio-radiothérapie associant les deux types de traitements (*p<0.05).

Les résultats de cette expérimentation chez l'animal montrent que la relation entre Fc-diOH et les rayonnements X est bien une relation synergique. En effet, comme observé dans les précédentes injections, il n'y a aucun effet *in vivo* de la molécule seule injectée en CED et la présence de sucrose n'améliore pas cet effet (Figure 18). En revanche, le groupe radiothérapie, qui a également reçu une CED de LNC blanches, voit sa médiane de survie augmentée à 33 jours. Le bénéfice de la radiothérapie classique dans le traitement des tumeurs gliales a montré son intérêt dans de nombreuses études [25-28], et ce depuis plusieurs années. En parallèle, le groupe de rats traités par chimio-radiothérapie a une médiane de survie de 37 jours avec la présence de deux rats long-survivants. Cette médiane est significativement différente de celle du groupe traité par une CED de LNC-Fc-diOH seule ($p<0.0001$), mais surtout significativement différente de celle du groupe traité par radiothérapie seule ($p<0.05$). Ce résultat confère au ferrociphénol des propriétés de molécule radio-sensibilisante. C'est un résultat majeur dans la mesure où les gliomes sont connus pour être des tumeurs hypoxiques très agressives [29] et le modèle murin 9L, comparé à d'autres modèles animaux, fortement radiorésistant [30].

En définitif, la survie des animaux est réellement effective pour deux types de traitements testés pour lesquels les LNC sont administrées par convection-enhanced delivery. Le premier est une radiothérapie interne à l'aide de LNC encapsulant le complexe de ^{188}Re pour une dose de 8Gy. Le second est un traitement par chimio-radiothérapie à l'aide de LNC encapsulant Fc-diOH pour une dose de 0.36 mg, suivi d'une radiothérapie externe externe de 3x6Gy. Si on ne compare que les données chiffrées des médianes et moyennes de survie, les résultats les plus probants semblent être obtenus par la radiothérapie interne (Tableau 1). Cependant, les groupes d'animaux variant du simple ou double : n=6 (^{188}Re) versus n=12 (Fc-diOH), les résultats sont difficilement comparables.

Traitement	**n**	**Temps de survie (jours)**			**Accroissement temps survie (%)**		
		Gamme	Médiane	Moyenne ± DS	Long survivants	ATS médiane	ATS moyenne
^{188}Re-SSS LNC 8 Gy	**6**	32-100	45.0	59.3 ± 32	33.3	80	137.2
LNC FcdiOH 0.36mg + radioT 3x6 Gy	**12**	32-100	37.0	51.3 ± 25.9	16.7	48	105.2
Témoins	**9**	23-27	25.0	25.0 ± 1.2	0	-	-

Tableau 1 : Tableau descriptif des données statistiques concernant les études de survie donnant lieu à l'existence de longs survivants : radiothérapie interne de ^{188}Re-SSS-LNC 8 Gy, et chimiothérapie de LNC-Fc-diOH 0.36mg suivie d'une radiothérapie externe délivrant 3x6 Gy.

De plus, si une administration intracérébrale de Rhénium-188 s'est avérée toxique pour le parenchyme cérébral, il reste à évaluer la toxicité d'un traitement local de ferrociphénol ainsi que celle de la radiothérapie externe. Le schéma de radiothérapie externe a été choisi comme le plus fidèle, en équivalent de dose, au traitement conventionnel des tumeurs cérébrales. Le fractionnement (3 séances de 6Gy) permet d'obtenir un effet différentiel entre les tissus sains et la tumeur, plus marqué que pour une fraction unique. En effet l'irradiation engendre chez toute cellule, qu'elle soit saine ou cancéreuse, des lésions sub-létales de l'ADN, c'est-à-dire des lésions qui peuvent être réparées par des mécanismes internes. Entre deux irradiations, les tissus sains ont une plus grande capacité de restauration et de prolifération que les populations tumorales. Le fractionnement exploite ce phénomène qu'il amplifie, créant un différentiel

favorable qui doit aboutir au terme de l'irradiation, à la destruction complète des cellules cancéreuses. Des effets toxiques de la radiothérapie externe sont décrits dans la littérature mais pour des doses délivrées en une seule fois et supérieures à 20 Gy [31].

Enfin, il est très difficile de mettre en parallèle ces résultats avec ceux d'autres études utilisant divers agents néoplasiques associés à la radiothérapie externe, dans la mesure où les protocoles expérimentaux sont tous très différents. Les variations sont nombreuses et proviennent de différentes sources : type de cellules (9L, F98, C6, U87, U251…), nombre de cellules implantées (500 à 500,000), jour de traitement (J5 à J14), dose totale d'irradiation (18-32Gy), et nombre de séances (1 à 9) [17, 32-36].

Références

1. Rainov NG, Soling A, Heidecke V. Novel therapies for malignant gliomas: a local affair? Neurosurg Focus 2006;20(4):E9.

2. Sawyer AJ, Piepmeier JM, Saltzman WM. New methods for direct delivery of chemotherapy for treating brain tumors. Yale J Biol Med 2006;79(3-4):141-152.

3. Wang PP, Frazier J, Brem H. Local drug delivery to the brain. Adv Drug Deliv Rev 2002;54(7):987-1013.

4. Ferguson S, Lesniak MS. Convection enhanced drug delivery of novel therapeutic agents to malignant brain tumors. Curr Drug Deliv 2007;4(2):169-180.

5. Lopez KA, Waziri AE, Canoll PD, Bruce JN. Convection-enhanced delivery in the treatment of malignant glioma. Neurol Res 2006;28(5):542-548.

6. Mamot C, Nguyen JB, Pourdehnad M, Hadaczek P, Saito R, Bringas JR, et al. Extensive distribution of liposomes in rodent brains and brain tumors following convection-enhanced delivery. J Neurooncol 2004;68(1):1-9.

7. Hillard E, Vessieres A, Thouin L, Jaouen G, Amatore C. Ferrocene-mediated proton-coupled electron transfer in a series of ferrocifen-type breast-cancer drug candidates. Angew Chem Int Ed 2006;45(2):285-290.

8. Lacoeuille F, Garcion E, Benoit JP, Lamprecht A. Lipid nanocapsules for intracellular drug delivery of anticancer drugs. J Nanosci Nanotechnol 2007;7(12):4612-4617.

9. Malzert-Fréon A, Vrignaud S, Saulnier P, Lisowski V, Benoit JP, Rault S. Formulation of sustained release nanoparticles loaded with a tripentone, a new anticancer agent. Int J Pharm 2006;320(1-2):157-164.

10. Ballot S, Noiret N, Hindre F, Denizot B, Garin E, Rajerison H, et al. 99mTc/188Re-labelled lipid nanocapsules as promising radiotracers for imaging and therapy: Formulation and biodistribution. European Journal of Nuclear Medicine and Molecular Imaging 2006;33(5):602-607.

11. Heurtault B, Saulnier P, Pech B, Proust J-E, Benoit J-P. A novel phase inversion-based process for the preparation of lipid nanocarriers. Pharm Res 2002;19(6):875-880.

12. Thorne RG, Nicholson C. In vivo diffusion analysis with quantum dots and dextrans predicts the width of brain extracellular space. Proc Natl Acad Sci U S A 2006;103(14):5567-5572.

13. Vessieres A, Top S, Pigeon P, Hillard E, Boubeker L, Spera D, et al. Modification of the estrogenic properties of diphenols by the incorporation of ferrocene. Generation of antiproliferative effects in vitro. J Med Chem 2005;48(12):3937-3940.

14. Garcion E, Lamprecht A, Heurtault B, Paillard A, Aubert-Pouessel A, Denizot B, et al. A new generation of anticancer, drug-loaded, colloidal vectors reverses multidrug resistance in glioma and reduces tumor progression in rats. Mol Cancer Ther 2006;5(7):1710-1722.

15. Roullin VG, Deverre JR, Lemaire L, Hindre F, Venier-Julienne MC, Vienet R, et al. Anti-cancer drug diffusion within living rat brain tissue: an experimental study using [3H](6)-5-fluorouracil-loaded PLGA microspheres. Eur J Pharm Biopharm 2002;53(3):293-299.

16. Allard E, Hindre F, Passirani C, Lemaire L, Lepareur N, Noiret N, et al. (188)Re-loaded lipid nanocapsules as a promising radiopharmaceutical carrier for internal radiotherapy of malignant gliomas. Eur J Nucl Med Mol Imaging 2008;35(10):1838-1846.

17. Lamfers ML, Idema S, Bosscher L, Heukelom S, Moeniralm S, van der Meulen-Muileman IH, et al. Differential effects of combined Ad5- delta 24RGD and radiation therapy in in vitro versus in vivo models of malignant glioma. Clin Cancer Res 2007;13(24):7451-7458.

18. Shapiro WR. The chemotherapy of intracerebral vs subcutaneous murine gliomas. A comparative study of the effect of VM 26. Archives of Neurology 1974;30(3):222-226.

19. Payen JF, Francony G, Fauvage B, Le Bas JF. [Contribution of magnetic resonance spectroscopy in predicting severity and outcome in traumatic brain injury]. Ann Fr Anesth Reanim 2005;24(5):522-527.

20. Schlemmer H-P, Bachert P, Herfarth KK, Zuna I, Debus J, Van Kaick G. Proton MR spectroscopic evaluation of suspicious brain lesions after stereotactic radiotherapy. American Journal of Neuroradiology 2001;22(7):1316-1324.

21. Zeng Q-S, Li C-F, Liu H, Zhen J-H, Feng D-C. Distinction Between Recurrent Glioma and Radiation Injury Using Magnetic Resonance Spectroscopy in Combination With Diffusion-Weighted Imaging. International Journal of Radiation Oncology Biology Physics 2007;68(1):151-158.

22. Iznaga-Escobar N. 188Re-direct labeling of monoclonal antibodies for radioimmunotherapy of solid tumors: Biodistribution, normal organ dosimetry, and toxicology. Nuclear Medicine and Biology 1998;25(5):441-447.

23. Mardor Y, Rahav O, Zauberman Y, Lidar Z, Ocherashvilli A, Daniels D, et al. Convection-enhanced drug delivery: increased efficacy and magnetic resonance image monitoring. Cancer Res 2005;65(15):6858-6863.

24. Perlstein B, Ram Z, Daniels D, Ocherashvilli A, Roth Y, Margel S, et al. Convection-enhanced delivery of maghemite nanoparticles: Increased efficacy and MRI monitoring. Neuro Oncol 2008;10(2):153-161.

25. Kristiansen K, Hagen S, Kollevold T, Torvik A, Holme I, Nesbakken R, et al. Combined modality therapy of operated astrocytomas grade III and IV. Confirmation of the value of postoperative irradiation and lack of potentiation of bleomycin on survival time: a

prospective multicenter trial of the Scandinavian Glioblastoma Study Group. Cancer 1981;47(4):649-652.

26. Sandberg-Wollheim M, Malmstrom P, Stromblad LG, Anderson H, Borgstrom S, Brun A, et al. A randomized study of chemotherapy with procarbazine, vincristine, and lomustine with and without radiation therapy for astrocytoma grades 3 and/or 4. Cancer 1991;68(1):22-29.

27. Walker MD, Alexander E, Jr., Hunt WE, MacCarty CS, Mahaley MS, Jr., Mealey J, Jr., et al. Evaluation of BCNU and/or radiotherapy in the treatment of anaplastic gliomas. A cooperative clinical trial. J Neurosurg 1978;49(3):333-343.

28. Walker MD, Green SB, Byar DP, Alexander E, Jr., Batzdorf U, Brooks WH, et al. Randomized comparisons of radiotherapy and nitrosoureas for the treatment of malignant glioma after surgery. N Engl J Med 1980;303(23):1323-1329.

29. Davis LW. Malignant glioma--a nemesis which requires clinical and basic investigation in radiation oncology. Int J Radiat Oncol Biol Phys 1989;16(6):1355-1365.

30. Bencokova Z, Pauron L, Devic C, Joubert A, Gastaldo J, Massart C, et al. Molecular and cellular response of the most extensively used rodent glioma models to radiation and/or cisplatin. J Neurooncol 2008;86(1):13-21.

31. Wong CS, Van der Kogel AJ. Mechanisms of radiation injury to the central nervous system: implications for neuroprotection. Mol Interv 2004;4(5):273-284.

32. Krauze MT, Noble CO, Kawaguchi T, Drummond D, Kirpotin DB, Yamashita Y, et al. Convection-enhanced delivery of nanoliposomal CPT-11 (irinotecan) and PEGylated liposomal doxorubicin (Doxil) in rodent intracranial brain tumor xenografts. Neuro Oncol 2007;9(4):393-403.

33. Roullin VG, Mege M, Lemaire L, Cueyssac JP, Venier-Julienne MC, Menei P, et al. Influence of 5-fluorouracil-loaded microsphere formulation on efficient rat glioma radiosensitization. Pharm Res 2004;21(9):1558-1563.

34. Rousseau J, Boudou C, Barth RF, Balosso J, Esteve F, Elleaume H. Enhanced survival and cure of F98 glioma-bearing rats following intracerebral delivery of carboplatin in combination with photon irradiation. Clin Cancer Res 2007;13(17):5195-5201.

35. Saito R, Krauze MT, Noble CO, Drummond DC, Kirpotin DB, Berger MS, et al. Convection-enhanced delivery of Ls-TPT enables an effective, continuous, low-dose chemotherapy against malignant glioma xenograft model. Neuro Oncol 2006;8(3):205-214.

36. Sugiyama SI, Yamashita Y, Kikuchi T, Sonoda Y, Kumabe T, Tominaga T. Enhanced antitumor effect of combinedmodality treatment using convectionenhanced delivery of hydrophilic nitrosourea with irradiation or systemic administration of temozolomide in intracranial brain tumor xenografts. Neurol Res 2008.

CONCLUSION ET PERSPECTIVES

Les LNC représentent un vecteur idéal pour l'administration locale par CED de complexes métalliques lipophiles dans le traitement des tumeurs gliales malignes. Les images réalisées en IRM, suite à l'injection de LNC encapsulant des oxydes de fer, montrent que les LNC diffusent largement dans le striatum et au-delà de la zone tumorale. De plus, les LNC permettent l'encapsulation de molécules lipophiles avec de forts rendements d'encapsulation proches de 100%. Cette encapsulation permet donc d'envisager une administration *in vivo* de ces molécules qui ne sont solubles que dans des solvants organiques non injectables. Les LNC encapsulant le complexe lipophile de Rhenium-188 permettent une rétention de l'émetteur β^- au niveau local et une éradication complète de la tumeur, pour une dose optimisée de 8Gy. L'activité du complexe Fc-diOH est conservée après encapsulation dans les LNC et s'avère majeure sur les cellules de gliome 9L (IC_{50}= 0.6µM) alors qu'elle est très réduite sur des astrocytes (IC_{50}= 60µM). De plus, les LNC sont quantitativement internalisées dans les cellules 9L, et entraînent une réduction du volume tumoral dans un modèle de gliome sous cutané. Cette réduction peut aller jusqu'à une éradication totale de la tumeur lorsque l'administration des LNC-Fc-diOH en CED est suivie d'une radiothérapie externe. En effet, l'association entre le complexe et les photons X est une association synergique conférant à Fc-diOH des propriétés de molécule radiosensibilisante.

Toutefois, ces protocoles restent perfectibles et de nombreuses améliorations restent à envisager. Dans l'optique d'améliorer l'efficacité thérapeutique, la lyophilisation qui a déjà été réalisée sur les nanocapsules lipidiques [1], permettrait d'augmenter la quantité de LNC injectée, et donc la dose de produit administrée. La lyophilisation est également en faveur d'une meilleure conservation des formulations et permettrait d'obtenir des suspensions à reconstituer extemporanément. Cependant, elle nécessite l'ajout d'un cryprotecteur en phase externe dont l'innocuité reste à confirmer une fois administrée dans le parenchyme cérébral.
Dans l'optique d'augmenter la dose injectée, il serait peut être judicieux d'envisager des multi-injections en CED. De plus, puisqu'il existe une étroite corrélation entre l'activité du complexe Fc-diOH et la radiothérapie externe, au lieu d'une administration néo-adjvuvante, il serait intéressant d'envisager une administration concomitante à la radiothérapie. Cette association pourrait également être suivie par une seconde administration de la chimiothérapie, comme ce qui se fait aujourd'hui en clinique avec l'administration du témozolomide (Témodal®)[2].

Dans le cas de la radiothérapie interne à l'aide des LNC encapsulant le ^{188}Re, les perspectives sont de tester d'autres modes d'administration et notamment des multi-injections. Afin de réduire les effets secondaires, la dose de 8Gy pourrait être fractionnée en plusieurs administrations et les volumes d'injection en CED pourraient être diminués minimisant ainsi les irradiations du tissu sain.

De manière à augmenter la spécificité des LNC pour les cellules cancéreuses, les perspectives seraient également d'injecter en CED une nanoparticule de troisième génération. Des travaux récents ont montré la possibilité de greffer de façon covalente des anticorps monoclonaux OX26 et des fragments issus de ce même anticorps, à la surface des LNC, formant ainsi des immunonanocapsules [3]. Ces anticorps permettent un ciblage du récepteur à la transferrine de rat, surexprimé au niveau de la BHE [4] mais aussi au niveau des cellules à forte activité mitotique comme les cellules de gliome. Le rayon de courbure des particules jouant un rôle prépondérant sur les capacités de greffage, cette étude a été réalisée sur des LNC natives de 100 nm. Par conséquent, il faudrait adapter la technologie de greffage à des LNC de 50 nm afin de conserver une bonne diffusion en CED.

Enfin, il serait intéressant de travailler sur un autre modèle que le modèle 9L. La lignée cellulaire de gliosarcome de rat 9L a été obtenue à partir d'une tumeur initialement chimio-induite par la N-méthyl nitroso-urée chez le rat Fisher 344 [5]. C'est un modèle syngénique très agressif avec une croissance très rapide [6], mais dont l'histopathologie et le potentiel invasif est souvent non-conforme à ceux des gliomes humains. Dans cette optique, il pourrait être intéressant de travailler sur des modèles associant des cellules de gliome humain à des animaux immunodéprimés (athymiques ou génétiquement modifiés) [7].

En conclusion, ce travail de thèse a permis d'explorer des stratégies très récemment décrites en testant le pouvoir thérapeutique de nouvelles substances actives issues de la recherche. Il offre un espoir dans le traitement des tumeurs gliales malignes qui, aujourd'hui, restent malheureusement de très mauvais pronostic.

Références

1. Dulieu C, Bazile D. Influence of lipid nanocapsules composition on their aptness to freeze-drying. Pharm Res 2005;22(2):285-292.

2. Stupp R, Mason WP, Van Den Bent MJ, Weller M, Fisher B, Taphoorn MJB, et al. Radiotherapy plus concomitant and adjuvant temozolomide for glioblastoma. N Engl J Med 2005;352(10):987-996.

3. Beduneau A, Saulnier P, Hindre F, Clavreul A, Leroux JC, Benoit JP. Design of targeted lipid nanocapsules by conjugation of whole antibodies and antibody Fab' fragments. Biomaterials 2007;28(33):4978-4990.

4. Beduneau A, Hindre F, Clavreul A, Leroux JC, Saulnier P, Benoit JP. Brain targeting using novel lipid nanovectors. J Control Release 2008;126(1):44-49.

5. Weizsaecker M, Deen DF, Rosenblum ML, Hoshino T, Gutin PH, Barker M. The 9L rat brain tumor: description and application of an animal model. J Neurol 1981;224(3):183-192.

6. Kimler BF. The 9L rat brain tumor model for pre-clinical investigation of radiation-chemotherapy interactions. J Neurooncol 1994;20(2):103-109.

7. Javerzat S, Bikfalvi A, Hagedorn M. [Understanding in treating gliomas: an adequate experimental model for each question]. Bull Cancer 2005;92(7):633-635.

.

CURRICULUM VITAE

Emilie ALLARD
10 rue botanique
49100 ANGERS
28 ans, née le 29/03/80
02 41 86 99 16
06 70 89 85 52
emilieallardfr@yahoo.fr

PHARMACIEN GALENISTE

FORMATION

2005 – 2008 — **THESE DE DOCTORAT DE L'UNIVERSITE D'ANGERS**
Pharmacotechnie et Biopharmacie
Dirigé par Pr JP Benoit et Dr C Passirani, INSERM U646, Angers

2003 – 2004 — **DESS PHARMACIE GALENIQUE INDUSTRIELLE, Mention bien**
Faculté de Pharmacie, Université de Lille II (Pr A. Gayot)

1998 – 2004 — **DIPLOME D'ETAT DE DOCTEUR EN PHARMACIE, UNIVERSITE D'ANGERS**
Thèse d'exercice : Mention Très Bien (Déc. 2004)

Formations : Expérimentation animale - Niveau I

RECHERCHE

2005 – 2008 — **THESE DE DOCTORAT**
INSERM U646, Ingénierie de la vectorisation particulaire, Université d'Angers

Mars – Août 2005 — **PROJET DE RECHERCHE ADEME, CDD 6 MOIS**
INSERM U 646, Ingénierie de la vectorisation particulaire, Université d'Angers
Microencapsulation en milieu CO_2 supercritique

Fév – Déc 2004 — **STAGE VALIDANT DESS ET 6EME ANNEE DE PHARMACIE**
Technologie SERVIER, Département Prospective Galénique, Orléans
Formulation de dispersions solides par extrusion à chaud dans le but d'augmenter la vitesse de dissolution d'un principe actif peu soluble.

Mai – Juillet 2002 — **STAGE ERASMUS - INITIATION A LA RECHERCHE** (Pr M.J. Alonso)
Laboratoire de Pharmacie Galénique, Université de Saint Jacques de Compostelle, Espagne
Les particules de PLA-PEG comme véhicules pour l'administration nasale.

Juin 2001 — **STAGE DE DECOUVERTE EN INDUSTRIE PHARMACEUTIQUE**
PFIZER, Angers, Laboratoire de contrôle analytique
Découverte des principales méthodes analytiques : HPLC, CPG, CCM, UV, IR, proche IR

ENSEIGNEMENT

MONITORAT CIES (centre d'initiation à l'enseignement supérieur)
Enseignements réalisés à UFR des Sciences Pharmaceutiques et ingénierie de la santé
3 x 64h équivalent TD

Travaux pratiques : Angles de contact *(6 x 3h x 3ans = 54h)*, tensiométrie des protéines *(3h)*, formulation de gel – Applications à la rhéologie *(6 x 3h = 18h)*, formulation de microémulsions *(3h)*, formulation de comprimés *(4 x 6h = 24h)*
Suivi de projet : UV formulation – comprimés pelliculés d'Ibuprofène *(40h)*
Travaux dirigés : Statistiques – (enseignement en binôme) *(88h)*

ENCADREMENT D'ETUDIANTS :
3 étudiants en 2ème année de pharmacie : stage d'initiation à la recherche (1 mois)
Formation d'1 étudiante en thèse d'Ankara, (Turquie) sur des techniques d'implantation intracérébrale chez le rat (7 mois)

PRODUCTIONS SCIENTIFIQUES

Communications orales

Immunociblage des cellules tumorales par les nanocapsules lipidiques
Allard E
Journée interne du GDR 2352 Immunociblage des tumeurs, Paris, Novembre 2005
2nd Journée Scientifique de l'Axe Vectorisation Tumorale, Angers, Décembre 2005

188-Rhenium loaded lipid nanocapsules as promising radiopharmaceutical carrier for internal radiotherapy of malignant glioma
Allard E, Hindre F, Passirani C, Lemaire L, Lepareur N, Menei P, Benoit JP
XXIIièmes Journées Scientifiques du GTRV, Strasbourg, Décembre 2007

Lipid nanocapsules loaded with ferrocenyl tamoxifen derivative as a novel drug-carrier system for experimental malignant glioma
Allard E, Passirani C, Garcion E, Vessières A, Jaouen G, Benoit JP
6 World meeting on Pharmaceutics biopharmaceutics and pharmaceutical technology, Barcelone, Avril 2008

Local delivery of ferrocifenol LNC as a novel drug carrier system against 9L glioma models
Allard E (conférencier invité)
Meeting COST D39 Metallo-Drug Design and Action, Paris, Octobre 2008

Communications écrites

Ferrociphenol-loaded Lipid nanocarriers as novel systems for experimental malignant glioma
Allard E, Passirani C, Garcion E, Vessières A, Jaouen G, Benoit JP
XXIièmes Journées Scientifiques du GTRV, Paris, Décembre 2006

Calcium carbonate microparticles formulation using CO2 in supercritical conditions: encapsulation of model proteins
K. Ahmed Ouamer, E. Allard, F. Tewes, N.Butoescu, P. Doan Thi, E. Garcion, JP Benoit, F. Boury
XXIIièmes Journées Scientifiques du GTRV, Strasbourg, Décembre 2007

Local delivery of ferrociphenol lipid nanocapsules followed by external radiotherapy as a synergistic treatment against intracranial 9l glioma xenograft
Allard E, Passirani C, Jarnet D, Petit S, Vessières A, Jaouen G, Benoit JP
XXIIIièmes Journées Scientifiques du GTRV, Angers, Décembre 2008

Solid Dispersion versus Particle Size Reduction to Improve the Dissolution Rate of a Poorly Water-Soluble Drug Substance from Fast-Disintegrating Tablets
Emilie Allard, Jean-Manuel Péan, Hervé Rolland, Patrick Wüthrich
Controlled Release Society, Miami, Juin 2005

Encapsulation of DNA into biomimetic lipid nanocapsules
Vonarbourg A, Passirani C, Desigault L, Allard E, Morille M, Saulnier P, Lambert O, Benoît JP, Pitard B
6 World meeting on Pharmaceutics biopharmaceutics and pharmaceutical technology, Barcelone, Avril 2008

Publications

188-Rhenium loaded lipid nanocapsules as promising radiopharmaceutical carrier for internal radiotherapy of malignant glioma
Allard E, Hindré F, Passirani C, Lemaire L, Lepareur N, Noiret N, Menei P, Benoît JP
European Journal of Nuclear Medicine and Molecular Imaging, 2008, 35 (10): 1838-1846.

Lipid nanocapsules loaded with an organometallic tamoxifen derivative as a novel drug-carrier system for experimental malignant gliomas
Allard E, Passirani C, Garcion E, Pigeon P, Vessières A, Jaouen G, Benoît JP
Journal of Controlled release, 2008, 130: 146-153

Local delivery of ferrociphenol lipid nanocapsules followed by external radiotherapy as a synergistic treatment against intracranial 9l glioma xenograft
Allard E, Passirani C, Jarnet D, Petit S, Vessières A, Jaouen G, Benoit JP (soumis Clinical Cancer Research)

Convection-enhanced delivery of nanocarriers for the treatment of brain tumors
Allard E, Passirani C, Benoit JP (Review soumise à Advanced Drug Delivery Review)

Encapsulation of DNA molecules into biomimetic lipid nanocapsules
Vonarbourg A, Passirani C, Desigault L, Allard E, Saulnier P, Lambert O, Benoît JP, Pitard B
(soumis à Biomaterials)

Résumé

Ce travail de thèse a pour objectif le traitement local des gliomes malins via l'administration de nanocapsules lipidiques (LNC) par convection enhanced delivery (CED). Deux types de complexes métalliques lipophiles aux propriétés thérapeutiques ont été encapsulés au sein des LNC. Le premier est un complexe radioactif de Rhénium-188 et le second, un agent anticancéreux dérivé du tamoxifène et du ferrocène, le ferrociphénol (Fc-diOH). Les LNC de ^{188}Re permettent une rétention de l'émetteur β^- au niveau local et une éradication complète de la tumeur est possible pour une dose de 8Gy puisque 33% des animaux sont de longs survivants. Cette dose optimisée s'est révélée être une dose efficace, intermédiaire entre des doses toxiques (10-12 Gy) ou inefficaces (3-4 Gy). Les LNC-Fc-diOH présentent des taux d'encapsulation élevés, et sont quantitativement internalisées dans les cellules 9L. De plus, l'activité du ferrociphénol est conservée après encapsulation et se révèle très efficace sur des cellules de gliome 9L (IC_{50}=0.6µM). En revanche, l'activité est très réduite sur les astrocytes, cellules au potentiel de division quasiment nul. L'action intratumorale des LNC-Fc-diOH dans un modèle de gliome sous-cutané entraîne une réduction significative des masses et volumes tumoraux. De plus, l'association entre le ferrociphénol et les photons X est une association synergique conférant à Fc-diOH des propriétés de molécule radio-sensibilisante. La médiane de survie du groupe traité par une CED de LNC-Fc-diOH suivie d'une radiothérapie externe de 18Gy (3x6Gy) augmente de 48% par rapport au groupe contrôle avec la présence de 17% de longs survivants.

Mots clés : Gliome, Nanocapsule lipidique, Rhénium-188, Fer, Convection-enhanced delivery

Abstract

The aim of this work is the use of lipid nanocapsules (LNC) infused by convection-enhanced delivery (CED) for the local delivery of brain tumors. For therapeutic applications, LNC were loaded with two lipophilic metal-based complexes. The first one is a lipophilic complex of Rhenium 188 (^{188}Re-SSS) which is investigated as a novel radiopharmaceutical carrier for internal radiation therapy of malignant glioma. The second one is an anticancer drug with a ferrocene grafted on a tamoxifen skeleton and called ferrociphenol (Fc-diOH). When administered in LNC, ^{188}Re tissue retention was greatly prolonged, and could eradicate tumors for an optimal dose of 8Gy as 33% of the animals were long-term survivors. The dose of 8 Gy proved to be a very effective dose, between toxic (10-12 Gy) and ineffective (3-4 Gy) ones. Fc-diOH-LNC showed many advantages such as a high drug loading capacity, and were able to be up-taken by glioma cells. Fc-diOH cytostatic activity was conserved after its encapsulation in LNC and was very effective on 9L-glioma cells as the IC_{50} was about 0.6µM. Interestingly, Fc-diOH-loaded LNC showed low toxicity levels when in contact with astrocytes which are slowly or non divided brain cells. Fc-diOH LNC treatment was able to lower significantly both tumour mass and volume evolution after 9L-cell implantation. Moreoever, the relationship between Fc-diOH-LNC and X-irradiations was synergistic. Combining an external irradiation of 18Gy (3x6 Gy) with CED of Fc-diOH-LNC increased the median survival time from 48% compared to the control group and 17% of the animals were long-terms survivors.

Keywords: Glioma, Lipid nanocapsules, Rhenium-188, Iron, Convection-enhanced delivery